LUND UNIVERSITY

Beyond Ethanol and Biodiesel

The Potential of Glycerol Derivatives and C_1–C_4 Alcohols for Motor Fuel Applications

Olson, Andre Louis

2024

Document Version:
Publisher's PDF, also known as Version of record

Beyond Ethanol and Biodiesel

The Potential of Glycerol Derivatives and C_1–C_4 Alcohols for Motor Fuel Applications

ANDRÉ LOUIS OLSON
DEPARTMENT OF ENERGY SCIENCES | FACULTY OF ENGINEERING | LUND UNIVERSITY

Printed by Media-Tryck, Lund 2024 NORDIC SWAN ECOLABEL 3041 0903

Faculty of Engineering (LTH)
Department of Energy Sciences

ISBN 978-91-8104-245-0

Beyond Ethanol and Biodiesel

Beyond Ethanol and Biodiesel

The Potential of Glycerol Derivatives and C_1–C_4 Alcohols for Motor Fuel Applications

av André Louis Olson

LUNDS
UNIVERSITET

AKADEMISK AVHANDLING
som för avläggande av teknologie doktorsexamen vid tekniska fakulteten vid Lunds universitet, kommer att offentligen försvaras den 29 november 2024, kl. 10.15 i M:B hörsal, M-huset, Lunds tekniska högskola, Ole Römers väg 1, Lund.

Handledare: Assoc. Prof. Sebastian Verhelst och Prof. Martin Tunér.
Fakultetsopponent: Assoc. Prof. Pierre Brequigny, Université d'Orléans, Orléans, Frankrike.

Organization	Document name
LUND UNIVERSITY Department of Energy Sciences Box 118 SE-221 00 LUND Sweden	**DOCTORAL DISSERTATION** Date of defense 2024-11-29 Sponsoring organization
Author(s) André Louis Olson	

Title and subtitle

Beyond Ethanol and Biodiesel: The Potential of Glycerol Derivatives and C_1–C_4 Alcohols for Motor Fuel Applications

Abstract

Certain oxygenated compounds, called oxygenates, when blended with gasoline, have the ability to inhibit the occurrence of engine knock, thus helping improve spark-ignition engine efficiency. Similarly, oxygenates can also be added to diesel fuel to decrease the exhaust emissions—soot in particular—from diesel engines. Although ethanol and biodiesel have had widespread use as oxygenates for gasoline and diesel fuel, respectively, certain types of glycerol-derived compounds—such as glycerol *tert*-butyl ether (GTBE)—as well as other alcohols may be technically superior in a number of aspects. This work provides an investigation into the potential of glycerol derivatives and C_1–C_4 alcohols to be used in motor fuel applications, focusing on engine performance and exhaust emissions. To that end, extensive engine tests were carried out on two diesel engines and on a modified spark-ignition CFR engine. The SI tests, which had a special focus on the knock behavior of the fuels, also included an investigation of the use of C_1–C_4 alcohols as neat fuels. The results showed that, in general, the glycerol derivatives and the C_1–C_4 alcohols were effective in decreasing the knock tendency of their blends with a gasoline surrogate, with the exception of *n*-butanol. When used as neat fuels, the results clearly showed the distinct knock behaviors exhibited by the different alcohols, with *n*-butanol again producing the poorest results, whereas isopropanol demonstrated excellent knock resistance. Regarding the diesel tests, the results showed that the glycerol derivatives and isobutanol (the only alcohol included in those tests), all performed well in decreasing soot emissions, highlighting the beneficial effect of fuel-bound oxygen. In summary, glycerol derivatives and C_1–C_4 alcohols can be effective in not only inhibiting knock in SI engines or decreasing soot emissions from diesel engines. When such compounds are produced from renewable sources, their usage may also displace the usage of fossil fuels, thus contributing to the decarbonization of the transportation sector.

Key words

biodiesel, gtbe, solketal, triacetin, methanol, ethanol, propanols, butanols

Classification system and/or index terms (if any)

Supplementary bibliographical information	Language
	English
ISSN and key title	ISBN
	978-91-8104-245-0 (print) 978-91-8104-246-7 (pdf)
Recipient's notes	Number of pages: 243 / Price
	Security classification

Beyond Ethanol and Biodiesel

The Potential of Glycerol Derivatives and C_1–C_4 Alcohols for Motor Fuel Applications

av André Louis Olson

LUNDS
UNIVERSITET

A doctoral thesis at a university in Sweden takes either the form of a single, cohesive research study (monograph) or a summary of research papers (compilation thesis), which the doctoral student has written alone or together with one or several other author(s).

In the latter case the thesis consists of two parts. An introductory text puts the research work into context and summarizes the main points of the papers. Then, the research publications themselves are reproduced, together with a description of the individual contributions of the authors. The research papers may either have been already published or are manuscripts at various stages (in press, submitted, or in draft).

Funding information: This work was supported by the European Union's Horizon 2020 Framework Program for Research and Innovation, Grant Agreement No. 818310.

Faculty of Engineering (LTH), Department of Energy Sciences

ISBN: 978-91-8104-245-0 (print)
ISBN: 978-91-8104-246-7 (pdf)

Printed in Sweden by Media-Tryck, Lund University, Lund 2024

Media-Tryck is a Nordic Swan Ecolabel certified provider of printed material. Read more about our environmental work at www.mediatryck.lu.se

MADE IN SWEDEN

He, O men, is the wisest, who, like Socrates, knows that his wisdom is in truth worth nothing.

— Plato, *Apology*

This documentation was prepared with LaTeX 2_ε

Contents

Acknowledgements

The decision of embarking on a "Ph.D. journey"—as many seem to call it—is never to be taken lightly. After all, that kind of endeavor takes patience, it takes time, it may take money, it takes precious years of one's life. So, it's a legitimate thing to wonder why making that decision seemed like the right thing to do in the first place. In my particular case, while I had at times entertained the idea of doing a Ph.D., that idea was always quickly dismissed, since I had always considered myself (1) too old for such a thing and also (2) hopelessly bereft of academic talent. However, by a series of unfortunate circumstances, I suddenly found myself out of a job and rapidly running out of money. Almost forty-two years-old. It was then that I had to reconsider the idea that, up to that point, had always been relegated to the back burner of my mind. I knew from the very outset that I was signing up for a rough ride. Yet, I was determined to face the storm. (And a storm did I face.)

This is how my midlife, unlikely Ph.D. journey started.

Therefore, a great deal of acknowledgement goes to the people whose support, in one way or another, helped me finish the Ph.D. program and to whom I'm very grateful. First off, I thank my supervisor, Sebastian Verhelst, for his guidance and—above all—his patience over all these years. I also thank Martin Tunér, my co-supervisor, whose support and friendliness also made a difference. Many thanks also to the other Professors in our division: Öivind Andersson, Marcus Lundgren, Per Tunestål, and also Magnus Genrup, the (now ex) head of our department. (Also, special thanks to Joakim Pagels and Vilhelm Malmborg from the Aerosol Lab, for providing instruments and helping me with particle measurements.) To the administrative staff I'm also grateful for helping me with practical matters, so many thanks go to Isabelle Frej, Anders Schyllert, and especially Catarina Lindén. For having always helped me with hands-on work in the test cells, I thank Patrik Johansson and especially Anders Olsson for their invaluable technical support. I'm definitely grateful to my fellow Ph.D. students and post docs—current and former—for supporting me, for being friendly, or simply for being around. The list includes: Ola Björnsson, Anupam Saha, Miaoxin Gong, Magnus Svensson, Peter Hallstadius, Beyza Dursun, Yachao Wang, Christoffer Ahrling, Menno Merts, Xinda Zhu, Vikram Singh, Carlos Jorque Moreno, Xiufei Li, Amir Bin Aziz, Brian Gainey, Nikolaos Dimitrakopoulos, Maja Novaković, and especially Nika Alemahdi.

Last, but not least, I thank Kenan Murić for being the one who ultimately started this whole mess.

So, as I turn the page on yet another chapter of my unsettled life—even without quite knowing what's going to happen next—I'm glad I made that decision over five years ago. After all the highs and lows, all the ups and downs, when I look back I realize that the ride was indeed very rough, but was worth it. In the end, I'm grateful for that storm.

A.L.O.

Lund
November 2024

Abstract

As the world is trying to be increasingly less dependent on fossil fuels, whose utilization contributes to climate change, the transportation sector, being responsible for a large part of the CO_2 emissions, is frequently the focus of much discussion on the subject. A range of strategies meant to address the issue of decarbonizing transport have been proposed, such as electrification and the use of carbon-free fuels, such as hydrogen and ammonia. However, due to the sheer magnitude of the problem and due to the existence of a vast fleet of vehicles powered by conventional internal combustion engines, it becomes clear that such engines are still going to be relevant for the foreseeable future. Moreover, due to economic reasons, many developing countries are likely to remain dependent on conventional engine technology for many years to come. Consequently, the types of fuels that existing and future engines will require can have a significant impact on net carbon emissions. As such, alternative fuels have the potential to play a significant role in the decarbonization process.

Today's most important biofuels, ethanol and biodiesel, have their weaknesses, beyond the fact that both are commonly produced from food-based crops. Ethanol exhibits negative aspects such as its affinity for water, corrosiveness, and ability to distort the vapor pressure characteristics of its blends with gasoline. In addition, largely because of those drawbacks, in some places the addition of ethanol to gasoline is capped by a "blend wall", an upper blending limit that effectively restricts the displacement of fossil energy. Biodiesel is plagued by poor cold-flow properties, restricting its use in colder climates. Besides, its production process produces sizable amounts of glycerol, a by-product that is commonly discarded as waste.

Against this backdrop there is a need to propose and develop new fuel alternatives with the potential to further displace fossil fuel usage, while having the ability to decrease exhaust emissions without compromising engine performance. Such fuels should be able to be used as "drop-in" fuels, that is, being able to use the same fuel infrastructure and be used on engines without extensive modifications (if any). Therefore, this work proposes and evaluates the use of alternative fuels and additives—for both gasoline and diesel engines—with the potential to diversify the range of fuel options and minimize the use of conventional fossil fuels. The first part of the proposed fuels is comprised of compounds derived from the aforementioned waste glycerol from the biodiesel industry. These compounds include

a number of ethers, acetals, and esters of glycerol that can be used as drop-in additives for both gasoline and diesel fuels, as oxygenates to enhance knock resistance and decrease smoke emissions. Moreover, such compounds may also be used to improve the cold-flow properties of biodiesel. The second group of fuels proposed by this work is represented by lower alcohols, other than ethanol, to be used in blends with gasoline. Among those, isobutanol is particularly attractive because of its higher heating value, lower corrosiveness and overall higher compatibility with gasoline, when compared to ethanol. Isopropanol, a less-studied alcohol also offers an enhanced potential to inhibit the occurrence of knock in spark-ignition engines. Finally, methanol, despite its relatively low heating value and high corrosiveness is also relevant since it is the cheapest alcohol, exhibits excellent combustion characteristics and can be used in the chemical industry as a raw material for several other compounds.

As described in this work, all those different compounds were evaluated in blends with either diesel fuel and a gasoline surrogate, through a series of testing campaigns, carried out on two diesel engines and on a spark-ignited CFR engine. Besides being evaluated in blends with the gasoline surrogate, the C_1–C_4 alcohols alcohols were also investigated in neat form, highlighting their potential to maximize the displacement of gasoline. The overall results showed that all compounds performed well when mixed to the base fuel in limited concentrations, as intended from a "drop in" perspective. Moreover, the tests on the CFR engine showed that the different fuel additives exhibited clearly distinct behaviors, regarding their knock-inhibiting abilities. Finally, in addition to their use as fuel components, clearly distinct behaviors were also seen in the tests with the alcohols in neat form, with both isopropanol and isobutanol performing particularly well. Therefore, it is hoped that the work presented in this dissertation will shine a light on promising fuels and fuel additives that have not received due attention from the engine and the fuel communities.

Populärvetenskaplig sammanfattning

Världen försöker gå bort från fossila bränslen, vars användning gör att nivåerna av koldioxid (CO_2) i atmosfären ökar, vilket bidrar till klimatförändringsproblemet. Transportsektorn står för en stor del av CO_2-utsläppen, därför pågår mycket forskningsarbete relaterat till användningen av biobränslen—bränslen som produceras från förnybara källor – eftersom deras förbränning inte leder till en ökning av den totala CO_2-nivån i atmosfären.

Förbränningsmotorer, som används i bilar, motorcyklar, bussar, lastbilar osv., finns i två huvudtyper: gnisttändningsmotorer (bensinmotorer) och kompressionständningsmotorer (dieselmotorer). För att förbättra förbränningsprocessen i dessa motorer, öka motorns prestanda och minska utsläppen av föroreningar kan speciella tillsatser blandas i bränslet. Sådana tillsatser innehåller ofta syre och kallas då ”oxygenater”. För dieselmotorer kan avgasröken reduceras avsevärt med oxygenater, medan de i bensinmotorer kan förhindra förekomsten av ”knack” (en förbränningsanomali som kan skada eller till och med förstöra motorer). Dessutom produceras de flesta oxygenater idag från förnybara källor, vilket innebär att deras användning bör ha mindre inverkan på CO_2-koncentrationerna i atmosfären. En annan egenskap hos dessa föreningar är att de är avsedda att blandas med fossila bränslen i låga koncentrationer, vilket gör att de kan betraktas som ”drop-in-bränslen”, det vill säga de kan användas på vanliga motorer som använder den befintliga bränsleinfrastrukturen. Även om elbilar blir allt vanligare kommer det fortfarande att finnas ett stort antal fordon som drivs av förbränningsmotorer på vägarna. Därför kommer det att finnas en marknad för sådana oxygenater under många år framöver.

Denna avhandling undersöker flera typer av oxygenater som kan blandas med bensin och dieselbränsle. De utvärderades genom motortester som utfördes i Lunds universitets motorlaboratorier. För dessa tester användes två dieselmotorer och en bensinmotor. Blandningar av oxygenaten med dieselbränsle och bensin framställdes och användes som bränslen under testerna. Huvudsyftet med testerna var att undersöka hur syrehalterna påverkade motorprestanda och utsläpp av föroreningar.

I den första delen av denna forskning testades oxygenater som härrör från glycerol (glycerin). Glycerol är en biprodukt av den process som producerar biodiesel (ett förnybart bränsle för dieselmotorer) och det kasseras vanligtvis som avfall. Därför

kan omvandling av det avfallsglycerol till användbara kemikalier bidra till biodieselindustrins miljömässiga hållbarhet samtidigt som det minskar användningen av fossila bränslen inom transportsektorn. De oxygenater som härrör från glycerol som undersöktes i detta arbete var den så kallade glycerol-*tert*-butyletern (GTBE), solketal och triacetin.

Förutom glycerolderivaten testades flera olika alkoholer på bensinmotorn. I den inledande delen av experimenten blandades alkoholerna med en bensinsurrogat (en typ av bensin-"ersättning", som används i motorforskning). Senare användes de i ren form. Etanol (etylalkohol) har varit den huvudsakliga alkoholen som använts som bränsle runt om i världen och som sådan ingick den i testerna. Förutom etanol undersöktes andra typer av alkoholer med potential att användas som bränsle under motortesterna. Dessa alkoholer var metanol, isopropanol, *n*-butanol och isobutanol (som även blandades med dieselbränsle). Isopropanol och butanolerna kan vara särskilt attraktiva eftersom de har ett högre energiinnehåll och är mindre korrosiva jämfört med etanol och metanol.

Resultaten av alla tester visade i allmänhet att båda typerna av kemiska föreningar, det vill säga glycerolderivaten och alkoholerna, framgångsrikt kunde användas som oxygenater när det gäller att bevara motorprestanda och minska utsläppen av föroreningar. Sammanfattningsvis visar den forskning som beskrivs i denna avhandling nya möjligheter att minska användningen av fossila bränslen, vilket bidrar till att minska koldioxidutsläppen inom transportsektorn.

List of Publications

Contents of this monograph have been or will be published in the following peer-reviewed journals:

I. **A concise review of glycerol derivatives for use as fuel additives**

A.L. Olson, M. Tunér, and S. Verhelst
Heliyon, vol. 9, no. 1, Jan. 2023, pp. 1–10, doi: 10.1016/j.heliyon.2023.e13041

II. **Experimental Investigation of Glycerol Derivatives as Low-Concentration Additives for Diesel Fuel**
A.L. Olson, N. Alemahdi, M. Tunér, and S. Verhelst
SAE Technical Paper 2023-24-0095, Aug. 2023, pp. 2–30, doi: 10.4271/2023-24-0095

III. **A Review of Isobutanol as a Fuel for Internal Combustion Engines**

A.L. Olson, M. Tunér, and S. Verhelst
Energies, vol. 16, no. 22, Nov. 2023, pp. 1–10, doi: 10.3390/en16227470

IV. **Experimental Investigation of Glycerol Derivatives and C_1-C_4 Alcohols as Gasoline Oxygenates**
A.L. Olson, M. Tunér, and S. Verhelst
Energies, vol. 17, no. 7, Apr. 2024, pp. 1–10, doi: 10.3390/en17071701

V. **Investigation of the combustion characteristics and knock tendencies of neat C_1-C_4 alcohol fuels using a CFR engine**[1]
A.L. Olson, M. Tunér, and S. Verhelst
Fuel, pp. 1–10

[1]Submitted to the journal *Fuel*; under review at the time of writing.

List of Tables

List of Figures

Nomenclature

ABE Acetone-butanol-ethanol

ASTM American Society for Testing and Materials

ATC After top-center crank position

BEV Battery-electric vehicle

BTC Before top-center crank position

CAD Crank-angle degree

CFC Chlorofluorocarbon

CFD Cumulative frequency distribution

CFR Cooperative Fuel Research

CI Compression-ignition

CORDIS Community Research and Development Information Service

COV Coefficient of variation

DAG Diacetyl glycerol

DMC Dimethyl carbonate

DME Dimethyl ether

E – fuel Electrofuel

ECU Electronic control unit

EGR Exhaust-gas recirculation

EV Electric vehicle

F – T Fischer-Tropsch

FAEE Fatty-acid ethyl ester

FAME Fatty-acid methyl ester

FAO Food and Agriculture Organization of the United Nations

FC Fuel cell

FTIR Fourier-transform infrared

GHG Greenhouse gas

GTBE Glycerol tertiary butyl ether

H/C Hydrogen/carbon ratio

H2ICE Hydrogen-fueled internal combustion engine

HC Hydrocarbon

HD Heavy-duty

HOV Heat of vaporization

HTC Hydrothermal carbonization

HVO Hydrotreated vegetable oil

IAT Intake air temperature

ICE Internal combustion engine

IMEP Indicated mean effective pressure

ISFC Indicated specific fuel consumption

ITE Indicated thermal efficiency

LCA Life-cycle analysis (or assessment)

LD Light-duty

LHV Lower heating value

LTC Low-temperature combustion

LUC Land-use change

MAG Monoacetyl glycerol

MAPO Maximum amplitude of pressure oscillations

MBT Maximum brake torque

MON Motor octane number

MSS Micro soot sensor

MSW Municipal solid waste

MTBE Methyl tertiary butyl ether

MW Molecular weight

NOx Nitrogen oxides

NVH Noise, vibration and harshness

OECD Organisation for Economic Co-operation and Development

PAH Polycyclic aromatic hydrocarbon

PM Particulate matter

RED Renewable Energy Directive

RON Research octane number

RP Rail pressure

SAE Society of Automotive Engineers

SAF Sustainable aviation fuel

SI Spark-ignition

ST Spark timing

STBE Solketal tertiary butyl ether

Syngas Synthesis gas

TAG Triacetyl glycerol (triacetin)

TBA Tertiary butyl alcohol

TC Top-center crank position

TEL Tetraethyl lead

THC Total hydrocarbons

TPRF Toluene primary reference fuel

Chapter 1

Introduction

1.1 Preliminary Remarks

In recent years, there has been intense scrutiny regarding the global energy production/consumption due to the impact of greenhouse gases (GHGs), especially carbon dioxide (CO_2), on the earth's climate, in particular. Because it represents a good portion of total GHGs emissions (See figure 1.3), and especially because of its visibility to the general public, the transport sector has been at the epicenter of such concerns. However, unlike the other exhaust pollutants (such as nitrogen oxides and particulate matter), CO_2 cannot be removed by the use of exhaust aftertreatment devices, which makes things more complicated. In fact, because CO_2 is the unavoidable product of the combustion of carbon-containing fuels, the mitigation of the impacts of climate change calls for the reduction of atmospheric CO_2 levels, that is, the *decarbonization* of the transport sector (and the entire energy sector in general) has become the top priority of the automotive industry. The reduction in the use of fossil fuels, since the carbon dioxide emissions from their combustion cannot be offset by the biomass that created them, has become the order of the day. However, since fossil fuels are the bedrock upon which the entire transport sector rests, the task of decarbonization is nothing less than an enormous and extremely complex endeavor. Therefore, several measures to reduce net CO_2 emissions and mitigate the climate-related issues associated with them have been put forth. Of particular importance is the proposed electrification of transport, especially regarding pure electricity-powered, battery-electric vehicles (BEVs). Because

BEVs obviously lack exhaust pipes, they are frequently claimed to be "zero emissions", an assertion that may or may not be true, depending on how the electricity to power them has been generated. Either way, electrification does represent a step forward towards a more decarbonized society. However, as it is the case with any technology, BEVs have their flaws and limitations, as discussed further ahead. Another approach that has been proposed is the use of hydrogen, either as a fuel for fuel cell vehicles or conventional internal combustion engines (ICEs). In either case, the use of hydrogen poses some serious challenges that call into question its viability as a fuel. Another carbon-free fuel, ammonia (NH_3), has its own issues but it seems to be more suitable for marine applications.

Besides the calls for a complete—and rapid—decarbonization of transport, one aspect that should be at the forefront of the public discourse is the recognition of the fact that there is a *legacy fleet* of over one billion cars on the world's roads nowadays, virtually all of them powered by ICEs. Those vehicles are expected to remain in operation for the foreseeable. In addition, in many parts of the world electrification is not expected to happen anytime soon, mostly for economic reasons, since the large-scale adoption of electric vehicles and building the necessary infrastructure require large investments. That means an energy transition is necessary, taking into account the different social and economic circumstances in different regions of the world. Therefore, within the range from 100% fossil-fuel transport to 100% electrified transport, there is a middle ground that can and should be explored as a feasible and potentially effective option during that transition, to reduce net carbon emissions. Biofuels, such as ethanol and biodiesel (FAME), have characteristics that make them attractive as transport fuels, since their production and use is commonplace in several parts of the world, such as Brazil and the United States (in the case of ethanol) and the European Union and parts of Asia (in the case of biodiesel). Nevertheless, biofuels are not without their drawbacks and limitations, especially in the case of first-generation biofuels such as sugar- or starch-based ethanol and vegetable-oil-based biodiesel. Yet, even though the technology for producing second-generation (i.e. lignocellulosic) biofuels does exist, their economic viability is still a matter of debate. Regardless, in the energy-transition scenario all options should be considered and their technical and economic feasibility will to a large extent depend on the local circumstances of the regions in which they are used. In other words, even the production and use of first-generation biofuels have their place and can be sustainable (which is the case of sugarcane ethanol in Brazil).

Expanding the range of options of potential biofuels is an attractive approach, since different chemical compounds may exhibit better characteristics when compared to the usual ones, and also because the diversification of the available biofuel options has the potential to benefit the transportation sector as a whole. For instance, glycerol, which is the waste that is generated by the production of biodiesel, can be converted into useful compounds that can be used as fuel additives, including for the biodiesel itself, because such compounds can improve some of biodiesel's properties, such as its cold-flow characteristics. Alternatively, the production and the utilization of other alcohols other than ethanol can be advantageous. For instance, isobutanol is an alcohol that has attractive properties, such as a higher heating value, lower water affinity and lower corrosiveness, when compared to ethanol. Moreover, isobutanol can be used as feedstock for several other useful chemicals. Another alcohol that is also an important commodity compound is methanol, a well-known and inexpensive chemical that is used extensively in the chemical industry and is also a clean-burning, low-carbon alcohol fuel for ICEs. The possibility of producing methanol as an electrofuel, using captured carbon dioxide and hydrogen, seems like a very promising and effective strategy to decarbonize transport. Other alcohols, such as isopropanol, which are widely used in several applications—except as ICE fuels—are also worth investigating, due to appealing characteristics such as superior knock resistance. Hence, from an overall perspective, this work attempts to address the topic of the diversification of the biofuel alternatives, by investigating compounds—glycerol derivatives and C_1–C_4 alcohols—that have the potential to play an important role in the energy transition. It is thus hoped that the present work will help fill some knowledge gaps and shine a light on potentially useful chemical compounds that have so far been given insufficient attention.

1.2 Climate-Related Issues

Climate can be defined as "the typical behavior of the atmosphere, the aggregation of the weather, and is generally expressed in terms of averages and variances of temperature, precipitation and other physical properties" [1]. The greenhouse effect, which is the ability of certain gases (such as carbon dioxide and water vapor) to trap some of the reemission of solar radiation by the earth, is necessary, otherwise the planet would be too cold for sustaining life. However, due to human activities, the concentration of greenhouse gases (GHGs) have been shown to

be steadily increasing, leading to widespread concerns about the warming of the earth. There has been an extensive amount of evidence to support the hypothesis that the earth's temperature has been increasing. Compiled data regarding global mean sea surface temperatures as well as surface air temperatures have indicated the climate is rapidly changing. Further evidence has been provided by measurements of atmospheric temperatures, obtained by meteorological balloons and satellites. In addition, proxy temperature indicators such as tree-ring width and density, the chemical composition and growth of corals, together with the characteristics of annual layers in ice cores, have been used to extend temperature records back as much as one thousand years. Besides temperature, the extent of alpine glaciers, sea ice, seasonal snow cover, and the lengths of the growing seasons have changed, consistent with the hypothesis that the planet is warming. The concentrations of many atmospheric gases would be expected to change slowly without human intervention. This scenario began to change after the start of the industrial age, when agriculture, industry, waster disposal, deforestation, and especially fossil fuel use, caused the levels of human-made emissions to rise rapidly. These include nitrous oxide (N_2O), chlorofluorocarbons (CFCs), and especially carbon dioxide (CO_2) and methane (CH_4), whose emissions are increasing at unprecedented rates.

Among the greenhouse gases, carbon dioxide has shown the largest-changing concentrations and it thus considered the gas of most concern regarding the human impacts on climate. As of July 2024, the monthly averaged atmospheric concentration of CO_2 was approximately 426 ppm [2], representing an increase of roughly 52% since before the Industrial Revolution, when such concentrations were estimated not only to be around 280 ppm, but also to have remained essentially constant for over a thousand years [1]. Figure 1.1 shows the long-term trends in atmospheric CO_2 concentrations, measured using preserved air samples from ice cores. The increase in CO_2 emissions are attributed primarily to two types of human activity: fossil fuel use (which has *increased* atmospheric carbon dioxide and production) and land use, including deforestation (which has *decreased* carbon storage in vegetation and soil). Energy from biomass represents a special case; while its combustion releases carbon into the atmosphere, the biomass has already absorbed an equal amount of carbon from the atmosphere prior to its emissions, thus the *net* carbon emissions are zero over its lifecycle.

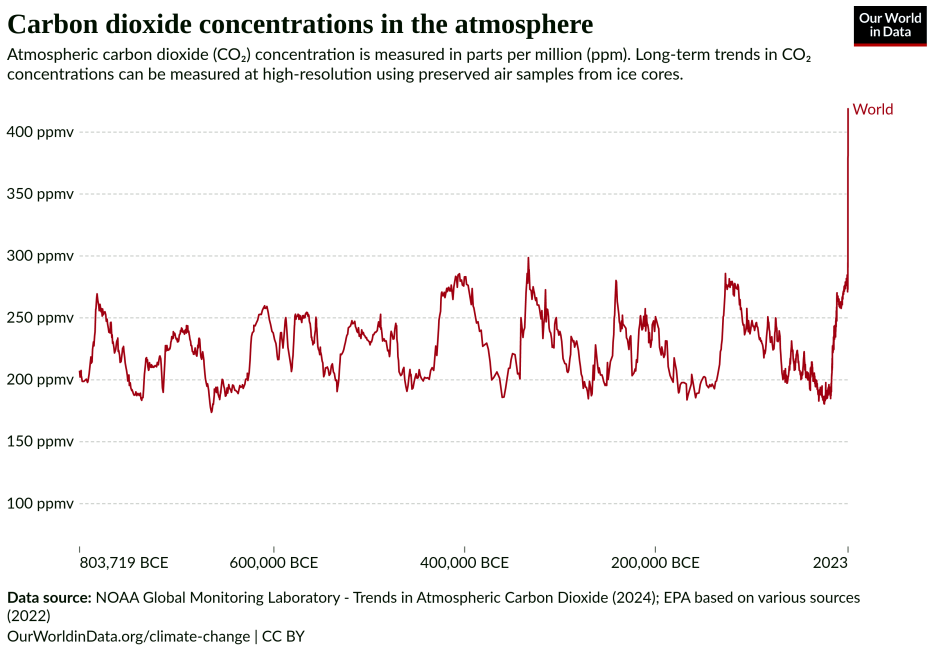

Figure 1.1: Carbon dioxide concentrations in the atmosphere.

Figure 1.2 shows the global average temperature relative to a baseline, defined as the average between 1961 and 1990. The plot shows that the average temperatures have risen by over 0.8°C since then. It also shows that the temperatures in 1850 were around 0.4°C cooler than the baseline, resulting in a total temperature rise of about 1.2°C compared to pre-industrial times.

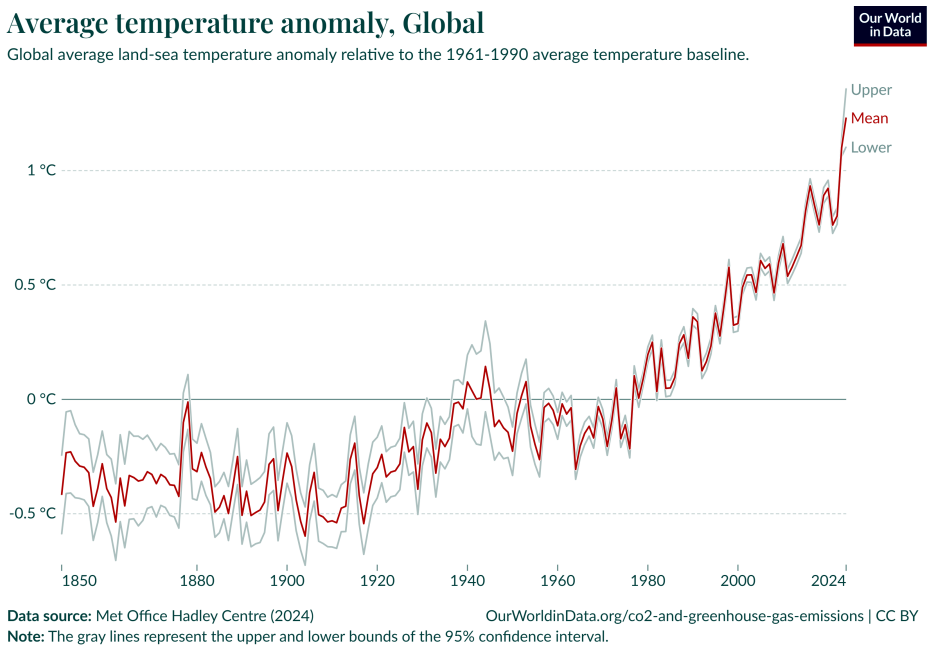

Figure 1.2: Average temperature anomaly, Global [3].

Studies have shown that the effects of climate change can impact several sectors such as human health, ecological systems, water resources, food production (agriculture), and coastal systems (sea levels).

The atmospheric concentrations of methane are much lower, on a molecule-by-molecule basis, representing less than 0.5% of the concentrations of carbon dioxide. However, as a greenhouse gas, CH_4 is about 50 times more powerful than CO_2, resulting in methane being the second most important gas regarding climate change. Methane emissions from anthropogenic sources are primarily related to agriculture and waste disposal, including enteric fermentation, animal and human wastes, rice paddies, biomass combustion, and landfills. Fossil-fuel-related sources include natural gas loss, coal mining, and the oil industry. Figure 1.3 shows a detailed allocation of GHG emissions by sector, from the year 2016 [3].

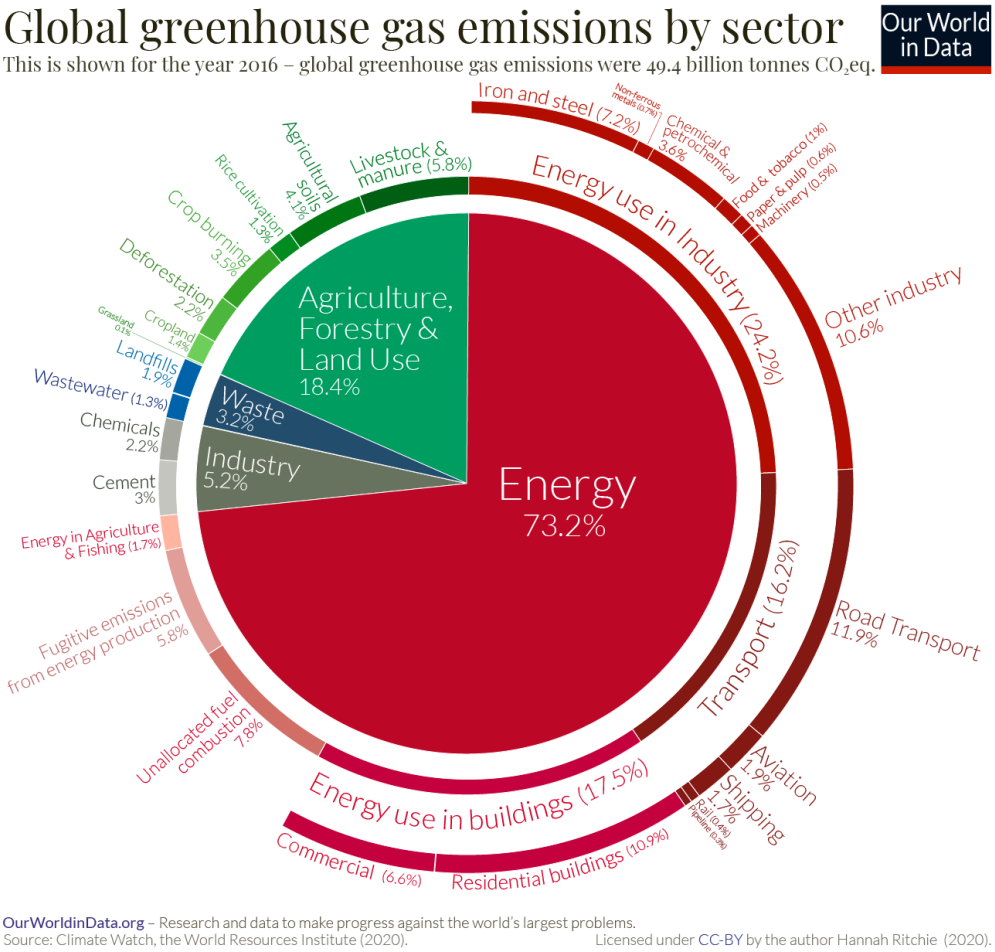

Figure 1.3: Global greenhouse gas emissions by sector, 2016 [3].

Aerosols have the potential to affect the climate directly by absorption and scattering of solar radiation and indirectly by acting as cloud-condensation nuclei. Such aerosols can originate from emissions of sulfur dioxide (SO_2) and other gases. Most of anthropogenic SO_2 in the atmosphere mainly results from the combustion of coal and other fossil fuels. Besides affecting the climate, sulfur dioxide emissions may form sulfuric acid (H_2SO_4) and eventually sulfate particles which can cause acid rain. Aerosols comprised of carbonaceous agglomerates, i.e. soot particles, are also relevant to climate change, since they can absorb solar and infrared radiation, potentially contributing to climate warming. The soot emissions from internal combustion engines can be significant and are therefore discussed in the next

chapters of this work.

1.3 The Future of the Internal Combustion Engine

As the concerns related to climate change have been amplified and become increasingly widespread, the long-term prospects and the very viability of internal combustion engines have been repeatedly called into question. Their reputation also suffered a blow, especially in the case of diesel engines, in the wake of Volkswagen's "Dieselgate" scandal of 2015 [4]. No technology lasts indefinitely (e.g. reciprocating steam engines) and, while ICEs can have a significant impact on the environment, so can their proposed alternatives. Therefore, it is crucial that the roles played by ICEs and their potential replacements, together with their strengths and shortcomings, be put into context and analyzed from a broad perspective. Two of such alternative technologies, electrification and hydrogen, have been heavily proposed and as such, deserve some attention.

1.3.1 Transport Electrification

As previously mentioned, road transport accounts for more than half of the GHG emissions of the transport sector, which in turn represents approximately a quarter of all global GHG emissions. Because of that, switching to electricity to fuel road transport has been proposed as the main tool to reduce CO_2 emissions. Therefore, vehicles, powered by electricity, have been touted as a promising alternative to conventional fossil-fuel ICE vehicles. Indeed, several governments around the world have set goals and timelines for the phase-out of vehicles powered by ICEs by 2050 [5]. Different types of EVs (battery EVs, hybrid EVs, and plug-in hybrid EVs) have been proposed and compared to determine which technology will likely dominate in the next decades, but many have already concluded that battery-electric vehicles (BEVs) should be prioritized [6].

When compared to conventional vehicles powered by ICEs, BEVs offer a number of attractive advantages. As listed by Senecal and Leach in their book [7], these include: the obvious absence of a tailpipe, reduced noise, high efficiency, cheap electricity (in some areas, at least), less maintenance, good vehicle driveability (quick acceleration), and the possibility of charging the batteries at home. Another advan-

tage mentioned by the authors is the possibility of using renewable electricity, and that is exactly where BEVs can make a significant difference—as long as renewable electricity is available.

While EVs themselves do not emit carbon dioxide, the electricity to charge their batteries must be generated somewhere and, depending on how that is achieved, significant CO_2 emissions may result. As the study by Zhang and Fujimori [8] points out, "transport electrification without the replacement of fossil-fuel power plants leads to the unfortunate result of increasing emissions instead of achieving a low-carbon transition". That is, as Kalghatgi pointed out [9], if carried out in such a way, electrification would simply shift emissions from the transport sector to the power sector. A large-scale transition to electric vehicles would also sharply increase the demand for electricity which, if not generated by carbon-free methods (such as solar, wind, hydro, or nuclear), the benefits of BEVs might be minimal or, at worse, the GHG emissions might even increase [9]. Therefore, as also mentioned in Zhang and Fujimori's study [8], transport electrification alone is not enough to reduce emissions and mitigate the effects of climate change. Instead, to meet stringent decarbonization targets, the link between the transport and energy sectors deserves special attention and the use of renewable—or nuclear—energy to decarbonize power generation will need to play a fundamental role together with the electrification of the transport sector.

Another factor that should be taken into consideration is the mining of lithium-ion battery materials, such as lithium and cobalt, and the battery manufacture itself. Life-cycle analyses have shown that these processes can produce substantial amounts of greenhouse gases, which could contribute to an increased carbon footprint [10]. In addition, as Kalghatgi pointed out [9], the mining and processing of battery metals, if not done properly, can pose a significant threat to the environment, in the form of freshwater contamination. Also to be considered is the recycling of BEV batteries at the end of their service life, since that can also have a negative impact on the environment [9, 11].

Last, but not least, one non-technical aspect of BEV battery manufacturing that deserves attention is that more than half of the world's cobalt is found in the Democratic Republic of Congo, one of the world's poorest countries. As reported by Amnesty International [12], 20% of that cobalt is mined by hand in artisanal mines, by adults and children as young as seven years-old working in appalling conditions,

at risk of fatal accidents and serious lung disease and earning as little as one dollar a day [13].

In summary, it is clear that electric vehicles have a number of advantages over their ICE-powered counterparts and they do have the potential to minimize the carbon footprint of the transport sector. However, the electrification of transport—with the technology currently available today—comes with some caveats that should not be overlooked. The pros and cons of mass electrification should be carefully considered, especially those issues regarding electricity generation and battery manufacture. Accordingly, policymakers should be aware that electrification—or any other proposed measures, for that matter—is no panacea and will not be able to mitigate the effects of climate change by itself, without putting into practice other potentially effective decarbonization strategies.

It seems inevitable that electrification will eventually dominate light-duty transportation. Electric motors are simple, robust, and efficient prime movers, and they have been so for over one hundred years. Once battery technology evolves, the advantages of electric traction will become undeniable.

1.3.2 Hydrogen Fuel

Just like battery-electric vehicles, in recent years, much has been said about hydrogen as a transportation fuel. Regarding GHG emissions, hydrogen is indeed a very attractive fuel, since in theory its combustion produces only water vapor. For transport applications, hydrogen can be utilized in two different ways: in fuel cells (FCs), in which case the vehicle is powered by an electric motor and hydrogen is used to generate electricity within the fuel cell, or burned in conventional internal combustion engines. Each approach has its pros and cons. Fuel cells, according to a 2018 study by Kalghatgi [9], is the preferred option, due to its higher efficiency (when compared to ICEs). In contrast, a 2022 editorial by the *International Journal of Engine Research* [14], stresses that the *overall* efficiency of current FC powertrains is much lower than that of the FC alone [15]. The article mentions other drawbacks of FCs, such as their need for high-purity hydrogen, the need to have large batteries to store the electricity and, of course—cost. The editorial maintains that hydrogen internal combustion engines (H2ICEs) can benefit from being able to take advantage of the advanced state of current ICE technologies, such as "reliability, durabil-

ity, existing supply chain, existing manufacturing plus recycling infrastructure and affordability". Furthermore, the authors continue, benefit from being able to use "existing advanced combustion and engine control technologies", including "direct injection, Miller cycle, lean/diluted combustion, pre-chamber ignition, etc".

Whatever technology is ultimately chosen—FCs or H2ICEs—the viable large-scale use of hydrogen as a fuel will require overcoming a number of significant practical hurdles that are caused by its own unique properties, such as its highly energy-intensive production[1] and its extremely low density, which makes its distribution and storage particularly challenging, since it requires it to be either highly compressed (to about 700 atm) or liquefied and stored in bulky and heavy cryogenic tanks (a process that consumes a large amount of energy). In addition, hydrogen's density makes it prone to leak through joints that are otherwise perfectly tight for other gases, posing a safety risk. This can be particularly worrisome, due to its wide flammability limits, meaning that very lean and very rich hydrogen-air mixtures are susceptible to easily ignite (since hydrogen also ignites easily, compared to most fuels). Therefore, in view of such shortcomings, it might make more sense to use hydrogen indirectly, through fuels that are significantly more practical, like methanol or even ammonia.

1.3.3 The Death—or Not—of the ICE?

In August 2017, the British newspaper *The Economist* ran a front-cover article titled "Roadkill" [17], predicting the imminent "death of the internal combustion engine", caused by the widespread electrification made possible because of advances in battery technology and the falling prices of battery components.

Also in August 2017, *The New York Times* published an article, with the title "The Internal Combustion Engine Is Not Dead Yet" [18], in which John B. Heywood, a professor at the Massachusetts Institute of Technology, predicted that in 2050 60% of light-duty vehicles are still going to be powered by ICEs, often working with electric motors in hybrid systems. On the other hand, BEVs, he estimated, will represent 15% of car sales by that time.

[1] The electrolysis of water, at a 100% theoretical efficiency requires roughly 142 MJ of electricity per kg H_2 produced (in contrast, hydrogen's lower heating value is 120 MJ/kg); in reality, the process consumes 180–230 MJ/kg H_2, requiring up to 95% more energy to produce hydrogen than the amount of energy contained in the fuel itself [16].

The starkly contrasting views presented by those two articles—both published by reputable media outlets and at around the same time—illustrate the uncertainties surrounding the prospects of either technology, that is, the dominance of EVs versus the survival of the ICE.

The prediction of the *Economist* article is not untrue: Internal combustion engines will not last indefinitely and many automakers have already been making the transition to BEVs, whose popularity has soared in some markets.

Indeed, according to the statistics [19], in Norway, in 2022, BEVs represented 79.3% of new car sales (if plug-in hybrids are included, the share of electric vehicles sold reaches 87.8%), see Figure 1.4.

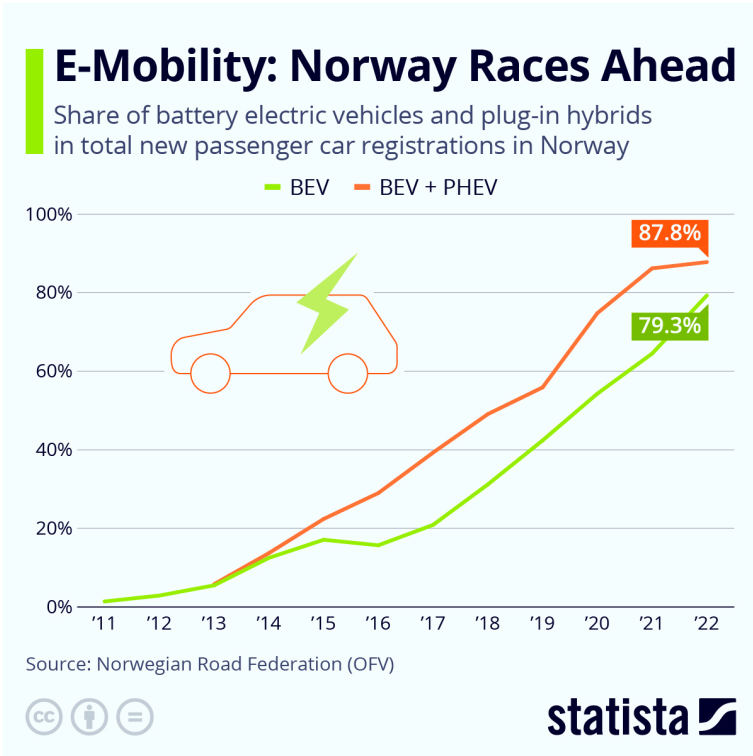

Figure 1.4: The share of electric vehicles on the Norwegian market [19].

However, Norway is a special case, since it is a wealthy country with a small population and extensive natural resources (such as abundant hydropower).

As the *New York Times* article also observed, the average age of the 270 million

light-duty vehicles on the road in the U.S. is approximately 12 years, meaning that, even if sales of new ICE-cars stopped right away, it would take longer than a decade for the fleet to switch over to EVs.

As stated in the 2020 editorial "The future of the internal combustion engine", by the *International Journal of Engine Research* [20], "... power generation sources will not become fully renewable and transport will not become fully electric for several decades, if ever". Regardless of how long it will take, this previously mentioned "legacy fleet" of over 1 billion vehicles powered by ICEs will remain in operation for the foreseeable future and their engines will need to burn some kind of fuel in the meantime. What *kind* of fuel they will burn can have an impact on the environment, hence the importance of investigating new biofuel options, the topic of next section.

1.4 The Role of Biofuels in the Energy Transition

1.4.1 Biomass Types

Biomass can be defined as renewable organic material obtained from plants, animals, and microorganisms. Biomass is an important fuel, especially in developing countries for cooking and heating [21].

Biofuels are ultimately based on the ability of photosynthetic organisms to use sunlight to convert CO_2 into glucose ($C_6H_{12}O_6$) and subsequently into plant biomass, according to the overall reaction [22]:

$$6CO_2 + 6H_2O \rightarrow C_6H_{12}O_6 + 6O_2$$

Cellulose is the name of the polysaccharide formed by the repeated connection of *D*-glucose building blocks [23]. This polymeric raw material is the main structural component of cell walls in higher plants and the most abundant form of living terrestrial biomass [24].

As explained further below, the photosynthetic efficiency of plants can be quite low, which raises doubts about the sustainability of converting food crops into biofuels [25].

Biomass feedstocks for energy include:

- Wood and wood processing waste: firewood, wood pellets, and wood chips, lumber and furniture mill sawdust and waste, and black liquor from pulp and paper mills.
- Agricultural crops and waste materials: corn (maize), soybeans, sugarcane, switchgrass, woody plants, algae, and crop and food processing residues.
- Biogenic materials in municipal solid waste (MSW): paper products, cotton and wool products, and food, yard, and wood wastes.
- Animal manure and human sewage.

Figure 1.5 illustrates the different types of biomass.

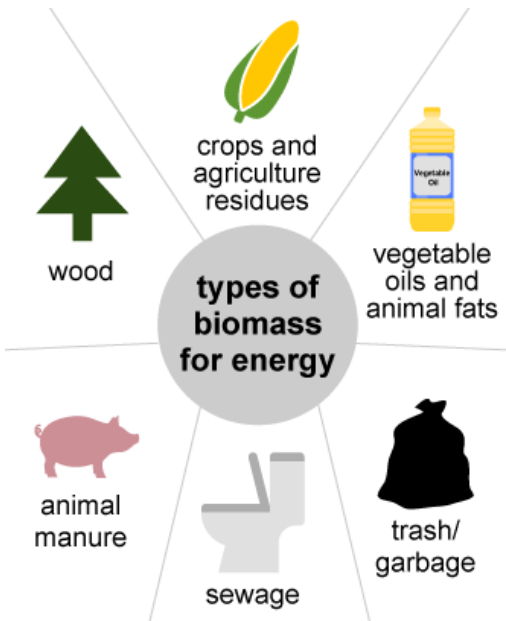

Figure 1.5: Biomass types [21].

1.4.2 Biomass Conversion Processes

Biomass conversion processes are the techniques through which biomass can be converted to energy, including biofuels, such as [21]:

- **Direct combustion**, the most common method for converting biomass to useful energy. All types of biomass can be directly burned for heating buildings and water, for providing heat to industrial processes, and for producing steam for steam turbines to generate electricity.

- **Thermochemical** conversion of biomass—including *pyrolysis* and *gasification*—is the thermal decomposition process in which the feedstock materials are subjected to high temperatures. The two proesses differ in the temperatures and in the amount of oxygen present during conversion:

  – Pyrolysis involves heating organic materials to between 400°C and 500°C in the absence of free oxygen. Biomass pyrolysis produces fuels such as charcoal, bio-oil, methane, and hydrogen.

  – Gasification involves heating organic materials to between 800°C and 900°C in the presence of controlled amounts of free oxygen or steam, producing a mixture of carbon monoxide and hydrogen called synthesis gas (syngas, essentially a mixture of hydrogen and carbon monoxide). Syngas can be used as a fuel for heating and for generating electricity in gas turbines. The hydrogen can be separated from the syngas and it can be used in fuel cells or burned in internal combustion engines. Syngas can also be further processed to produce liquid fuels using the Fischer–Tropsch process.

- **Biochemical** conversion of biomass includes *fermentation* of sugars to make ethanol and *anaerobic digestion* to produce biogas. Ethanol is used as a motor fuel. Biogas, comprised primarily of methane (CH_4) and carbon dioxide, can be produced through the anaerobic digestion of various types of biomass and waste, such as the organic fraction of MSW, agricultural waste, manure, sewage sludge, among others [26]. Properly treated biogas has the same uses as fossil natural gas.

- **Chemical conversion** includes the transesterification process, in which vegetable oils, animal fats, and greases are converted into fatty acid alkyl esters (biodiesel).

1.4.3 Biofuel Types

Biofuels are solid, liquid, or gaseous fuels that are derived from biomass, that is, plant or algae material or animal waste [27]. They are considered a renewable source of energy, since such feedstocks can be readily replenished. Because of that, biofuels are commonly proposed as environmentally-friendly alternatives to fossil fuels.

According to the *OECD-FAO Agricultural Outlook 2024-2033* report [28] (which describes market developments and medium-term projections for world biofuel—ethanol and biodiesel—markets for the period 2024-2033), in 2023, approximately 83% of ethanol was produced from corn or sugarcane, whereas roughly 65% of biodiesel was based on vegetable oils (see below).

More advanced biofuel technologies based on lignocellulosic feedstocks (e.g. crop residues, wood, or dedicated energy crops) do not account for large shares of total biofuel production. However, they are often seen as relevant technologies for the future, since they are supposed to cause less competition with food products and result in lower levels of GHG emissions.

Biofuels usually belong to three different categories, according to the nature of the feedstock and the technology used for their production, as follows:

- **First-generation** biofuels: By far the most common type, are obtained from traditional agricultural commodities as feedstock, such as sugarcane, corn, soybeans, rapeseed, etc. The foremost biofuels, conventional bioethanol and biodiesel (fatty-acid mono-alkyl esters), are first-generation biofuels.
- **Second-generation** biofuels: Produced from non-edible plant material, such as lignocellulosic biomass (such as agricultural and forest residues) and refuse such as municipal solid waste.
- **Third-generation** biofuels: Obtained from algal feedstocks.

First-generation *ethanol* is produced from sugars and from starch. Simple sugars are extracted from a variety of sugar crops and are then fermented, with the resulting wine distilled into ethanol. Starch requires an additional step—saccharification—in which it is broken down by enzymes to convert it into sugars, which are subsequently fermented. The saccharification of starch uses additional energy, increasing production costs.

Biodiesel is derived from vegetable oils, animal fats, or other materials consisting mainly of triacylglycerols [29]. It is obtained by reacting the oil with an alcohol (such as methanol or ethanol) in the presence of a catalyst, through the chemical process of transesterification, producing fatty-acid alkyl esters—fatty-acid methyl esters (FAME) if methanol is used (which is the most common route), or fatty-acid ethyl esters (FAEE), in the case of using ethanol. The hydrotreatment of vegetable oils or animal fats is an alternative process to esterification for producing renewable diesel fuel. Hydrotreated vegetable oil (HVO, also simply called "renewable diesel") [30] are mixtures of paraffinic hydrocarbons that are free of sulfur and aromatics, featuring a high cetane number, similar to diesel fuel produced via Fischer-Tropsch (F-T) synthesis.

First-generation biofuels, even though they are still dominant, exhibit a major drawback, which is the fact that the production of their feedstocks competes with food crops for arable land, even though the extent to which they impact food prices is debatable and can be hard to estimate. However, the fact that 46% of the corn produced in the U.S. is intended for ethanol production alone—to supply 3% of the total transport energy used [9]—is a typical example of the issues associated with first-generation biofuels, made even worse in this case, since corn is a staple crop. The main rationale behind second- and third-generation biofuels is to avoid such dilemma.

Lignocellulosic feedstocks can be converted into biofuels through biochemical and thermochemical routes, typical examples of which are:

- Second-generation ethanol, obtained through the fermentation of lignocellulosic biomass. In this approach, the polysaccharides comprising cellulose are broken down and converted into simple sugars through hydrolysis or chemical (or combined) processes. The obtained sugars are subsequently fermented into ethanol using conventional fermentation technology.
- Gasification of lignocellulosic biomass to produce syngas, which can be subsequently synthesized into various fuels via the Fischer-Tropsch process. The pyrolysis of lignicellulosic biomass is another approach, producing bio-oils that can subsequently be refined to be used as fuel components.

The successful development of commercially feasible second-generation biofuels could significantly increase the amount of feedstocks for biofuel production, since

lignocellulosic biomass is, as previously noted, the most abundant biological material on earth [24]. However, even though the cost of lignocellulosic feedstock can be much lower than that of first-generation ones, lignocellulosic material is significantly more difficult to break down into sugars, when compared to starch, and the technology to convert it into liquid fuels is more expensive [31]. Therefore, while first-generation biofuels have already been in commercial production for many years in several countries, the same does not apply to second- and third-generation technologies yet.

Finally, the use of micro-algae for biodiesel production seems very appealing, since 80% or more of their dry weight can be extracted as oil (compared to 5% for some food crops) [32]. Additionally, algae have little impact on arable land because they can be grown in a wide variety of conditions, even in salt water and water from polluted aquifers [31]. However, algal biofuel still faces significant hurdles to become a more economically viable alternative to biofuels obtained from conventional oilseeds, mainly due to feedstock costs, but also due to the labor-intensive process [33].

Electrofuels

Even though they are not technically considered biofuels, electrofuels, or *e-fuels*, are advanced carbon-based fuels produced from captured carbon dioxide and electrolysis-derived hydrogen [34]. Such fuels are also called power-to-gas/liquids/fuels [35]. Methanol is the typical example of a fuel that can be produced in such manner, along with dimethyl ether (DME), though other types of fuels and synthetic hydrocarbons can be produced [16]. The main appeal of e-fuels is that, if renewable electricity is used in the water electrolysis process, they offer a possibility to decrease carbon emissions by chemically recycling captured CO_2. Additionally, they exhibit a relatively high energy density, can use the existing energy infrastructure and are mostly compatible with existing internal combustion engines. Indeed, in a recent article, Ramirez *et al.* [36] argue that, because it is expected that much of road transport is going to rely on liquid hydrocarbon fuels for the foreseeable future, the ideal drop-in fuels are non-oxygenated hydrocarbons with molecular structures resembling those found in fossil fuels, in order to be as physically and chemically similar to gasoline and diesel as possible. However, in spite of their potential, the large-scale deployment of e-fuels in the short to medium term is unrealistic, since

they are still very expensive to produce [9]. (As mentioned previously, the production of electrolysis-derived hydrogen is very energy-intensive and, according to a recent study [37], a price of around US$ 2.50 per kg of green H_2 is predicted for the next decade.)

1.4.4 Impact of Biofuels on Climate Change Mitigation

Biofuels are a potential low-carbon energy source and, as such, are intended to replace fossil fuels, supposedly avoiding associated GHG emissions. In reality, whether they are able to offer carbon savings depends on how they are produced. In fact, their large-scale adoption could increase the release of GHG emissions to the atmosphere through land-use change (LUC) as landowners might clear existing forests to meet the increased crop demand to supply feedstock for biofuels [38]. Moreover, the climate change mitigation potential due to fossil fuel replacement varies depending on feedstock type and production process/technology and on the amount of fossil fuel consumed, both in the production of feedstocks and in the subsequent conversion to biofuels. Even in the case of a particular feedstock, the life-cycle analyses (LCAs) of biofuels found in the literature may exhibit wide variations regarding the overall reduction in GHG emissions because of different underlying assumptions regarding system boundaries, co-product allocation, and energy amounts used in the production of agricultural inputs and feedstock conversion to biofuels.

Nevertheless, many studies show that biofuels can indeed result in emission reductions, compared to their fossil fuel counterparts, *when the emissions from land-use changes caused by biofuel feedstock production are excluded* [31].

Indeed, the often-advertised overly optimistic outlook on the GHG savings potential of biofuels may disappear in practice, once the release of carbon stored in forests or grasslands during land conversion to crop production is taken into account. According to Fargione *et al.* [38], converting rainforests, peatlands, savannas, or grasslands to produce first-generation biofuels creates what they called a "biofuel carbon debt", which can release 17 to 420 times more carbon dioxide than the annual GHG reductions that these could provide by displacing fossil fuels. Several other studies have found that, if the GHG emissions related to LUC caused by biofuel cultivation are included, it would take tens to hundreds of years to offset those

land-conversion emissions with the emission reduction resulting from the replacement of fossil fuels with biofuels. This is known as the "carbon payback period" [38, 39, 40]. To make things worse, even second-generation biofuels may not be attractive from this perspective. For example, according to the study by Searchinger *et al.* [39], if switchgrass were grown for biofuels on U.S. corn lands, the indirect LUC would have a carbon payback period of 52 years and would increase emissions over 30 years by 50%. Additionally, biodiversity can be significantly reduced in fields dedicated to the cultivation of biofuel crops, compared to the unconverted habitat [41]. In view of all those issues, Danielsen *et al.* [40] maintain that, instead of converting forest for biofuel production, reducing deforestation may be a more effective climate-change mitigation approach. The advantages of reforestation over growing dedicated biofuel crops were also mentioned by Michel [25], based on the intrinsic low efficiency of the photosynthesis process itself in converting sunlight energy into biomass (4.5% theoretical best, around 1% in practice), meaning that the amount of solar irradiation energy that is ultimately stored in biofuels is less than 0.1% for rapeseed biodiesel and less than 0.2% in the case of ethanol[2].

As a result, all those authors stress the importance of, instead of growing dedicated crops, producing biofuels from waste biomass or from biomass grown on degraded or abandoned agricultural lands planted with perennials, since this strategy incurs little or no carbon debt and can offer immediate and sustained GHG benefits [38, 39, 40].

1.4.5 The Prospect of Global Biofuel Production and Use

This section is based on the *OECD-FAO Agricultural Outlook 2024-2033* [28] report, previously mentioned.

Biofuels, overall, are projected to remain important renewable alternatives to fossil fuels within the transportation sector, with demand expected to increase by 1.2% annually over the coming decade. This growth rate, however, is less than half the growth rate over the last ten years. This slowdown is attributed to slower economic growth and diminished demand for transport fuel in developed countries, as a result

[2]Those figures, however, do not even take into account the energy inputs necessary to prepare and fertilize the fields, sow and harvest the crops, transport the feedstock, produce the biofuels, etc.—much of which comes from fossil sources

of the improvements in vehicle efficiency and the increasing popularity of electric vehicles.

On the other hand, the demand for biofuels in emerging economies—notably Brazil, Indonesia, and India—is anticipated to increase (see Figure 1.6), primarily due to the greater demand for transport fuels, energy security concerns, and initiatives to decrease GHG emissions in those countries. In the U.S., however, the focus is expected to shift towards biodiesel (including renewable diesel—HVO), a result of higher targets for renewable fuel programs and the extension of biomass-based diesel tax credits.

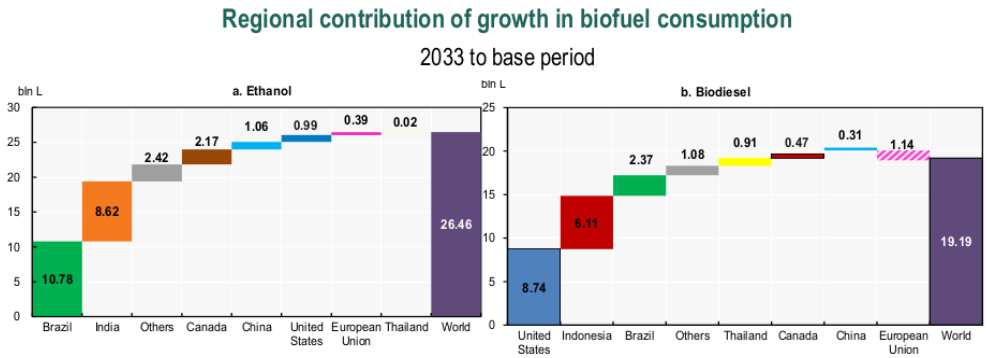

Figure 1.6: Regional contribution of growth in biofuel consumption (Adapted from [28]).

As Figure 1.7 shows, biofuel use is projected to expand faster than the total demand for transport fuel, indicating an increase in the biofuel share within total transport fuels. By 2033, the global production of ethanol and biodiesel is expected to increase to 155 billion liters and 79 billion liters, respectively.

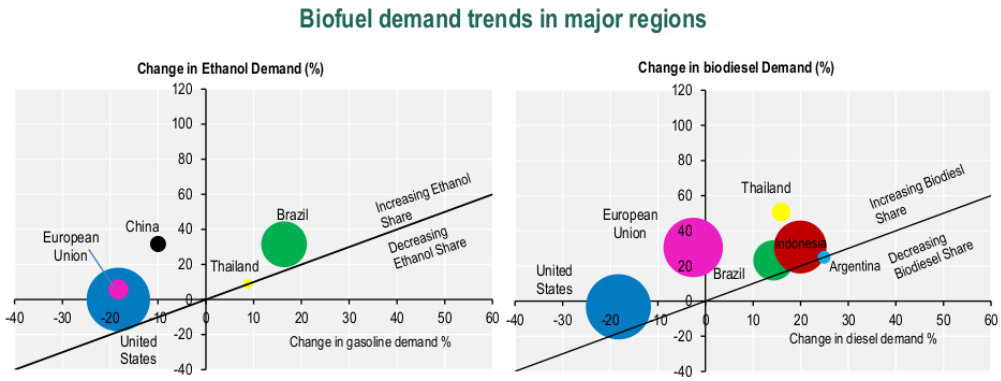

Figure 1.7: Biofuel demand trends in major regions (Adapted from [28]).

Overall, first-generation biofuels are expected to remain the dominant biofuel type, with most of the ethanol being produced from corn and sugar products, whereas vegetable oils (soybean, rapeseed, and palm oil) making up most of the feedstock for biodiesel production:

- In 2023, the total feedstock for ethanol production was comprised of 59% corn, 24% sugarcane, 6% molasses and 2% wheat, with the other 9% being a mix of assorted grains, cassava, and sugar beets.
- Biodiesel's total feedstock was made up of 65% vegetable oils (30% palm oil, 20% soybean oil, 11% rapeseed oil) and 27% used cooking oils, with the remaining 8% consisting of non-edible oils and animal fats.

The table depicted in Figure 1.8 shows the typical feedstocks—*all of them food-related*—used in different regions, as well as the ranking of global biofuel production.

Biofuel production ranking and major feedstocks

	Production #ranking in 2021-2023 (market shares)		Major feedstock used in base period 2021-2023	
	Ethanol	Biodiesel	Ethanol	Biodiesel
United States	#1 (46.9%)	#2 (19.2%)	Maize	Soybean oil, used cooking oils
European Union	#4 (4.9%)	#1 (31.3%)	Maize / wheat / sugar beet	Rapeseed oil /Palm oil/ used cooking oils
Brazil	#2 (24.9%)	#4 (11.7%)	Sugarcane / maize / molasses	Soybean oil / used cooking oils
China	#3 (8%)	#5 (4.2%)	Maize / cassava	Used cooking oils
India	#5 (4.8%)	#15 (0.3%)	Sugarcanes / molasses / maize / wheat / rice	Used cooking oils
Canada	#6 (1.5%)	#12 (0.7%)	Maize / wheat	Used cooking oils / Canola oil/ soybean oil
Indonesia	#18 (0.1%)	#3 (18.9%)	Molasses	Palm oil
Argentina	#8 (1%)	#6 (3.1%)	Maize / sugarcane/ molasses	Soybean oil
Thailand	#7 (1.2%)	#7 (2.6%)	Molasses / cassava/ sugarcane	Palm oil
Colombia	#15 (0.3%)	#9 (1.3%)	Sugarcane	Palm oil

Figure 1.8: Biodiesel production ranking and major feedstocks (Adapted from [28]).

Despite the increasing scrutiny of the sustainability of biofuel production seen in many countries, and despite the fact that cellulosic feedstocks—such as agricultural waste, dedicated energy crops, or woody biomass—are promising alternatives that avoid competition with food sources, biofuels from such advanced feedstocks are not expected to experience a substantial increase in their share of total biofuel production, as Figure 1.9 shows.

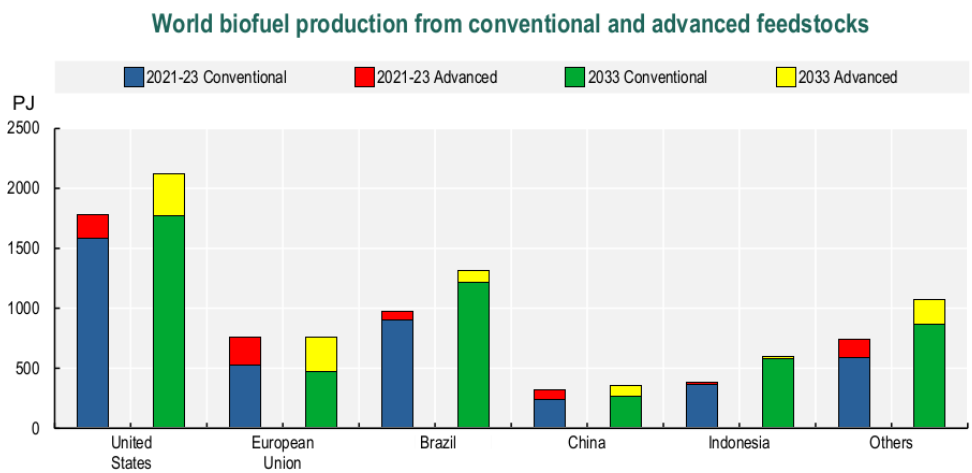

Figure 1.9: World biofuel production from conventional and advanced feedstocks (Adapted from [28]).

Biofuels in the European Union

The so-called Renewable Energy Directive (RED) serves as the legal framework governing the advancement of clean energy across multiple sectors, including transportation, within the European Union. Under the RED, specific targets are set for the share of renewable energy within total energy consumption of each E.U. member state, currently aiming for 29% by 2030.

The RED, which originally included mandates for the blending of biofuels with conventional fuels, aiming to reduce GHG emissions and dependency on fossil energy, has undergone two significant revisions: initially amended under Directive (EU) 2018/2001 (RED II), and subsequently under Directive (EU) 2023/2413 (RED III). Since RED II, there are limits for using feedstocks from food and feed crops, which restricts the expansion of agricultural feedstocks to be used in biofuel production. In addition, the Directive's latest revision, RED III, includes sustainability criteria setting a maximum limit for the production of first-generation biofuels, which is part of the reason why the E.U.'s contribution to global biofuel use is expected to decrease. At the same time, RED III has increased the target for advanced biofuels, derived from waste or residues, from 3.5% to 5.5% by 2030.

Future Trends for Biofuels

There are uncertainties regarding biofuel market predictions, and those are mainly due to the policy landscape (blending mandates), feedstock availability, and oil prices. Exploring advanced biofuels can open opportunities beyond conventional crops, with cellulosic feedstocks like agricultural waste and energy crops offering potential for expanded production without affecting food supplies. In addition, waste-based feedstocks such as MSW and used cooking oil are promising alternatives, while providing additional benefits for waste management.

Consequently, technological advances, along with regulatory changes in the transportation sector have the potential to significantly affect biofuel market predictions. Countries are expected to implement policies promoting new biofuel technologies to reduce GHG emissions, which may not only influence future biofuel demand, but may also introduce uncertainty into agricultural markets. Trends of biofuel usage over the coming decade and beyond may also be largely determined by how the

private sector will response to these measures, particularly by industries investing in EVs and SAFs (sustainable aviation fuels).

1.5 The *BioRen* Project

BioRen was a *Horizon 2020* E.U.-funded project[3] running from November 1st, 2018 through January 31st, 2023. As stated by its slogan ("Development of competitive, next generation biofuels from municipal solid waste"), *BioRen*'s objective was to produce biofuels from municipal solid waste, which is essentially a cellulosic material, through fermentation routes. Two alcohols were targeted: ethanol and isobutanol, though the latter had a stronger focus, since it is an intermediate compound for the production of another *BioRen* focus product: glycerol tertiary ether (GTBE), a chemical compound with potential to be used as a fuel component in both gasoline and diesel fuels. The project's required engine testing of the different additives was the task assigned to Lund University (those engine tests are described in Chapters 3–5). Especially modified microorganisms were developed for the pretreatment of the MSW and subsequent fermentation. The fermentation residues were then treated by hydrothermal carbonization (HTC) to convert them into biocoal pellets [42].

The information below is based on the European Union's Community Research and Development Information Service (CORDIS) website [43].

Worldwide, the majority of municipal solid waste is either landfilled or incinerated. The E.U. has a policy to reduce the amount of MSW that is incinerated, while realizing that it contains valuable components with the potential to be either recycled or transformed into energy resources (e.g. electricity, biofuels, syngas, methane, etc.). This is very important for the environment, since it can lead to decreased net CO_2 emissions while at the same time producing sustainable energy, products and materials.

The objective of the *BioRen* project was the development of a sustainable and technically and economically viable production of transport biofuels obtained from the organic fraction of MSW (consisting mostly of paper and cardboard). The project focused on the conversion of that cellulosic waste material into ethanol and isobu-

[3]Grant Agreement no. 818310.

tanol via enzymatic hydrolysis followed by fermentation.

Besides ethanol and isobutanol, another target chemical of the project was the so-called glycerol *tert*-butyl ether (GTBE) (which will be described at length in Chapter 2). This glycerol derivative is a promising compound that can be used as a fuel additive for both gasoline and diesel, having the potential to further displace fossil fuels and decrease exhaust emissions, without compromising engine performance.

GTBE can be produced through the catalytic dehydration of isobutanol into isobutylene, which is in turn converted into GTBE via the acid-catalyzed reaction with glycerol—preferably the waste glycerol that is the by-product of the transesterification process that produces biodiesel (FAME).

The fermentation residues, together with any leftover MSW can be further processed into biocoal via hydrothermal carbonization (HTC). Therefore, by producing fuels, fuel additives, and biocoal from waste streams (MSW and by-product glycerol), *BioRen* demonstrated a way to valorize those low-value materials into useful products, potentially benefiting both the transportation and the waste-management sectors, in the framework of the circular economy.

Additional publications related to the *BioRen* project are the works by Kowalski *et al.* [44] and Verhé *et al.* [45].

The overall processes of the *BioRen* project are illustrated in Figure 1.10.

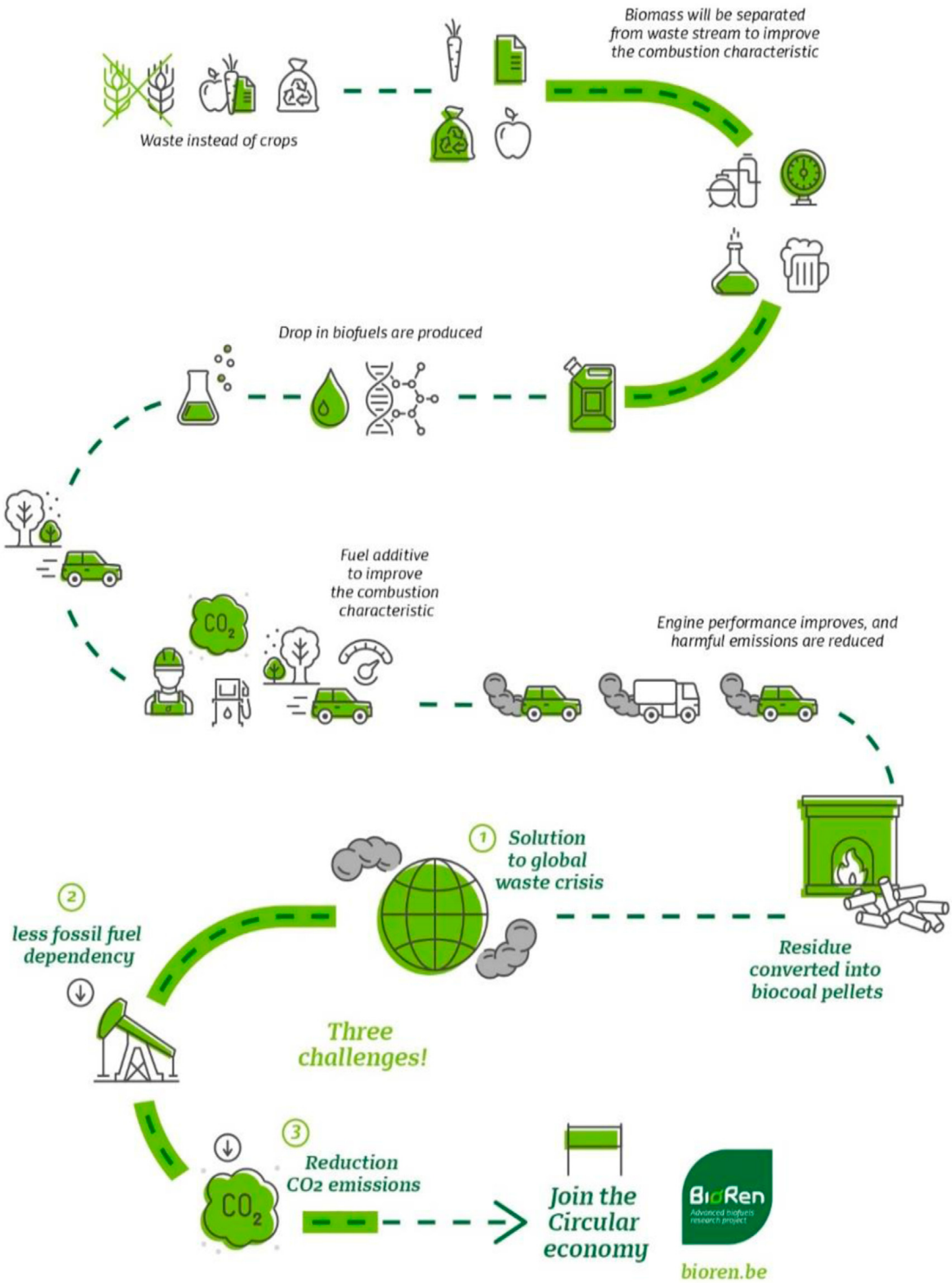

Figure 1.10: The *BioRen* processes [44, 42].

The *BioRen* Tasks

The first step in the *BioRen* process was the design of an MSW separation line using a combination of techniques to isolate its organic fraction[4], separating it from the other components based on its different physical and chemical properties, whereas the remaining material present in the waste stream was eventually sorted and transformed into biofuels via pyrolysis and used as energy sources.

Subsequently, a rapid acid-based pre-treatment of the waste that had been sorted was developed, leading to an improved enzymatic hydrolysis of the cellulose and hemicellulose, producing a solution consisting of C5 (pentose) and C6 (hexose) sugars.

Improved second-generation yeast strains were developed, capable of efficiently fermenting both C5 and C6 sugars. Moreover, the xylose fermentation performance of the engineered strains was enhanced. Laboratory experiments were carried out under various conditions in order to evaluate the efficiency of both the enzymatic hydrolysis and the subsequent fermentation. This was done with the goal of achieving a high hydrolysis yield (above 90% of total sugars), together with a productivity of at least 11.5 g/l/h ethanol and a final ethanol titer of over 6% v/v.

Using specially-developed enzymes, a saccharification (i.e. the breakdown of cellulose into sugars) efficiency of 75-90% was achieved, depending on the nature of the samples and the pre-treatment conditions.

Several saccharification and fermentation experiments using a clean mixture of paper and cardboard were performed both at lab-scale and at pilot-plant scale. The saccharification was executed according to a fed-batch strategy. The paper/cardboard was pulped (15%) and subsequently treated with 5% of the specially-developed enzymes. After 60 hours, an ethanol concentration of 8.5% v/v was obtained.

After the fermentation was complete, the solid residues in the fermentation broth were separated and were sent to the HTC facility in order to be transformed into biocoal. The carbonization itself was performed in a reactor at 200–225°C and 18 bar. The experiments showed that the process was able to increase the fixed carbon amount in the biocoal by at least 50%, when compared to the its original amount in the fermentation residues, giving a yield of 65-70%.

[4]On average, MSW consists of 30–40% biomass.

Meanwhile, the GTBE samples needed for the engine tests were produced. The first step in their production being carrying out the dehydration of isobutanol to produce isobutylene, to be subsequently reacted with glycerol, using sulfuric acid as a catalyst, forming GTBE. Initially, commercial isobutylene was used as feedstock, instead of the isobutylene originating from the dehydration of the isobutanol produced from MSW fermentation. Likewise, commercial glycerol was used for the production of GTBE, instead of the crude glycerol residue from biodiesel production. The obtained samples, comprising the different GTBE components, were sent to Lund University to be used in the engine tests.

Work Package 5 ("biofuel testing") was assigned to Lund University and became the doctoral project of the present author. The package's overall task was to evaluate the target chemical compounds (initially, isobutanol plus the different GTBE types) as fuel additives, through engine experiments carried out in the test cells of the Division of Combustion Engines, at the Department of Energy Sciences of Lund University. The main goal was to investigate the effect of the different additives on engine performance and emissions. Both diesel (light-duty and heavy-duty) and spark-ignition engines were used. The engine tests were divided into different parts, starting with initial screening experiments (which are treated in Chapter 3), followed by more extensive tests, which also investigated glycerol-derived compounds other than GTBE. Such tests form the basis of Chapters 4 and 5.

In addition to the engine experiments, described in Chapters 3 through 6, a literature study dealing with life-cycle analyses related to the environmental impact of biofuels production, distribution and combustion was performed, involving both first- and second-generation biofuels, together with data and information obtained from the *BioRen* project's partners.

1.6 Goal and Motivation

As discussed in this introductory chapter, climate change and the negative effects associated with it are real and the last years have seen an increased awareness and a deepened concern regarding the impact of a rapidly changing climate on the environment and on human life in general. More than ever, governments around the world and society at large have acknowledged the need to mitigate those effects by limiting, as much as possible, the emissions of greenhouse gases, especially carbon

dioxide. In particular, the transport sector, being responsible for a significant share of total CO_2 emissions (and playing an essential role in people's everyday lives), has been the focus of intense scrutiny regarding its carbon footprint. Therefore, it is not surprising that several measures have been put forth, with the ultimate goal of curtailing the overall CO_2 emissions from the transport sector.

Among such measures, two of them have been discussed in this chapter and are particularly noteworthy: the electrification of transport and the use of hydrogen as a fuel. While both measures can be effective to a certain extent, they are not without their flaws.

As previously discussed, while electric vehicles (EVs)—especially the purely electric battery-electric vehicles (BEVs)—represent a promising alternative for the decarbonization of transport, their beneficial environmental effects are invariably linked to how the electricity to charge their batteries was generated. In the case of carbon-free electricity (such as wind, solar, hydro, and nuclear), BEVs do have the potential to decrease net-CO_2 emissions and thus mitigate the negative effects of global warming. On the other hand, if their batteries were charged with electricity from coal-fired plants, their environmental benefits are questionable. Moreover, the issues associated with the production of their lithium-ion batteries should also be considered.

Hydrogen seems like an outstanding fuel at first, since its combustion should produce only water vapor as a product, and its mass-based lower heating value of 120 MJ/kg is indeed impressive. Unfortunately, hydrogen's density is extremely low, making its heating value on a volume base much lower. Besides, its low density also makes hydrogen's storage challenging, especially on a vehicle. Plus, the production of hydrogen from water electrolysis is known to be very energy intensive and might not be economically feasible in areas where electricity is not particularly cheap.

Having discussed the clear limitations of the two major options that have been recently proposed to decarbonize the transport sector, it becomes more or less evident that no single solution is—contrary to what their advocates may say—effective enough to accomplish that mission. Instead, it is *a combination of different approaches* that is necessary to deal with the GHG issues more effectively. In addition, which strategies make more sense will also depend on the local conditions of a particular region [46]. For instance, in a country that relies heavily on coal to pro-

duce its electricity (such as Poland), BEVs do not make much sense. Instead, they fit much better in countries with abundant carbon-free electricity (like Norway or Iceland).

Such a combination of different decarbonization strategies should invariably include biofuels, since their use is fairly widespread around the world. As mentioned above, first-generation biofuels may make more sense in some regions, while making less sense in others—or not making any sense at all in yet another place. The feedstock used for their production can make a significant difference, a typical example of which being the differences in productivity exhibited by corn ethanol in the U.S. and ethanol made from sugarcane in Brazil [47]. This is another example of how different approaches may be either more effective or less effective, depending of the region in which they are implemented. Although biofuels produced from food crops—such as ethanol and biodiesel—may not be ideal, they can represent a transition towards a more diverse range of biofuels, and hopefully this is where this work fits.

Ethanol and biodiesel have, for quite some time, been the foremost examples of biofuels for spark-ignition and compression-ignition engines, respectively. Even though both fuels are typically used in their respective blends with gasoline and diesel fuel, their use in neat form is also possible, though some engine modifications might be required for that purpose.

However dominant their status as biofuels may be, ethanol and biodiesel are hardly the sole examples of biomass-derived fuels with the potential to displace fossil fuels and reduce net carbon emissions. Even though the current energy transition requires the diversification of energy carriers, when it comes to alternative biofuels, missed opportunities seem to exist. There are a number of other promising alternative biofuels that have not been properly explored. There are several chemical compounds, related to biodiesel and alcohols, whose untapped potential has not been duly investigated yet. Consequently, there are knowledge gaps that need to be addressed and their existence, together with the current climate-related concerns, are enough reasons to warrant further investigation of such lesser-studied compounds.

Therefore, the overall purpose of this monograph is to, starting from the original *BioRen*-related activities, investigate and propose alternatives to ethanol and biodiesel in order to fill those gaps to help further displace fossil usage in transport.

Such fuel alternatives should preferably also have the possibility to be produced from renewable feedstocks and to decrease exhaust emissions without compromising engine performance, while being able to use the existing fuel storage and distribution infrastructure as drop-in fuels.

The chemical compounds described and investigated in this work fall into two categories. First, compounds derived from glycerol—ideally, the by-product from the biodiesel industry—such as the glycerol *tert*-butyl ethers (GTBE), solketal, and triacetin (glycerol triacetate). Such compounds have the potential to be used as fuel additives, improving the cold-flow properties of biodiesel, decreasing the PM formation tendency of diesel fuels, and boosting the octane rating of gasoline. Moreover, the fact that it is possible to use waste glycerol means that waste-management issues can be tackled at the same time.

The second category is represented by the C_1–C_4 alcohols (other than ethanol, obviously). That includes methanol and the most common propanol and butanol isomers, namely isopropanol, *n*-butanol, and isobutanol, for a total of four additional alcohols.

The use of methanol as a fuel for spark-ignition engines has long been documented, but by far most of that fuel has been produced from fossil sources, namely coal and natural gas. The possibility of obtaining methanol from biomass gasification and even from hydrogen and carbon dioxide, as an e-fuel, greatly increases its environmental potential, making it a very promising alternative to ethanol.

In spite of being widely used in industry as solvents and in household products as a disinfectant, isopropanol (2-propanol) has been virtually unexplored as a fuel for internal combustion engines. The limited available data on its fuel properties, such as octane numbers, indicate good potential to be used as an SI fuel. It is typically produced from fossil sources, but recent advances in biotechnology have made it possible to synthesize isopropanol from renewable feedstocks via biochemical routes.

Compared to isopropanol, *n*-butanol and isobutanol (2-methylpropan-1-ol) have attracted significantly more attention as potential IC engine fuels, due to their favorable properties and the fact that significant advances have been made regarding their biosynthesis via fermentation, using genetically modified yeasts and bacteria. As a matter of fact, substantial efforts have been made by companies like Butamax

Advanced Biofuels and Gevo (see Section 2.5.4) to commercialize their biomass-derived butanol. Besides, when compared to ethanol, both isomers exhibit attractive properties such as higher energy density, lower water affinity, lower corrosiveness, and a smaller impact on the vapor pressure of their blends with gasoline. In other words, they are more compatible with existing engines and infrastructure. Finally, because butanol has a lower oxygen content than ethanol (21.6% vs. 34.8%, respectively), a larger amount of it can be blended with gasoline to achieve a fixed fuel oxygen content (overcoming the so-called ethanol "blend wall"). In turn, this means that larger amounts of fossil fuel—gasoline—can be displaced by using butanol as oxygenate.

This study therefore attempts to make a small contribution towards the diversification of the energy mix in the transport sector by investigating and proposing feasible and sustainable alternatives beyond the currently dominant biofuels ethanol and biodiesel, thus contributing to a decreased carbon footprint. Even though the production of alternative biofuels often requires large investments (as well as government subsidies), most of the necessary infrastructure already exists (in the form of ethanol or biodiesel plants, for instance) and could be retrofitted for that purpose, which has already happened [48].

The engine tests discussed in this work, along with the analysis of their results can provide valuable insights into the viability of each of the different compounds, from an engine perspective. In addition to engine experiments, this work provides a review and an assessment of the state-of-the-art in the production and utilization of current biofuels, highlighting not only their potential, but also their shortcomings.

In summary, what needs to be acknowledged is the fact that the world is diverse, and so should be the range of the fuel options that are going to power the existing legacy fleet and also new vehicles in the future. When it comes to fuel technology, there are several available alternatives, more than many people seem to realize. There exist potentially promising, largely untapped, fuel alternatives to be investigated, beyond gasoline, beyond diesel fuel—even beyond ethanol and biodiesel—and hopefully the information provided by this work could be of interest not only to the engine and fuel communities, but also to policymakers and to the general public.

1.7 Dissertation Outline

This introductory chapter "sets the stage" for the subsequent material. setting the main subject of this work—alternative fuels for transportation—in the context of the current environmental and energy-related issues, while discussing the merits and the shortcomings of the solutions that have generally been proposed. Additionally, it introduces the chemical compounds (the glycerol derivatives and the C_1–C_4 alcohols), suggesting their potential for fuel applications. Finally, a description of the *BioRen* project is presented, followed by the author's outlook on the main topics discussed in this dissertation, concluding with an explanation of the motivation behind this work. Then, the subsequent chapters are as follows:

- **Chapter 2** introduces and discusses the theoretical concepts that are relevant for the analysis of the experimental results presented in the following chapters. More specifically, Chapter 2 introduces and discusses the basics on the topics of soot formation in diesel engines and knock in spark-ignition engines, since they are of fundamental importance for the next chapters. Then, the properties and characteristics of the glycerol derivatives and the C_1–C_4 alcohols are described in more detail, followed by a brief explanation of their production methods, from both fossil and renewable routes.
- **Chapter 3** describes the light-duty (LD) diesel engine testing and evaluation of the glycerol derivatives and the alcohols as diesel fuel components.
- **Chapter 4** describes the heavy-duty (HD) diesel engine testing and evaluation of the glycerol derivatives and the alcohols as diesel fuel components.
- **Chapter 5** then introduces the spark-ignition (SI) engine tests, performed on a Waukesha CFR engine, where the glycerol derivatives and the alcohols are evaluated as gasoline oxygenates, that is, as blend components.
- **Chapter 6** evaluates the performance of the C_1–C_4 alcohols as neat fuels, through tests also carried out using the CFR engine.
- **Chapter 7** finally discusses the overall results, from a broad perspective, after which the limitations of the study are presented, along with suggestions for future work.

Chapter 2

Background

2.1 Introduction

The previous chapter set the "boundary conditions" to which the remainder of this work is related. It addressed the current climate-related challenges, that is, reducing the emissions of greenhouse gases—mainly CO_2—and discussed the role the internal combustion engine should play in the transition to a decarbonized transport sector. Chapter 1 also assessed the potential of alternative transportation technologies, such as transport electrification and the use of hydrogen as a fuel, along with a discussion of the role biofuels can play. It was concluded that a *combination* of different strategies—including ICEs—will be necessary. Finally, Chapter 1 introduced the E.U. project *BioRen*, upon which the work contained in this dissertation was based. Having laid that preliminary foundation, it is now time to proceed further into this investigation of alternative fuels that could play an important role in that energy transition.

Because this work is essentially about alternative fuels and fuel additives, the present chapter discusses some practical aspects of engine performance that can be significantly affected by different fuel properties, such as soot emissions from diesel engines and knock resistance in spark-ignition engines. Both soot formation and the occurrence of knock can pose a significant constraint on overall engine behavior and, as such, their characterization and control is of fundamental importance whenever new fuel types are proposed. Regarding knock measurement and char-

acterization, the CFR engine—the engine used for the SI tests in this work—and which has long been considered the *de facto* standard device for evaluating the knock resistance of fuels, is introduced. Some of its history and design characteristics are presented, together with a description of the ASTM methods used for assessing the octane rating of practical fuels using it.

Afterwards, the fuels and the fuel additives that are at the core of this work are presented. Glycerol, being the main by-product of biodiesel production and the raw material for several additives, is introduced and the important topic of "glycerol valorization" is discussed. Because that glycerol is usually treated as a waste product, its conversion into high-value and useful chemicals—such as fuel additives—represents an extra environmental benefit, since it also addresses waste-management issues. The main types of glycerol derivatives with the potential to be used as fuel components are introduced, most notably glycerol *tert*-butyl ether (GTBE), one target chemical of the *BioRen* project. GTBE is discussed, along with a description of its potential to be used as a fuel component for gasoline, biodiesel, and diesel fuel. Besides GTBE, other potentially useful glycerol derivatives are introduced and discussed. Alcohols are the other category of fuels included in this work, more specifically, the C_1–C_4 alcohols. Isobutanol, in particular, has a special place since it was also a target fuel in the *BioRen* project. The fact that there have been advances in its production via fermentation routes makes it especially attractive. Besides isobutanol, *n*-butanol is also discussed, since it has for long been considered an alternative fuel. The inclusion of a less-studied compound having fuel potential—isopropanol—represents an attempt to widen the range of the available fuel options that could become more important in the future. Methanol, being the cheapest alcohol, is always a good choice, especially with the growing possibility of synthesizing it from hydrogen and carbon dioxide. Finally, the foremost biofuel—ethanol—is included due to its ubiquity and attractive characteristics, though one focus of the present work is to present alternatives to it.

2.2 Rudiments of Soot Formation in Diesel Engines

Soot, in the form of smoke, is the hallmark of diesel exhaust pollution. It is the main component of diesel particulate matter (PM), however, it is not, as pointed out by Smith and Tree and Svensson [49, 50], a uniquely defined substance. It

consists mainly of carbon but it also contains hydrogen, roughly at the ratio of 8:1, respectively. Its density was reported to be 1.84 $\mathrm{g/cm^3}$, by Choi *et al.* [51]. In general terms, soot is formed from unburned diesel fuel, nucleating in fuel-rich regions of the diesel spray at high temperatures [50]. The time available for its formation is of the order of a few milliseconds [52]. At the same time it is formed, soot is also being oxidized in regions of the flame where oxidizing species are present [49]. Such species include $\mathrm{O_2}$, O, OH, $\mathrm{CO_2}$, and $\mathrm{H_2O}$. The eventual emission of soot from the engine depends on the balance between the processes of formation and burnout. In reality, almost all the soot formed within the fuel spray is oxidized before the exhaust process starts. As discussed below, soot is one component of diesel PM, a complex combination of organic and inorganic species, solid and volatile, that is produced not only during combustion but also during the diluting and cooling of the exhaust gases after they leave the engine.

From a thermodynamic point of view, according to Haynes and Wagner [52], in premixed flames, soot should form only when, in the following reaction

$$\mathrm{C_mH_n + yO_2 \rightarrow 2yCO + \frac{n}{2}H_2 + (m - 2y)C_s}$$

m becomes larger than 2*y*, that is, when the C/O ratio exceeds unity. However, in reality, the authors pointed out that the limits of soot formation are tied to the onset of luminosity, and this usually occurs at roughly C/O = 0.5. As noted by Smith [49], the fact that soot may form even in well-mixed systems starting at a C/O ratio as low as 0.5 suggests that some of the oxygen is unavailable to react with carbon, a finding that can have implications for the efficacy of fuel oxygenates, a topic discussed in the section further below.

In diffusion flames, the C/O ratio will always exceeds 0.5 in some regions, so it becomes clear that soot will always be formed in such areas. Conversely, soot may be oxidized in regions of the flame where C/O < 0.5.

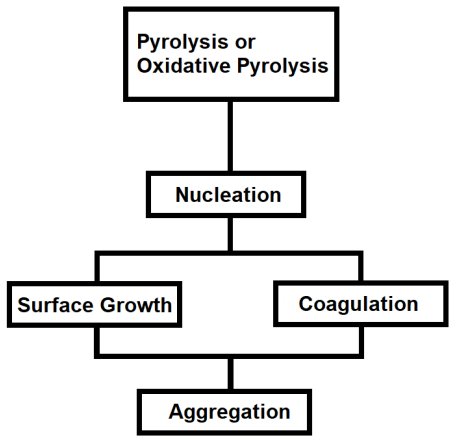

Figure 2.1: The steps in the soot formation process. Adapted from [49].

The fundamental processes of soot formation, in the context of diesel engines, are extremely complicated, due to the inherently high temperatures and pressures, complex fuel composition, turbulent mixing, the unsteady nature of diesel combustion, and the extremely reactive intermediate species formed. However, a simplified idea of such processes can be developed, and the mechanism by which soot is believed to be formed can be divided into the following steps: pyrolysis, nucleation (or inception), surface growth, coagulation (or coalescence), and agglomeration [52, 49, 50]. See Figure 2.1. These processes are discussed as follows:

- **Pyrolysis** is the process through which the molecules of organic compounds break down in the presence of high temperatures and in the relative absence of oxygen. This leads to the formation of products such as unsaturated hydrocarbons, especially acetylene (C_2H_2) and its higher analogues ($C_{2n}H_2$), and the so-called polycyclic aromatic hydrocarbons (PAHs). These molecules are considered the main soot precursors in flames.

- **Nucleation** is the formation of "embryonic" particles (as Glassman [53] described them) originating from gas-phase reactants (i.e., the soot precursors described above). Such particles, commonly referred to as *nuclei*, are very small (diameters in the range 1.5–2 nm) and grow faster than they decompose or otherwise react [49].

- **Surface growth**, where the bulk of the solid-phase material is generated, is the process of adding mass to the surface of the soot nuclei. During this phase, gas-phase hydrocarbons (mainly acetylenes, according to Smith [49] and Tree and Svensson [50]) attach to the hot and reactive surface of the nuclei, becoming incorporated into the particulate phase. Surface growth leads to an increase in soot mass, while keeping the number of soot particles constant.

- **Coagulation** is the process by which small spherical soot particles collide and coalesce to form a larger spherical particle [50]. Coagulation, as opposed to surface growth, leads to a decrease in the number of soot particles, while the total particle mass remains essentially constant. These primary soot particles, that have nucleated, grown, and coagulated, are sometimes referred to as "elementary soot particles" [52] or "spherules" [54], and their diameters are typically in the range of 15–30 nm. These are the particles that undergo agglomeration, as mentioned below.

- **Agglomeration** takes place after particle nucleation and growth have ceased and it causes the primary soot particles (the spherules) to stick together, forming larger groups of particles. These aggregates may range in appearance from resembling a cluster of grapes to resembling a chain of beads [54].

Subsequently, soot **oxidation** takes place in regions of the flame where oxidizing species are present. As mentioned above, usually most of the soot is oxidized and the amount of it that is emitted is typically just a very small fraction of the amount actually generated within the engine [52].

Ultimately, the total mass of the emitted soot particles usually becomes larger as the exhaust gases dilute and cool with air, therefore turning the "raw" soot particles into components of diesel particulate matter. This occurs because, as the temperature drops, heavy organic compounds including unburned hydrocarbons, oxygenated hydrocarbons, and polycyclic aromatic hydrocarbons (PAHs) adsorb and condense onto the surfaces of the soot agglomerates, increasing their masses. Similarly, inorganic materials such as sulfur dioxide (SO_2), sulfuric acid (H_2SO_4), sulfates, and water, also adsorb and condense onto the soot particles [55]. The amount of condensed sulfur compounds depends on the sulfur content of the diesel fuel [56]. The composition and structure of diesel PM is illustrated in Figure 2.2.

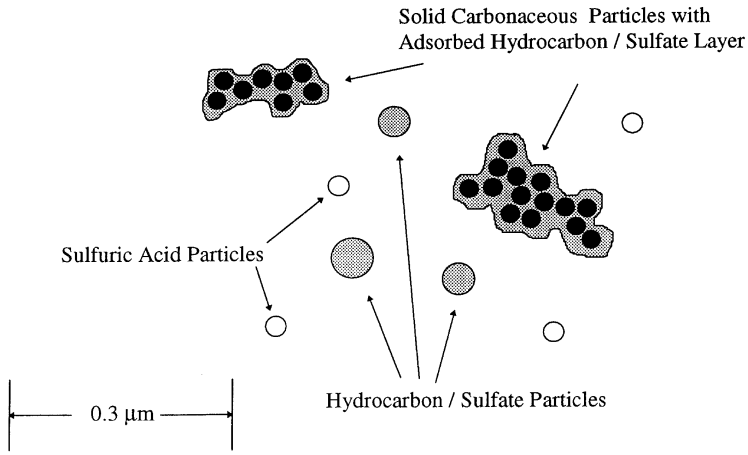

Figure 2.2: Typical composition and structure of diesel engine exhaust particles [55].

The conceptual model of diesel combustion developed by Dec [57] describes the major chemical and physical processes that occur during diesel combustion and lead to the production of soot in direct-injection diesel engines [58]. Figure 2.3 illustrates such processes and steps leading to soot formation, as mentioned above. According to Dec's model, diesel fuel is injected shortly before the compression stroke into hot, highly compressed air and combustion residuals, in the form of liquid fuel sprays. Each spray then quickly vaporizes and entrains and mixes with the hot surrounding air, as shown by the arrows in the figure. This region is characterized by the so-called *lift-off* length. This fuel-air mixture ignites in the gas phase, while its equivalence ratio is locally still very high (around 3). This rich, premixed ignition location is represented in the figure by the dashed curve. The products of this ignition do not oxidize completely, since there is not sufficient oxygen. The fuel then pyrolyzes, giving rise to intermediate species such as acetylene, ethylene, propylene, and others. These products of partial combustion lead to the formation of PAHs, which are considered to be the buiding blocks for soot formation in flames. These precursor species then move downstream into the hot, oxygen-depleted inner regions of the diffusion flame, where they nucleate into tiny soot nuclei. These early particles then increase in size through surface growth and coagulation, arriving at the region of maximum soot concentration in the flame (represented by the dark circular region in Figure 2.3). Finally, these freshly-created soot spherules reach the outer regions of the diffusion flame, in its periphery, where

they are ultimately burned. Naturally, this process is eventually quenched during the expansion stroke, and the soot that escaped oxidation exits the engine.

According to Dec's model, the equivalence ratio of the rich premixed region is determined by how much oxygen has been entrained along the lift-off length. Consequently, the lift-off length determines how rich the premixed region—where the soot precursors are initially formed—will be. Thus, as the lift-off length increases, the spray's propensity for forming soot decreases, since more oxygen has been mixed with the vaporized fuel prior to combustion [50]. Moreover, in their study [59], Siebers and Higgins also observed that soot formation became negligible when enough air was entrained to result in an equivalence ratio of approximately 2 at the time of ignition [58]. In practice, an increase in the lift-off length can be achieved, for instance, by using diesel injectors with very small nozzle diameters, combined with very high fuel injection pressures, which are commonplace features of modern diesel engines.

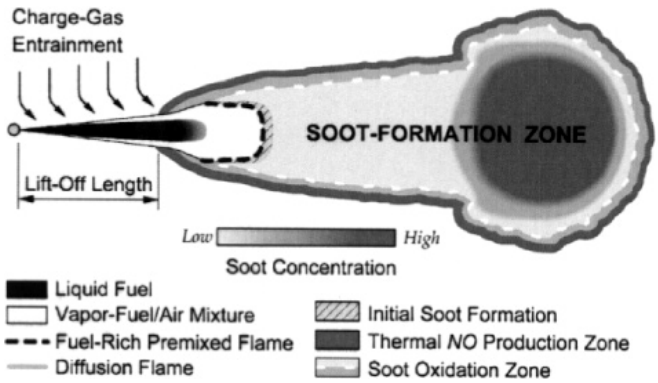

Figure 2.3: Phenomenological description of the main features of diesel combustion based on Dec's experimental work [57], from [58].

The Effect of Diesel Fuel Oxygenates

As discussed above, soot precursors originate in the fuel-rich areas of premixed flames and the nucleation and growth of soot particles themselves occur in the subsequent diffusion flames during the diesel combustion process. Most of the soot that has been formed eventually undergoes oxidation in leaner zones of the diffusion flame and also during the expansion stroke. However, this burnout is not complete, and soot is emitted as black smoke. A method which is commonly

employed to reduce engine-out soot (and consequently, PM) emissions from diesel engines is the addition of oxygen-bearing compounds (referred to as *oxygenates*) to conventional fossil diesel fuel. The use of oxygenates has become more common as a result of both stringent emissions standards and also due to the promotion of the use of naturally oxygenated renewable fuels, such as biodiesel, in diesel engines.

The understanding of the fundamental mechanisms responsible for the soot reduction with oxygenated fuels has been the focus of intense research activity over the years. Basically, nowadays it is widely believed that the introduction of fuel-bound oxygen into the combustion process decreases the formation of *soot precursors* during the thermal cracking (pyrolysis) of the fuel, a phenomenon that has been investigated in numerous studies, a few of which are discussed in the next paragraphs.

A few well-known studies by researchers at Hokkaido University, Japan, in the mid to late 1990s and early aughts investigated the impact of several fuel oxygenates on the emissions from diesel engines [60, 61, 62]. The main takeaway from their studies was that the oxygenates significantly decreased smoke and particulate matter emissions and that the pollutant reduction was a linear function of the oxygen content of the fuel blend, regardless of the type of oxygenate being used. In addition, the authors found that the PM emissions could be essentially eliminated once the concentration of fuel-bound oxygen in the fuel blend reached a certain amount. In one of the articles [61], the authors found that the exhaust's Bosch smoke number decreased from 55% for neat diesel fuel to less than 1% when the mass concentration of oxygen in the fuel blend was above 25–30%. In a subsequent study [62], it was reported that the exhaust smoke decreased linearly with increasing fuel oxygen content until it reached zero when the fuel blend's oxygen content was 38 wt.% and above, even at high EGR levels and stoichiometric operating conditions. The findings of those studies were confirmed by the subsequent works of other researchers, as mentioned below.

However, according to other studies, the structure of the oxygenate did impact PM emissions. For instance, in a study by Hallgren and Heywood [63], in which several oxygenates of different chemical structure were evaluated, the reduction in PM emissions with increasing oxygenate amount appeared to be logarithmic. Furthermore, some oxygenates were observed to be more effective than others in decreasing the PM levels, when the blends were tested at a fixed oxygen content of 8 wt.%. They also reported that the effect of increasing fuel oxygen content was less pro-

nounced at lower engine loads, compared to higher loads. In addition to ultra-low-sulfur diesel, they also used a Fischer-Tropsch synthetic diesel fuel and measured the impact on the exhaust PM emissions when 8 wt.% of an oxygenate (diglyme) was added to it, compared to the emissions obtained with the Fischer-Tropsch fuel in neat form. Interestingly, they found that the particle emissions were unaffected by the addition of oxygen to the F-T fuel.

Several studies sought to explain the mechanism through which an oxygenate can impact the soot levels produced by a given fuel. As previously stated, according to the work by Dec [57], the fuel molecules in the rich premixed reaction zone downstream of the lift-off lenghth undergo pyrolysis and decompose to form species (such as acetylene) which in turn lead to the formation of polycyclic aromatic hydrocarbons, which are considered to be the building blocks of soot formation. According to the chemical kinetic modeling results from the aforementioned work by Flynn *et al.* [64], oxygenates inhibit the formation of soot precursors, thus decreasing the amount of soot that can be formed. More specifically, when oxygenates are mixed with the fuel, the rich premixed reaction becomes leaner and the extra oxygen promotes carbon oxidation to CO, thus decreasing carbon availability for the production of soot precursors, such as acetylene, ethylene, and 1,3 butadiene, as well as propargyl and vinyl radicals. Such compounds are responsible for the production of aromatic species and PAHs, which in turn may lead to soot formation. Besides, their work demonstrated that the tendency to form precursors disappeared once the oxygen-to-fuel mass ratio reached 25%. This elimination of precursor formation agrees with the earlier results by Miyamoto *et al.* [61].

Another chemical kinetic modeling work on diesel oxygenates was carried out by Curran *et al.* [65], in which the authors examined the influence of the addition of five different oxygenated compounds on fuel ignition and soot precursor formation. *n*-Heptane was used as representative diesel fuel, since its cetane number, 56, is representative of common diesel fuels and the products of its rich ignition include many of the species believed to lead to soot formation [58]. Their results also showed that the addition of oxygenated compounds to diesel fuel reduced the production of precursors (e.g. acetylene, ethylene, and propargyl radicals) which may eventually form soot. Moreover, their study showed that when the oxygen content in the fuel blend reached 30–40 wt.%, the production of precursors decreased to zero, in agreement with earlier studies by Miyamoto *et al.* [61] and others.

Besides carrying out engine experiments—in which the authors found that oxygen content was the main parameter controlling PM reduction—the work by Cheng *et al.* [66] also included numerical modeling to investigate the effect of oxygenate addition on soot formation. *n*-Heptane was again used as base fuel. Once more, inhibiting the production of soot precursors in the fuel-rich premixed flame was shown to be the main factor responsible for the ability of an oxygenate to reduce engine-out soot emissions. More specifically, they attributed this ability to these key mechanisms:

- The oxygenate shifts the pyrolysis and decomposition products, displacing the long carbon chains that exist in the conventional diesel fuel. This may lead to the production of different decomposition products, with lower tendencies for soot formation
- During the premixed combustion phase, oxygenates may significantly increase the concentration of free radicals such as O, OH, and HCO. These radicals help oxidize carbon to CO and CO_2. As a result, the availability of carbon to form soot precursors is decreased
- High concentrations of those free radicals (OH in particular) can also oxidize soot precursors in the subsequent diffusion flame, limiting the formation and growth of PAHs and inhibiting the inception of soot particles

The authors also pointed out that the presence of C-C bonds facilitates the eventual formation of aromatics, which may lead to soot. On the other hand, C-O bonds, present in oxygenates, are stronger and in this particular case the production of soot precursors is less straightforward. Finally, the authors also found that oxygenate addition would reduce PM emissions to essentially zero at an oxygen content of 28 wt.%, in accordance with the influential work by Miyamoto *et al.* [61].

A 2006 study by Westbrook *et al.* [58], also used detailed chemical kinetic modeling to investigate sooting reduction in diesel engines through the addition of oxygenates to the base fuel (which was, once again, *n*-heptane). Their key takeaway from their work is that the C-O bonds—which are part of oxygenated molecules—displace carbon in the original diesel fuel. That is, the C-O bond survives the fuel-rich premixed reaction zone intact, thus resulting in less carbon being available for soot formation in the post-ignition environment. The authors also stressed that some

oxygenated species, due to details in their molecular structures, use their oxygen atoms less effectively than others.

The authors also emphasized that their analysis is only valid in the case of *premixed* ignition, in which fuel-bound oxygen inhibits soot production, whereas the presence of oxygenates in *diffusion* flames can have the opposite effect, that is, they may *increase* soot formation, a phenomenon reported in studies by McEnally and Pfefferle [67, 68]. McNesby *et al.* [69] observed that it may happen if the oxygenate is added to the fuel stream, instead of the air stream, causing it to interact primarily with the fuel pyrolysis process. This effect was reported by studies by due to . The authors therefore conclude that the ignition in diesel engines, where soot production may (or may not) happen, is best characterized as a rich *premixed* process. Interestingly, this goes against the common perception of diesel combustion being a process that takes place in a diffusion-controlled environment. However, the fact that the presence of oxygenates may actually promote soot formation in diffusion-flame studies suggests otherwise. The *oxidation* of the soot that has been formed, on the other hand, is characterized as a diffusion process. Therefore, the authors suggest that diesel ignition (where soot production occurs) is an inherently premixed process, while the subsequent soot burnout happens in a diffusion flame, in agreement with Dec's model [57].

The works mentioned above, about the effect of oxygenates on soot emissions, have mostly been kinetic modeling studies, but the work by Rubino and Thomson [70] is a good example of an experimental investigation. In it, the authors used a counterflow propane-air diffusion flame, at an equivalence ratio of 1.79, to study the effect of adding oxygenate compounds on soot precursor formation. The oxygenates used were dimethy carbonate (DMC) and ethanol. According to their results, the addition of 10 vol.% DMC significantly reduced acetylene (by 15%), benzene (by 15%), among other pyrolysis products. Ethanol, also added at 10 vol.% concentration, on the other hand, exhibited smaller reductions for acetylene (about 8%), while the benzene concentrations increased slightly. Their results suggest that the reduction in acetylene production was related to both the oxygen content and the presence of C-C bonds in the oxygenates' molecules. In summary, both DMC and ethanol were able to reduce the production of soot precursors, and therefore soot, and this effect was shown to decrease linearly with increasing fuel oxygen content.

While it has been shown by numerous studies that the addition of oxygenates to the

base fuel may result in lower soot emissions by inhibiting the formation of precursors in the rich premixed ignition zone, the same can also be achieved by providing additional oxygen through extra entrained air into the fuel spray, as noted in the work by Westbrook *et al.* [58]. However, it should be kept in mind that oxygen—either coming from the fuel or from the entrained air—is hardly the only factor controlling soot formation in diesel engines, due to the sheer complexity of this phenomenon. Indeed, as Hallgren and Heywood pointed out in their study [63], decreasing the diesel fuel's aromatic content, sulfur content, distillation temperatures, and density may also reduce soot (and even NO_x) emissions. (The influence of the fuel's aromatic content helps explain why, in their study, adding an oxygenate to a Fischer-Tropsch synthetic diesel fuel—whose aromatic content is essentially zero—did not produce any reductions in the particle emissions, compared to the F-T diesel in neat form.) Moreover, they emphasized that it is difficult to attribute changes in the emissions behavior when so many fuel properties are simultaneously changed. Finally, they stressed that the benefits of adding oxygenates to a fuel can also be engine-specific and test-specific, that is, dependent on the engine's operating conditions.

2.3 Rudiments of Knock in SI Engines

Engine knock (historically referred to as detonation) is a combustion anomaly in spark-ignition engines that is caused by the autoignition of the fuel-air mixture ahead of the propagating flame [71], in the so-called end-gas region. This abnormal ignition causes the entire unburned charge to burn suddenly, giving rise to intense shock waves that are repeatedly reflected from the walls of the combustion chamber, thus communicating the sound to the atmosphere. The phenomenon is named after the characteristic noise associated with such pressure oscillations.

Figure 2.4 illustrates the differences beetween normal SI combustion and knocking combustion.

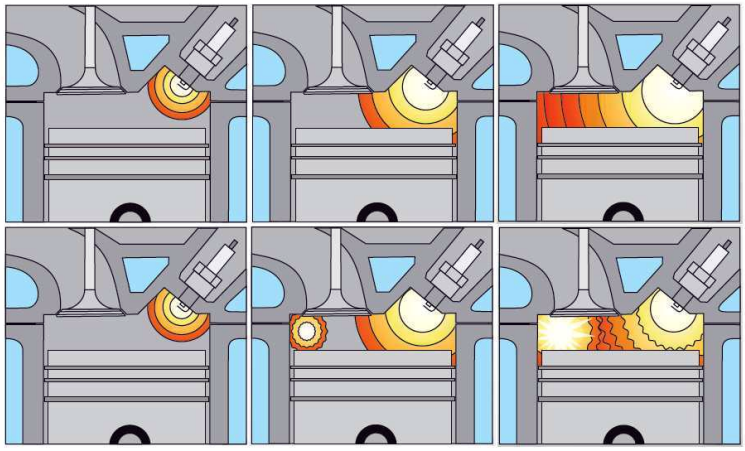

Figure 2.4: Normal SI combustion (top) versus knocking combustion (bottom) [72].

Because knock is essentially an acoustic phenomenon, it can be characterized by the frequencies of the pressure oscillations it creates. These frequencies, in turn, are associated with the resonant acoustic modes of the combustion chamber, which depend on the excited oscillation modes, cylinder geometry, and combustion gas properties [73].

In an early study, Draper [74], in order to calculate the relevant frequencies induced by knock, analyzed the resonant acoustic modes associated with a cylindrical shape with flat ends, representing a simplified geometry of a combustion chamber. The three modes investigated were the so-called circumferential mode, the radial mode, and the axial mode. Most of the wave energy is typically found in the lowest mode, i.e the 1st circumferential mode [75], which is also the mode responsible for the basic audible knock frequency.

The oscillation frequency of the 1st circumferential mode is given by the equation

$$f = \frac{\sqrt{\gamma RT}}{\alpha B} \tag{2.1}$$

where $\sqrt{\gamma RT}$ represents the speed of sound (C) for an ideal gas, α is the vibration mode factor determined by the solution of the wave equation, and B is the cylinder bore. For the 1st circumferential mode, α is equal to 1.7062 [76]. Using air properties, the speed of sound at 2000 K is approximately 896 m/s. From these results,

for typical automotive size engine cylinders ($B \approx 85$ mm), the frequency associated with the 1st circumferential mode is approximately 6 kHz [77]. Furthermore, the mean velocities of shock wave propagation in the products of combustion range from 1000 to 1200 m/s [78].

Knock is a constraint that depends on both fuel quality and engine design. It can lead to extensive—even catastrophic—engine damage, since the shock waves sharply increase the rate of heat transfer from the combustion products to the susceptible parts. This may lead to engine overheating and destruction of some combustion chamber components, such as piston edges, gaskets between the cylinder and its head, electrodes and spark plug insulators [78]. In addition, the vibrational nature of the load on the pistons may destroy the antifriction layers of the connecting rod bearings and intensify the wear of the upper part of the cylinder liners, since the shock waves destroy the oil film on the surface of the metal, leading to dry friction and also corrosive wear by active substances (particularly nitrogen oxides) contained in the combustion products [78].

The occurrence of knock is facilitated by all the factors that increase the rate of preflame reactions in the end-gas region, namely [78]:

- Increasing the reactivity of the fuel, which means lowering its octane rating.
- Increasing the compression ratio, which increases the pressure and the temperature of the end-gas.
- Advancing the spark timing, shifting the peak combustion pressure closer to TC.
- Enriching the fuel-air mixture to an equivalence ratio ϕ of around 1.1, which corresponds to the highest pressures and temperatures of combustion and to the maximum velocities of preflame reactions in the mixture heated by compression.
- Poor cooling of the areas around the cylinder.

Conversely, knock occurrence is suppressed by the factors that accelerate the combustion of the end-gas by the flame front or hamper the explosive autoignition of the end-gas in any other way. These include: (a) increased turbulence of the

charge; (b) a shorter path traveled by the flame front to the farthest regions of the combustion chamber; (c) the use of squish recesses in the combustion chamber, facilitating the cooling of the end-gas region and suppressing the appearance of spots of explosive autoignition that may produce shock waves [78].

Knock is closely related to the autoignition properties of a fuel, which, in turn, are connected to the fuel's ignition delay characteristics [79]. Knock-resistant fuels tend to exhibit long ignition delays [80, 81]. In other words, there is a strong relationship between the magnitude of the ignition delay period and the fuel's knock resistance. The presence of fuel-bound oxygen, through the addition of an oxygen-containing substance to the base gasoline (see section on oxygenates further below) has the potential to significantly decrease the fuel's reactivity and suppress autoignition, thus increasing the ignition delay period and inhibiting the occurrence of knock [82]. Moreover, this knock-suppressing mechanism is usually more pronounced at regimes of low temperature, characteristic of the beginning of the ignition process [83, 84, 85, 86, 87].

2.3.1 Knock Measurement and Characterization

The presence or absence of knock in engines is often detected by ear, since the human ear is a surprisingly sensitive knock detector [88, 77]. In automotive applications, for knock-control purposes, piezoelectric accelerometers are mounted on the engine block and vibrations resulting from knock are converted to electrical signals. These signals are input to the engine's electronic control unit (ECU) and are processed to determine the signal strength during a period when knock is expected to occur [89].

For research and development purposes, knock intensity is routinely measured and characterized through the processing of the amplified and filtered signal obtained with a pressure transducer installed in the cylinder head. After amplification, this signal is then bandpass-filtered so that the desired range of frequencies is centered roughly at the relevant frequency (as stated above, a value of 6 kHz is representative of typical automotive applications).

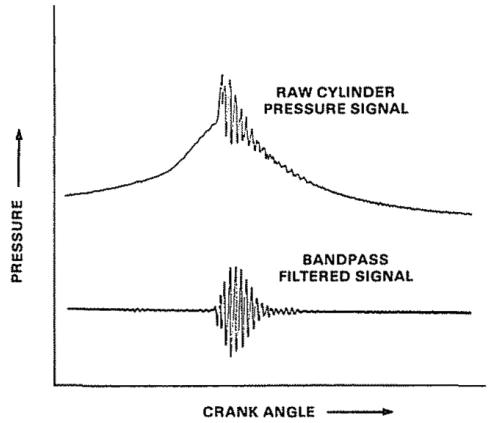

Figure 2.5: Signal processing of a typical in-cylinder pressure signal for knocking operation. (Adapted from [90].)

Figure 2.5 illustrates the processing of a typical in-cylinder pressure signal obtained during knocking operation. It shows the raw pressure signal and the corresponding bandpass-filtered signal. Once this signal has been properly filtered, several manipulations for the determination of knock intensity have been devised and the studies by Puzinauskas [76], Xiaofeng *et al.* [91], and Shahlari and Ghandhi [73] describe several methods to characterize knock intensity. In this monograph, the chosen method is the so-called Maximum Amplitude of Pressure Oscillations (MAPO), a simple measure that is useful because the amplitude of such oscillations is a function of the amount of end-gas that ignites and burns spontaneously and rapidly [77]. It is simply defined as the maximum (absolute) value of the band-pass-filtered pressure signal for each cycle, according to Equation 2.2.

$$MAPO = maximum\{P_{filtered}\} \tag{2.2}$$

2.3.2 The CFR Engine and the Knock Rating of SI Fuels

In the United States, in the first decades of the 20$^{\text{th}}$ century, as the automobile started to quickly grow in popularity, it became evident that the chemical composition of a fuel had a direct influence on its knock tendency and, consequently, on engine performance. Therefore, there was an increasing need for establishing tech-

nical protocols aimed at evaluating the knock resistance of the automobile fuel. The fuel in question, gasoline, had been for many years a waste product from kerosene refining and its quality was not a subject of much concern. However, because engine performance problems related to the quality of gasoline became more common, the petroleum and the automotive industries—which, up to that point, had antagonistic views on many technical matters—felt the need to cooperate with each other. Then, in 1922, the so-called Cooperative Fuel-Research (CFR) Committee was created, comprising members of both industries, under the guiding principle of mutually adapting the fuel to the engine and the engine to the fuel. This was accomplished through the first individual projects undertaken by the CFR committee, the first ones being related to (a) the relationship between gasoline volatility and fuel economy, (b) crankcase-oil dilution, (c) the relationship between gasoline volatility and engine starting (which also included the effect of volatility on engine acceleration). Finally, the fourth major project of the Committee was to devise a "satisfactory apparatus and technique for the measurement of the knock characteristics of fuel" [92].

This is how the CFR engine and the standardized knock testing methods came into being.

After years of intense work, the "apparatus" (i.e. the test engine), developed by Waukesha Motor Company and meeting the requirements of having (a) universality, (b) ruggedness, and (c) low cost, was finally unveiled in January, 1929, at the Annual Meeting of the Society of Automotive Engineers (SAE). Subsequently, by 1931, the "technique" (i.e. the testing procedures), together with the standardized engine, plus the reference fuels and a rating scale, became a reality [93]. That engine—the "CFR engine", as it is simply known—remains, even to this day, in upgraded form, the *de facto* standard device for the octane rating of SI fuels [94].

The original 1929 engine is shown in Figure 2.6, equipped with two different cylinder head configurations, while cross-sectional views of it, illustrating its simple design, are shown in Figure 2.7.

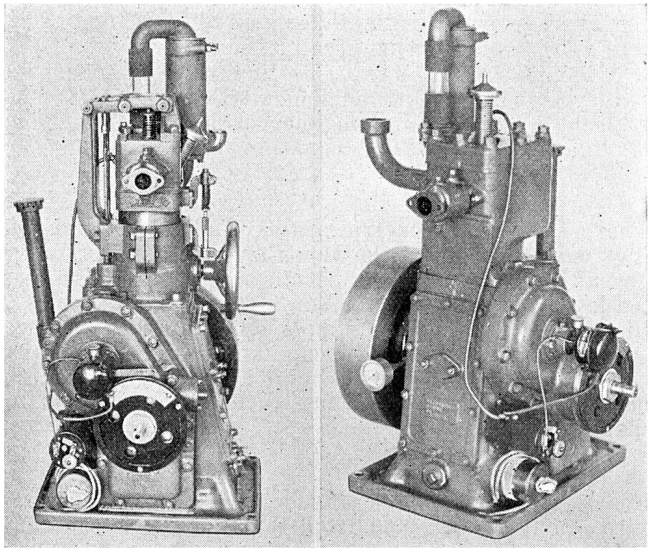

Figure 2.6: Two views of the original CFR engine [93].

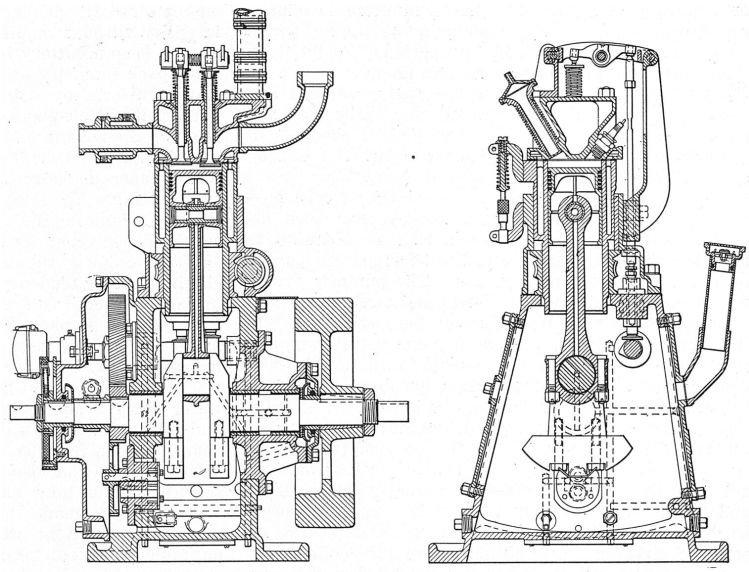

Figure 2.7: Longitudinal and transverse cross sections of the CFR engine [93].

The CFR engine is a naturally-aspirated, throttle-less single-cylinder engine featuring a variable compression ratio. In addition, it exhibits some design characteristics that are considered odd by modern standards, such as a flat piston top, a nearly

cylindrical combustion chamber, and a side-mounted spark plug. As a result of that, the CFR engine tends to produce knock at much lower compression ratios when compared to a modern engine running on the same fuel [95], which is not surprising, since its primary function is to evaluate the knock resistance of SI fuels. In other words, it an engine that is specifically designed for knocking operation. Some of the technical specifications of the CFR engine are shown in Table 2.1.

Table 2.1: Basic specifications of the CFR engine [94].

Waukesha CFR F-1/F-2 Engine Specifications	
Cylinder type	Cast iron, flat combustion surface, integral coolant jacket
Compression ratio	Adjustable 4:1 to 18:1
Bore	82.55 mm (3.25 in.)
Stroke	114.3 mm (4.5 in.)
Displacement	611.7 cm^3
Connecting rod length	254 mm
Piston	Cast iron, flat top
Intake valve opens	10° ATC
Intake valve closes	34° ABC
Exhaust valve opens	40° BBC
Exhaust valve closes	15° ATC
Ignition	Electronically triggered capacitive discharge through coil to spark plug

As already mentioned, the CFR engine is characterized by a simple design and a basic structure that is extremely rugged, being designed to withstand continuous operation under heavy knock conditions [93][1]. Such qualities make it an attractive research engine in its own right and not only a device for fuel testing.

The standardized ASTM test methods evaluate the knock resistance of fuel in terms of two arbitrary scales, in the form of the *octane numbers* of SI fuels. Those octane number scales correspond to the RON (research octane number) and MON (motor octane number) test methods. The testing procedures prescribed by these two methods are carried out on the CFR engine and are described in the ASTM standards D2699 and D2700, corresponding to the research octane number (RON) and motor octane number (MON) methods, respectively [97, 98].

Essentially, those methods consist of running the fuel to be tested under the stan-

[1] In one instance, it was reported that it withstood mean piston speeds higher than 15 m/s, and an indicated mean effective pressure (IMEP) of over 68 bar [96].

dard conditions and adjusting the compression ratio that gives a standard knock intensity, measured by the engine's knockmeter. While keeping the compression ratio and the other operating conditions constant, blends of the two reference fuels (isooctane and *n*-heptane) are tried until the blend that gives the same knock intensity as the fuel being tested is discovered[2] The percentage of isooctane in the matching mixture is the octane number of the fuel being tested [88].

The two testing methods differ regarding their standard operating conditions. A summary of the main differences is shown in Table 2.2.

Table 2.2: Engine operating conditions for the RON and MON tests.

Test	RON	MON
ASTM method	D2699	D2700
Engine speed [rpm]	600	900
Intake air temperature [°C]	Based on barometric pressure	38
Mixture temperature [°C]	Not controlled	149
Spark timing [deg BTC]	13	Based on compression ratio
Coolant temperature [°C]	100	100

Because knock limits the maximum allowable compression ratio, the possibility of knock essentially limits the maximum engine thermal efficiency that can be achieved in practice [99]. It is and has been a hurdle in the development of spark-ignition engines since their inception [100]. Indeed, it has been said that more research has been devoted to a study of knock than to any other aspect of internal combustion engines [88]. Furthermore, due to the more demanding operating conditions brought about by modern engine technologies such as downsizing and high boosting [101], as well as stoichiometric operation over the entire speed-load range, the avoidance of knock occurring becomes even more important, since it can hinder the achievement of the desired performance targets. At the same time engines develop, so does fuel technology, and there have been efforts to develop advanced fuels to match the demanding requirements of advanced engine designs.

[2]The final blend is determined by bracketing two blends, one of which produces slightly more knock and one slightly less, than the fuel being tested [88].

2.3.3 Gasoline Oxygenates

The octane rating of a fuel, and therefore its knock resistance, can be improved by adding certain types of compounds to it. This improvement can be significant, as it is—or, rather, was—the case with tetraethyl lead (TEL), $(C_2H_5)_4Pb$, which was first introduced in 1923 [102]. Considered the most effective antiknock element known [77] (just a few grams per liter would significantly raise the octane number of a fuel), its discovery and use made a huge contribution towards increasing the efficiency and the specific output of SI engines [88]. However, TEL was phased out after decades of widespread use, due to lead's toxicity.

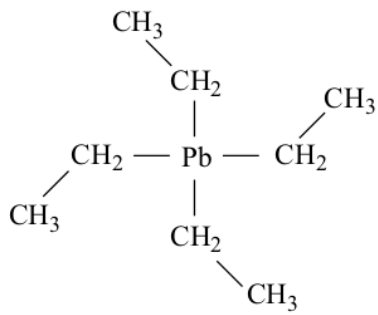

Figure 2.8: Tetraethyl lead' structure.

High-quality gasolines can also be obtained by the addition of oxygen-containing fuel components, known as *oxygenates*, to unleaded gasoline. As a less toxic alternative to lead, methyl *tert*-butyl ether (MTBE), $C_5H_{12}O$, is very effective as an octane booster and was widely used as such [103]. However, it has also been discontinued in some markets (most notably, the U.S.) due to its tendency to contaminate ground water in the event of gasoline spills [104, 105].

As alternatives to MTBE, other classes of oxygenates also have the potential to be used as blend components for gasoline, in order to improve its anti-knock properties and also promote cleaner combustion. Ethanol is the main example of an alcohol being used as an SI fuel, most notably in Brazil, where it has long been used as a gasoline blend component and also as a neat fuel (in hydrous form, at about 95%) [106, 107]. Ethanol is of particular relevance due to the fact that it can easily be biologically produced from a wide range of sugary or starchy feedstocks by fermentation and distillation processes [108]. The main feedstocks for

bioethanol production are corn (especially in the U.S.), sugarcane (especially in Brazil), sugar beets (in Europe), other cereals (such as wheat, rye, sorghum, etc.), and cassava [103]. The use of lignocellulosic ethanol is particularly promising since, as a second-generation biofuel, its production does not impact food crops.

However, several other oxygenated compounds have the potential to be used as promising alternatives to ethanol and MTBE and, as such, are worth investigating. As an example, the other lower alcohols (methanol, the propanols, plus the butanols) and also a number of glycerol derivatives, such as GTBE, solketal, and triacetin. The following sections discuss these compounds, starting with the glycerol derivatives, followed by the alcohols.

2.4 The Glycerol Derivatives and Their Use in Motor Fuel Applications

In much the same way as the alcohols (see section further below), glycerol-derived compounds also have the potential for fuel applications as blend components to gasoline, diesel fuel, or biodiesel. Ideally, such compounds should be produced using the by-product glycerol generated by the biodiesel industry in order to increase the value of a substance that is considered waste and is typically disposed of as such. In this work, the glycerol derivatives considered are the glycerol *tert*-butyl ethers (GTBE), solketal, and triacetin, which are introduced in the next section. (For further information regarding the use of glycerol derivatives as fuel additives, a review on the subject has been published by the author and colleagues [109].)

2.4.1 The Valorization of Waste Glycerol

Glycerol (1,2,3-propanetriol, also known as glycerin or glycerine) is a clear, colorless, odorless, sweet-tasting, hygroscopic, viscous liquid at room temperature. Glycerol, found in all natural fats and oils as fatty esters, is an important intermediate in the metabolism of living organisms [110]. Its boiling point is 290°C at atmospheric pressure and its freezing point is ca. 18°C. It is an example of a polyalcohol, featuring a three-atom carbon chain with a hydroxyl group attached to each carbon. These groups make it completely miscible with water, methanol, ethanol, and the isomers of propanol, butanol, and pentanol, but it is virtually insoluble in

hydrocarbons [111]. It is also biodegradable and has a very low toxicity. A representation of the glycerol molecule is shown in Figure 2.9 and Table 2.3 lists some of its properties.

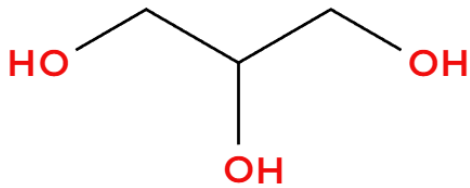

Figure 2.9: Glycerol's skeletal formula.

Table 2.3: Select properties of glycerol [112].

Glycerol (1,2,3-propanetriol)						
Molecular Weight	Melting Point [°C]	Boiling Point [°C]	Density (20°C) [kg/dm^3]	Viscosity (20°C) [mm^2/s]	HV[a] [MJ/kg]	Flash Point [°C]
92	18.0	290.0	1.261	1118	16.0	177

[a]Heating value

Even though a few isolated studies have reported diesel engine operation running on glycerol [113, 114], its direct utilization as a neat fuel is precluded by physicochemical properties such as a very high viscosity, high melting point, low heating value (16 MJ/kg), and high autoignition temperature (370°C) [115]. To complicate the issue even further, glycerol has a tendency to polymerize and to form propenal (also known as acrolein) during combustion, a toxic compound that causes irritation on the skin, eyes, and nasal mucosa [116]. For that reason, for engine applications, glycerol has to be converted into compounds that can be mixed with fuels such as gasoline, biodiesel, or diesel.

As discussed in Chapter 1, in order to address the environmental concerns caused by the use of fossil energy, the production and use of renewable fuels in the transportation sector has been mandated by law in several countries. This means that conventional fossil fuels must be gradually replaced by biofuels such as ethanol and biodiesel. Ethanol, which has become the foremost biofuel [117, 9, 46] (see below), is primarily intended to be used in spark-ignition engines, in combination with (or

as a replacement for) gasoline, in light vehicles such as passenger cars and motorcycles. Biodiesel, on the other hand, is meant to be used in compression-ignition (i.e. diesel) engines, in blends with conventional diesel fuel, or even in neat form, powering passenger cars but also heavy-duty vehicles, such as buses and long-haul trucks.

Chemically, biodiesel is defined as the mono-alkyl esters of long-chain fatty acids [118]. It is traditionally produced by the transesterification of triglycerides (that is, vegetable oils and/or animal fats) with an alcohol in the presence of a catalyst. Figure 2.10 depicts the transesterification reaction, where a triglyceride reacts with an alcohol, producing fatty-acid alkyl esters (biodiesel). Methanol is typically the alkylation agent used, in which case the products are called fatty-acid methyl esters (FAME) [29]. The main purpose of the transesterification reaction is to improve the properties of the original oil, such as lowering its viscosity, to make it suitable to be used as engine fuel.

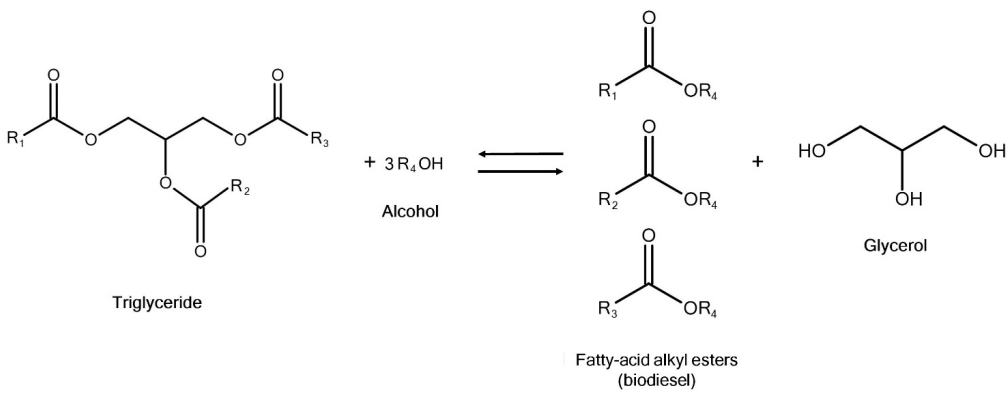

Figure 2.10: The transesterification reaction.

In Europe, over 200,000 barrels of biodiesel are produced daily [119] and it has become the leading biofuel in the European Union. A 2014 report by the European Commission indicated that the biodiesel production capacity had increased to about 26.3 billion liters per year, with an annual production of about 10.5 billion liters [120]. Moreover, according to data published by the Organization for Economic Co-Operation and Development (OECD), global biodiesel production is projected to increase from 36 billion liters in 2017 to 44 billion liters by 2028, when the EU is expected to remain the world's major producer [121].

According to the stoichiometry of the transesterification reaction, one mole of triglyceride reacts with three moles of alcohol, producing three moles of fatty acid alkyl esters and one mole of glycerol, corresponding to roughly 10 wt.% of the biodiesel produced [122, 123, 124, 125]. As an unavoidable consequence, the rapid growth of the biodiesel industry has caused an oversupply of glycerol (a "glycerol glut") on the markets, with its supply growing faster than the demand for its traditional applications (e.g. in foods, cosmetics, and pharmaceuticals) [111].

A consequence of such glycerol oversupply is the possibility of sharp drops in the glycerol prices, which represents a burden to the biodiesel industry and a threat to its sustainability as a whole.

Because of that, it has become necessary to find alternative ways of utilizing the glycerol from biodiesel production and turning it into valuable products. Hence, innovative processes to convert the surplus glycerol into valuable chemicals have been investigated and developed, a topic commonly called *glycerol valorization* [126, 127, 128, 129].

The production of oxygenated fuel additives is therefore one of the most important chemical routes that can be used for glycerol valorization and such additives can serve different purposes, depending on the base fuel to which they are added [130]. More specifically, glycerol derivatives, when used as motor fuel additives, can be used as gasoline octane boosters, biodiesel cold-flow improvers, or as diesel fuel oxygenates (mainly to reduce PM emissions).

Though there exist several different chemical pathways to turn glycerol into fuel additives, a few deserve a more detailed description, namely the acetalization, etherification, and esterification routes (which produce glycerol acetals, ethers, or acetates, respectively). The products obtained from such processes are the subject of the next paragraphs.

2.4.2 Glycerol Acetals

Fuel additives can be obtained from the acetalization of glycerol with an aldehyde, producing acetals. The so-called glycerol formal, the product of the reaction between glycerol and formaldehyde (see Figure 2.11), is an example of a glycerol acetal. It is a compound comprised of two cyclic isomers: 1,3-dioxan-5-ol and 1,3-

dioxolane-4-methanol. This mixture of five- and six-membered cyclic isomers is a characteristic of the reaction of glycerol with aldehydes and ketones [131].

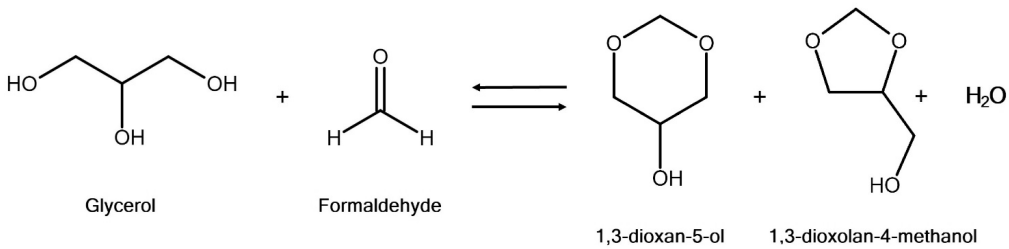

Figure 2.11: The acetalization of glycerol with formaldehyde.

When glycerol, instead of reacting with an aldehyde, reacts with a ketone, the reaction is commonly called ketalization, and the product is called a ketal. A typical example is the reaction of glycerol with acetone (see Figure 2.12), which yields the five-membered ring compound 2,2-dimethyl-1,3-dioxolane-4-methanol, also known as solketal. In theory, besides solketal, this reaction also produces the six-membered ring 2,2-dimethyl-1,3-dioxan-5-ol. However, in practice, due to thermodynamic reasons, solketal is the only product [132, 133]. The acetalization (or ketalization) of glycerol is usually a simple process that can be done under mild conditions at atmospheric pressure using standard acid catalysts, with high selectivities to products [134].

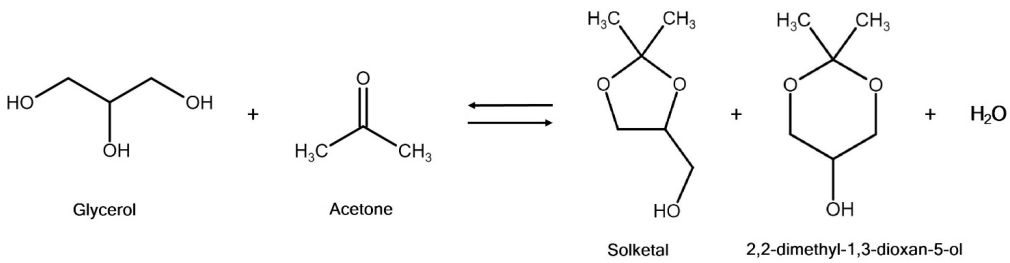

Figure 2.12: The ketalization of glycerol with acetone.

2.4.3 Glycerol Ethers

Ethers of glycerol have been investigated for several decades. In 1934, Evans and Edlund described a method for producing tertiary ethers of aliphatic polyhydric

alcohols—such as glycerol—with tertiary-base olefins [135] and in 1941, Doelling found that certain glycerol mono- and di-ethers could be used as antiseptics [136]. Indeed, glycerol etherification has been extensively investigated to produce a wide variety of products, from food flavoring agents to solvents, surfactants, and fuel additives.

For motor fuel applications, glycerol is typically etherified through the reaction with alkylation agents, such as alcohols or olefins (alkenes), in the presence of a strongly acidic catalyst. Several processes for the etherification of glycerol with ethanol, *tert*-butanol, *n*-butanol, and higher alcohols have been proposed as well as its alkylation with alkenes such as isobutylene.

The most commonly investigated glycerol ether, GTBE, is introduced in the following paragraphs, followed by a discussion about the other types of glycerol ethers.

Glycerol *tert*-Butyl Ethers (GTBE)

A well-known glycerol etherification reaction is its *tert*-butylation, which replaces one or more hydroxyl groups in the original glycerol molecule with one or more *tert*-butyl groups, yielding the so-called glycerol *tert*-butyl ethers (GTBE) [137, 138]. The *tert*-butylation of glycerol has been extensively investigated and industrial productions methods have been proposed [139]. This reaction is usually carried out when the alkylation agent is either isobutylene or *tert*-butanol (*tert*-butyl alcohol, TBA). It is possible to achieve a combination of 100% glycerol conversion and very high selectivity (> 92%) towards di- and tri-ethers (the GTBE components with best potential as fuel additives, see below) [140]. However, the process can be costly, isobutylene needs to be pressurized to be in liquid phase and it has low solubility in glycerol [141]. The use of TBA does not pose such problems and it also inhibits secondary reactions like isobutene oligomerization [142], but it creates water as a by-product, which can hamper the reaction by inhibiting catalyst activity [143].

GTBE is not a single compound, but rather a mixture of five component ethers, which are formed depending on the extent of etherification underwent by the glycerol molecule (i.e. depending on how many hydroxyl groups were replaced with the *tert*-butyl group). These five components are represented by three types of ethers: a monoether (mono-GTBE, representing two isomers), a diether (di-GTBE, two isomers), and a triether (tri-GTBE), all of which are shown in Figure 2.13. Due to

the poor miscibility of mono-GTBE in hydrocarbons, the *tert*-butylation reaction should be designed for high selectivities towards the di- and tri- components. The latter exhibits the best hydrocarbon solubility, but its synthesis is more expensive since it consumes more alkylating agent.

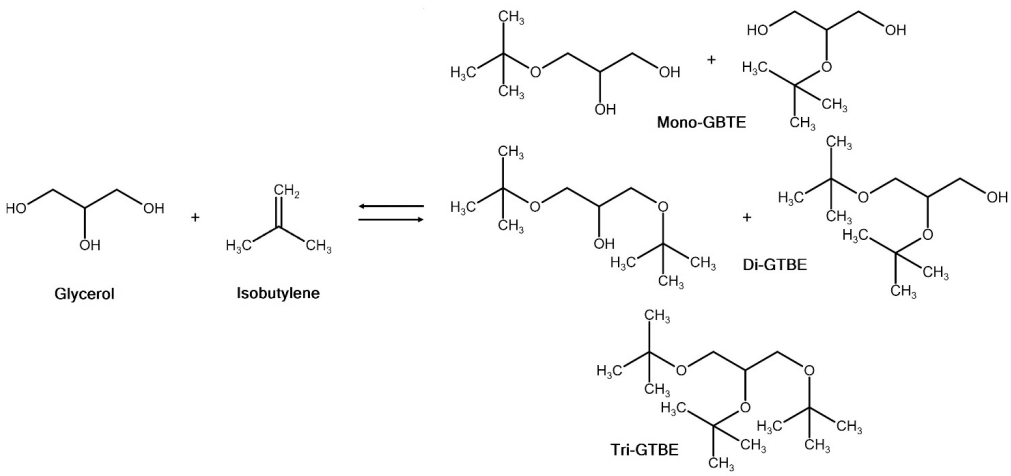

Figure 2.13: The etherification of glycerol with isobutylene.

Other Types of Glycerol Ethers

In their 2009 patent, Kousemaker and Thiele [144] described a method for producing ethers of glycerol acetals or ketals, intended to be used as fuel additives for diesel fuels, gasoline, and biodiesel. As an example, the patent describes the reaction of glycerol with acetone, producing solketal, followed by the etherification of solketal with isobutylene, producing the compound called solketal *tert*-butyl ether (STBE). It can also be obtained in the other direction, through the ketalization of mono-GTBE with acetone, as described by Samoilov et al. [145]. The rationale for the additional etherification (or ketalization) step is to remove the hydroxyl group still present in the solketal molecule, replacing it with an alkoxy group, thus enhancing the compound's hydrophobicity and oxidation stability, and increasing its heating value [145]. Therefore, STBE has the potential for becoming a promising fuel additive. A discussion on other types of glycerol ethers—obtained by reacting glycerol with ethanol, propanol, butanol, and even pentanol, hexanol, octanol, and decanol—can be found in the 2023 review article by the author and colleagues [109].

2.4.4 Glycerol Acetates

Another way of producing glycerol-derived fuel additives is to react it with carboxylic acids to form esters. For fuel additive applications, a typical conversion pathway is the acid-catalyzed esterification of glycerol with acetic acid or acetic anhydride to yield glycerol acetates (also called acetins); this reaction is illustrated in Figure 2.14. Depending on the extent of the reaction, three components are formed: monoacetin, diacetin, and triacetin [also known as monoacetylglycerol (MAG), diacetylglycerol (DAG), and triacetylglycerol (TAG), respectively]. Among these, triacetin (TAG) is particularly suited as a fuel additive—usually as a biodiesel cold flow improver or gasoline octane booster—due to its better solubility in hydrocarbons, which is caused by the elimination of all three of glycerol's hydroxyl groups. A 2016 patent by Puche [146], extensively describes a process for producing triacetin and alkyl esters of fatty acids.

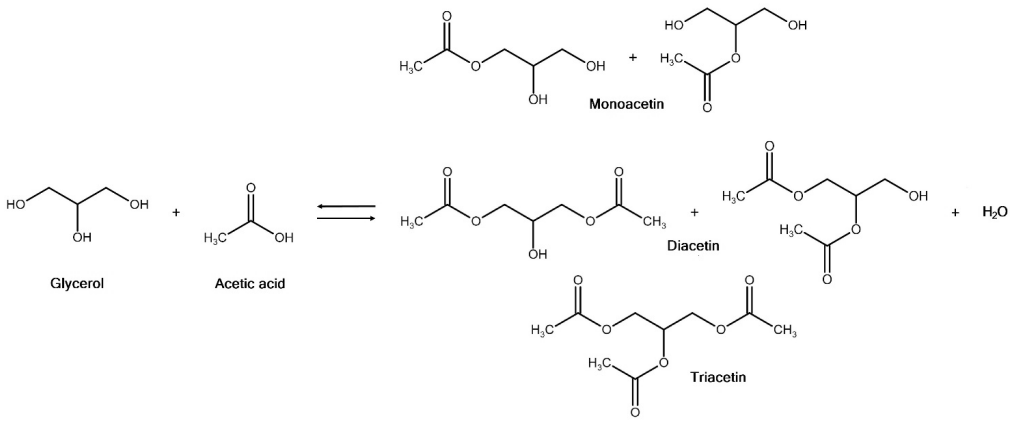

Figure 2.14: The acetylation of glycerol with acetic acid.

2.5 The C_1–C_4 Alcohols and Their Use in Motor Fuel Applications

In comparison with conventional gasolines, the C_1–C_4 alcohols (that is, methanol, ethanol, and the isomers of propanol and butanol) possess properties that make them particularly suitable to be used as spark–ignition engine fuels, such as higher heat of vaporization and superior knock resistance [147]. The enhanced cooling ef-

fect caused by their high heat of vaporizations can increase an engine's volumetric efficiency, while an improved knock resistance enables the use of higher compression ratios, leading to higher engine efficiency.

In addition, the possibility of obtaining the C_1–C_4 alcohols from renewable feedstocks and using them as drop-in gasoline oxygenates is another attractive feature, making it possible to use them in the transportation sector as promising alternatives to fossil fuels.

This study includes the most common isomers of propanol and butanol, namely isopropanol, *n*-butanol and isobutanol. A summary of relevant properties for the alcohols included in this work is shown in Table 2.4.

A brief introduction to each of the alcohols used in this work follows, addressing their production routes and use as fuels for IC engines.

2.5.1 Ethanol

Ethanol (ethyl alcohol or grain alcohol or simply "alcohol"), being the main component of alcoholic beverages, is the most widespread alcohol compound. Moreover, ethanol is the most common biofuel [117, 9, 46]. It is typically obtained through the fermentation of sugar- or starch-containing materials, such as sugarcane or corn, though it is also produced through synthetic routes from fossil feedstocks. As a transportation fuel, it has first been put into large-scale use in Brazil in the 1970s, where both neat hydrous ethanol and ethanol blends with gasoline are marketed [106, 107]. It is also a well-established gasoline blend component in the United States, as well as in other countries [103].

In its pure form, ethanol is a colorless liquid, miscible in all proportions with water and also with ether, acetone, benzene, and some other organic solvents. The azeotropic mixture contains 95.6 wt.% ethanol and 4.4 wt.% water, meaning that the highest concentration of ethanol that can be obtained by distillation is 95.6 wt.% [148].

Figure 2.15 shows ethanol's skeletal structure.

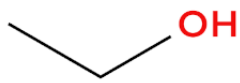

Figure 2.15: Ethanol's skeletal structure.

Even though ethanol is commonly associated with alcoholic beverages and engine fuels, it has several other applications in the chemical industry, as Figure 2.16 shows.

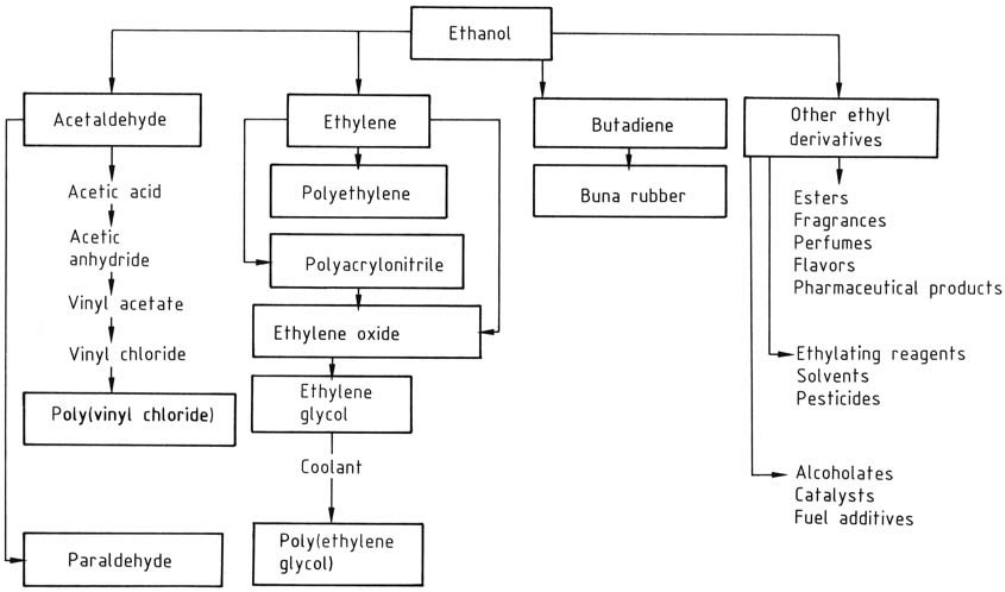

Figure 2.16: An example of chemicals obtained from ethanol [148].

Ethanol Production

Synthetic ethanol is most commonly produced by the direct catalytic hydration of ethylene, according to the reaction:

$$C_2H_4 + H_2O \rightarrow C_2H_5OH$$

This reaction is usually carried out over phosphoric acid catalysts, with the molar ratios of ethylene to water in the range 1:0.3–1:0.8, at 250–300°C and 5–8 MPa [148].

Ethanol is widely produced through fermentation of sugars, using yeasts such as *Saccharomyces cerevisiae*, *S. uvarum* (formerly *S. carlsbergensis*), and *Candida utilis*. Its production by yeast is characterized by high selectivities, low formation of by-products, high ethanol yields and fermentation rates, good tolerance regarding ethanol and substrate concentrations, and lower pH values [148]. Yeasts are capable of metabolizing various carbon compounds using different pathways, under aerobic and anaerobic conditions.

Under *anaerobic* conditions, the yeast produces ethanol, from hexoses, according to the Gay-Lussac reaction:

$$C_6H_{12}O_6 \rightarrow 2C_2H_5OH + 2CO_2$$

Theoretically, for each gram of glucose, 0.51 g of ethanol can be produced; the actual ethanol yield being around 90–95% of that value.

The work by Rogers *et al.* [149], showed that the bacterium *Zymomonas mobilis* has a number of favorable characteristics for efficient production of ethanol from glucose. However, it is incapable to ferment pentose sugars, such as xylose and arabinose, into pure ethanol. (In fact, up to now, no natural yeast or bacterial strains are capable to ferment pentoses into ethanol as efficiently as these organisms can ferment hexoses like glucose or fructose.) To circumvent this, various approaches have been made to genetically engineer microorganisms such as *Z. mobilis* to broaden its range of utilizable substrates.

Cellulosic Ethanol Second-generation bioethanol, on the other hand, is achieved through the fermentation of non-food, lignocellulosic biomass, including forest and agricultural residues or municipal solid waste [150, 151].

Ethanol Use in Internal Combustion Engines

Ethanol has been regarded as a fuel for internal combustion engines since the early years of their development. References [152] and [153] are interesting examples. Besides, being the foremost example of a biofuel, it comes as no surprise that the literature on ethanol fuel is vast; a good recent review on the topic can be found in the 2022 article by Mendiburu *et al.* [154].

2.5.2 Methanol

Methanol, also called methyl alcohol or wood alcohol, is the simplest alcohol. At ambient conditions, it is a colorless, volatile liquid with a faint alcoholic odor. It is completely miscible with water, other alcohols, various organic solvents, and to a limited extent with oils and fats.

Figure 2.17 shows methanol's very simple skeletal formula.

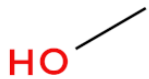

Figure 2.17: Methanol's skeletal structure.

It is one of the most important raw materials in the chemical industry. Nowadays, approximately 70% of the worldwide methanol production is used for chemical synthesis, to produce a wide variety of chemicals such as formaldehyde, methyl tertbutyl ether (MTBE), acetic acid, dimethyl ether (DME), propylene, among others. However, its use for energy and fuel applications, either directly or in form of methanol-derived products, is gaining more importance [155].

Methanol Production

Methanol was originally produced by the destructive distillation of wood—hence the name—and it was not until 1923 that an industrial process using syngas as feedstock, became available [156]. As such, methanol can be made from virtually any carbon source, fossil or renewable, via gasification to syngas and the subsequent catalytic synthesis.

Therefore, the first step for the industrial methanol synthesis is the production of syngas.

Due to cost and availability, natural gas has long been the major source for syngas production, the most widely used technology used to produce it being the steam reforming of methane, according to the reaction:

$$CH_4 + H_2O \rightarrow CO + 3H_2 \tag{2.3}$$

A partial oxidation reaction may be used in combination, in a process called autothermal reforming:

$$CH_4 + \frac{1}{2}O_2 \rightarrow CO + 2H_2 \tag{2.4}$$

Coal is another fossil raw material used for syngas production. Its gasification can be done at different pressures (0.5–8 MPa) and temperatures (400–1500°C). It combines partial oxidation (2.5) and steam treatment (2.6) [16]:

$$C + \frac{1}{2}O_2 \rightarrow CO \tag{2.5}$$

$$C + H_2O \rightarrow CO + H_2 \tag{2.6}$$

Because coal has a low H/C ratio, coal-based syngas is deficient in hydrogen, which drastically reduces the selectivity to methanol during its subsequent synthesis [155]. Therefore, to adjust its composition (a CO/H_2 ratio close to 1:2 is ideal [16]), the syngas must be subjected to a shift conversion with water, according to the water-gas shift reaction:

$$CO + H_2O \leftrightarrows CO_2 + H_2 \tag{2.7}$$

Alternatively, syngas can also be obtained from biomass gasification [157, 158].

Once the CO/H_2 ratio has been adjusted, the syngas is ready for conversion into methanol, according to reaction (2.8), which is typically done at 5–10 MPa, 200–300°C, using copper/zinc oxide catalysts:

$$CO + 2H_2 \rightarrow CH_3OH \tag{2.8}$$

CO_2-to-Methanol

The syngas-based production of methanol generates large amounts of carbon dioxide. Due to an increasing awareness of the necessity to reduce CO_2 emissions for

environmental reasons, the chemical recycling of CO_2 by catalytic hydrogenation to methanol is a topic that has attracted significant attention.

The most direct route to methanol from CO_2 is represented by the so-called catalytic regenerative conversion of carbon dioxide with hydrogen, according to the reaction [16]:

$$CO_2 + 3H_2 \rightarrow CH_3OH + H_2O \tag{2.9}$$

Optimized catalysts, combinations of copper and zinc oxides, have been developed to increase the efficiency of the process and its selectivity to methanol.

The carbon dioxide necessary for the reaction can be captured from natural and industrial sources, as well as from human activity or even from the air. Hydrogen for the chemical recycling of CO_2 to methanol can be produced either by using conventional, fossil-based methods (i.e. using natural gas) or, preferably, by splitting water using renewable (or nuclear) electricity, in which case the methanol becomes an example of an *e-fuel*. When water-electrolysis-derived hydrogen is produced using renewable electricity, the produced methanol can—at least theoretically—have a zero carbon footprint.

There are a few commercial CO_2-to-methanol plants in operation, most notably the Iceland-based company Carbon Recycling International [159]. The main challenge of this technology is the economically feasible production of both green hydrogen from various energy sources and clean CO_2 from waste gas streams [155].

Methanol Use in Internal Combustion Engines

The literature on methanol fuel is extensive; however, comprehensive reviews on its production and use as a fuel for IC engines can be found in the works of Landälv [160] and Verhelst *et al* [161].

2.5.3 Propanols

Propanols are clear, colorless liquids with an odor resembling that of ethanol. They comprise two isomers, 1-propanol and 2-propanol (also called isopropyl alcohol),

of which the latter is industrially the more important [162]. Both isomers are completely miscible with water and readily soluble in a variety of common organic solvents, such as ethers, esters, acids, ketones, and other alcohols. They are mainly used as solvents and chemical intermediates for the production of esters, amines, and other organic derivatives. The propanols are also effective antiseptics and disinfectants [163]. Isopropanol, the simplest secondary alcohol, is produced by the hydration of propylene or the hydrogenation of acetone, whereas 1-propanol is manufactured by the hydrogenation of propanal [162].

Figure 2.18 shows the skeletal formula of both propanol isomers.

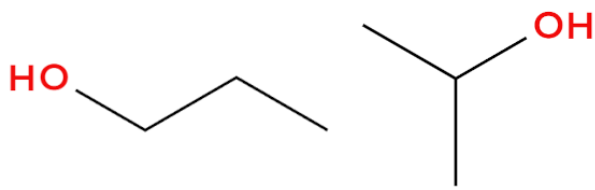

Figure 2.18: The skeletal structures of both isomers of propanol.

The remainder of this section deals with isopropanol only.

Isopropanol Production

There are two main industrial processes for the production of 2-propanol, the indirect and direct hydration of propylene. Smaller amounts are produced by the hydrogenation of acetone [162]. In the indirect method, propylene first reacts with sulfuric acid, forming sulfate esters, which are subsequently hydrolyzed to yield isopropanol.

In the direct hydration process, propylene reacts with water according to the reaction:

$$C_3H_6 + H_2O \rightarrow C_3H_7OH \tag{2.10}$$

Obtaining isopropanol from renewable sources does not seem to have achieved a level of maturity sufficient for large-scale commercialization [164, 165], compared to other C_1–C_4 alcohols. However, there are studies in the literature re-

porting its successful production via fermentation using bacteria such as *Escherichia coli*, *Clostridium beijerinckii Corynebacterium glutamicum*—see references [166, 167, 168, 169, 170]. In addition, an interesting recent study by Liew *et al.* [171] describes the production of isopropanol (and acetone) through the fermentation of low-cost waste gas feedstocks (such as industrial emissions) using the engineered bacterium *Clostridium autoethanogenum*. The authors claim that the process has a carbon-negative footprint, since it fixes CO_2 instead of producing it.

Isopropanol Use in Internal Combustion Engines

The state of the technology to produce isopropanol from biomass has prevented it from receiving much attention as a potential engine fuel and is likely the primary technical barrier to its use as a gasoline oxygenate. Nevertheless, a few recent engine studies on the use of gasoline-isopropanol blends can be found in the literature; for instance, the articles by Gong *et al.* [172], Sivasubramanian *et al.* [173] and Kumar *et al.* [174].

There seem to be even fewer studies dedicated to neat isopropanol fuel, with notable exceptions being the recent works by Gainey *et al.* [147, 175, 176], who investigated neat C_1–C_4 alcohols, mostly focusing on low-temperature combustion (LTC) applications.

2.5.4 Butanols

The butanols are aliphatic saturated C_4 alcohols (C_4H_9OH), comprising four structural isomers: two primary (*n*-butanol and isobutanol), one secondary (*sec*-butanol), and one tertiary (*tert*-butanol) [177]. At ambient conditions, they are colorless liquids (except for *tert*-butanol, whose melting point is 25.6°C) having a characteristic odor. All four isomers are completely miscible with common organic solvents, but only *tert*-butanol is completely miscible with water.

Figure 2.19 shows the skeletal structures of the four butanol isomers.

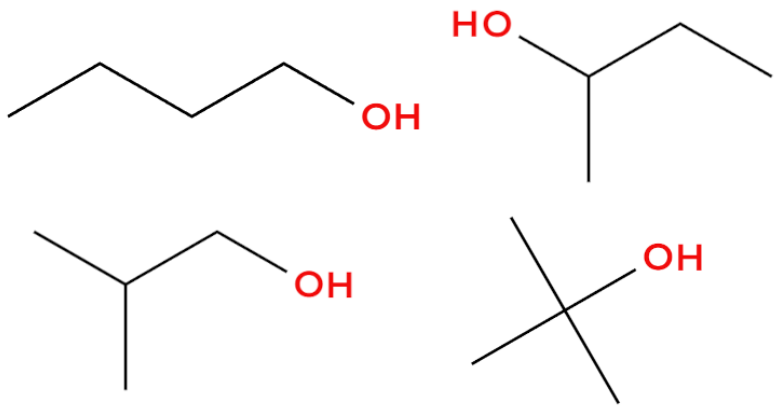

Figure 2.19: The skeletal structures of the four isomers of butanol.

n-Butanol (1-butanol) and isobutanol (2-methyl-1-propanol) are the butanol isomers most commonly considered for fuel applications [178]. Both are mainly used as industrial solvents and are typically obtained from fossil sources, though they can also be obtained from renewable feedstocks (see below) [177].

The remainder of this section deals with *n*-butanol and isobutanol only.

n-Butanol and Isobutanol Production

n-Butanol occurs in nature in compound form and so does isobutanol (2-methyl-1-propanol), which occurs in natural products as well as in fusel oils, from which it can be separated [177]. Even though both isomers can be obtained from fermentation (see below), the renewable production routes could not compete with decreasing oil prices, so they became obsolete and nowadays *n*-butanol and isobutanol—along with the other two isomers—are mainly produced from fossil sources.

Both *n*-butanol and isobutanol are mainly produced by the hydroformylation of propylene, with the subsequent hydrogenation of the aldehydes formed (a process known as *oxo synthesis*) [177].

In the oxo reaction (see Figure 2.20), carbon monoxide and hydrogen are added to a carbon–carbon double bond in the liquid phase in the presence of catalysts, forming aldehydes that are subsequently hydrogenated. In the case of propylene these consist of 1-butanal and 2-ethylpropanal.

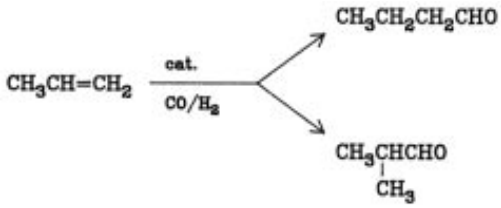

Figure 2.20: The Oxo synthesis.

n-Butanol and isobutanol can also be produced in large scale by the carbonylation of propene, a method known as the *Reppe process* (Figure 2.21) [177]. In this process, alkenes, carbon monoxide, and water are reacted under pressure in the presence of a catalyst.

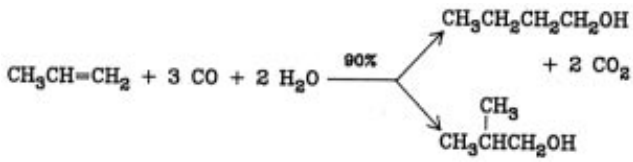

Figure 2.21: The Reppe process.

The first large-scale production of *n*-butanol, in the early 20th century, was based on the discovery of the bacterium *Clostridium acetobutylicum*, which has the ability to ferment carbohydrates, yielding acetone, *n*-butanol, and ethanol, at ratios of approximately 3:6:1, respectively (this is the well-known ABE—acetone-butanol-ethanol—fermentation method [179]). In addition to *C. acetobutylicum*, other *n*-butanol-producing bacteria of the *Clostridia* type were eventually developed, such as *C. beijerinckii*, *C. saccharoperbutylacetonicum*, and *C. saccharobutylicum* [180].

Regarding isobutanol, it can be synthesized by a number of microorganisms, such as *Escherichia coli* and *Saccharomyces cerevisiae*, utilizing various biomass feedstocks [181]. It is worth mentioning that, because most microorganisms do not produce isobutanol on their own, they need to be genetically manipulated to enhance the expression of the key enzymes, to inhibit byproduct formation, and to strengthen their resistance against the cytotoxicity of the alcohol. *E. coli* and *S. cerevisiae* are also able to synthesize isobutanol from lignocellulosic material, along with bacteria, such as *Clostridium cellulolyticum* and *Clostridium thermocellum*, for instance [181]. However, when cellulose is used as a substrate, usually much lower product

concentrations are achieved in comparison with isobutanol obtained from sugar or starch, due to the challenges associated with the breaking down of cellulose into simple sugars [182].

An overview of biomass-produced isobutanol can be found in a recent article by Dedov *et al.* [183].

n-Butanol and Isobutanol Use in Internal Combustion Engines

Isobutanol, in particular, has been considered as a feasible alternative to ethanol as a gasoline oxygenate, primarily due to its good octane-boosting capacity and its higher heating value. In addition, it exhibits lower water affinity, lower corrosiveness, and lower impact on the fuel's vapor pressure (see discussion in the following paragraph). Moreover, recent advances in biotechnology have increased the efficiency of isobutanol production through biochemical routes, using microorganisms such as *Escherichia coli* and *Saccharomyces cerevisiae*, among others, which can make it more economically feasible. A review of isobutanol as a fuel for IC engines has been recently published by the author and colleagues [178].

Commercial Production of Isobutanol The commercial production of bioisobutanol has been carried out by a number of companies, most notably Butamax Advanced Biofuels (a joint venture between BP and DuPont) [184] and Gevo [185], the latter of which has developed a technology for not only retrofitting existing ethanol plants to produce isobutanol [186], but also to produce it from lignocellulosic biomass [187]. A 2012 article published by *The New York Times* [48] highlighted the work of both companies and their technologies. The article also discussed the advantages of isobutanol over ethanol, as a gasoline oxygenate, such as its higher energy content, lower affinity for water, as well as its ability to overcome the aforementioned "blend wall" commonly associated with ethanol. Moreover, that article stated the fact that isobutanol does not distort the volatility characteristics of gasoline, allowing for a cheaper gasoline to be used when making the final blend.

2.5.5 Practical Aspects of Alcohols as ICE Fuels

In spite of their attractive properties, the use of alcohols in blends with gasoline involves some practical aspects that must be taken into consideration. Alcohols tend to be corrosive, especially the ones with shorter molecules [188], which can damage fuel system components. The corrosiveness of methanol is particularly well-documented [189]. An alcohol's water affinity can restrict its transportation in pipelines, due to the risk of corrosion and also due to the possibility of water-induced phase separation of gasoline–alcohol blends [190]. Finally, alcohols may distort the vapor pressure behavior and the distillation properties of their blends with gasoline, which can have a negative impact on the evaporative emissions, engine cold start, and drivability [191, 192, 193].

2.6 Fuels and Fuel Additives Investigated in This Work

All fuels and fuel additives used in this work, along with some of their key properties, are listed in Table 2.4. For the alcohols, additional properties are listed in Table 6.1.

Table 2.4: All fuel and additives used in this dissertation.

Compound	Chemical Formula	MW[a]	Specific Gravity	Viscosity [mm^2/s]	LHV[b] [MJ/kg]	RON[c]	Oxygen [wt.%]
Diesel	$C_nH_{1.8n}$	170	810	—	43.2	—	0
B7 Diesel	—	—	—	—	—	—	—
Mono-GTBE[d]	$C_7H_{16}O_3$	148	1.000	187	28.0	—	32.4
Di-GTBE	$C_{11}H_{24}O_3$	204	0.890	13.9	32.6	—	23.5
Tri-GTBE	$C_{15}H_{32}O_3$	260	0.860	7.55	37.9	—	18.5
Mono-shifted GTBE[e]	—	158	0.975	—	29.8	—	—
Di-shifted GTBE[f]	—	185	0.925	—	31.6	—	—
Solketal	$C_6H_{12}O_3$	132	1.065	10.3	23.0	—	36.4
Triacetin	$C_9H_{14}O_6$	218	1.159	19.8	18.0	—	44.0
Methanol	CH_4O	32	0.792	—	20.0	109	50.0
Ethanol	C_2H_6O	46	0.785	—	26.9	109	34.8
Isopropanol	C_3H_8O	60	0.785	—	30.4	117	26.7
n-Butanol	$C_4H_{10}O$	74	0.810	—	33.1	98	21.6
Isobutanol	$C_4H_{10}O$	74	0.803	—	33.0	105	21.6
TPRF[g]	—	103	0.742	—	43.1	91	0

[a] Molecular weight
[b] Lower heating value
[c] Research octane number
[d] mono-GTBE
[e] "Mono-shifted" GTBE
[f] "Di-shifted" GTBE
[g] Toluene primary reference fuel

2.7 Summary

This Chapter initially discussed some engine-related phenomena, such as soot emissions in diesel engine and knock in SI engines, that can be strongly affected by the use of alternative fuels. More specifically, since biofuels typically have oxygen in their chemical composition, the role it plays on soot formation and knock occurrence was presented. The presence of fuel-bound oxygen is usually associated with a reduction in the formation of soot in diesel engines and the suppression on the onset of knock in SI engines. However, it is known that chemical structure can also play a role in the soot and knock processes in engines. In addition, the well-known CFR engine was introduced. Subsequently, the topic of glycerol valorization was presented, along with a discussion of how the glycerol derivatives investigated in this work could be used. Likewise, the C_1–C_4 alcohols were introduced and their potential for fuel applications was discussed. Having introduced the "boundary conditions" surrounding the present work in Chapter 1, then the background information on the topics relevant to this study in this chapter, it is now time to delve into the experimental part of the dissertation, the core of the study, and the subject matter of Chapters 3 through 6.

Chapter 3

Light-Duty Diesel-Engine Tests

3.1 Introduction

After a presentation of the pressing issues regarding environmental concerns, and the role of internal combustion engines and biofuels as a motivation for carrying out this work (Chapter 1), along with a review of the pertinent background related to it (Chapter 2), the present chapter introduces the experimental core of this dissertation. The engine experiments described herein represent the preliminary assessment of the *BioRen*'s project target compounds, namely GTBE and isobutanol, as diesel fuel oxygenates. These tests were performed on a light-duty (i.e. passenger car) 4-cylinder Volvo engine installed in a test cell at Lund University. This experimental campaign was aimed at evaluating the potential of GTBE and isobutanol, when used as fuel additives, to reduce the exhaust emissions from the engine without compromising its performance. Blends of conventional fossil diesel fuel with either GTBE or isobutanol were prepared and tested, while fossil diesel was used as a baseline. Since the emission-reducing benefits of oxygenated fuels are a function of their oxygen content, the diesel-GTBE and diesel-isobutanol blends were prepared based on a fixed fuel oxygen content, so that a more meaningful comparison could be made. The exhaust emissions investigated included soot and NO_x, that are critical for diesel engines, plus unburned hydrocarbons and carbon monoxide. Being fundamental engine performance measures, the brake power was also measured, along with the brake specific fuel consumption.

In the wake of Volkswagen's "Dieselgate" scandal [4] and also due to the broader climate-related issues, the popularity of diesel-powered passenger cars has waned in recent years (as an example, Volvo Cars has recently discontinued the production of diesel vehicles [194]. Understandably, the rationale for doing experiments on light-duty diesel engines in the first place can be called into question. However, light-duty diesel powertrains will continue to be an important part of the so-called "legacy fleet" and diesel-powered cars will continue to be sold in many parts of the world in the foreseeable future. Therefore, the topic of diesel fuel additives—and the experiments described in this chapter—are still relevant nowadays, even in the case of light-duty applications.

In the remainder of this chapter, as in subsequent ones, the engine characteristics are introduced, along with the specifications of the measuring instruments and a description of the fuels tested, followed by the test procedures. Then, the main results are presented and discussed, before an overall summary of the key findings concludes the chapter.

3.2 Materials and Methods

3.2.1 Engine

The light-duty diesel engine tests were performed on a 4-cylinder, Volvo D4204T diesel engine (Figure 3.1). It is a typical example of a modern passenger car diesel, which has been used in the company's compact and mid-sized models such as the Volvo V40, V60, and V70. In its stock configuration, the engine was fitted with a turbocharger, which was subsequently removed for installation in the test cell, where intake air was supplied by an external compressor (as per usual practice).

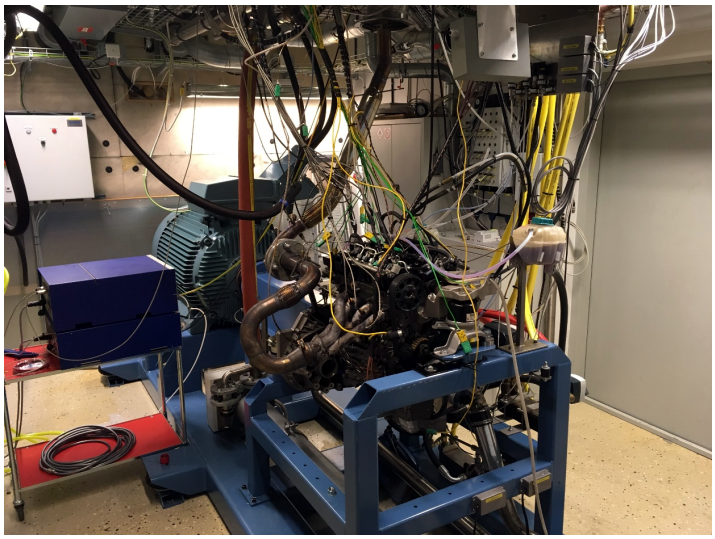

Figure 3.1: The Volvo D4204T engine in the test cell at Lund University.

Some basic specifications of the Volvo D4204T are shown in Table 3.1. As it is usually the case for a production engine, it is offered in several variants exhibiting different performance characteristics, depending on the vehicle in which it is installed, as the ranges for rated torque and power in the table show.

Table 3.1: Basic specifications of the production Volvo D4204T engine.

Volvo D4204T Engine	
No. of cylinders	4
Compression ratio	15.8:1
Bore	82 mm
Stroke	93.2 mm
Displacement	1.969 L
Rated torque	280–480 N·m
Rated power	88–174 kW

3.2.2 Instrumentation

To provide mechanical load to the engine at the desired speeds, the engine was coupled to an ABB M2BA 355SMB 3-phase electric motor. Its rated power and speed were 335 kW and 2200 rpm, respectively. It was controlled by a stock ABB controller with an accuracy of 1 rpm. To measure brake torque, the Volvo D4204T

engine was fitted with an HBM T40B torque transducer mounted on the shaft from the ABB motor and the crankshaft position was determined by a Leine & Linde RSI503 incremental encoder. The in-cylinder pressure traces were obtained with a AVL GH14P piezoelectric pressure transducer, flush-mounted in the cylinder head. The in-cylinder pressure was pegged to the pressure in the intake manifold when the piston is in the bottom dead center position. Moreover, the absolute crank position was calibrated based on the peak motoring in-cylinder pressure having an offset of 0.4 crank angle degree before top dead center. This "thermodynamic loss angle", as it is sometimes called, is due to heat and blowby losses, which prevent the peak pressure from occurring at TDC [195, 196]. For the determination of the fuel consumption, the supply fuel tank was placed on a Sartorius MSE12201S scale and the fuel mass flow rate was obtained through the calculation of the rate of change of the fuel mass, which was done by the linear fitting of the fuel mass data measured by the scale. The intake air mass flow rate was measured with a Bronkhorst F106CI mass flow meter. The gaseous emissions (HC, NO_x, CO, CO_2, and O_2) were sampled and measured by an AVL AMA i60 emission bench whereas the soot emissions were sampled and measured with an AVL Micro Soot sensor (MSS). The engine was controlled and several test variables were recorded by a LabVIEW-based program.

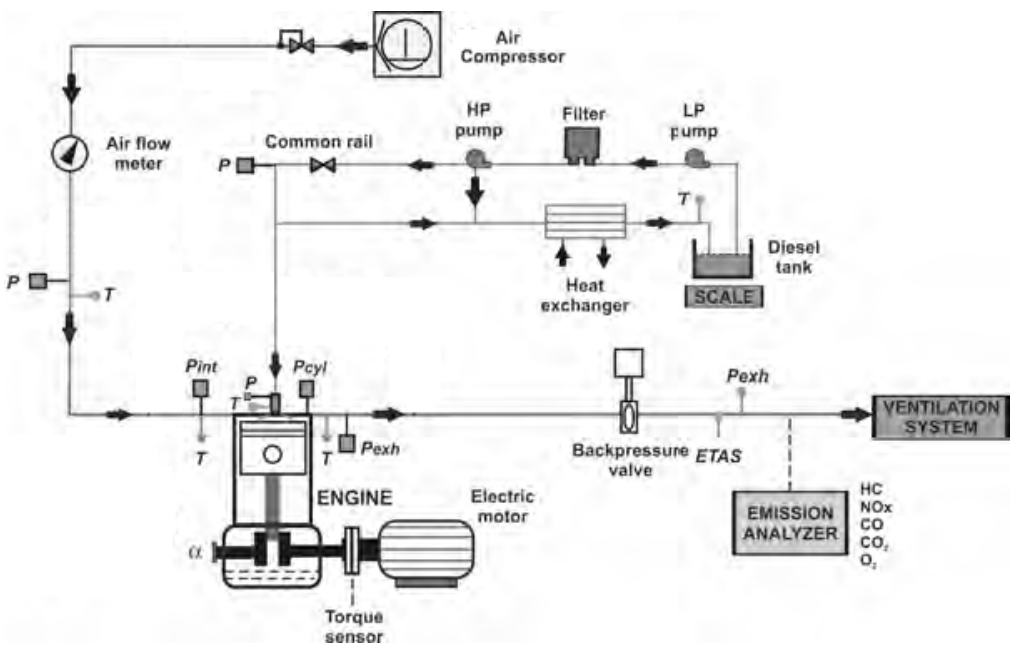

Figure 3.2: Schematic of the Volvo D4204T engine in the test cell.

A schematic of the test cell setup is shown in Figure 3.2 and the technical specifications of key instruments are shown in Table 3.2 [197].

Table 3.2: Specifications of key measuring instruments used in the tests.

Variable	Sensor Model	Measurement Range	Accuracy
Crankshaft position	Leine & Linde RSI503	0–6000 rpm	0.02 CA
In-cylinder pressure	AVL GH14P	0–250 bar	-
Fuel injection pressure	OEM sensor	0–2750 bar	-
Brake torque	HBM T40B	0–10000 Nm	0.05 % FS
Temperature	Pentronic 8105000	0–1100 degC	2.5 degC
Pressure	Keller 23SY	0–5 bar	0.7% FS
Intake air flow rate	Bronkhorst F106CI	0–900 kg/h	0.1% FS
Fuel flow rate	Sartorius MSE12201S	0–12200 g	0.1 g
Exhaust oxygen	ETAS ES635 + LSU4.9	0–25%	-
CO/CO_2	AVL AMA i60	0–1/16%	1% FS
NO_x		0–25%	
HC		0–10000 ppm	
O_2		0–25%	
Soot	AVL Micro Soot Sensor	0–50 mg/m^3	5 mg/m^3

3.2.3 Fuels Tested

As explained in Chapter 2, the GTBE compounds are comprised of three different components (mono-, di-, and tri-GTBE), depending on the extent to which glycerol has reacted with the etherification compound (isobutylene or *tert*-butanol), for a total of five isomers. In reality, however, the etherification reaction results in the simultaneous formation of all components, and the separation of any of them incurs additional costs. Therefore, for practical applications, GTBE is produced as a mixture of all three components, and the relative amounts of each are determined by the reaction conditions (such as temperature, pressure, reactant amounts, catalyst used, etc.) [138]. In other words, an "out-of-reactor" GTBE mixture (that is, without any component separation) is what would be typically used as an additive for motor fuel applications.

To prepare the fuel blend used in this chapter (see below), an out-of-reactor GTBE[1] was used, having the composition and properties shown in Table 3.3:

[1]The GTBE samples used in this work was supplied by Procede N.V. (Enschede, Netherlands), a *BioRen* project partner.

Table 3.3: Composition and properties of the "out-of-reactor" GTBE mix.

"Out-of-Reactor" GTBE					
mono-GTBE [wt.%]	**di-GTBE [wt.%]**	**tri-GTBE [wt.%]**	**Molecular Weight**	**Density [kg/dm^3]**	**LHV[a] [MJ/kg]**
18	64	18	197	0.911	32.6

[a]Lower heating value

For the light-duty engine experiments described in this chapter, the following fuels were used during the light-duty diesel test campaign. Some of their properties are listed in Table 3.4.

- Fossil diesel (reference fuel)
- A blend of 5.0 vol.% of the out-of-reactor GTBE with fossil diesel
- A blend of 6.5 vol.% isobutanol with fossil diesel
- A blend of 10.0 vol.% of the out-of-reactor GTBE with fossil diesel[2]

Table 3.4: Key properties of the fuels used in the tests.

Fuel/blend	**Molecular Weight**	**Density [kg/dm^3]**	**LHV[a] [MJ/kg]**
Fossil diesel[b]	170	0.810	43.2
5 vol.% GTBE	171	0.815	43.2
6.5 vol.% i-BuOH	157	0.810	42.5
10 vol.% GTBE	173	0.820	42.0

[a]Lower heating value
[b]Obtained from [77].

3.2.4 Test Matrix

The engine experiments were conducted at a constant speed of 2000 rpm, which is representative of regular driving, and at three torque levels: 70 N·m (referred to as "low load"), 140 N·m ("mid load"), and 280 N·m ("high load"). Table 3.5 shows

[2]This blend was used only at the 2000 rpm, 140 N·m operating condition.

the engine speed and load conditions used throughout the light-duty engine tests. No EGR was used throughout the tests.

Table 3.5: Experimental test matrix.

Point	Speed [rpm]	Brake Torque [N·m]	Brake Power [kW]	Rail Pressure [bar]
A1	2000	70	14.7	600
A2				800
B1		140	29.3	800
B2				1000
C1		280	58.6	1200
C2				1400

3.2.5 Test Procedure

At each speed/load condition, the following engine variables were varied:

- Start of (main) injection (SOI): 4 timings were tested, at 2 degree-intervals
- Rail pressure (RP): 2 different pressures were tested at each operating point

The variation of these two variables gives a valuable overview of the engine's behavior, which can be useful when testing different fuels. Overall, when the repetitions were taken into consideration, the results obtained in the tests comprised a total of 128 measurements.

Note on pilot injections

It should be noted that, as it is typical for modern production diesel engines, small pilot fuel injections are used. Especially in the case of high-speed light-duty diesel engines such as the Volvo D4204T, pilot injections have a significant influence on the engine's noise, vibration, and harshness (NVH) characteristics and vehicle drivability in general. For the experiments described in this chapter, the use of a pilot injection was necessary, since the Volvo engine would not run smoothly without one. Consequently, pilot injections with a constant separation of **8 crank angle degrees** before the main injection were always used. Table 3.6 shows the percentage of the total fuel represented by the pilot injections, for each fuel and

operational point. It can be seen that the contributions from the pilot injections tend to increase with decreasing load, since more fuel needs to be injected early to avoid the unstable combustion that may happen at such lower loads.

Table 3.6: Percentage of fuel energy from pilot injections.

Point	Diesel	5 vol.% GTBE	6.5 vol.% i-BuOH	10 vol.% i-BuOH
A1	27%	27%	27%	—
A2	28%	30%	30%	—
B1	25%	26%	26%	25%
B2	26%	27%	27%	27%
C1	21%	21%	21%	—
C2	24%	24%	24%	—

3.3 Results and Discussion

The tests results presented and discussed below include the brake power, main exhaust emissions and the brake specific fuel consumption. For the sake of conciseness, most of the presented results are from the mid-load engine operating condition (2000 rpm, 140 N·m), since this is the operating point at which the 10%-GTBE blend was tested.

3.3.1 Brake Power

Some variants of the Volvo D4204T engine offer 280 N·m as maximum brake torque. Therefore, for the experiments, the ”100% load” condition was chosen as corresponding to a brake torque of 280 N·m. At the speed of 2000 rpm, this torque level translates into a brake power of 58.6 kW (79.7 PS). Figure 3.3 shows the attainment of this power output at both rail pressure settings.

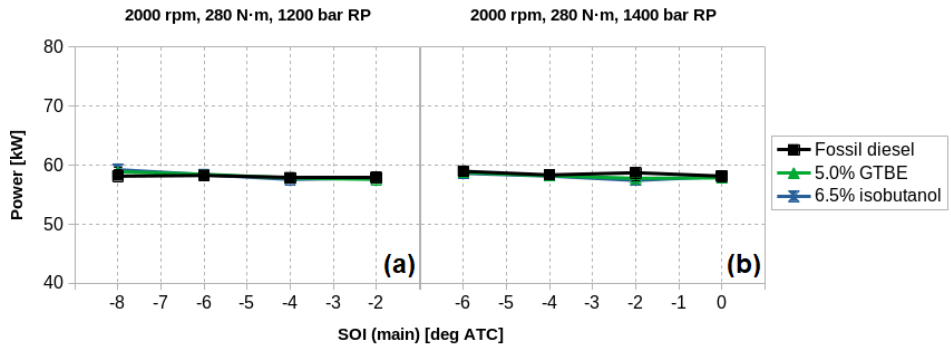

Figure 3.3: The maximum brake torque achieved during the experiments.

At this ”full load” condition, the relative air/fuel ratio (λ) was aimed at 1.4. The lambda values achieved at this operating point are shown in Figure 3.4.

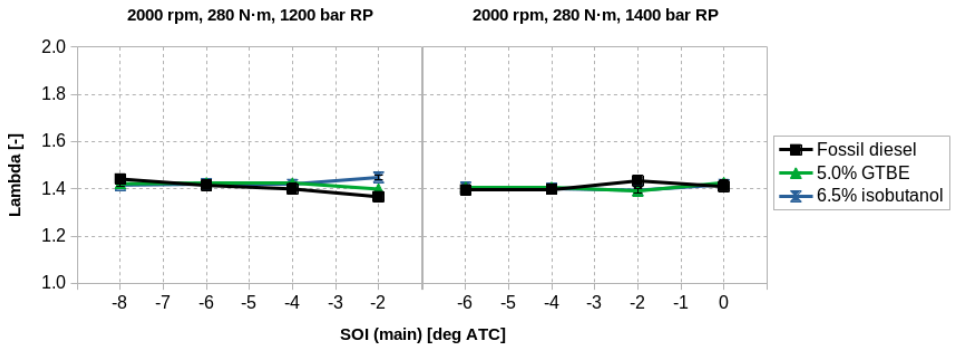

Figure 3.4: The measured relative air/fuel rations (lambdas) at full load.

3.3.2 Soot Emissions

Visible exhaust smoke is historically the pollutant most commonly associated with diesel engines, with soot being the major constituent of it. Therefore, it is not surprising that much effort has been spent on mitigating soot emissions, which can be accomplished by means of improvements in engine design, exhaust aftertreatment devices, or through fuel modification, which is the case in this work. The soot emissions corresponding to the low- and mid-load conditions—at both of their rail pressure settings—are shown in Figures 3.5 and 3.6.

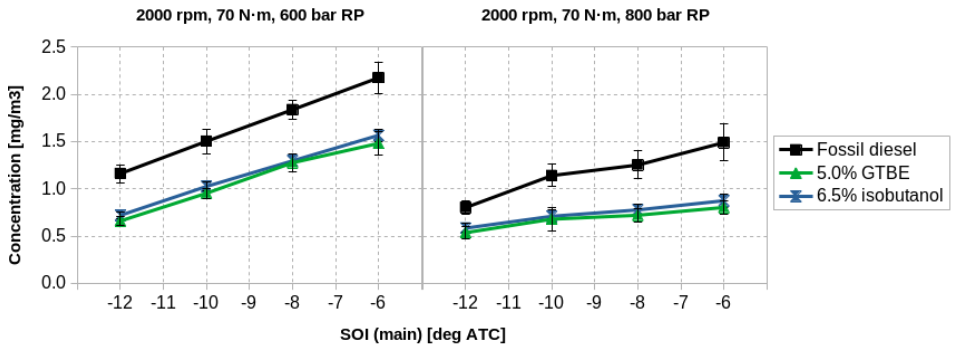

Figure 3.5: Soot emissions, 70 N·m.

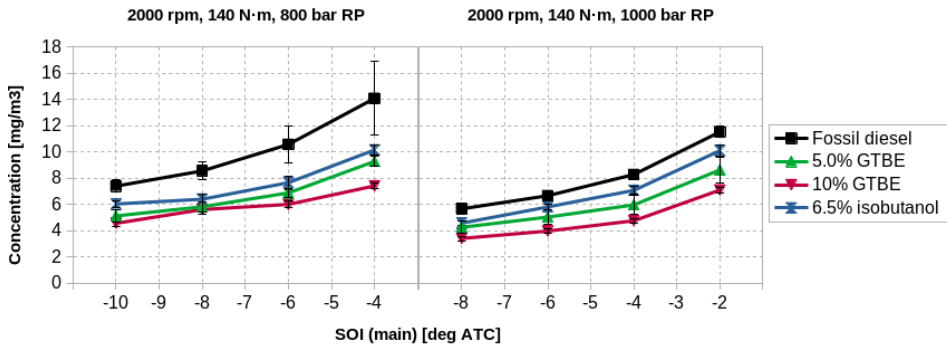

Figure 3.6: Soot emissions, 140 N·m.

At both of these engine operating conditions, the soot-inhibiting effect of the oxygenated compounds is evident. At the low-load condition, 70 N·m, a clear difference can be seen between the soot emissions from the fuel containing no oxygen—fossil diesel—and from the GTBE and isobutanol blends, although there was no obvious distinction between the performances of these two fuels. (It is also worth mentioning that, as expected, the soot emissions produced with the 800-bar rail pressure were lower than the soot concentrations obtained with the rail pressure of 600 bar.) In the 140 N·m case, however, the results show a clear correspondence between fuel oxygen content and soot emissions: the higher soot emissions were produced by fossil diesel, whereas the 10% GTBE blend, being the fuel with the highest levels of oxygen, gave the lowest concentrations. Intermediate values are exhibited by the 6.2% isobutanol and the 5% GTBE blends, with both blends containing the same amount of fuel oxygen. The lower emissions produced by the

GTBE blend may suggest a possibly lower tendency for soot formation in the case of GTBE, compared to isobutanol.

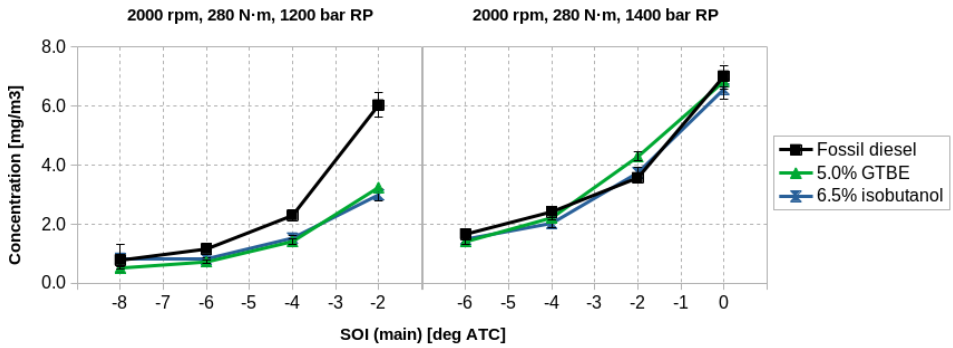

Figure 3.7: Soot emissions, 280 N·m.

However, at the full load condition (see Figure 3.7), the soot-reduction ability of the oxygenates was less evident. The results from the 1400-bar rail-pressure case seem very unclear, since the presence of fuel oxygen did not seem to produce any benefit at all, even though the soot concentrations in this case were far from negligible.

3.3.3 Hydrocarbon Emissions

The emissions of unburned hydrocarbons seemed to be the highest in the case of the isobutanol blend, Figure 3.8. This result does not seem at first to be related to the amount of fuel-bound oxygen, since the blend containing 10% GTBE gave results very similar to the results obtained with fossil diesel, a fuel without any oxygen. Regardless, the HC levels are very low, which is usually the case with diesel engines.

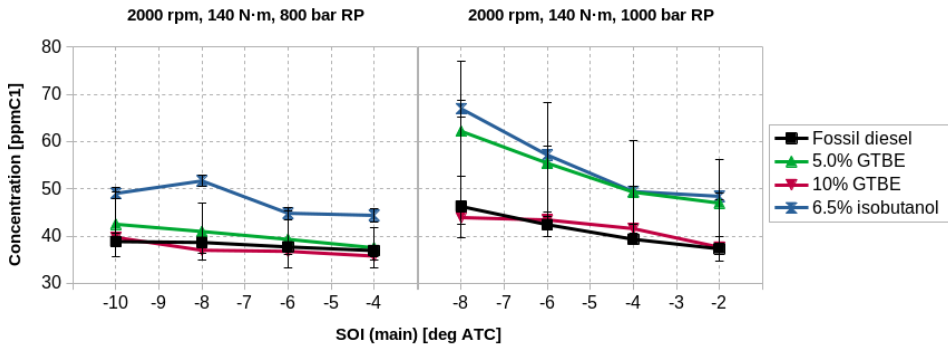

Figure 3.8: Hydrocarbon emissions, 140 N·m.

3.3.4 Carbon Monoxide Emissions

The trend corresponding to the emissions of carbon monoxide is not very clear, as seen in Figure 3.9. The oxygenated blends gave results showing CO emissions that were both lower and higher than the baseline diesel fuel. In any case, engine-out CO emissions from diesel engines are typically low (compared to SI engines) and are therefore not a matter of concern.

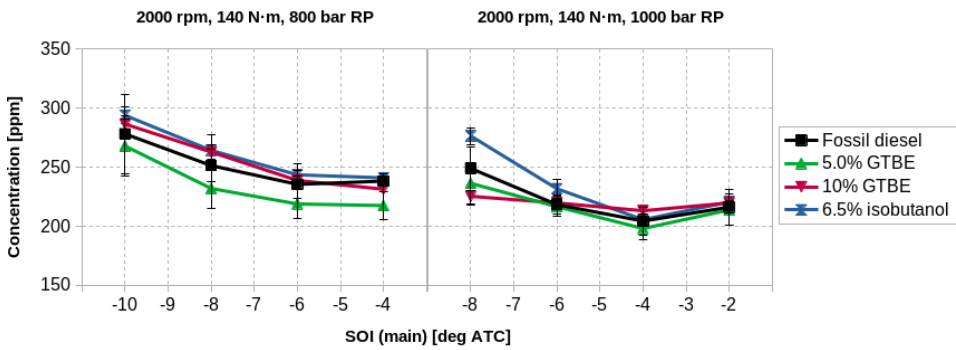

Figure 3.9: Carbon monoxide emissions, 140 N·m.

3.3.5 Nitrogen Oxide Emissions

The emissions of NO_x (the combination of the NO and NO_2 emissions), are very significant in the case of diesel engines. However, in the present case, an anomaly

was detected in the results: as Figure 3.10 shows, the NO_x concentrations related to the earliest SOI settings were virtually unchanged, when compared to the previous SOI values. This effect is more evident in the case of the rail pressure of 800 bar, where the NO_x emissions of the 5% GTBE blend were *lower* at the SOI of -10 deg BTC, compared to the previous SOI, 8 deg BTC. Interestingly, this anomalous behavior was exhibited by all fuel blends, at all operating conditions.

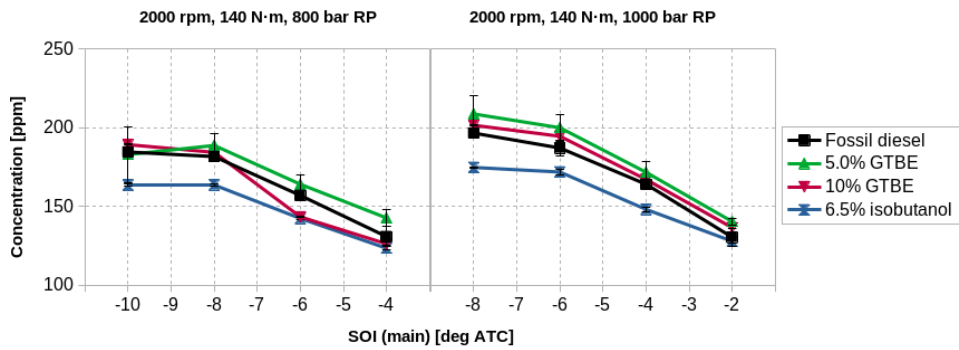

Figure 3.10: Nitrogen oxide emissions, 140 N·m.

3.3.6 The Soot-NO_x Trade-Off

The combined behavior of the soot and NO_x emissions is very important in the case of diesel engines, running on conventional fuels, due to the fact that mitigating one typically causes an increase of the other, the so-called soot-NO_x trade-off. The presence of fuel-bound oxygen—through the addition of oxygenated compounds to the base diesel fuel—is known to minimize or even eliminate this phenomenon [61].

Figures 3.11, 3.12, and 3.13 show the soot-NO_x behavior at all three speed-load testing conditions. The arrows indicate the direction of advancing injection timings.

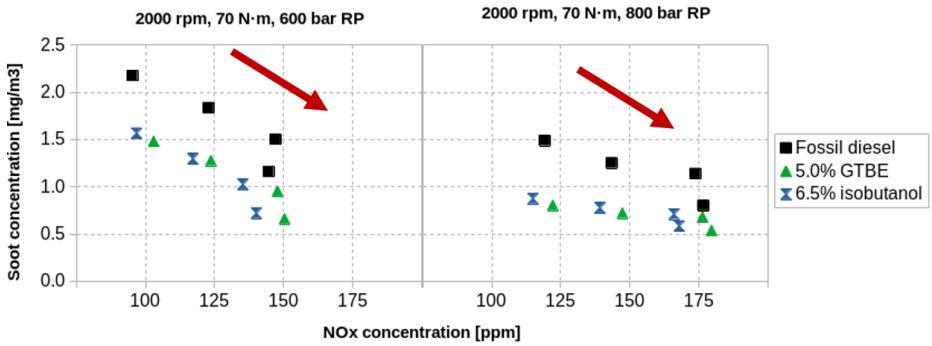

Figure 3.11: The soot-NO_x trade-off, 70 N·m.

At both 70 N·m and 140 N·m conditions, the presence of fuel oxygen caused the soot concentrations to drop, at the NO_x levels shown, represented by the markers below the diesel fuel's black square markers. The previously mentioned NO_x anomaly is displayed in both plots, where the markers corresponding to the last SOIs are essentially below the markers corresponding to the SOI immediately before, indicating a NO_x level that has not changed.

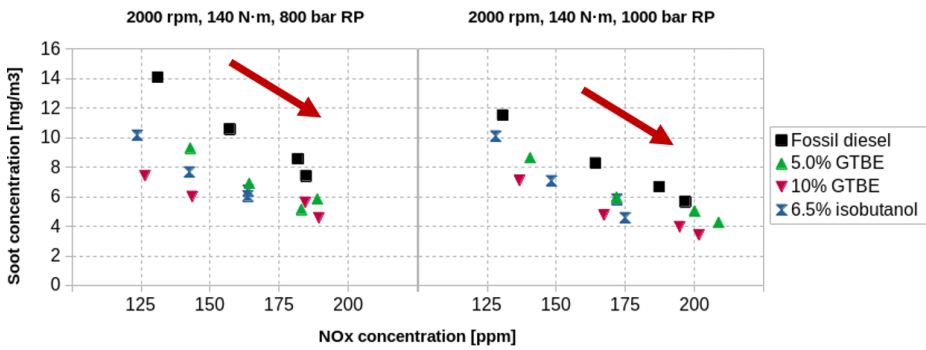

Figure 3.12: The soot-NO_x trade-off, 140 N·m.

In the case of the highest load (Figure 3.13), the influence of the oxygenates was less clear, since most of the markers are clustered together, especially in the 1400-bar case (in agreement with the soot levels seen in Figure 3.7 above). Moreover, the NO_x anomaly can still be seen in the plots, especially also in the 1400-bar rail pressure condition, in the clusters located in the lower right corner of the plot.

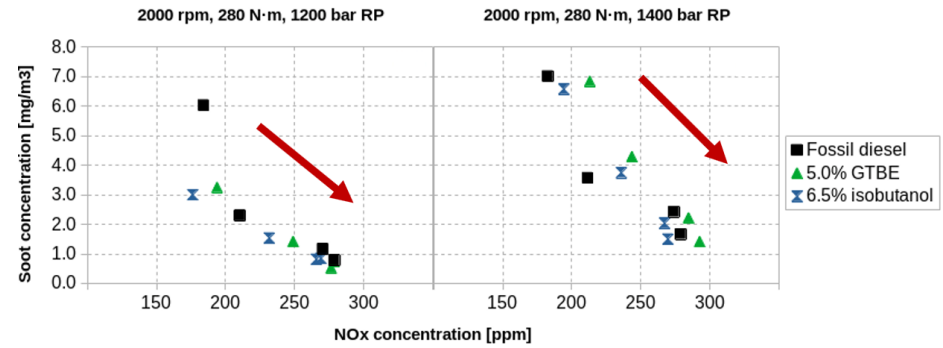

Figure 3.13: The soot-NO_x trade-off, 280 N·m.

3.3.7 Fuel Consumption

The brake specific fuel consumption results are shown for the full load and also for the mid-load (2000 rpm, 140 N·m) conditions. In the 140 N·m case, Figure 3.14, the results were rather consistent, since the blend that supposedly has the lowest heating value (the one containing 10% GTBE) corresponded to the highest fuel consumption, whereas fossil diesel exhibited the lowest consumption, due to its higher heating value.

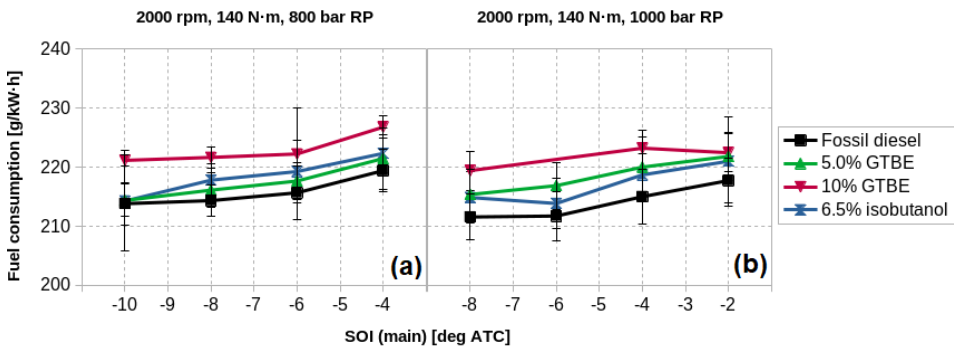

Figure 3.14: Brake specific fuel consumption, 140 N·m.

However, in the full-load case, Figure 3.15, the situation is unclear since there are no obvious differences among the fuels. Also, the large error bars seen in the plots, which indicate a large variability in the measurements, suggest that the fuel consumption data were not reliable in this particular condition.

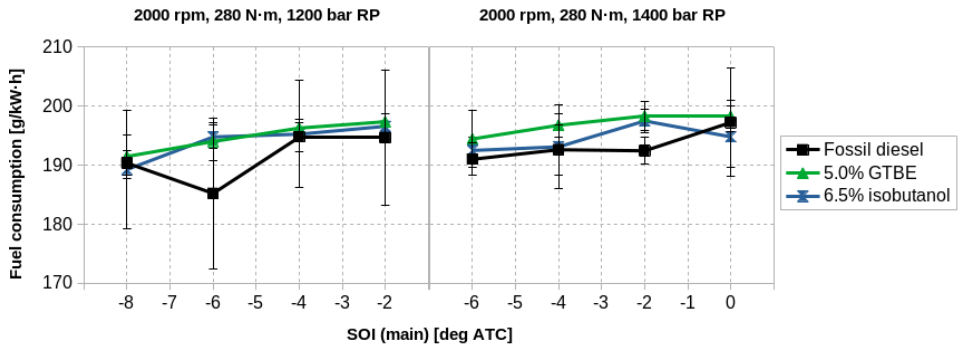

Figure 3.15: Brake specific fuel consumption, 280 N·m.

3.4 Summary

This chapter is the first of the ”experimental” chapters in this monograph. It describes engine experiments designed to investigate the influence of GTBE and isobutanol, as fuel blend components, on the performance and emissions of a light-duty multi-cylinder diesel engine. Those experiments served as an initial screening for the subsequent, heavy-duty tests described in the next chapter. More specifically, the diesel-GTBE and the diesel-isobutanol fuel blends were prepared in such a way as to exhibit the same fuel oxygen level, that is, the amount of oxygen of the 5 vol.% GTBE blend. The first results described in this chapter show that both oxygenated blends were able to produce the same maximum torque levels as in a production Volvo engine of the same type. In other words, the blends could deliver the same brake power as a corresponding stock Volvo engine installed on a vehicle. These results are not exactly surprising, since the intention of such low-concentration blend is to be able to be used in unmodified engines (or at least as minimally modified as possible) as ”drop-in” fuels. Regarding the exhaust emissions, both the GTBE and the isobutanol blends performed well in the case of the soot emissions, an important finding since soot (i.e. exhaust smoke) is the pollutant against which diesel oxygenates are primarily expected to be effective. The soot-reducing abilities of both GTBE and isobutanol were particularly evident in the low-load (70 N·m) and mid-load (140 N·m) cases. However, in the ”full-load” operating condition (280 N·m), the soot-reducing effect was less clear. This might have been due to the fact that the higher cycle temperatures at higher loads had

a stronger influence on soot oxidation, thus masking the soot-decreasing effects of the oxygenates. In the case of the hydrocarbon and carbon monoxide emissions, the performance of both blends was not as apparent as in the soot case. The hydrocarbon levels produced by the fossil diesel fuel seemed to be the lowest, and so did the levels from the 10% GTBE blend. According to the results of the carbon monoxide emissions, the situation was less clear in the sense that the oxygenated blends produced CO emissions at levels that could be either lower or higher than the fossil diesel emission results. In any case, regarding both the HC and CO emissions, their levels were always low (as expected from a diesel engine) and should not be a matter of concern. On the other hand, the NO_x emissions are very important in the case of diesels and, additionally, they can be difficult to control. Unfortunately, the NO_x emissions presented in this chapter exhibited an anomalous behavior in which the NO_x levels obtained at the most advanced SOI could remain essentially unchanged—or be even *lower*—than the levels produced by the immediately preceding, and later, SOI setting. What is interesting is that such behavior was seen at all engine operating conditions and with all tested fuels. Without taking this anomaly into consideration, the soot-NO_x trade-off results, in general, showed that the oxygenated blends were able to lower the soot emissions while keeping the NO_x levels constant, a pattern that was not visible in the full load condition (in which the soot-reducing benefits of the oxygenated blends were less evident). Finally, the fuel consumption data showed that the oxygenated blends increased the brake specific fuel consumption, a fact that is not surprising, since the presence of fuel-bound oxygen lowers the heating value of the base fuel, leading to worse fuel economy. This fuel consumption trend, however, was not evident in the full load case which, given the relatively large measurement variability (as evidenced by the large error bars), could indicate issues in the fuel flow measurement affecting the reliability of the fuel consumption data. All in all, the oxygenated blends seemed to perform well, particularly regarding the soot emissions without causing any negative impact on engine performance, therefore laying the groundwork for the heavy-duty diesel tests of the next chapter.

Chapter 4

Heavy-Duty Diesel-Engine Tests

4.1 Introduction

As previously discussed, the addition of oxygenated compounds to diesel fuel can reduce the exhaust particulate matter (PM) emissions from diesel engines due to, among other factors, the suppression of soot formation [66, 58]. As an example, oxygen-containing compounds that are derived from glycerol can effectively be used as diesel fuel additives, such as the glycerol *tert*-butyl ethers (GTBE) and also solketal and triacetin. The previous chapter demonstrated the use of such derivatives—and also isobutanol—as diesel oxygenates through engine tests carried out on a light-duty diesel engine. The results showed that those additives were effective in decreasing exhaust soot emissions and other pollutants. However, even though diesel is still widely used in light-duty applications (e.g. passenger cars), it has always mostly been used as a fuel for commercial vehicles, such as trucks, that are powered by medium- and heavy-duty engines. So, from a practical perspective, heavy-duty diesel engine applications are still relevant, while—as stated in the previous chapter—the popularity of light-duty diesels declined in the years after Volkswagen's "Dieselgate" scandal in 2015 [4]. Therefore, the present chapter complements the previous one by investigating the use of oxygenated compounds as blend components, this time on a heavy-duty engine.

The engine during the heavy-duty test campaign was a modified 13-liter Scania truck engine, originally having six cylinders, but converted to single-cylinder op-

eration. Regarding the fuels tested, in this chapter, the blends of the oxygenated compounds with fossil diesel fuel were prepared in two different ways: by mixing them based on a fixed fuel oxygen content (in which case their *concentrations* varied) and by mixing them at a constant ratio (in which case the blends' *oxygen content* varied). Thus, the experiments described in this chapter were divided into two parts, one for each of those conditions. However, the experimental setup, the test conditions and the test procedure were exactly the same in both cases.

4.2 Materials and Methods

This section describes the engine, the main test cell instrumentation, as well as the fuels tested and the test matrix and procedure.

4.2.1 Engine

The engine used in the tests was a Scania DC13 engine (Figure 4.1), originally having six cylinders, but converted to single-cylinder operation. This engine, in its stock configuration, is a typical example of an on-highway, long-haul, heavy-duty diesel engine. Its basic specifications are shown in Table 4.1 and a schematic of the test cell layout is shown in Figure 4.2.

Table 4.1: Basic specifications of the single-cylinder Scania DC13 engine.

	Scania DC13
No. of cylinders	1
Compression ratio	20:1
Bore	130 mm
Stroke	160 mm
Displacement	2.124 L

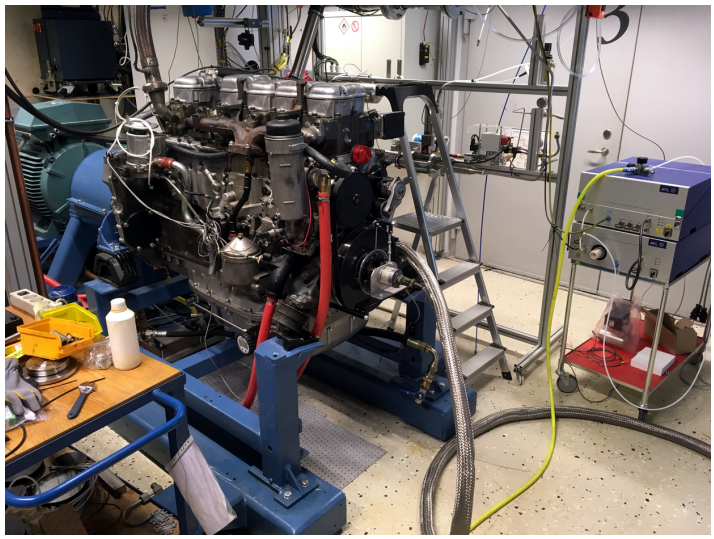

Figure 4.1: The Scania DC13 engine in the test cell at Lund University.

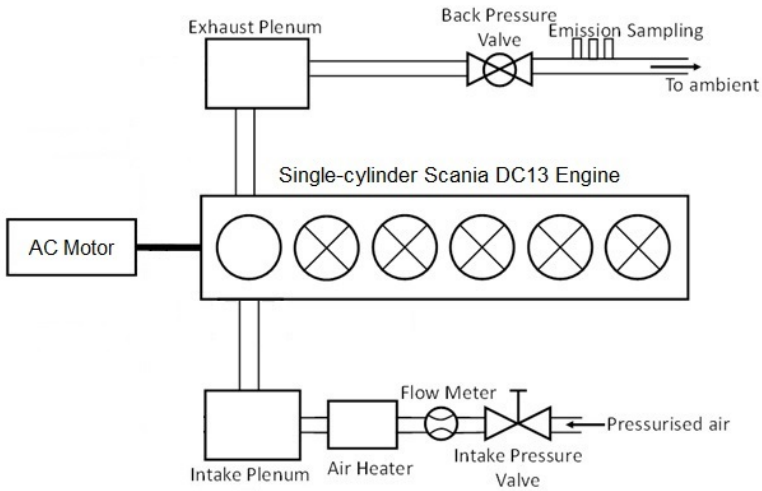

Figure 4.2: Simplified schematic of the engine installation in the test cell.

4.2.2 Instrumentation

The engine was coupled to an ABB M2BA 280SMB 3-phase electric motor, rated at 90 kW, acting as a dynamometer and the crankshaft position was determined by a Leine & Linde Model 520026011 incremental encoder. The in-cylinder pressure

traces were obtained with a Kistler Type 7061B piezoelectric pressure transducer, flush-mounted in the cylinder head. The pressure traces were amplified by a Kistler Type 5011 charge amplifier. The in-cylinder pressure was pegged to the pressure in the intake manifold when the piston is in the bottom dead center position. Moreover, the absolute crank position was calibrated based on the peak motoring in-cylinder pressure having an offset of 0.4 crank angle degree before top dead center, as in the previous chapter. For the determination of the fuel consumption, the supply fuel tank was placed on a Radwag APP 10.R2 scale and the fuel mass flow rate was obtained through the calculation of the rate of change of the fuel mass, which was done by the linear fitting of the fuel mass data measured by the scale. The intake air mass flow rate was measured with a Bronkhorst F106CI mass flow meter. The gaseous emissions (HC, NO_x, CO, CO_2, and O_2) were sampled and measured by an AVL AMA i60 emission bench whereas the soot emissions were sampled and measured with an AVL Micro Soot sensor (MSS). The engine was controlled and test measurements were logged by a LabVIEW-based program.

The technical specifications of key instruments are shown in Table 4.2.

Table 4.2: Specifications of key measuring instruments used in the tests.

Variable	Sensor Model	Measurement Range	Accuracy
Crankshaft position	Leine & Linde Model 520026011	-	0.2 CA
In-cylinder pressure	Kistler Type 7061B transducer & Type 5011 amplifier	0–250 bar	-
Fuel flow rate	Radwag APP 10.R2	0–10 kg	0.01 g
CO/CO_2	AVL AMA i60	0–1/16%	1% FS
NO_x		0–25%	
HC		0–10000 ppm	
O_2		0–25%	
Soot	AVL Micro Soot Sensor	0–50 mg/m^3	5 mg/m^3

4.2.3 Heat Release Calculation

The rate of heat release was evaluated, based on the in-cylinder pressure trace, at each engine firing cycle and the results were obtained from the average value of 300 firing cycles. The heat release calculations were done according to the single-zone method outlined by Gatowski *et al.* [198] according to Equation (4.1) below,

assuming the crevice flows to be negligible. In this equation, Q is the *gross* heat release, θ is the crank-angle degree, γ is the ratio of specific heats, p is cylinder pressure, V is cylinder volume, and Q_{HT} is the heat transfer to the cylinder walls. In addition, the working fluid's temperature and composition were assumed to be uniform. Heat transfer was calculated from Woschni 's well-known correlation [199].

$$\frac{dQ}{d\theta} = \frac{\gamma}{\gamma - 1} p \frac{dV}{d\theta} + \frac{1}{\gamma - 1} V \frac{dp}{d\theta} + \frac{dQ_{HT}}{d\theta} \tag{4.1}$$

4.2.4 Test Matrix

The engine experiments were conducted at the engine operation conditions described in Table 4.3, whose designation is explained as follows: The "A" points represent a low-speed idle running condition, the "B" points are typical of a medium-speed high load condition, and the "C" points represent a higher-speed, mid-load condition. Each of these speed-load conditions was run at a higher ("1") and lower ("2") fuel rail pressure.

No EGR was used throughout the engine tests.

Table 4.3: Experimental test matrix.

Point	Speed [rpm]	Load (IMEP[a], gross) [bar]	Rail Pressure [bar]
A1	600	5	800
A2			600
B1	1200	20	1400
B2			1200
C1	1500	10	1200
C2			1000

[a]Indicated mean effective pressure

4.2.5 Test Procedure

The evaluation of the fuel blends was carried out by running the engine at the three speed and load conditions, and at the rail pressures described above, for a total

of six operating conditions. At each of those points the start of injection (SOI) timing was varied by two-degree increments, for a total of four SOI timings, and two consecutive one-minute measurements were taken at each point.

Therefore, one full experimental test matrix, as described by Table 3, comprised 48 one-minute measurements, representing three speed-load conditions run at two different rail pressures, with four SOI angles at each of those conditions, taking two consecutive one-minute measurements at each SOI setting. Except for the tri-GTBE blend (for which the matrix was run only once, due to the limited amount of additive available), the blends were tested by running the full matrix at least twice, meaning that at least a total of 96 measurements were carried out for each fuel blend. In other words, each test variable was logged for a total minimum of four minutes (two times two consecutive one-minute measurements).

Upon changing the fuel blends, the fuel lines were flushed thoroughly with the new blends, after which the engine ran for at least 15 minutes at medium load. Besides, before taking a measurement, the engine was left to stabilize until the exhaust temperature was roughly constant, which could take about two minutes at high load and up to 15 minutes at light load.

During the experiments, the intake air temperature was kept at 30°C and both the oil and coolant temperatures were kept at roughly 90°C.

4.3 Fuel Blends with Fixed Oxygen Content

In this section, the evaluation of the diesel-GTBE and the diesel-isobutanol blends was done by preparing the mixtures in such a way that they all had the same oxygen content as the diesel-5% GTBE blend. This is in accordance with the procedure employed in Chapter 3. However, unlike the previous chapter, in the present one the base diesel (with which the additives were mixed) was not neat fossil diesel, but rather B7 diesel (see paragraph below). Fossil diesel was used as a non-oxygenated reference fuel.

4.3.1 Fuels Tested

Throughout the tests, the fuels used as reference were:

- Fossil diesel
- B7 diesel

B7 diesel is a mixture of fossil diesel with 7 vol.% biodiesel (fatty acid methyl esters, FAME). This fuel is particularly relevant, as the diesel fuel sold at fuel stations in the E.U. contains a certain amount of biodiesel blended into it. (The European norm EN590 [200] allows up to 7 vol.% biodiesel to be blended into fossil diesel for transportation, hence the name B7). Another reason was the fact that, serving as a co-solvent, biodiesel was supposed to improve the miscibility of the "mono-shifted" GTBE (see below), in fossil diesel. Because of that, all of the fuel blends in this study were prepared using B7 as the base fuel.

To ensure that the B7 diesel used in the tests actually contained 7 vol.% biodiesel, the exact amounts of it were carefully measured and mixed with fossil diesel before the experiments.

In addition to fossil diesel and B7 diesel, the following oxygenated fuel blends were tested (all of which were made by mixing the additives with the previously prepared B7 diesel):

- 4.5 vol.% of a 75%/25% mixture of mono- and di-GTBE (representing a "mono-shifted" GTBE mixture[1])
- 5.0 vol.% di-GTBE (reference blend, see below)
- 6.4 vol.% tri-GTBE
- 6.2 vol.% isobutanol

The oxygen content of the 5 vol.% di-GTBE blend was estimated as being approximately 2 wt.% oxygen, assuming that biodiesel contains 11 wt.% oxygen, a typical value [202, 203].

Key properties of the fuels/blends used are listed in Table 4.4.

[1]Due to the fact that the reaction conditions were tweaked in order to shift the final composition towards mono-GTBE, as described in a patent by Versteeg and Wermink [201]. In other words, it is a mono-GTBE-rich mixture

Table 4.4: Key properties of the fuels/blends used in the tests (fixed oxygen content).

Fuel/Blend	Molecular Weight	Density [kg/dm^3]	LHV[a] [MJ/kg]
Fossil diesel[b]	170	0.810	43.2
B7 diesel[c]	176	0.815	42.7
4.5 vol.% M-S GTBE[d]	157	0.810	42.5
5.0 vol.% di-GTBE	177	0.819	42.1
6.4 vol.% tri-GTBE	180	0.818	42.4
6.2 vol.% i-BuOH	162	0.814	42.1

[a]Lower heating value
[b]Obtained from [77].
[c]Biodiesel properties obtained from [203].
[d]"Mono-shifted GTBE", i.e. a mix of 75 vol.% mono- and 25 vol.% di-GTBE.

4.3.2 Results and Discussion

The tests results shown below include fuel consumption and the exhaust emissions of soot, hydrocarbons (HC), carbon monoxide (CO), and oxides of nitrogen (NO_x). In order to save space, the focus is on the results corresponding to the lower rail pressures at each speed-load condition (see Table 4.3.. However, in the discussion related to the soot-NO_x trade-off, the results obtained with both lower and higher rail pressures are shown.

As the plots show, for all engine conditions tested, the results exhibited a clear and consistent trend, which is a good indicator of the quality of the data. The overall results can be summarized as follows:

Soot

Exhaust smoke is historically the pollutant most commonly associated with diesel engines, with soot being the major constituent of it. Therefore, it is not surprising that much effort has been spent on mitigating soot emissions, which can be accomplished by means of improvements in engine design, exhaust aftertreatment devices, or by fuel modification, which is the case in this work.

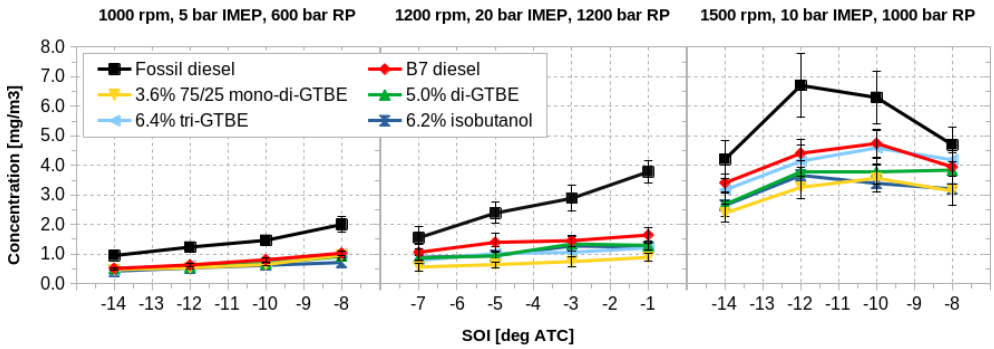

Figure 4.3: Soot emissions.

As expected, the results consistently show that fossil diesel, a fuel that contains no oxygen, produced the highest soot concentrations in all cases, as Figure 4.3 clearly shows. Moreover, and in accordance with its oxygen content, B7 diesel seemed to produce lower soot emissions than neat fossil diesel. The other oxygenated blends, which have a higher fuel oxygen level than B7, resulted in even lower soot levels. Even though the results exhibit some variability (as illustrated by the error bars), the 3.6% 75/25 mono-di-GTBE blend did seem to give the lowest soot emissions overall.

Hydrocarbons

Unlike the majority of spark-ignition engines, the fuel-air mixture in diesel engines is non-homogeneous and it is also overall lean (i.e. it contains excess air), therefore the hydrocarbon emissions are typically low for diesel engines, and this has been the case for all of the test results, see Figure 4.4. Moreover, as can be seen in all plots, fossil diesel produced the lowest hydrocarbon emissions, when compared to the oxygenated blends. The discrepancy was more evident at the low-speed, low-load condition (1000 rpm, 5 bar IMEP). A possible explanation is that, at the lower cycle temperatures characteristic of such light-load conditions, the presence of the oxygenated compounds worsened the combustion efficiency of the blends, resulting in higher unburned HC emissions. On the other hand, at the inherently high cycle temperatures of the high-load conditions, that decrease in combustion efficiency was much less noticeable, since the higher temperatures promoted fuel oxidation to some extent, regardless of the presence of the oxygenates.

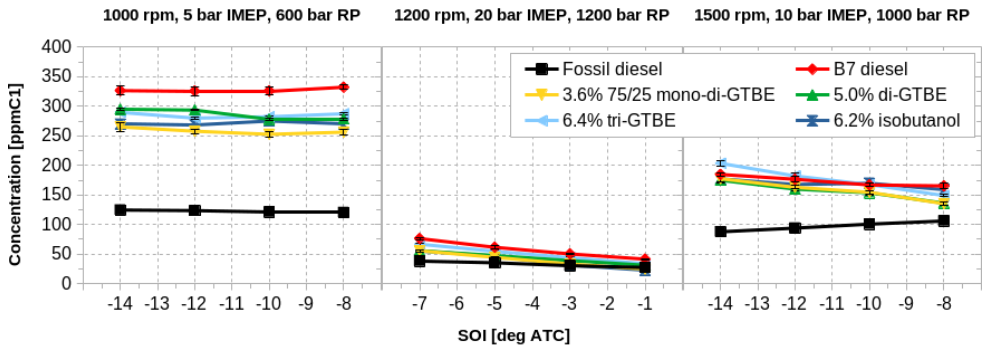

Figure 4.4: Hydrocarbon emissions.

Carbon Monoxide

As stated above, diesel engines always operate lean of stoichiometric and therefore the CO emissions are typically very low for diesel engines. In the test results, as seen in Figure 4.5, the CO levels increase with increasing load (and therefore, decreasing air/fuel ratio), since the behavior of CO formation is directly linked to the relative air/fuel ratio (λ). In most cases all fuels resulted in approximately the same CO levels. The increase in CO emissions with increasing engine speed might be attributed to the shorter combustion times at higher speeds, meaning that a larger fraction of CO will not be fully oxidized to CO_2.

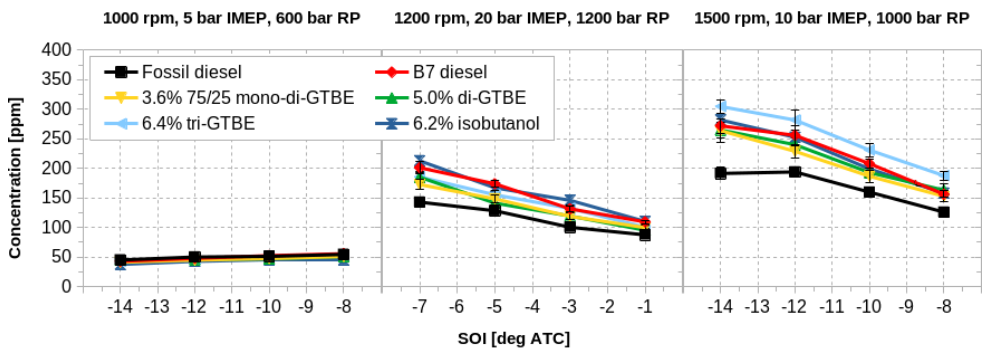

Figure 4.5: Carbon monoxide emissions.

Nitrogen Oxides

If the fuel does not contain any nitrogen—which is usually the case—the formation and emission of oxides of nitrogen (mostly nitric oxide, NO) is basically a function of the peak temperatures occurring during the combustion process. Because all of the oxygenated fuel blends contained additives in low amounts of oxygenates (biodiesel and GTBE), it is not expected that such compounds would cause a significant cooling of the combustion temperatures. Therefore, according to Figure 4.6, the NO_x emissions were very consistent for all fuel blends tested.

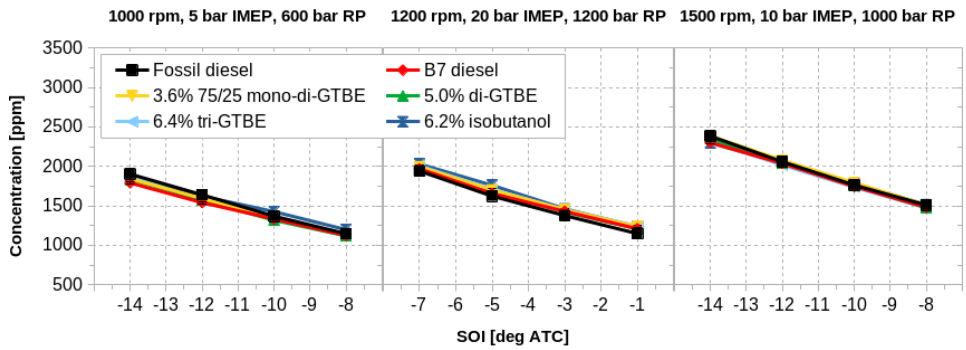

Figure 4.6: NO_x emissions.

The Soot-NO_x Trade-Off

As already mentioned in the previous chapter, the emissions of soot and oxides of nitrogen, when analyzed together, are very important in the case of diesel engines because mitigating one typically causes an increase of the other (the well-known soot-NO_x trade-off exhibited by diesel engines when running on conventional fuels).

The three plots in Figure 4.7 show the emissions of NO_x and soot for each fuel blend at each speed-load condition. At each plot, the results were obtained by varying the SOI angle at two-crank-angle-degree intervals, for a total of four measurements. For the sake of comparison, the three plots are shown with the same y-axis (soot) and x-axis (NO_x) scales. The arrows indicate the direction of advancing injection timings.

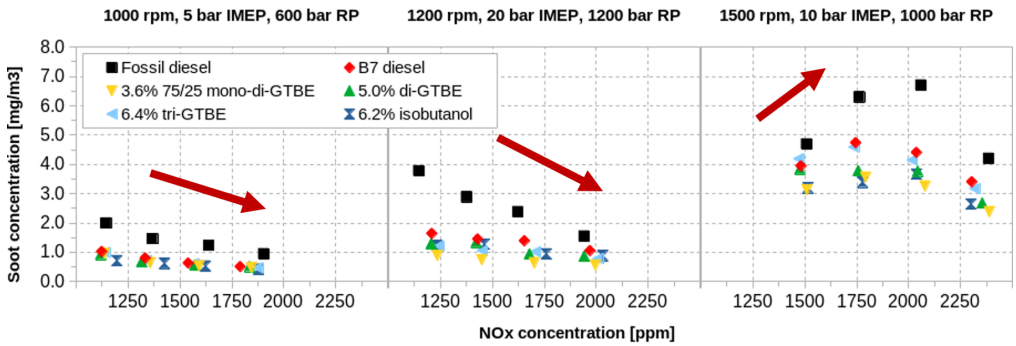

Figure 4.7: The soot-NO_x trade-off—lower rail pressures.

The plots show some interesting features. The soot-NO_x trade-off was clearly exhibited by fossil diesel in the 1200 rpm, 20 bar IMEP, 1200 bar RP case (the middle plot), since advancing the start of injection caused a significant decrease in soot emissions while at the same time increasing the NO_x emissions appreciably. On the other hand, the oxygenated fuel blends (appearing as the four "clusters" at the bottom of the plot), exhibited a rather different behavior. In this case, the soot emissions, as the SOI angles were changed, were essentially unchanged while the NO_x concentrations varied appreciably, producing "flat" soot-NO_x curves. Moreover, the GTBE blends, along with the isobutanol blend, despite containing more fuel-bound oxygen (approximately 2 wt.%), produced essentially the same reduction in soot emissions as the B7 diesel (which contains around 0.8 wt.% oxygen). Even though the soot levels are low relative to the range shown in the y-axis, a similar situation can be observed in the 1000 rpm, 5 bar, 600 bar RP case, where the oxygenated blends seemed to produce soot concentrations that were both lower and relatively constant as the NO_x values changed. In the 1500 bar, 10 bar IMEP, 1000 bar RP case, however, the overall results were less clear, since the soot emissions seemed to increase and then decrease with advancing SOI angles (a behavior which was more evident with fossil diesel). Other than that, the oxygenated blends resulted in lower soot emissions, this time with the blends containing more oxygen producing the lowest soot levels, compared to B7 diesel.

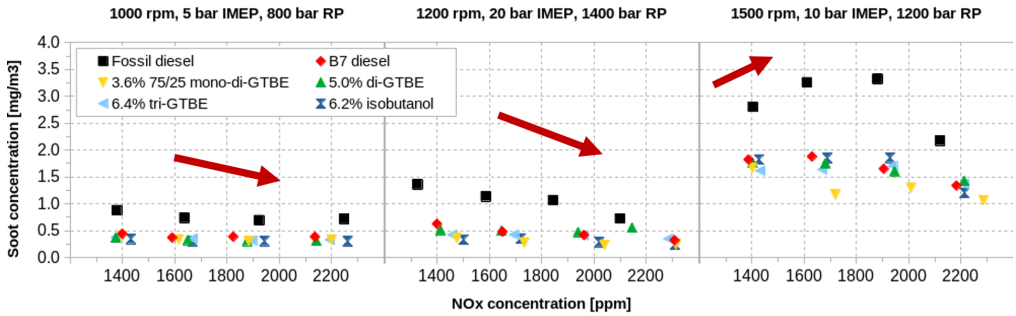

Figure 4.8: The soot-NO_x trade-off—higher rail pressures.

In the case of the higher rail pressures (800, 1400, and 1200 bar, Figure 4.8), besides the obvious lower soot and higher NO_x ranges displayed by the plots, the situation is slightly different, compared to the lower rail pressure case. First, at the high-load condition (1200 rpm, 20 bar IMEP), the oxygenated blends did decrease the soot emissions, since they are located below the black square markers representing fossil diesel. However, they also seemed to increase the NO_x emissions. This could be a result of the higher rail pressure—1400 bar—being more dominant, that is, increasing the NO_x emissions to a higher extent than decreasing the soot levels. On the other hand, this behavior was different for the low-load condition (1000 rpm, 5 bar IMEP). Here it is more evident that the oxygenated blends were able to lower the soot emissions without a NO_x penalty, as the clusters seem to be immediately below the black diesel markers. For the mid-load case (1500 rpm, 10 bar IMEP), the situation was less clear, as in the low rail pressure case described above, since the soot concentrations seemed to increase and then decrease with earlier SOI angles, a behavior that was more prominent in the case of fossil diesel.

For illustration purposes, the plot in Figure 4.9 shows the soot-NO_x results for all fuels, at all engine operating conditions tested, comprising a total of 144 measurements. The results from the "sootiest" condition (fossil diesel, 1500 rpm, 10 bar IMEP, 1000 bar rail pressure) are clearly seen at the top, whereas the oxygenated blends are clustered towards the bottom.

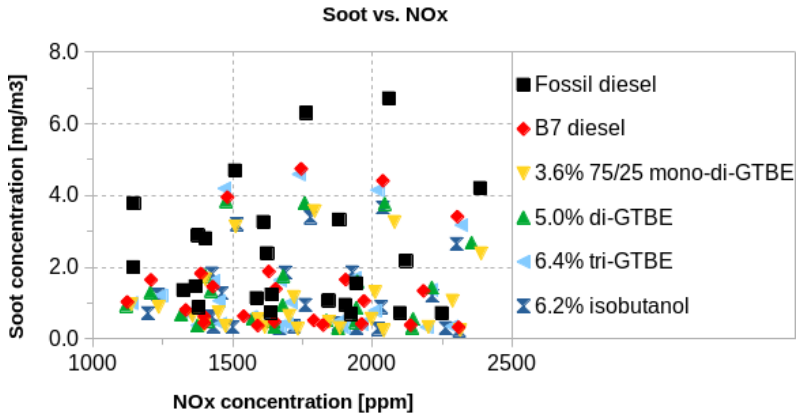

Figure 4.9: All soot-NO_x measurements.

Fuel Consumption

Fuel consumption is—unsurprisingly—essentially a function of the fuel's heating value. Because all blends tested contained the oxygenated additives mixed at low concentrations, the measured fuel consumption figures were not much different compared to the fossil diesel baseline. In addition to that, experimental issues in the fuel consumption equipment caused the final results to be rather unclear (especially in the 1000 rpm, 5 bar, 600 bar RP case). However, the difference in fuel consumption between the fuels tested is expected to be minimal, due to the differences in heating value not being very significant[2]. Therefore, fossil diesel should result in the lowest fuel consumptions, a fact shown in some of the plots in Figure 4.10.

[2]As an example, assuming diesel fuel to have a heating value of 43 MJ/kg, the addition of 7 vol.% of isobutanol (which has an LHV of 33 MJ/kg) would cause the blend to have an LHV of approximately 42.9 MJ/kg.

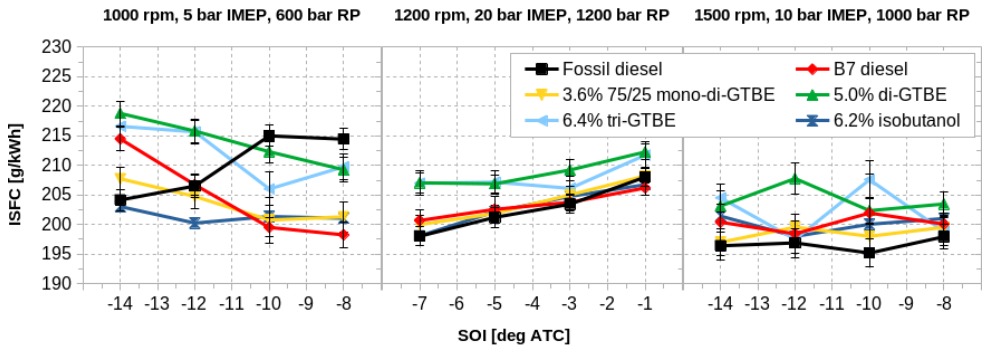

Figure 4.10: Indicated specific fuel consumption.

In-Cylinder Pressure and Rate of Heat Release

In the combustion analysis that follows, in addition to fossil diesel, only the 6.2 vol. % blend of isobutanol—the fuel containing the largest amount of oxygenate—was included. In this particular case, the plots correspond to the high-load (1200 rpm, 20 bar IMEP), high rail pressure (1400 bar) and earliest SOI (7 deg BTC) operating condition, the one that produced the highest peak value (slightly over 200 bar) and the highest rate of increase of in-cylinder pressure. It can be clearly seen from the plots in Figure 4.11 that the addition of the oxygenate compounds to the B7 base fuel did not result in any marked effect on the cylinder pressure traces and the corresponding heat release calculations. In other words, the effect of the oxygenated blends on the pattern and phasing of the combustion process was negligible. This is not surprising, since previous studies have reported similar results when GTBE was added in 10 vol.% concentration [204, 205] and even at a concentration of 20 vol.% [206, 207].

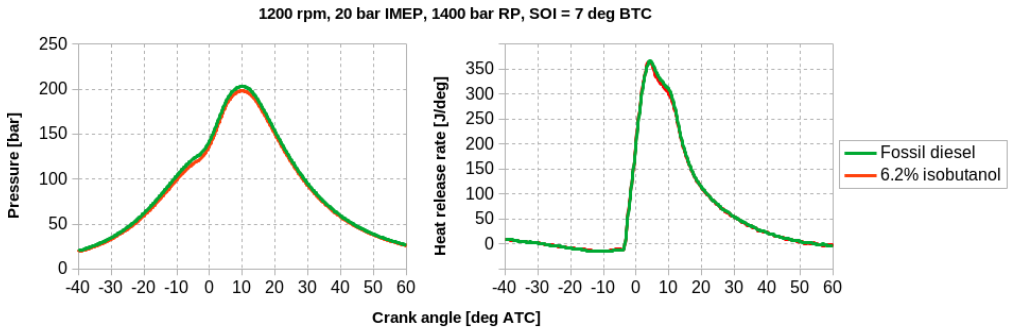

Figure 4.11: In-cylinder pressure and computed rate of heat release.

4.4 Fuel Blends with Fixed Additive Amount

In this section, the oxygenated fuel blends made for the engine experiments contained a fixed amount of the oxygenated compounds, in contrast with the previous section, where the blends had a fixed amount of fuel-bound oxygen.

4.4.1 Fuels Tested

For the engine tests described in this chapter, as before, two fuels were used as reference: neat fossil diesel and B7 diesel. As in the case of blends with fixed oxygen content, described in the previous section, the B7 diesel was the base fuel with which the oxygenated compounds were mixed.

In order to broaden the scope of this work, besides the GTBE compounds already mentioned, two additional glycerol derivatives were included in the present section: **solketal**, and **triacetin**. As discussed in Chapter 2, these compounds are the products of the reaction of glycerol with acetone and acetic acid, respectively, and also have the potential to be used as fuel additives.

Some relevant properties of the oxygenated additives are listed in Table 2.4, in Chapter 2.

The Oxygenated Blends

The oxygenated fuel blends investigated in this section were prepared by mixing the compounds listed below with B7 diesel at a *fixed* concentration of 4.0 vol.%. One reason for such low concentration relies on the estimated assumption that the amounts of biodiesel-derived glycerol available on the markets—based on the maximum 7 vol.% prescribed by the EN 590 standard [200]—would not be enough for the production of higher-concentration fuel blends in large scale. Indeed, since the amount of by-product glycerol is around 10 wt.% of the biodiesel output, the B7 mandate means that the actual concentrations of GTBE—or some other glycerol-based additive—mixed with the diesel fuel would be rather small. On the bright side, low-concentration blends are more likely to comply with the existing fuel standards and thus be used as drop-in fuels, that is, they should meet current fuel specifications and be able to be used in existing engines and infrastructure without modifications. The 4 vol.% additive amount was chosen in the hope of detecting noticeable effects.

Accordingly, the following 4 vol.% fuel blends with B7 diesel were prepared and investigated in this section:

- A 75%/25% mixture of mono- and di-GTBE (the "mono-shifted" GTBE—see above)
- di-GTBE
- tri-GTBE
- Solketal
- Triacetin (glycerol triacetate)
- Isobutanol

As discussed in Chapter 2, among the GTBE components, mono-GTBE is the cheapest one to produce, but in pure form it has poor solubility in diesel fuel. However, the addition of di-GTBE can improve its miscibility. Therefore, the GTBE mixture comprised of 75% mono- and 25% di-GTBE (i.e. the "mono-shifted" GTBE mix) represents a compromise between cost and solubility in diesel fuel, and for that reason it was included among the fuel blends investigated.

The GTBE samples used in the tests were provided by the *BioRen* project partner Procede B.V. (Enschede, Netherlands) and both solketal and triacetin were purchased from Sigma-Aldrich.

Key properties of the fuels/blends used are listed in Table 4.5.

Table 4.5: Key properties of the fuels/blends used in the tests (all additives blended with B7 at 4.0 vol.%).

Fuel/Blend	Molecular Weight	Density [kg/dm^3]	LHV[a] [MJ/kg]
Fossil diesel[b]	170	0.810	43.2
B7 diesel[c]	176	0.815	42.7
"Mono-shifted" GTBE	175	0.821	42.1
di-GTBE	177	0.818	42.3
tri-GTBE	178	0.817	42.5
Solketal	173	0.825	41.7
Triacetin	178	0.829	41.3
Isobutanol	167	0.815	42.3

[a] Lower heating value
[b] Obtained from [77].
[c] Biodiesel properties obtained from [203].

The results obtained with the oxygenated blends are presented and discussed in the following section.

4.4.2 Results and Discussion

For the sake of brevity, only the results for the "B2" condition (1200 rpm, 20 bar imep, 1200 bar RP) are discussed. Furthermore, due to the number of blends tested, in order to avoid clutter, the results are shown in two separate plots, both showing the results from fossil diesel and B7 diesel (as reference fuels).

All LabVIEW-based engine control program logged engine variables such as temperatures, flow rates, gaseous emissions and fuel consumption at a rate of 2 Hz. In addition, data from the micro soot sensor (MSS) was logged at 0.67 Hz. Finally, as previously stated, crank-angle based quantities were logged with a resolution of 0.2 crank angle degree.

Therefore, at 1200 rpm (i.e. 10 engine cycles per second) each one-minute individual measurement is a sample of 600 engine cycles, and the various test variables

were logged at the frequencies described above. As previously explained, except for the tri-GTBE blend, each result shown in the plots represents the average from at least four one-minute individual measurements combined. As in the previous cases, the error bars in the plots represent the variability in the results, calculated using the standard deviation of the logged measurements.

Soot Emissions

As commented before, it is well known that fuel-bound oxygen helps decrease exhaust soot emissions [61, 50, 208]. Therefore, the addition of the glycerol-derived oxygenates to the base diesel fuel was expected to lower the emissions of soot to some extent, when compared to the case of neat fossil diesel, since it does not contain any oxygen. In agreement with that, the plots in Figure 4.12 show that, in general, fossil diesel produced the highest exhaust soot concentrations, when compared to the oxygenated blends. However, even though the fuel blends containing oxygenates produced less soot than neat fossil diesel, the ability of the individual blends in lowering soot formation was not straightforward. The GTBE blends, despite containing more fuel-bound oxygen (approximately 2 wt.%), resulted in roughly the same decrease in soot emissions as the B7 diesel (which contains around 0.8 wt.% oxygen). This result should not be entirely unexpected, since a given fuel oxygen content can have different amounts of percent soot reduction [50], so there is not a fixed correlation between these two variables. In other words, more fuel oxygen does not necessarily result in less PM emissions. In their 2007 work, Tree and Svensson [50] discuss the results of a number of studies about the influence of oxygenated soot structure on soot reduction. While there are studies indicating that soot reduction is primarily a function of fuel oxygen content [61], in their article, Tree and Svensson also mention several studies concluding that fuel structure does play a role in reducing soot formation. In other words, fuels containing the same amount of oxygen—but with different structure—may produce significantly distinct levels of soot. Other studies indicating that an oxygenate's chemical structure has an influence on the overall PM reductions include the works of Delfort *et al.* [209] and Frusteri *et al.* [210]. In any case, the engine-out soot emissions for all tested fuels were very low, as is the case with a modern diesel engine equipped with a high-pressure common-rail fuel injection system.

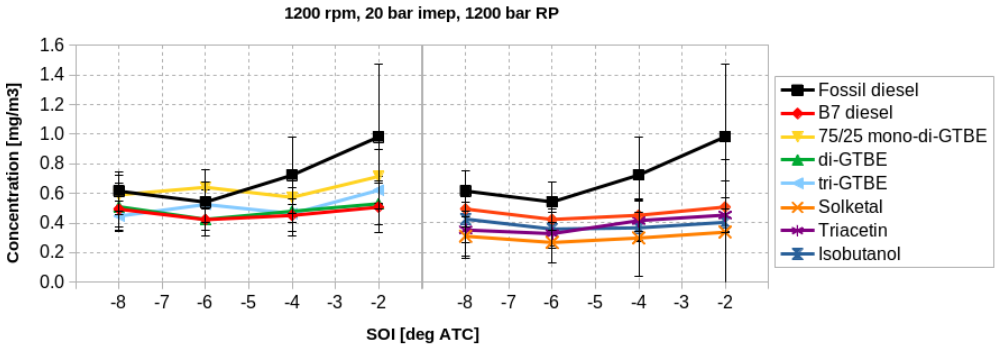

Figure 4.12: Soot emissions.

Hydrocarbons and Carbon Monoxide Emissions

Unlike spark-ignition engines, the fuel-air mixture in diesel engines is as a whole both non-homogeneous and lean. Therefore, the hydrocarbon emissions are typically low for diesel engines, and this has been the case for all of the test results. Moreover, as it can be seen in the plots in Figure 4.13, the oxygenated fuel blends produced the lowest hydrocarbon emissions, compared to fossil diesel. These results were likely due to a slightly improved combustion efficiency.

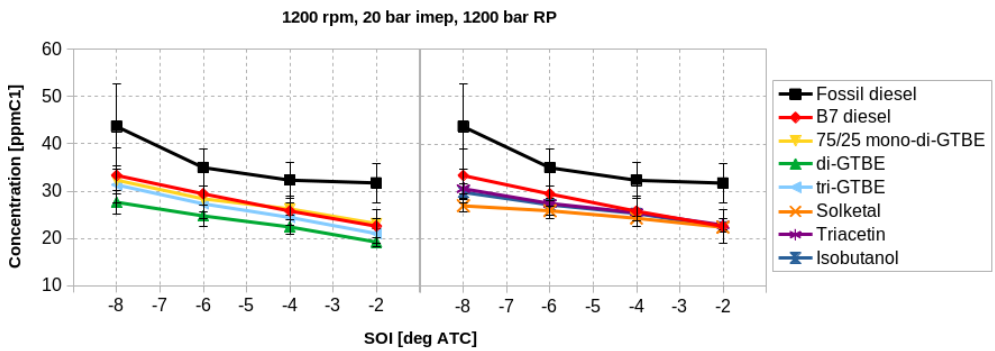

Figure 4.13: Hydrocarbon emissions.

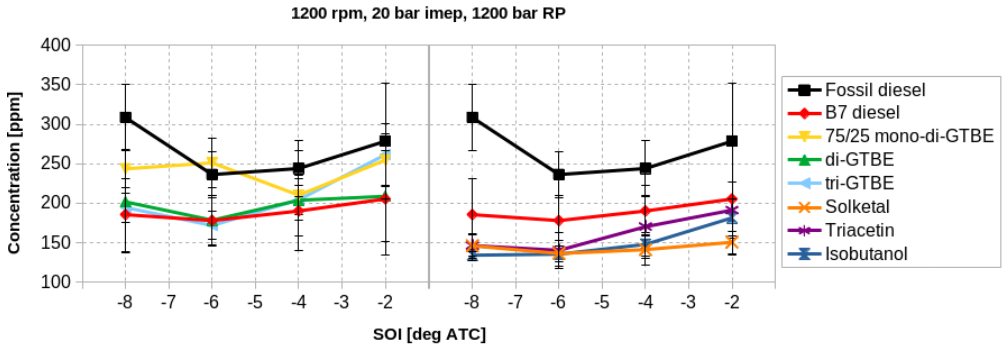

Figure 4.14: Carbon monoxide emissions.

Diesel engines always operate globally lean of stoichiometric and therefore the emissions of carbon monoxide are typically very low and as such they are usually not a matter of concern. In any case, based on the test results, shown in Figure 4.14, the CO emissions seemed to be slightly lower with the oxygenated blends.

The emissions of hydrocarbons and carbon monoxide can be thought of as a measure of combustion efficiency and, accordingly, a decrease in the cetane number of a fuel may result in higher concentrations of HC and CO in the exhaust [211]. In the present case, however, the low concentration of oxygenates in the fuel blends was most likely not enough to affect combustion completeness, which could have increased the emissions of hydrocarbons and carbon monoxide.

Nitrogen Oxide Emissions

In general, oxygenated fuels tend to result in higher NO_x emissions [212, 213, 214, 215]. This may be due to the increase in peak temperatures resulting from a more complete combustion process in locally rich zones, caused by the presence of oxygen in the fuel [206]. In addition, the extra oxygen available may either contribute to increase the formation of NO_x [207] or to decrease it, by lowering flame temperatures. In the present case, once more, the low concentration of oxygenates in the fuel blends was not enough to affect the NO_x emissions to a significant degree, as the plots in Figure 4.15 show that the NO_x variations are roughly in the range defined by the error bars (plus and minus one standard deviation of the mean value).

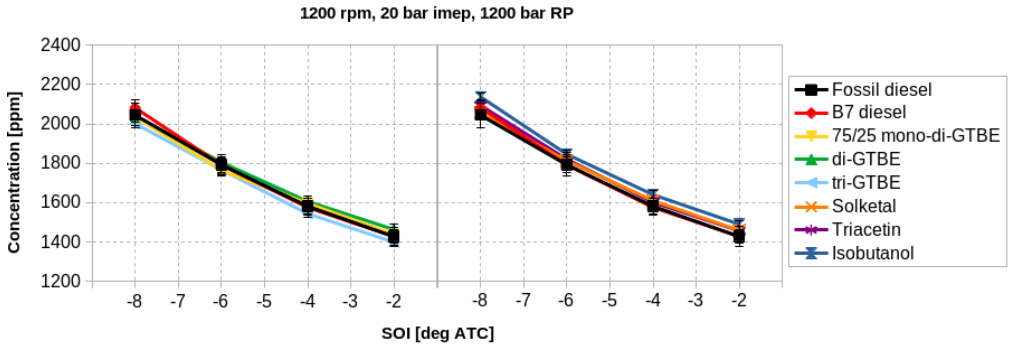

Figure 4.15: NO_x emissions.

The Soot-NO_x Trade-Off

As shown in Figure 4.16, fossil diesel clearly exhibits the soot-NO_x trade-off: advancing the start of injection (as illustrated by the measured points towards the right of the plots) causes a significant decrease in soot emissions while the NO_x emissions increase appreciably. The oxygenated blends, represented by the four "clusters" at the bottom of the plots, exhibited a different behavior, in which the NO_x emissions can be decreased without a significant penalty in soot formation—that is, the soot-NO_x curves are more or less "flat". In other words, the oxygenated blends exhibit the highest soot reduction at the same NO_x levels, a behavior that is typical of oxygen-containing fuels [206]. Also, for a given NO_x value, the oxygenated blends always produced lower soot levels, compared to fossil diesel. The arrows indicate the direction of advancing injection timings.

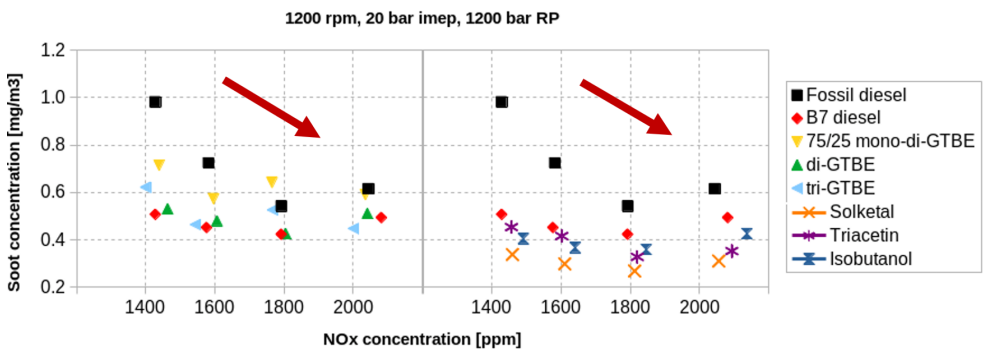

Figure 4.16: The soot-NO_x trade-off.

Indicated Specific Fuel Consumption

Fuel consumption is essentially due to the fuel's heating value, and variations in engine efficiency: the higher the heating value or the engine efficiency, the lower the fuel consumption for a given engine condition, and vice versa. Due to the small additive concentrations, the heating values of the fuel blends were not significantly different from the heating value of fossil diesel (see Table 4.5). Consequently, the fuel consumption figures with the oxygenated blends were not expected to be significantly higher than the fossil diesel fuel consumption (due to the decrease in heating value caused by the presence of oxygen in the fuel). In addition, it was not expected that the addition of small amounts of the oxygenated compounds would affect the engine's thermal efficiency. Finally, experimental uncertainty caused the final fuel consumption results to be fairly unclear and that might have exaggerated the differences among the tested fuel blends. It is also assumed that the uncertainty in fuel consumption was further amplified by the persistent presence of air bubbles in the engine's fueling system. Those were likely the result of the frequent fuel changes during the experiments with the corresponding flushing of the old fuel blends with the new ones. Regardless of all that, it can be noticed that fossil diesel, having a slightly higher heating value than the oxygenated blends, had the lowest fuel consumption in comparison to those blends, as the plots in Figure 4.17 illustrate.

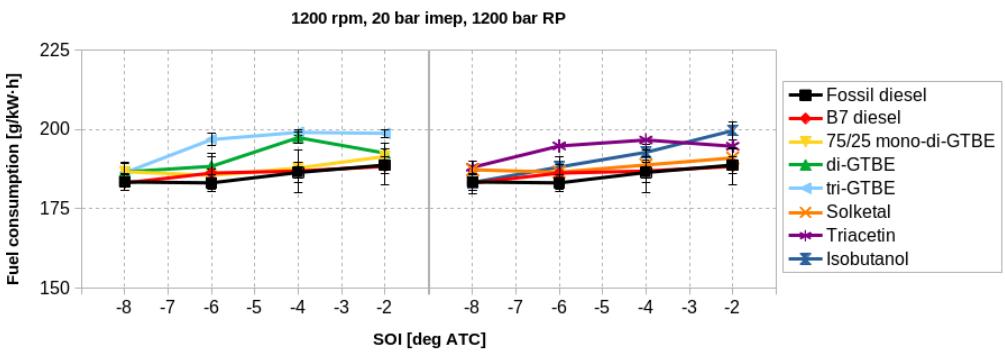

Figure 4.17: Indicated specific fuel consumption.

In-Cylinder Pressure and Rate of Heat Release

In the combustion analysis that follows, in addition to fossil diesel and B7 diesel, only the 4 vol. % blends of mono-, di-, and tri-GTBE, plus solketal and triacetin were included. As in the first part of this chapter, the chosen engine operating condition was 1200 rpm, 20 bar IMEP, 1400 bar RP, and an SOI of 7 deg BTC. Interestingly, as Figure 4.18 shows, the oxygenated blends exhibited lower peak release rates, when compared to fossil diesel. The reason this behavior is unclear, since the addition of those compounds, whose cetane numbers are believed to be low, should promote higher peak heat release rates. In a best case scenario their addition would not result in any significant impact, due to their low concentrations.

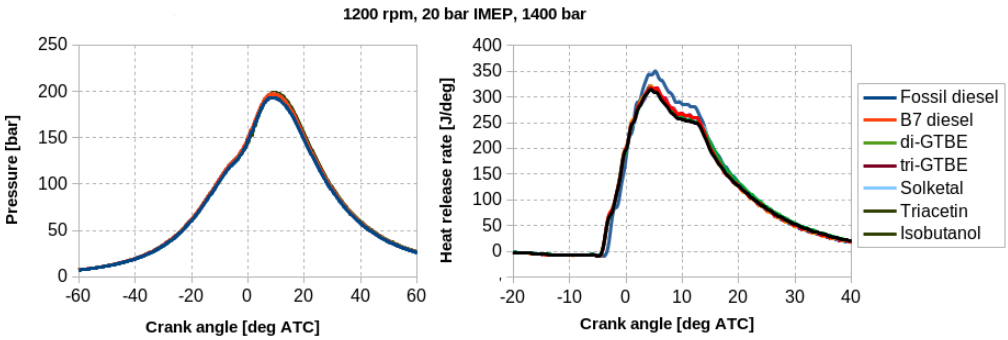

Figure 4.18: In-cylinder pressure and computed rate of heat release.

4.5 Summary

According to the results obtained from the heavy-duty diesel engine experiments, the emissions data, in general, were quite consistent. They also showed that the addition of the oxygenates in low concentrations—either at fixed oxygen or at a fixed additive content—did not cause any significant negative effects on engine performance and emissions.

Regarding the emissions, as expected, fossil diesel produced the highest levels of soot, since it has no fuel-bound oxygen. The oxygenated compounds, in general, seemed to improve the engine-out emissions of soot, hydrocarbons, and carbon monoxide, without compromising the NO_x emissions significantly. As seen in

the first part of this chapter, the GTBE blends, regardless of their higher oxygen content, did not always seem to perform better than B7 diesel, regarding soot emissions, suggesting that their different chemical structures, in addition to their oxygen contents, had an influence on the soot emissions.

The fuel consumption results, on the other hand, were unfortunately not very clear. This may be due to the minimal differences in heating value among the fuels tested, and also to instabilities in the fuel measuring equipment used throughout the experimental campaign. In any case, the volumetric fuel consumption with the oxygenated fuels was found to increase slightly, due to their lower heating value.

The overall findings suggest that the oxygenated diesel fuel blends containing the glycerol derivatives and the isobutanol described in this study, in low concentrations, have the potential to be used as drop-in fuels, that is, without requiring any engine modifications or changes to the already existing fuel infrastructure. However, one should interpret these findings with caution, since any commercial fuel blend must conform to the applicable fuel standards, which means that all the regulated physicochemical fuel properties (such as density, lubricity, volatility, etc.) must be within specified ranges. Therefore, a comprehensive fuel certification process would need to be carried out before the blends are commercialized.

Chapter 5

Spark-Ignition Engine Tests I: Surrogate-Oxygenate Blends

5.1 Introduction

As described in the previous two chapters, the glycerol derivatives, plus isobutanol, in general performed well as blend components for diesel fuel, being able to improve the soot-NO_x trade-off due to the presence of fuel-bound oxygen. Those results were observed in both the light-duty (Chapter 3) and heavy-duty (Chapter 4) diesel engine tests. This chapter now introduces and describes the spark-ignition (SI) engine tests, more specifically the evaluation of the different oxygenated compounds as gasoline blend components, whereas Chapter 6 deals with neat alcohol fuels. Moreover, in contrast with the preceding chapters, the present one expands the research scope even further, by including four new compounds to be investigated, namely methanol, ethanol, isopropanol, and *n*-butanol. In this chapter, these alcohols are evaluated in addition to isobutanol and the glycerol derivatives already introduced. For the SI tests, a modified Waukesha CFR engine was used throughout. A special focus of this—as well as the next—chapter is the characterization of the knock propensities of the different compounds studied. Being the standard device for the octane rating of SI fuels, the CFR engine proved to be a valuable and reliable tool for such purpose. This chapter then concludes with a general assessment and recommendations regarding the performance of the different compounds as gasoline oxygenates.

As discussed in Chapter 2, engine knock has a negative influence on the efficiency of spark-ignition engines, since it limits the maximum compression ratios that can be achieved. In addition, the possibility of knock occurrence may also restrict the ignition timings corresponding to MBT (maximum brake torque) operating conditions, especially at higher loads. These limitations on both the compression ratio and the spark timings preclude the attainment of higher overall engine efficiencies. Therefore, this negative impact of knock must be minimized as much as possible. Even if the likelihood of knock occurrence cannot be completely eliminated, it can be significantly decreased.

One way this can be achieved is by adding specific chemical compounds to the fuel, aiming at increasing its knock resistance. For instance, adding a suitable oxygenate to the base gasoline can improve its octane rating, which results in the attainment of higher compression ratios, boosting engine efficiency. Furthermore, if the oxygenate in question is produced from renewable sources, it has the potential to decrease net CO_2 emissions, thus contributing to the decarbonization of the transportation sector.

Ethanol is of particular relevance among gasoline oxygenates due to the fact that it can easily be biologically produced from a wide range of sugary or starchy feedstocks by a variety of techniques [108].

Even though ethanol is by far the most widely used gasoline oxygenate, other alcohols and also other types of chemical compounds have the potential to be used as gasoline additives. Therefore, this chapter describes engine experiments that were conducted to evaluate the potential of the glycerol-derived compounds and the alcohols introduced in Chapter 2, whereas Chapter 6 addresses the use of the C_1–C_4 alcohols as neat fuels for SI engines.

5.2 Methods and Materials

5.2.1 The CFR Engine

The Waukesha CFR engine, already introduced in Chapter 2, was the engine used for the SI experiments described in this work. Its technical specifications are shown in Table 2.1, and therefore will not be reproduced here. A picture of the CFR engine

used in this study is shown in Figure 5.1, and a schematic representing the overall experimental setup is shown in Figure 5.2.

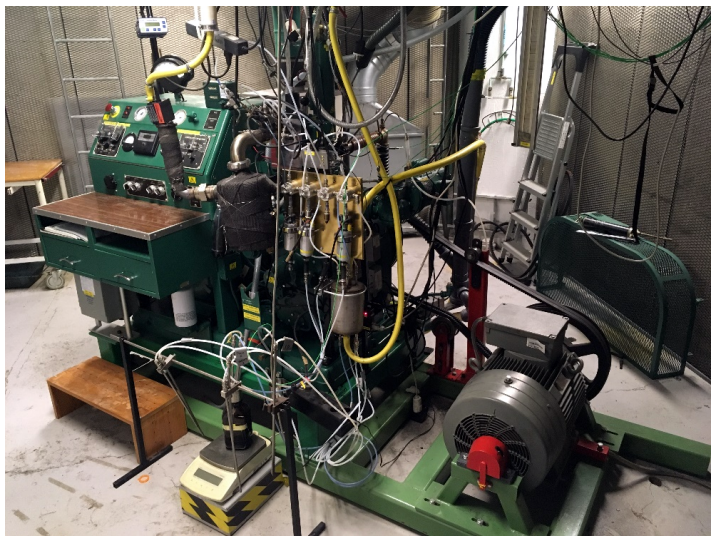

Figure 5.1: The CFR engine in the test cell at Lund University.

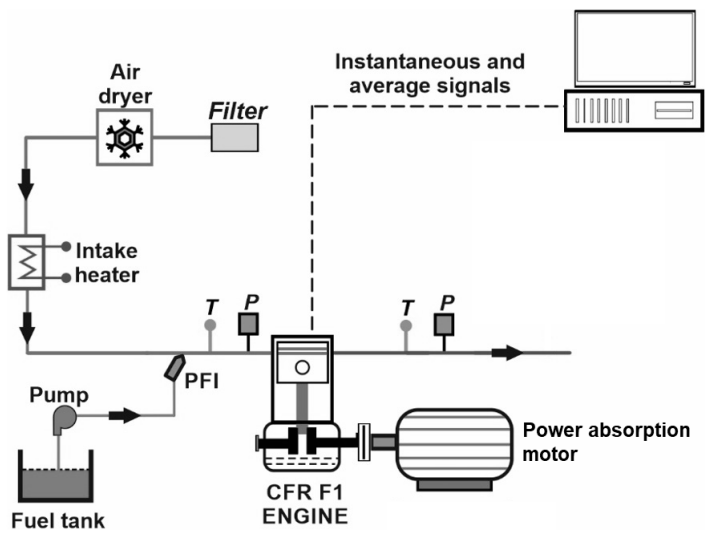

Figure 5.2: Schematic of the CFR engine setup. (T: temperature; P: pressure; PFI: port fuel injection).

5.2.2 Additional Instrumentation

For the tests described in this chapter, some of the engine's original systems remained unmodified, including the intake air refrigeration unit, which provides filtered and dehumidified combustion air, and also the cylinder jacket cooling system.

The main modification made on the engine was the removal of the original four-bowl carburetor assembly and the installation of four electronically controlled Bosch 0280150712 fuel injectors installed in the engine's intake runner. Additionally, the original power absorption electric motor was substituted with a Lönne 14BG 206-2AA60-Z motor, which was used to start the engine, absorb the power output of the engine and maintain constant engine speed. The modifications also included a Leister LE 3000 intake air heater mounted on the intake manifold. To measure fuel consumption, a Sartorius CPA62025 scale was used. The in-cylinder pressure trace was measured with a water-cooled Kistler Type 7061B piezoelectric pressure transducer mounted in the cylinder head and connected to a Kistler Type 5011 change amplifier. This transducer was installed in the same hole normally used by the D-1 Detonation Pickup, the pressure sensor used by the CFR engine in its original configuration. Crankshaft position was measured by a Leine & Linde RSI 503 22990963-06 shaft encoder, with a resolution of 1800 pulses per crankshaft revolution. The relative air–fuel ratio (lambda) was measured by a Bosch UEGO (universal exhaust–gas oxygen) sensor mounted on the exhaust pipe and coupled to an ETAS LA4 Lambda Meter. The control of the engine, as well as the logging of the experimental data were done by a custom-built LabVIEW 2011 program.

The in-cylinder pressure was pegged to the pressure in the intake manifold when the piston was in the bottom dead-center position (BC) of the intake stroke. Moreover, the absolute crank position was calibrated based on the peak motoring in-cylinder pressure having an offset of 0.4 crank angle degree before top dead center, according to the recommendations by Tunestål [195].

The measurement specifications of key measuring instruments are listed in Table 5.1.

Table 5.1: Measurement range and resolution of select measuring instruments.

Variable	Device	Range	Resolution
In-cylinder pressure	Kistler 7061B	0-250 bar	1.25 bar
Intake pressure	Keller PAA-33X	0-5 bar	250 Pa
Exhaust pressure		0-10 bar	500 Pa
Crank angle, engine speed	Leine & Linde RSI 503	0-6000 rpm	0.2 CAD [a]
Fuel consumption	Sartorius CPA6202S	0-6200 g	0.01 g
Gaseous emissions	AVL SESAM i60FT	0-max 10000 ppm	≤ 2% of the measured value

[a] CAD: crank angle degree.

5.2.3 Heat Release Calculation

The rate of heat release was evaluated, based on the in-cylinder pressure trace, at each engine firing cycle and the results were obtained from the average value of 1000 firing cycles. The heat release calculations were done according to the single-zone method outlined by Gatowski *et al.* [198] according to Equation (5.1) below, assuming the crevice flows to be negligible. In this equation, Q is the *gross* heat release, θ is the crank-angle degree, γ is the ratio of specific heats, p is cylinder pressure, V is cylinder volume, and Q_{HT} is the heat transfer to the cylinder walls. In addition, the working fluid's temperature and composition were assumed to be uniform.

$$\frac{dQ}{d\theta} = \frac{\gamma}{\gamma - 1} p \frac{dV}{d\theta} + \frac{1}{\gamma - 1} V \frac{dp}{d\theta} + \frac{dQ_{HT}}{d\theta} \tag{5.1}$$

Heat transfer was calculated from Woschni 's well-known correlation [199] and the heat release from motored cycles was subtracted from the fired heat release to reduce measurement and model errors [216]. The heat transfer model required the determination of the in-cylinder gas temperature at the time of inlet valve closing. This was calculated from the measured intake temperature, which was then corrected with a simple temperature model, taking into account the heating from intake walls and from mixing with hot residuals. A detailed description of the heat release calculations can be found in a previous study by Truedsson *et al.* [216], carried out on exactly the same engine.

5.2.4 Fuels Tested

The fuel matrix was comprised of a pure-hydrocarbon gasoline surrogate plus oxygenated fuel blends; that is, mixtures of that surrogate with each of the several oxygenated compounds, as described below.

The gasoline surrogate, referred to as TPRF (toluene primary reference fuel) in this chapter, is the non-oxygenated reference fuel in this chapter. This surrogate, described in a 2014 study by Foong *et al.* [217], was a blend of 53 vol.% isooctane, 17 vol.% *n*-heptane, and 30 vol.% toluene, resulting in a RON of around 91 and an H/C ratio of approximately 1.85. The H/C ratio is a very important property, because it determines the equivalence ratio, has an impact on the fuel's emission characteristics and on parameters such as the burning characteristics, adiabatic flame temperature, and heat of combustion [218, 219], and an H/C value of 1.85 represents a "customer average" regular-grade gasoline without added oxygenates [220]. Test reproducibility was the main reason for choosing a surrogate, instead of using commercial gasoline.

Some select properties of the TPRF blend are shown in Table 5.2.

Table 5.2: Select properties of the TPRF blend used in this chapter.

Toluene Primary Reference Fuel (TPRF)							
Isooctane [vol.%]	*n*-Heptane [vol.%]	Toluene [vol.%]	RON[a]	H/C	MW[b] [g/mol]	Density (20 °C) [g/L]	LHV[c] [MJ/kg]
53	17	30	91	1.85	103.1	742.1	43.1

[a]Research octane number
[b]Molecular weight
[c]Lower heating value

The oxygenated compounds that were blended with the surrogate consisted of a number of glycerol derivatives and C_1–C_4 alcohols, with the exception of the less common isomers of propanol and butanol, namely *n*-propanol, *sec*-butanol, and *tert*-butanol.

The oxygenated reference fuels, to which the oxygenated blends were compared were mixtures of TPRF with ethanol, at 10 and 20 vol.% blending ratios, referred to in this study as EtOH10.0 and EtOH20.0, respectively. The rationale for choosing

these particular blending amounts is that E10 and E20 (gasolines containing 10 and 20 vol.% ethanol, respectively) are relatively common in several countries. Those blends contained 3.7 and 7.4 wt.% oxygen, respectively, and all other oxygenated blends in this study were prepared by blending the various oxygenates with TPRF in the amounts necessary to achieve those fuel oxygen levels (3.7 wt.% being the maximum fuel oxygen allowed according to the European standard EN 228 **??**). However, three compounds could not be mixed at the 7.4% oxygen level: triacetin, due to miscibility issues, and the two GTBE mixes, due to the excessive viscosity of the blends they produced.

Properties of the oxygenated compounds can be found in Table 2.4, in Chapter 2, whereas the fuel blends are listed in two separate tables according to their oxygen content. Table 5.3 shows the oxygenated blends containing 3.7 wt.% oxygen and the blends containing 7.4 wt.% oxygen are listed in Table 5.4.

In both tables, the name of each fuel blend indicates the amounts of oxygenate, in vol.%, that was blended with TPRF to achieve the desired oxygen contents. (As an example, "Triacetin5.5" represents a mixture of 5.5 vol. % triacetin with the gasoline surrogate.) It should be noted that the RON values of the neat glycerol derivatives are not listed because their octane testing is not easily performed, due to their low volatility and/or high viscosity.

Table 5.3: Key properties of the 3.7 wt.%-oxygen-blends (all additives mixed with the TPRF surrogate, see Table 5.2.)

Blend Name	Additive	Molecular Weight	Density [kg/dm^3]	LHV[a] [MJ/kg]
EtOH10.0	Ethanol	91	0.746	41.4
MeOH7.0	Methanol	88	0.746	41.4
i-PrOH13.0	Isopropanol	94	0.748	41.4
n-BuOH16.0	*n*-Butanol	97	0.753	41.4
i-BuOH16.0	Isobutanol	97	0.752	41.4
75M25D9.5	M-S GTBE[b]	108	0.764	41.5
25M75D11.7	D-S GTBE*c*	110	0.763	41.4
Solketal7.3	Solketal	105	0.766	41.1
Triacetin5.5	Triacetin	108	0.765	41.0

[a]Lower heating value
[b]"Mono-shifted" GTBE, a mix of 75 vol.% mono-GTBE and 25 vol.% di-GTBE
c"Di-shifted" GTBE, a mix of 25 vol.% mono-GTBE and 75 vol.% di-GTBE

Table 5.4: Key properties of the 7.4 wt.%-oxygen-blends (all additives mixed with the TPRF surrogate, see Table 5.2.)

Blend Name	Additive	Molecular Weight	Density [kg/dm^3]	LHV[a] [MJ/kg]
EtOH20.0	Ethanol	82	0.751	39.7
MeOH14.0	Methanol	76	0.749	39.7
i-PrOH26.0	Isopropanol	86	0.753	39.7
n-BuOH32.0	*n*-Butanol	91	0.764	39.7
i-BuOH32.0	Isobutanol	91	0.762	39.7
Solketal14.6	Solketal	108	0.789	39.1

[a]Lower heating value

5.2.5 Test Procedure

The calibration of the compression ratio was done according to the procedure described in the engine's documentation [94].

The evaluation of the fuel blends described in this chapter was done at the constant engine speed of 600 rpm and at an intake air temperature (IAT) of 52 °C, as prescribed by the ASTM RON test protocol [97]. At those conditions, spark timing sweeps comprising three timings were then done at the compression ratios (r_c) of 6:5 and 7:5. The three spark timings were chosen so that the intermediate ignition timing produced a 50% mass fraction burned angle (CA50) around 8° ATC. This value was based on the empirical rule described by Heywood [77], which states that, with optimum spark timing, half of the charge is burned at about 8° after TC. Subsequently, based on that intermediate spark timing, one timing 6° earlier and another one 6° later were also tested. Spark timing was changed manually by rotating the ignition timer's shaft until the desired timing was displayed on the engine's digital timing and tachometer indicator, installed on the CFR engine's control panel.

The higher compression ratio (7.5:1) was determined based on the knock intensity obtained by running the engine on the least knock-resistant fuel, i.e. the gasoline surrogate, at the earliest timing. This "worst-case scenario" was determined to ensure that the knock levels obtained when testing the other fuel blends would not be extreme. Then, the lower compression ratio (6.5:1) was arbitrarily chosen as being one unit below the higher one. This lower compression ratio was run to investigate the behavior of the blends also at less demanding engine conditions.

Table 5.5 shows the selected compression ratios and spark timings.

Table 5.5: Compression ratios and spark timings used in the experiments.

Compression Ratio [-]	Spark Timings [deg BTC]
6.5:1	23; 17; 11
7.5:1	16; 10; 4

5.2.6 Knock Measurement

Because engine knock is essentially an acoustic phenomenon, the resulting resonant vibration modes of the combustion chamber are a function of both cylinder geometry and gas properties [74, 221, 222]. Additionally, the in-cylinder pressure signal has to be filtered to remove the undesirable frequencies, leaving only the ones associated with those relevant vibration modes. Therefore, the in-cylinder pressure signal was band-pass filtered using a Butterworth filter implemented in the LabVIEW code. In this work, the frequencies of interest were the ones associated with the so-called first circumferential mode, whose resonant frequencies have been described in the literature as being around 5.8–6.9 kHz for the CFR engine [74, 221, 223, 224]. This mode is particularly important since it contains most of the energy of the knocking vibrations [225]. Accordingly, the in-cylinder pressure signal was filtered with a 10th-order Butterworth filter having cut-off frequencies of 4 and 8 kHz (i.e. centered at the critical frequency of 6 kHz). According to a 2019 study by Swarts *et al.* [224], filters with high orders give better transient response and remove the bulk cylinder pressure.

The metric chosen to characterize knock intensity was the so-called absolute value of the maximum amplitude of pressure oscillations (MAPO), which is defined at the maximum amplitude of the filtered in-cylinder pressure signal [99, 76, 73, 226]. Figure 5.3 shows an example of a knocking cycle where the knocking oscillations are evident, whereas Figure 5.4 illustrates how MAPO is defined. Moreover, the MAPO was determined and logged for each engine cycle, in the crank angle range from 10° BTC to 70° ATC to avoid interference from ignition noise and/or valve closing events [224].

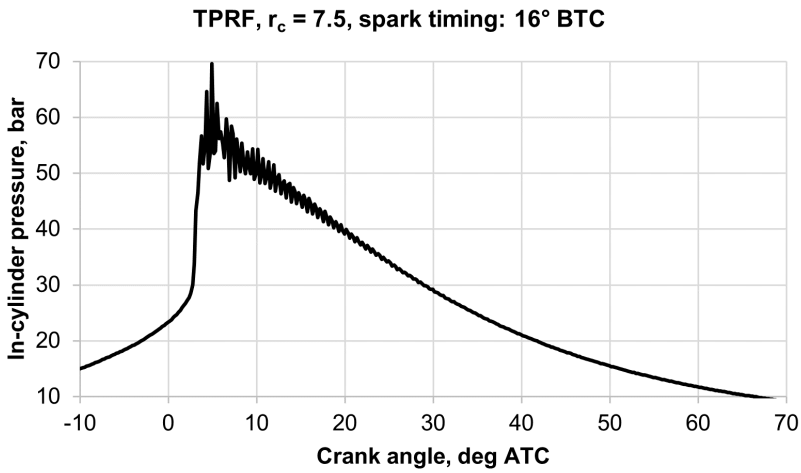

Figure 5.3: In-cylinder pressure oscillations caused by engine knock.

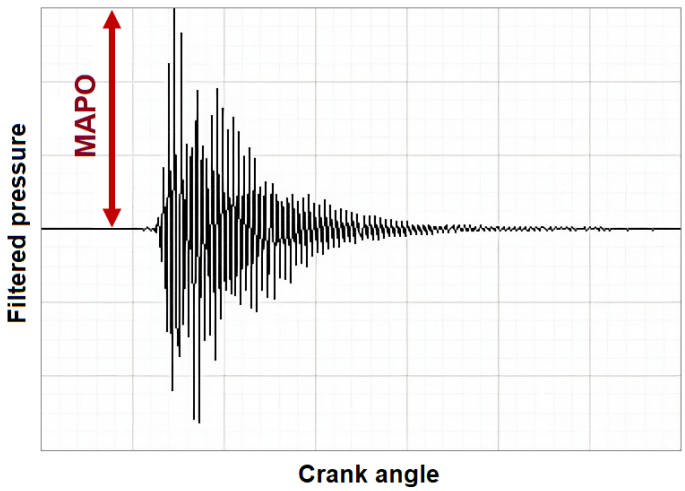

Figure 5.4: A graphical description of MAPO, as indicated by the arrow.

At each operating condition, after stabilizing the engine for about ten minutes, indicated data corresponding to a total of 1000 consecutive firing engine cycles were logged for each experimental point in order to improve any subsequent statistical analysis of knock intensity, as recommended by Brunt *et al.* [227]. During that time, 70 low-speed, time-based measurements were also logged. In addition, motoring cycles were sampled at both compression ratios, to be used in the heat release

calculation.

5.3 Results and Discussion

This section presents the overall results obtained with the different fuel blends throughout the test campaign. The combustion analysis, based on the heat release data, shows the impacts of fuel composition on the combustion process and the corresponding performance characteristics of the engine. Then, the important issue of how the fuel oxygenates affect engine knock is introduced and discussed.

5.3.1 Selection of Operational Parameters

This section presents and discusses the main experimental results. Due to the large amount of data that were produced and due to space limitations, only a part of all results, corresponding to just one spark timing and one compression ratio, is considered in this chapter. The choice of these two engine parameters was based on the combustion phasing and the corresponding engine efficiency obtained with the gasoline surrogate (TPRF) baseline fuel. The chosen spark timing was determined based on the peak thermal efficiencies, as the following plots show. They show how the spark timings and the compression ratios affected engine performance, as represented by the CA50 angle, the indicated thermal efficiency (ITE), and the indicated mean effective pressure. For the indicated results, at each experimental point, the error bars in the plots represent the variability in the measurements, defined as the standard deviation of the measured values corresponding to 1000 engine cycles.

At this point, it is worth mentioning that the overall approach in this work is to assess how a minimally-modified production engine might behave, performance-wise, to the use of the different alcohols as fuels. In other words, to investigate how an engine in a near-stock configuration would react to such alcohols being used as drop-in fuels. Even though the use of neat alcohols in a production engine obviously does require engine modifications (hence the ”minimally-modified”), this ”drop-in” approach is focused on the basics. A modern engine could be retrofitted and be calibrated to obtain the maximum performance when using any of those alcohols. That would also be a valid comparison. However, any differences in engine

performance could also be largely attributed to hardware changes and calibration optimization, in which case the direct impact of the fuels could become masked and harder to discern. The CFR engine, having such a simple design, is particularly useful in that regard, since it makes it possible to compare different fuels with minimal hardware influence.

Figure 5.5 illustrates the combined influence of the "intermediate" spark timings at the compression ratios used in this study. The plot on the left shows that those timings gave CA50 angles of around 8° ATC. Moreover, as the plot in the middle shows, these intermediate timings also resulted in improved thermal efficiencies. (As expected, the compression ratio of 7.5 resulted in slightly higher thermal efficiencies, compared to the compression ratio of 6.5.) Finally, the plot on the right shows that the maximum loads (expressed as indicated mean effective pressure, IMEP), achieved with the surrogate fuel at both compression ratios were slightly above 8 bar.

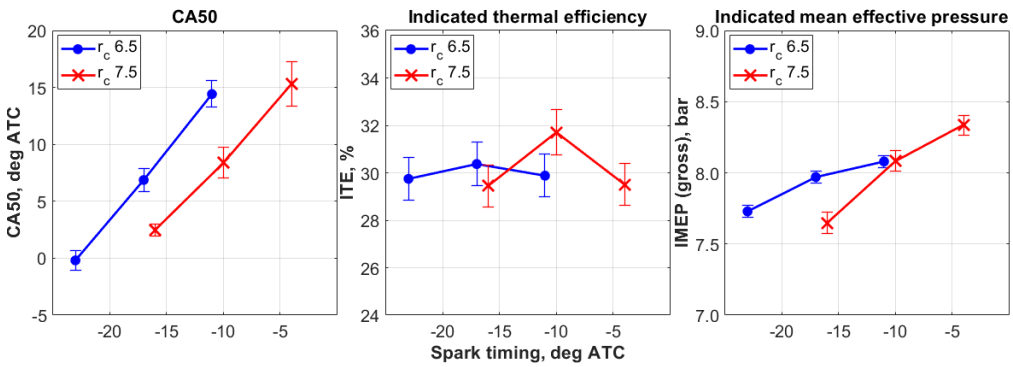

Figure 5.5: CA50 angles, indicated thermal efficiencies and mean effective pressures obtained with the TPRF blend.

It is also worth discussing how the IMEP varied among all tested fuel blends, as Figure 5.6 shows. (The black color was chosen to differentiate the TPRF blend, since it does not contain any fuel-bound oxygen.) It can be seen that the blends produced roughly the same output of 8 bar IMEP.

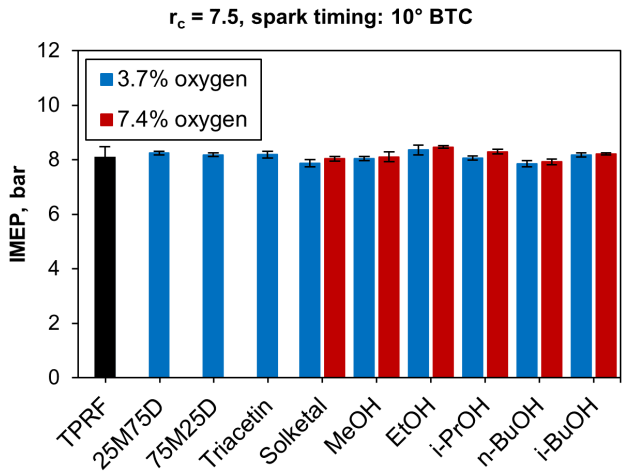

Figure 5.6: Indicated mean effective pressures produced by all the tested blends.

Therefore, based on these data, the compression ratio of 7.5, together with the spark timing of 10° BTC, were chosen to represent the experimental results for the remainder of this chapter.

Furthermore, due to the large number of fuel blends tested (16 in total), the results are divided into three parts, based on fuel oxygen content, keeping in mind that the number in each compound's name represents the vol.% amount of that compound that was mixed with the gasoline surrogate.

1. **3.7 wt.% oxygen part I:** Includes the reference blends TPRF and EtOH10.0, plus the glycerol derivatives:
    - TPRF
    - EtOH10.0
    - 25M75D11.7
    - 75M25D9.5
    - Solketal7.3
    - Triacetin5.5
2. **3.7 wt.% oxygen part II:** Includes the reference blends TPRF and EtOH10.0, plus the other alcohols:

- TPRF
- EtOH10.0
- MeOH7.0
- i-PrOH13.0
- n-BuOH16.0
- i-BuOH16.0

3. **7.4 wt.% oxygen:** Includes the alcohols plus solketal (the only glycerol derivative that could be blended at that oxygen level). The EtOH20.0 blend is the only reference fuel in this part:
    - EtOH20.0
    - MeOH14.0
    - i-PrOH26.0
    - n-BuOH32.0
    - i-BuOH32.0
    - Solketal14.6

5.3.2 Knock Characterization

This subsection briefly describes some important features of engine knock and the means to characterize its occurrence and intensity. Afterwards, the experimental results related to knock are presented and analyzed using the methods introduced in the next paragraphs. At this point, it is worth mentioning that the criterion used to define knock occurrence can be rather arbitrary. In this work, a firing engine cycle was considered to be knocking if its measured MAPO value exceeded 1.0 bar, which is a commonly used threshold [226, 224]. However, any cycle will have some MAPO value associated with it, ranging from background noise to heavy knock. Moreover, the occurrence of one single cycle having a MAPO above the chosen threshold does not necessarily mean that the engine is knocking—hence, the usefulness of the statistical approach described below. That being said, it should be kept in mind that the choice of the threshold value can have an influence on how the results as a whole are interpreted, as illustrated in the following paragraph.

The fact that the combustion process in spark-ignition engines exhibits relatively large cycle-to-cycle variations has been known for a long time [228, 229], even at constant speed and load conditions. The existence of knock only complicates the situation even further. As a typical example, Figure 5.7 shows the knock intensity, expressed as MAPO, for 1000 consecutive measured engine cycles under knocking conditions. In this particular case, the engine was running on the TPRF surrogate, at the compression ratio of 7.5 and a spark timing of 10° BTC, in which conditions 96.7% of the cycles were knocking (i.e their measured MAPO values were above 1.0 bar).

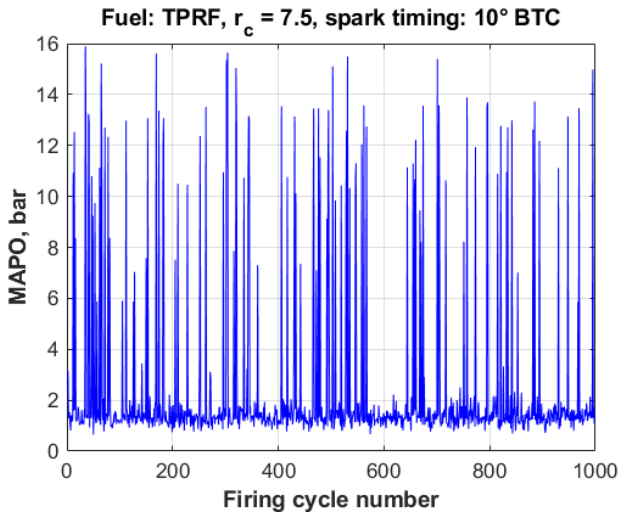

Figure 5.7: Cycle-to-cycle variations in knock intensity, TPRF, r_c = 7.5, spark timing: 10° BTC.

The stochastic nature of such large cyclic variations benefits from statistical analysis [230]. Indeed, the characterization of the magnitude of knock can be effectively described as a statistical distribution of its intensity values measured over a sufficiently large number of cycles and calculated at each individual firing cycle. Therefore, in this study, the experimental knock data were processed and characterized using a few basic statistical techniques, as described below.

Histograms are a useful tool to visualize and characterize random data, a good example of which is the representation of engine knock intensity [99]. The histograms shown in Figure 5.8 illustrate the general features of typical knock events; in this particular case, caused by differences in fuel quality. Those histograms show the distributions of the measured MAPO values for the ”neat” TPRF and the 10 vol.%

and 20 vol.% ethanol blends, at the compression ratio of 7.5 and the spark timing of 10° BTC. A few things can be inferred from those histograms. First, it is evident that the presence of ethanol significantly inhibits the occurrence and the intensity of knock, especially at the 7.4 wt.% fuel oxygen level (i.e., blend EtOH20.0). Secondly, all three distributions are skewed to the right, towards higher MAPO values, suggesting the existence of knock events of comparatively higher magnitude, although occurring much less frequently in the case of the oxygenated blends. Especially in the case of the TPRF distribution, there are some cycles with much higher MAPO values than the mean. Thirdly, the spread of knock intensity decreases with decreasing MAPO values.

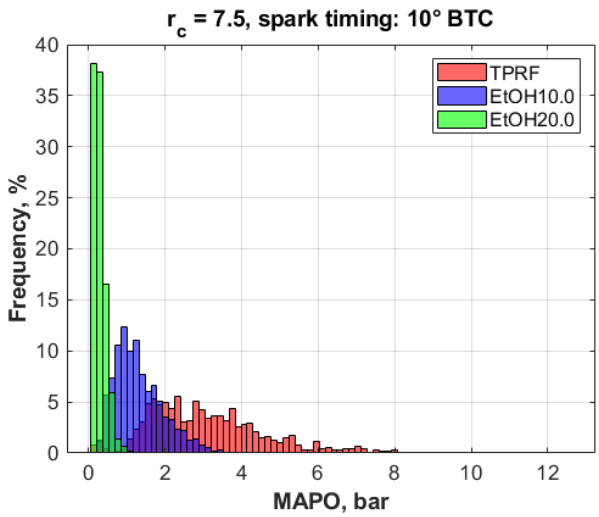

Figure 5.8: Knock intensity (MAPO) distributions, r_c = 7.5, spark timing: 10° BTC.

Those histograms can be further described by calculating some relevant statistics pertaining to the MAPO distributions produced by each fuel blend, as shown in Table 5.6. A fact not shown in the table is that, according to the results of a Shapiro–Wilk test at the 5% significance level, all three datasets in Figure 5.8 were found to be normally distributed, a fact that can be partly attributed to the central limit theorem of statistics, which states that large enough samples converge to a standard normal distribution.

Table 5.6: Knock intensity statistics for the fuel blends described in Figure 5.8.

Fuel Blend	Mean MAPO [bar]	MAPO Standard Deviation [bar]	COV[a] MAPO [%]	Skewness [-]	Kurtosis [-]
TPRF	3.10	1.58	51.0	1.16	5.64
EtOH10.0	1.32	0.644	48.8	0.942	3.81
EtOH20.0	0.295	0.154	52.2	1.28	5.10

[a]Coefficient of variation

As the histograms in Figure 5.8 show, the increase in knock resistance, brought about by the addition of ethanol to the fuel, causes significant decreases in the mean MAPO values. Moreover, the spread of the distributions, represented by their standard deviations, decreases with increasing ethanol content. Finally, the statistical concepts of *skewness* and *kurtosis* can be useful in characterizing the shape of the MAPO distributions [90]. Skewness is a measure of the asymmetry of the shape of the distribution, while kurtosis is a measure of the "peakedness" of the distribution relative to the length and size of its tails [231, 232, 233]; in other words, it can be interpreted as a measure of the prevalence and influence of outliers. These two statistics can also be used to help assess departures from normality in a distribution. (The skewness and the kurtosis of a normal distribution are by definition 0 and 3, respectively.)

All three fuel blends exhibited positive skewness values, implying that their MAPO distributions were skewed to the right, that is, towards higher knock intensities, as is usually the case. Compared to the TPRF and the EtOH20.0 blends, the EtOH10.0 blend had a lower skewness associated with it, implying a more symmetric distribution. Moreover, that blend, when compared to the other two cases, produced a MAPO distribution with a lower kurtosis, closer to that of a normal distribution, indicating a less peaked and less "tail-heavy" shape, implying that outliers were not as prevalent and influential as in the other two blends; in other words, a more consistent pattern, a fact reflected in the COV (coefficient of variation) of MAPO of the EtOH10.0 blend, the lowest among the three cases, which suggests a more stable MAPO behavior.

Cumulative Frequency Distributions

Besides ordinary histograms, empirical cumulative frequency distribution (CFD) plots are a convenient way of characterizing knock intensity [90]. In such plots, the x-axis represents an appropriate range of MAPO values, while the y-axis shows the proportion (usually expressed in percentage) of the measured data points having values less than or equal to a given MAPO. In practice, the more a curve is shifted to the right-hand side, the higher the overall knock intensities. Thus, cumulative frequency distribution plots provide a good way to distinguish between the knock intensity levels caused by different fuels and different engine operating conditions, as the results below show.

3.7. wt.% Fuel Oxygen Blends The plots that follow show the cumulative frequency distributions of the MAPO for all fuel blends tested, at the compression ratio of 7.5 and a spark timing of 10° BTC. Each curve was calculated based on a minimum of 1000 engine cycles.

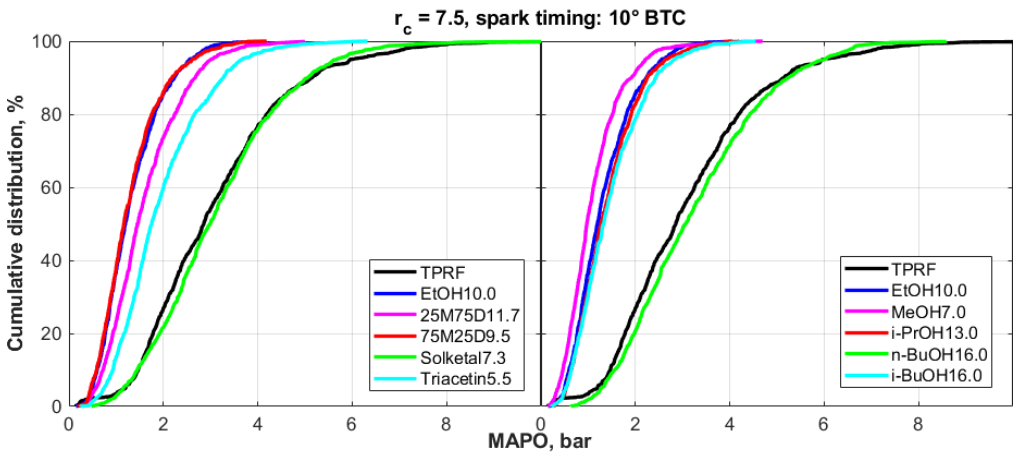

Figure 5.9: MAPO cumulative frequency distributions for the fuel blends, 3.7% fuel oxygen. Part I (left), Part II (right).

Figure 5.9 shows the cumulative frequency distributions for the MAPO obtained from the gasoline surrogate (TPRF) and the 10 vol.% ethanol–surrogate blend (EtOH10.0) as baseline, plus the 3.7%-oxygen blends of TPRF with the glycerol derivatives, i.e. Part I of the 3.7% oxygen blends.

Figure 5.9 clearly shows that both the 75M25D9.5 and EtOH10.0 blends gave the best results, that is, they caused the largest decrease in the MAPO levels compared to the reference TPRF blend. Another feature is that their MAPO distributions are nearly colinear. Indeed, a two-sample z-Test at the 5% significance level and a Mann–Whitney U test were performed on those distributions, with both suggesting that there was no statistical difference between them. The 25M75D11.7 and the Triacetin5.5 blends gave intermediate results, with the former causing higher knock inhibition. Finally, the plot demonstrates that the Solketal7.3 blend, when compared to the TPRF, did not seem to cause a significant improvement, if any, in knock resistance.

Among the 3.7% oxygen blends of TPRF with the alcohols, i.e. 3.7% oxygen, Part II (Figure 5.9), the situation was similar. In this case, the *n*-butanol-surrogate performed very poorly, showing even MAPO values slightly higher than the ones produced by the TPRF blend, a suspicion confirmed by a two-sample z-Test at the 5% significance level and a Mann–Whitney U test. In contrast, methanol performed the best among the alcohol oxygenates while ethanol, isopropanol and isobutanol also produced significant reductions in knock intensity. The results of both tests suggested that the knock intensities produced by the ethanol and isopropanol blends were slightly different, whereas the isobutanol and isopropanol blends did not produce statistically different results.

Table 5.7 contains the relevant statistics for the MAPO distributions of all tested blends having 3.7 wt.% oxygen, displayed in ascending order of their mean MAPO values. Those statistics show that the fuel producing the highest knock intensities, the *n*-butanol blend, resulted in the narrowest, most symmetrical MAPO distribution and the one with comparatively fewer outliers, as evidenced by the distribution's COV of MAPO, skewness, and kurtosis. These numbers suggest that most knock events were roughly evenly distributed over a relatively narrow interval of high MAPO values centered around the mean, hence the COV of MAPO exhibited by that distribution being the lowest among all blends. This behavior also implies that the distribution tended towards symmetry, resulting in the lowest skewness overall. Finally, it is suggested that a very large fraction of the firing cycles was knocking (as confirmed by the bar plot in Figure 5.12) at high intensity, a consistency that left less room for outliers, resulting in a kurtosis value close to 3. On the other hand, the fuel that produced the distribution with lowest MAPO values, the methanol blend, exhibited the highest COV of MAPO, skewness, and kurtosis.

The existence of fewer knocking cycles (see bar plot in Figure 5.12) implies more randomness, leading to knock events that are more widely distributed around the mean, which helps explain the highest overall COV of MAPO. Also, due to the overall low mean MAPO value, an occasional, more intense knock event would be considered extreme, and it could disproportionately cause the distribution to skew to the right, explaining the relatively high skewness. In addition, the occurrence of such occasional outliers would result in a distribution with heavier tails, hence the higher kurtosis.

Table 5.7: Knock intensity statistics for TPRF and the 3.7 wt.% fuel oxygen blends.

Fuel Blend	**Mean MAPO [bar]**	**MAPO Standard Deviation [bar]**	**COV[a] MAPO [%]**	**Skewness [-]**	**Kurtosis [-]**
MeOH7.0	1.10	0.607	55.2	1.55	7.17
75M25D9.5	1.30	0.660	50.8	1.11	4.34
EtOH10.0	1.32	0.644	48.8	0.942	3.81
i-PrOH13.0	1.40	0.673	48.2	0.996	4.17
i-BuOH16.0	1.46	0.730	50.2	0.994	4.08
25M75D11.3	1.60	0.785	48.9	0.984	4.28
Triacetin5.5	1.96	0.945	48.3	1.05	4.43
TPRF	3.10	1.58	50.9	1.16	5.64
Solketal7.3	3.15	1.42	45.1	0.836	4.28
n-BuOH16.0	3.25	1.43	44.0	0.644	3.06

[a]Coefficient of variation

7.4. wt.% Fuel Oxygen Blends In the case of the blends containing 7.4 wt.% fuel oxygen, Figure 5.10, the reference fuel was the 20 vol.% ethanol-TPRF blend, EtOH20.0. In this case, the n-BuOH32.0 blend produced the worst results, followed by the Solketal14.6 blend. The results obtained with the other compounds were clearly superior and, while their distributions are close to each other, a pattern can be discerned, with the ethanol blend exhibiting the overall best knock-inhibiting behavior.

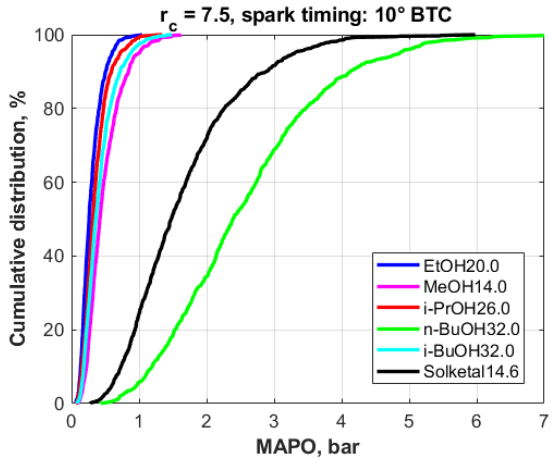

Figure 5.10: MAPO cumulative frequency distributions for the fuel blends (7.4% fuel oxygen).

Table 5.8 shows the relevant statistics for the MAPO distributions corresponding to the fuel blends shown in Figure 5.10, i.e. the blends containing 7.4 wt.% oxygen. As in Table 5.7, the blends are displayed in ascending order of mean MAPO values. Compared to the previous case, similar patterns can be recognized here, but only in the case of the fuel producing the highest knock levels, the *n*-butanol blend. As shown in the table, its MAPO distribution exhibits the lowest values of the COV of MAPO, skewness, and kurtosis, a result likely caused by the existence of higher intensity knock events occurring narrowly about the mean, with relatively fewer outliers. However, the picture is less clear in the case of the blends producing the lowest MAPO levels as they did not seem to follow the same trends displayed in the previous table. The ethanol blend resulted in the lowest mean MAPO, while it was the isopropanol blend that exhibited the highest skewness and kurtosis. This can be partly explained by the fact that, as previously stated, the results of a two-sample Z-test showed that the MAPO characteristics of these two blends were not significantly different at the 5% significance level. Moreover, in the case of such low mean MAPO values, corresponding essentially to knock-free operation, the distributions tend to be more random in nature.

Table 5.8: Knock intensity statistics for the 7.4 wt.% fuel oxygen blends.

Fuel Blend	Mean MAPO [bar]	MAPO Standard Deviation [bar]	COV[a] MAPO [%]	Skewness [-]	Kurtosis [-]
EtOH20.0	0.295	0.154	52.2	1.28	5.10
i-PrOH26.0	0.354	0.186	52.6	1.41	5.75
i-BuOH32.0	0.414	0.228	55.2	1.37	5.25
MeOH14.0	0.481	0.258	53.5	1.28	4.92
Solketal14.6	1.65	0.857	51.9	1.18	4.90
n-BuOH32.0	2.57	1.17	45.4	0.779	3.60

[a]Coefficient of variation

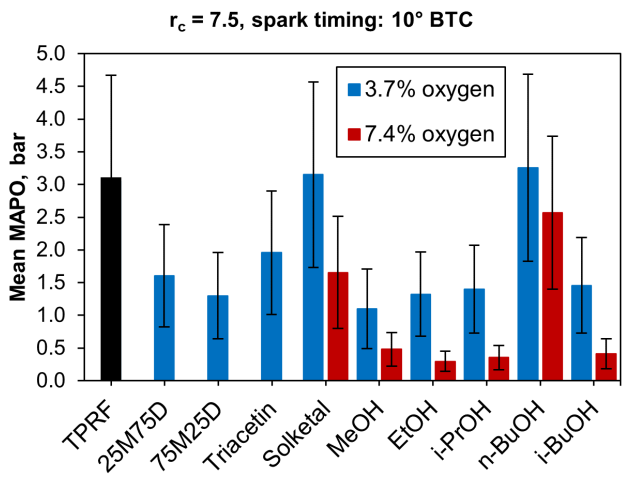

Figure 5.11: Mean values of knock intensities (MAPO).

Being a stochastic phenomenon, engine knock is more properly characterized by methods that take into account the variability and randomness of its occurrence. Statistical plots such as histograms and cumulative frequency distributions are very useful in describing knock. However, simple metrics such as mean MAPO values, representing an aggregate contribution of many firing cycles, can provide a quick and convenient quantitative measure of knock intensity. Bar plots displaying mean MAPO values can, therefore, be effective in illustrating the overall knock-inhibiting performance of different fuels, as is the case in Figure 5.11 which shows the mean MAPO values for all blends tested. This plot confirms the fact that both the ethanol

and the 75M25D blends exhibit essentially the same knock behavior, as previously discussed.

Moreover, Figure 5.11 illustrates the poor performance of solketal and *n*-butanol in enhancing the knock resistance of the base fuel (i.e. the TPRF), particularly at the 3.7 wt.% oxygen level. At that level, the blends achieved with those compounds seemed to produce even slightly higher mean MAPO values, compared to the TPRF fuel, though the variability in the data was significant, as displayed by the large error bars. (It should be kept in mind that those error bars represent the standard deviation of the measured values, *not* the uncertainties in those measurements.)

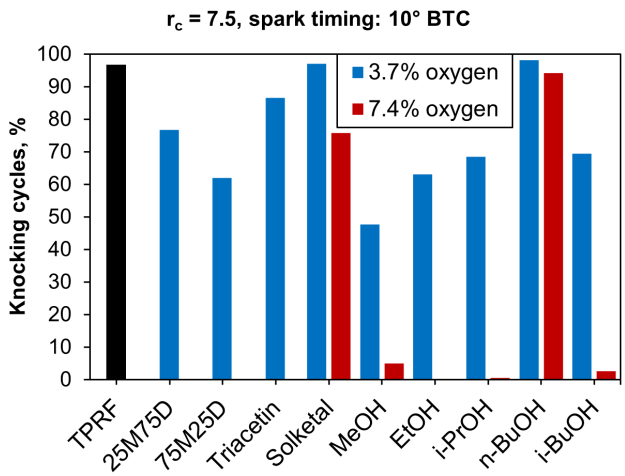

Figure 5.12: Fractions of knocking cycles to sampled firing cycles.

Besides the calculated mean MAPO values, another metric that demonstrates the presence of knock is an increasing ratio of knocking cycles to the total number of firing cycles measured. As stated above, in this work, a knocking cycle is defined as one whose measured MAPO was above 1 bar. Figure 5.12 shows the fractions of cycles where knock is occurring, for all blends tested, at a compression ratio of 7.5 and a spark timing of 10° BTC. This plot shows the exact same patterns displayed in Figure 5.11, where both the EtOH10.0 and the 75M25D9.5 blends exhibited essentially the same knock behavior while the Solketal7.3 and the n-BuOH16.0 performed very poorly. The low knock-inhibiting capacity of solketal and *n*-butanol was also evident among the 7.4 wt.% fuel oxygen level, as their blends produced the worst outcomes. On the other hand, the high-concentration blends containing

ethanol and isopropanol gave excellent results, followed closely by the isobutanol and methanol blends.

As shown in the previous paragraphs, there was a considerable variability in the knock-inhibiting capacity of the oxygenates tested. The C_1–C_3 alcohols performed particularly well, while, among the glycerol derivatives, both GTBE types gave the best results. On the other hand, *n*-butanol and solketal did not seem to produce any significant improvement in knock resistance.

5.3.3 Combustion Characteristics

In this subsection, the characteristics of the combustion process of the different fuel blends that can influence knock onset and intensity are presented and discussed.

Combustion Phasing

The 50% fuel mass fraction burned angles (CA50) for the tested fuel blends are shown in Figure 5.13 below. It can be noticed that the addition of any of the oxygenated compounds to the TPRF blend extended the 50% burn angles, suggesting relatively slower combustion rates with the oxygenated blends. In particular, the results from the butanols show that *n*-butanol burned faster than isobutanol, in agreement with the literature [79]. However, the relatively slow combustion of the methanol-containing blends may seem like an odd results, since methanol exhibits—at least in neat form—a high burning velocity. (For comparison, the reader is referred to the plot in Figure 6.12, in the next chapter, where methanol did exhibit the shortest CA50 angle among all tested alcohols.)

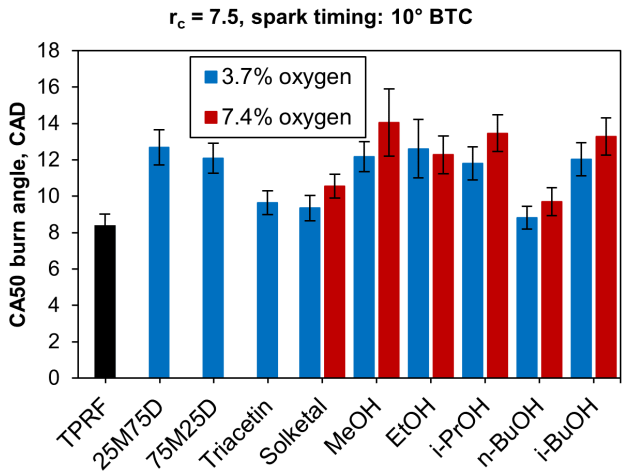

Figure 5.13: 50% burn angles for all blends.

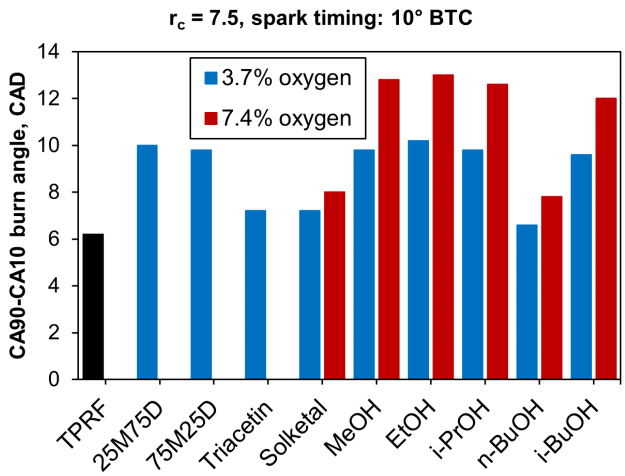

Figure 5.14: 90%-10% burn angles for all blends.

Exhaust Gas Temperatures

Figure 5.15.

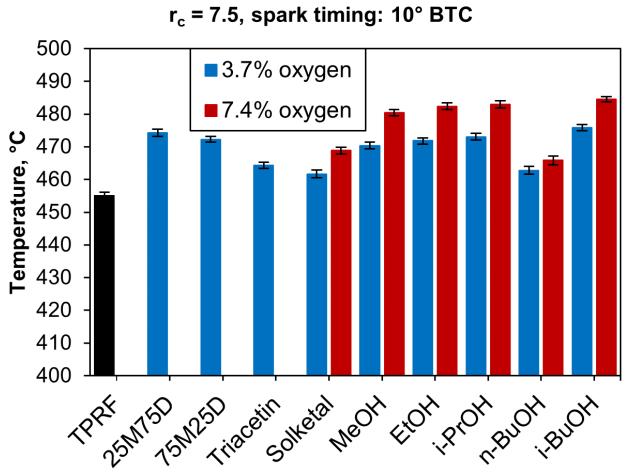

Figure 5.15: Exhaust gas temperatures for all blends.

Heat Release Rates

The plots in figure 5.16 show the impact of the oxygenates on the heat release behavior of the fuel blends. Plots (a) and (b) show the glycerol derivatives and the alcohols, respectively, representing the blends of "low" (3.7 wt.%) oxygen content, in addition to the "neat" TPRF as reference fuel. Plot (c) displays the "high" oxygen (7.4 wt.%) blends. In this particular case, the blend containing 20 vol.% ethanol (EtOH20.0) was used as reference. For ease of comparison, all plots have the same scale on the y-axis.

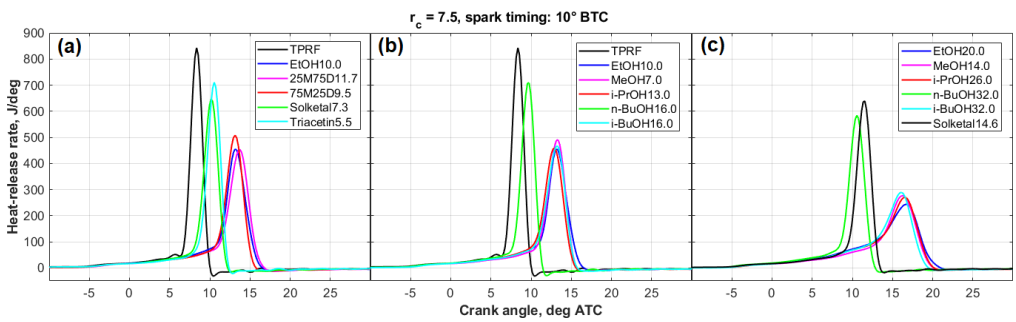

Figure 5.16: Heat release rates (a) 3.7 wt.% fuel oxygen blends, Part I (b) 3.7 wt.% fuel oxygen blends, Part II (c) 7.4 wt.% fuel oxygen blends.

As discussed in more detail further ahead, the engine was knocking to some extent in the case of all 3.7%-oxygen blends, though knock was more intense with the TPRF (as expected, due to it being the "weakest" fuel), Triacetin5.5, and Solketal7.3 blends. At the 7.4% oxygen level, except for the Solketal14.6 and n-BuOH32.0 blends, engine operation was essentially knock-free.

At the 3.7% oxygen level the oxygenated blends both delayed the combustion process and decreased the peak heat release rates. However, this effect was less pronounced with the triacetin, solketal, and *n*-butanol blends, a fact reflected in their inferior knock resistance. At the 7.4% oxygen level, compared to the other fuels, the solketal and *n*-butanol blends exhibited a much shorter combustion development, together with a higher and sharper heat release peak, which is consistent with their worse knock performance.

This behavior is in line with the results from a 2018 article by Hoth *et al.* [234], in which the authors found that the MAPO intensity correlated well with the peak heat release rate and the rate of heat release after the onset of autoignition leading to knock. They also observed that adding ethanol to the base fuel reduced both MAPO and the heat release rate after knock onset. Similar conclusions were drawn by Rockstroh *et al.* in their 2018 article [226], in which they found a correlation between MAPO and the heat release rate after knock onset.

To summarize, the heat release patterns displayed in these plots are closely related to the knock behavior of the fuel blends, as described in the previous section of this chapter.

5.3.4 Exhaust Emissions

In this section, the exhaust emissions produced by the various fuel blends are discussed. In each of the figures that follow, the first two plots show the results from the blends containing 3.7 wt.% fuel oxygen, whereas the third plot, on the right, shows the results from the 7.4 wt.% oxygen blends.

It should be kept in mind that, in the first case, the gasoline surrogate (TPRF) and the its blend with 10 vol.% ethanol (EtOH10.0) are the reference fuels and, as such, appear on both plots in the 3.7 wt.% oxygen case. Among the 7.4 wt.% fuel blends, the mixture of TPRF with 20 vol.% ethanol (EtOH20.0) is the reference

fuel, as stated previously. All concentrations are shown in ppm, as a function of spark timing.

As previously, plots (a) and (b) show the glycerol derivatives and the alcohols, respectively, representing the blends of "low" (3.7 wt.%) oxygen content, in addition to the "neat" TPRF as reference fuel. Plot (c) displays the "high" oxygen (7.4 wt.%) blends.

In general, according to the results seen in the plots, the emission trends—if any—seem to be subtle and no obvious behaviors can be identified, even if the pollutant concentrations were not negligible. In other words, it seems as if the presence of the oxygenates at such concentrations did not cause any significant impact, compared to the baseline fuel, TPRF.

Carbon Monoxide

As seen in Figure 5.17, the different blends produced a wide scatter of carbon monoxide concentrations, ranging from about 2000 to 6000 ppm. Yet, the results did not seem to exhibit any clear trends. The 2000 to 6000 ppm range appeared to be roughly the same for both the 3.7 and 7.4 wt.% fuel blends. Moreover, the CO emissions from the non-oxygenated fuel, the TPRF, did not show any distinguishable behavior, except that in plot (c) of the figure, the carbon monoxide emissions from that fuel *appear* to be the lowest, but this result might simply be random.

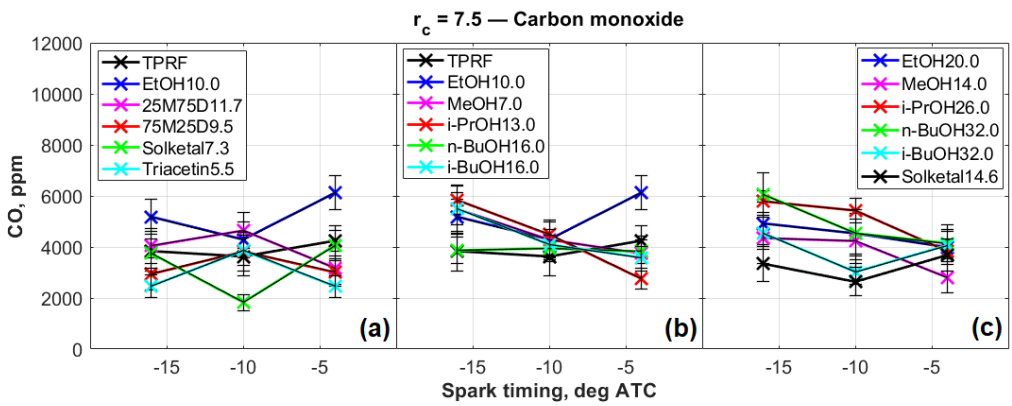

Figure 5.17: Carbon monoxide emissions.

Hydrocarbons

In the case of unburned hydrocarbons, as Figure 5.18 shows, the results at first do not seem exhibit any clear trends. However, the "neat" TPRF fuel seemed to produce lower emissions, compared to the oxygenated blends. If that is indeed the case, this might be due to the presence of the oxygenates interfering with—or, rather, enhancing—flame quenching on the cylinder wall and crevices.

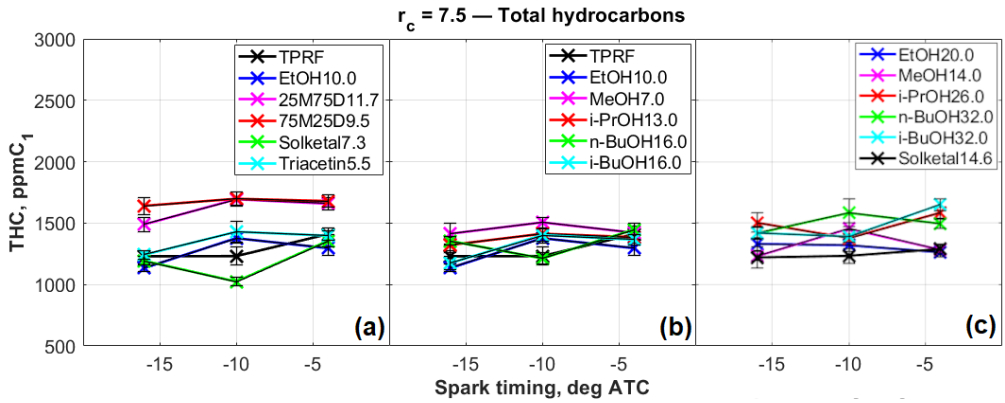

Figure 5.18: Hydrocarbon emissions.

Nitric Oxide

Even though it is more difficult to see it in the plots representing the 3.7 %-oxygen blends, plot (c) seems to show that the oxygenated blends produced lower nitric oxide levels, compared to TPRF, which could suggest that oxygenate addition resulted in lower peak combustion temperatures.

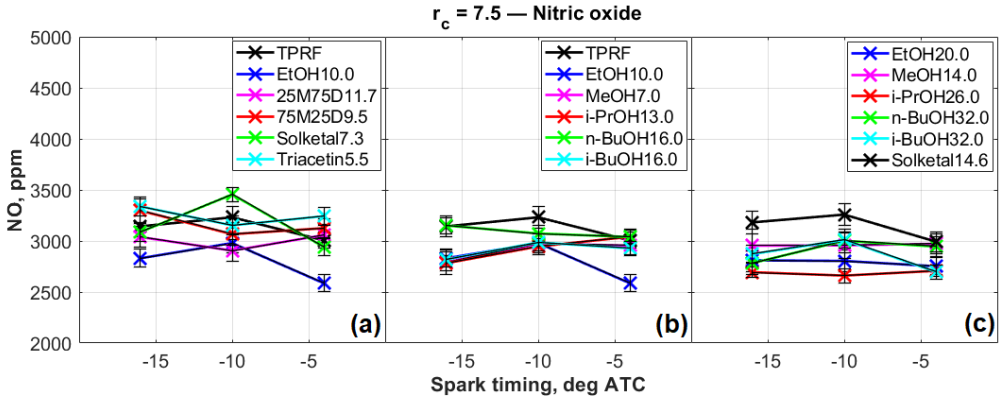

Figure 5.19: Nitric oxide emissions.

Formaldehyde

As the plots in 5.20 show, the formaldehyde emissions from the MeOH7.0 and MeOH14.0 blends seem to be slightly higher than the rest—or it might just be a random result—in accordance to the fact that formaldehyde is an common intermediate product of methanol combustion. However, there is a chance the aldehyde emissions in this work may not be accurate, as explained further ahead.

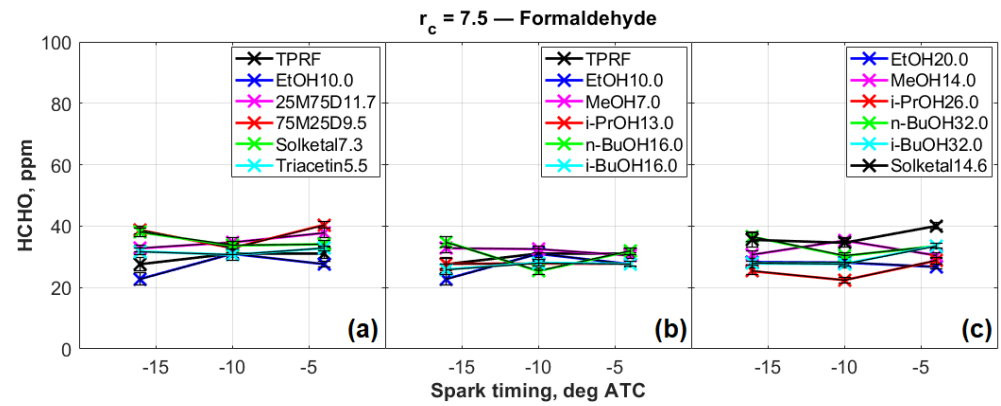

Figure 5.20: Formaldehyde emissions.

Acetaldehyde

Acetaldehyde is the aldehyde that is typically associated with ethanol combustion. As Figure 5.21 shows, it is hard to identify any trend in the plots. Moreover, a close examination of plot (c) reveals that the emissions from the MeOH14.0 blend are missing. In fact, those values were negative. The same phenomenon was even more evident in the case of neat alcohols, described in the next chapter. As discussed in more detail in Chapter 6, the explanation might be that the FTIR analyzer, due to its factory settings, was not calibrated to measure exhaust containing methanol, ethanol, or any of the alcohols included in this work [235]. Therefore, it is safe to say that the aldehyde emissions presented in this work, unfortunately, may not be accurate.

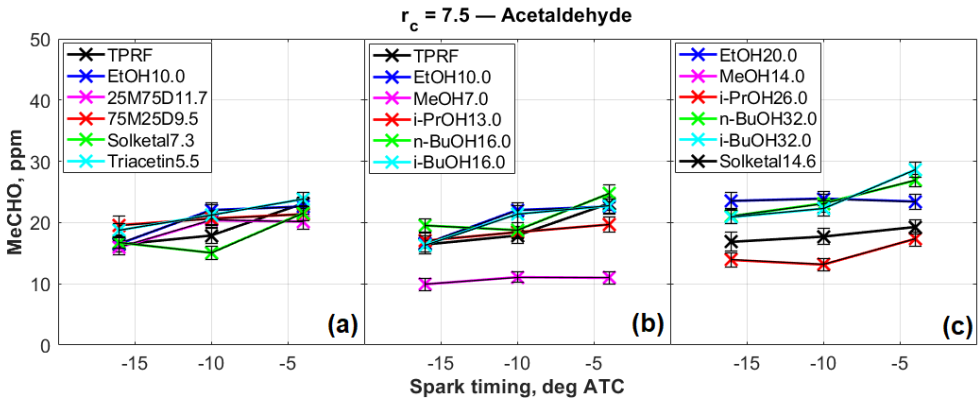

Figure 5.21: Acetaldehyde emissions.

5.4 Summary

This chapter investigated the suitability of a number of potentially renewable compounds to be used as gasoline oxygenates, as alternatives to the usual blendstocks ethanol and MTBE. Those compounds comprised glycerol derivatives and C_1–C_4 alcohols (including ethanol itself as the reference oxygenate). The main focus of the experiments was on the knock propensity of the fuels. To this end, tests were performed on a modified spark-ignition Waukesha CFR engine operating at a fixed speed, at different compression ratios and spark timings. A gasoline surrogate containing toluene was used as baseline fuel, along with a blend of that surrogate with

10 vol% ethanol. In addition, blends of the surrogates were prepared so as to match the oxygen content of the reference ethanol blends.

According to the results, there were distinguishable trends among the knock-inhibiting characteristics of the different oxygenates. Among the glycerol derivatives, both GTBE types, when considered together, performed the best, resulting in significant reductions in knock intensity when added to the "neat" TPRF blend. However, GTBE's relatively high viscosity and low vapor pressure precluded it from being blended with gasoline at higher concentrations. Solketal, while having better miscibility with the TPRF, produced inferior knock-inhibiting capacity.

All alcohols also increased the knock resistance of the base fuel appreciably, with the notable exception of *n*-butanol, likely due to its straight-chain molecular structure. Both methanol and ethanol, despite performing well, exhibit well-known issues like their corrosiveness, affinity for water, and negative impact on the fuel blend's vapor pressure, as discussed earlier. Therefore, if such non-combustion-related characteristics are taken into consideration, one could say that isopropanol and isobutanol were the best overall performing alcohols, regarding their knock-inhibiting properties.

In summary, the main conclusions from the experiments described in this chapter can be listed as follows:

- Among the glycerol derivatives, both GTBE mixtures resulted in good knock reduction, while the performance of solketal was inferior.
- Triacetin gave good results, but its miscibility with hydrocarbons may pose a problem at higher concentrations and/or cold temperatures.
- Among the alcohols, all performed quite well, with the notable exception of *n*-butanol, which gave very poor knock results, likely by virtue of its straight-chain molecular structure.
- Methanol and ethanol, unsurprisingly, exhibited very good knock inhibition performance, but their effect on the volatility of their blends with gasoline can be an issue.
- Isopropanol was also very effective in decreasing knock and its ability to distort the volatility characteristics of the base fuel is lower, compared to

methanol and ethanol. However, the available technology to produce it feasibly from renewable sources does not seem to be very developed yet.

- Isobutanol exhibited very good knock-inhibiting characteristics, while having a higher energy density and lower water affinity, when compared to the smaller alcohols, due to its molecular structure.

In general terms, glycerol derivatives can possess superior knock-inhibiting capacities, but their miscibility with hydrocarbons may be an issue at higher concentrations and/or lower temperatures. In general, the C_1–C_4 alcohols also have the potential to perform very well, but it must be kept in mind that the smallest ones (methanol and ethanol) present issues such as corrosiveness, water miscibility, and blend vapor pressure distortion. In this regard, isobutanol seems very promising among the alcohols. Finally, isopropanol performed well enough to warrant further work, since there are relatively very few studies dedicated to its use as a fuel for internal combustion engines.

Chapter 6

Spark-Ignition Engine Tests II: Neat Alcohol Fuels

6.1 Introduction

Chapter 5 introduced the part of this work dealing with spark-ignition engines. More specifically, it addressed the topic of gasoline oxygenates, that is, oxygen-containing substances that are added to the base gasoline to promote more complete combustion and—perhaps most importantly—enhance its knock resistance. In addition, the fact that oxygenates are usually obtained from renewable sources is another reason for their adoption. The chemical compounds investigated in the preceding chapter, that is, the glycerol-derived compounds, plus the C_1–C_4 alcohols, were evaluated on a modified Waukesha CFR engine, focusing on their knock-inhibiting characteristics. In a similar fashion, this chapter now evaluates and discusses the performance of those C_1–C_4 alcohols when used as *neat* fuels, as opposed to being used merely as gasoline fuel components. For that purpose, the same CFR engine is used and the test procedures are similar to the ones already presented. Moreover, the evaluation of the knock tendency when using different fuels is once more the focus of the investigation. Finally, the present chapter offers an assessment regarding the suitability of each of the alcohols, from a neat-fuel perspective.

Using alcohols as fuels has been considered since the early years of the internal

combustion engine era [152, 153]. Indeed, the ICE pioneer Sir Harry R. Ricardo studied extensively the use of alcohols as engine fuels and advocated their use as such [236]. Through his early work on pre-ignition, he showed that, with ethanol, due to its decreased pre-ignition propensity, it was possible to achieve higher compression ratios, compared to pure hydrocarbon fuels. Furthermore, Ricardo also found that the higher latent heats of vaporization and lower flame temperatures of alcohols could be exploited to increase power output and decrease thermal losses [79].

As previously discussed, for motor fuel applications, biologically-produced ethanol is primarily used as a gasoline extender and, as such, it is nowadays widely used. However, ethanol possesses qualities that make it highly suitable for utilization as a neat fuel for spark–ignition engines, such as a high heat of vaporization and superior resistance to engine knock [147]. Indeed, it has already been used as a transportation fuel in large-scale, most notably in Brazil, where neat hydrous ethanol has been available since the late 1970s. In contrast with its adoption as gasoline blend component, the use of bioethanol in neat form has the potential to displace even larger amounts of fossil fuels, offering an additional route to achieve further reductions in net CO_2 emissions. Besides ethanol, other lower alcohols, by virtue of their properties, also have the potential to be used as neat spark-ignition fuels.

Accordingly, and similarly to Chapter 5, where, besides ethanol, additional chemical compounds were tested as gasoline oxygenates, the present chapter proposes additional alcohols—other than ethanol—to be used as neat fuels for SI engines. Therefore, besides ethanol, the alcohols evaluated in this chapter are the ones already introduced: methanol, isopropanol, *n*-butanol and isobutanol. A summary of some of their relevant properties is shown in Table 6.1, whereas a more detailed description of each of these alcohols is presented in Chapter 2.

Therefore, this chapter presents a direct comparison, performed on the same modified CFR engine, of neat C_1–C_4 alcohols, with ethanol being the reference fuel. The tests focused on the combustion characteristics and on the knock tendencies exhibited by the different compounds. As in the previous chapter, the experimental test procedure was comprised of spark-timing sweeps carried out at two different compression ratios, at stoichiometric conditions, nominally constant intake air temperature[1] and constant engine speed.

[1]See explanation in section "Test Procedure"

6.2 Materials and Methods

The experimental setup for the engine tests discussed in this chapter is identical to the setup described in the previous chapter. That is, the engine used herein—the Waukesha CFR engine—and all the measuring instruments are exactly the same. Table 2.1 shows a list of key engine specification and subsection 2.3.2 gives a description of the CFR engine itself. A picture of it, along with a schematic representing the overall experimental setup are also shown in Chapter 5, in Figures 5.1 and 5.2, respectively. Moreover, the heat release calculation procedure is identical. Finally, the overall description of engine knock and the procedure for its measurement are the same and have already been discussed. Thus, the reader is referred to Chapter 5 for a more detailed description of those topics. The test procedure used for the experiments described in this chapter, however, is slightly different and is explained further below.

6.2.1 Fuels Tested

The fuels studied in this chapter are the C_1–C_4 alcohols, used in neat form, as opposed to being gasoline blendstocks. Ethanol, being the foremost example of an alcohol fuel, was the reference compound. Regarding the propanol and butanol isomers, *n*-propanol, plus *sec*-butanol and *tert*-butanol were not included in this study.

A summary of relevant properties of the alcohols included in this study are listed in Table 6.1.

Table 6.1: Physicochemical properties of the tested alcohols [175]. (RON: research octane number; MON: motor octane number).

Alcohol	Molecular Weight [g/mol]	Specific Gravity at 20°C	Lower heating value [MJ/kg]	Stoich. Air/Fuel Ratio	Heat of Vaporization at 25°C [kJ/kg]	Solubility in Water at 25°C [wt.%]	RON	MON
Methanol	32.04	0.792	19.95	6.46	1168	Miscible	109	89
Ethanol	46.06	0.794	26.95	9.00	920	Miscible	109	90
Isopropanol	60.09	0.789	30.54	10.33	757	Miscible	117	99
n-Butanol	74.11	0.810	33.21	11.17	708	7.7	98	85
Isobutanol		0.802	33.29		686	8.7	105	90

6.2.2 Test Procedure

For the present chapter, the test procedure was identical to the procedure in Chapter 5, except for differences in the chosen compression ratios, spark timings, and intake air temperatures. As in the previous chapter, the calibration of the compression ratio was done in accordance with the procedure described in the engine's operating manual [94].

In this chapter, the evaluation of the alcohol fuels was conducted under operating conditions that are partly similar to the conditions used in the RON test, that is, at a constant engine speed of 600 rpm [97]. It is also worth pointing out that, because the CFR engine features throttle-less operation, the different alcohols were tested at roughly stoichiometric "full load" conditions, at similar, but not constant levels of the (gross) indicated mean effective pressure (IMEP) (see Figure 6.3 further below). Furthermore, the intake air temperature (IAT) was set to 25°C, about room temperature, a level intended to subdue the cooling effect caused by the relatively high heat of vaporization (HOV) of the alcohols, which can be significant, especially in the case of methanol and ethanol. Unfortunately, due to their lower HOVs, it was not possible to achieve the 25°C target with *n*-butanol and isobutanol, and their average intake air temperatures were about 31°C and 27°C, respectively. The average IAT values during the tests are shown in Figure 6.1.

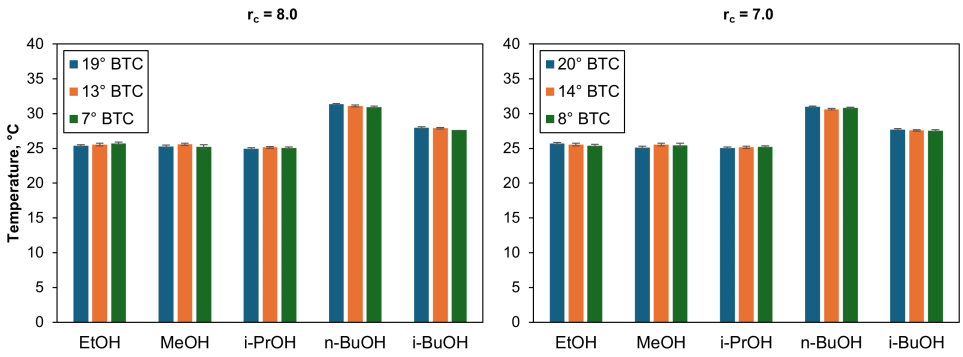

Figure 6.1: Intake air temperatures throughout the tests (compression ratios and spark timings indicated).

Under these conditions, spark timing sweeps were done at the compression ratios of 8:1 and 7:1.

The higher compression ratio (8:1) was selected based on the knock intensity observed when operating the engine on the least knock-resistant fuel (*n*-butanol in this chapter) at the earliest timing. This represented a worst-case scenario, to ensure that the knock intensity with all other fuels and all timings remained within reasonable limits.

The lower compression ratio (7:1) was then arbitrarily chosen as being one unit lower than the compression ratio of 8:1. The rationale for including a lower compression ratio was to investigate the knocking behavior of the different alcohols also at less demanding—or even knock-free—engine operating conditions.

Being the reference alcohol fuel, ethanol was used for the determination of the spark timings used throughout the tests as follows: At each compression ratio, an optimum spark timing, that resulted in a 50% mass burned fraction angle (CA50) of about 8° after top-center crank position, was found. As mentioned in Chapter 5, this value of the CA50 angle was chosen based on the empirical rule that relates the maximum brake torque (MBT) timing to the mass burning profile, as mentioned in the textbook by Heywood [77].

Subsequently, two additional spark timings were investigated, one set 6° earlier and the other 6° later, relative to the optimum timing. It should be noted that, at each compression ratio, the same spark timings were used for all alcohols. In this case, all alcohols other than ethanol might have been tested at non-optimal engine

conditions, which might also have affected their knocking behavior. However, since the C_1–C_4 alcohols are not radically different from each other, it can be assumed that the effect of such discrepancies might not have been significant.

As in Chapter 5, adjustments to spark timing were made manually by rotating the ignition timer's shaft until the desired timing was indicated on the engine's digital timing and tachometer display, installed on the instrument panel of the unit.

Table 6.2 shows the selected compression ratio and spark timings.

Table 6.2: Compression ratios and spark timings used in the experiments.

Compression Ratio [-]	Spark Timings [deg BTC]
7.0:1	20; 14; 8
8.0:1	19; 13; 7

6.3 Results and Discussion

This section presents and discusses the main experimental findings. The knock tendencies of the various alcohols are presented using some of the statistical concepts presented in Chapter 5. Additionally, the combustion analysis using the heat release data, shows the influence of the alcohols' molecular structures on their combustion processes and, consequently, knocking behavior.

6.3.1 Selection of Operational Parameters

As mentioned previously, the selection of compression ratios was determined based on knock considerations, while the spark timings were selected based on combustion phasing and the optimum values of the mean effective pressure and thermal efficiencies. Those parameters were determined using ethanol, which is the reference fuel in this chapter.

The plots in Figure 6.2 depict the impact of spark timings and compression ratios on the 50% mass burned fraction angle (CA50), indicated thermal efficiency (ITE), and on the (gross) IMEP.

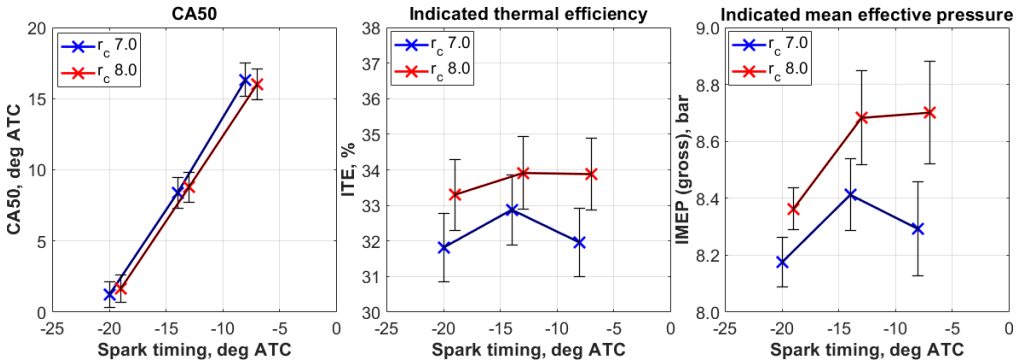

Figure 6.2: CA50 angles, indicated thermal efficiencies and mean effective pressures obtained with ethanol.

The plot on the left shows that the intermediate spark timings, at the compression ratios employed in this investigation, resulted in CA50 angles of approximately 8° after top-center crank position (ATC), as intended. Moreover, as shown in the middle plot, these intermediate timings led to improved thermal efficiencies. (As expected, the 8:1 compression ratio yielded marginally higher thermal efficiencies, when compared to the 7:1 compression ratio.) Finally, according to the plot on the right, the maximum engine outputs, expressed as gross indicated mean effective pressure (IMEP), achieved with the baseline ethanol fuel at both compression ratios, exceeded 8.5 bar slightly.

(Again, it should be noted that the "error" bars in those plots, strictly speaking, do not represent the actual measurement uncertainties, but the standard deviation of the measured values calculated based on 1000 engine cycles. A discussion about uncertainties is given in Appendix A. For now, using the method described in that Appendix, it is sufficient to state that the uncertainty in the IMEP was about 0.05 bar, while the ITE had an uncertainty of roughly 0.3%, negligible compared to the variability in the measurements, which, under these circumstances, dominate the experimental uncertainties.)

The gross IMEP values for all the alcohols tested, at both compression ratios, are shown in Figure 6.3.

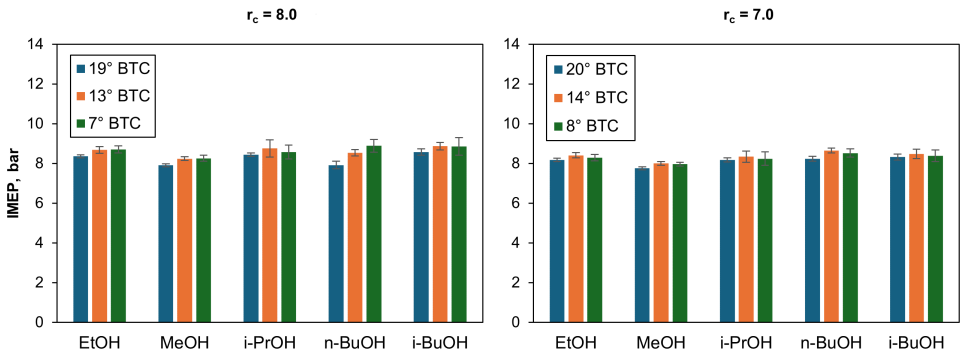

Figure 6.3: Average IMEP for all the tested alcohols. The maximum observed differences were about 1.0 bar for the 8:1 compression ratio and 0.8 bar for the 7:1 compression ratio.

These two plots show slight variations in engine load, which could be due to differences in fuel properties. The decrease in the heating values of the fuels associated with their decreasing molecular sizes can be offset by the increasing stoichiometric fuel/air ratios with the smaller alcohol molecules (such as methanol and ethanol). In other words, for a given amount of air inducted by the engine (which is naturally aspirated), larger amounts of the smaller alcohols can be stoichiometrically burned, thus compensating for their lower energy content. However, a careful analysis of the plots in Figure 8 reveals that methanol consistently produced the *lowest* gross IMEP values at both compression ratios and at all spark timings. The reason for that can be explained by determining the volumetric efficiencies, based on the intake air mass flow rates, for each alcohol, as shown in Figure 6.4.

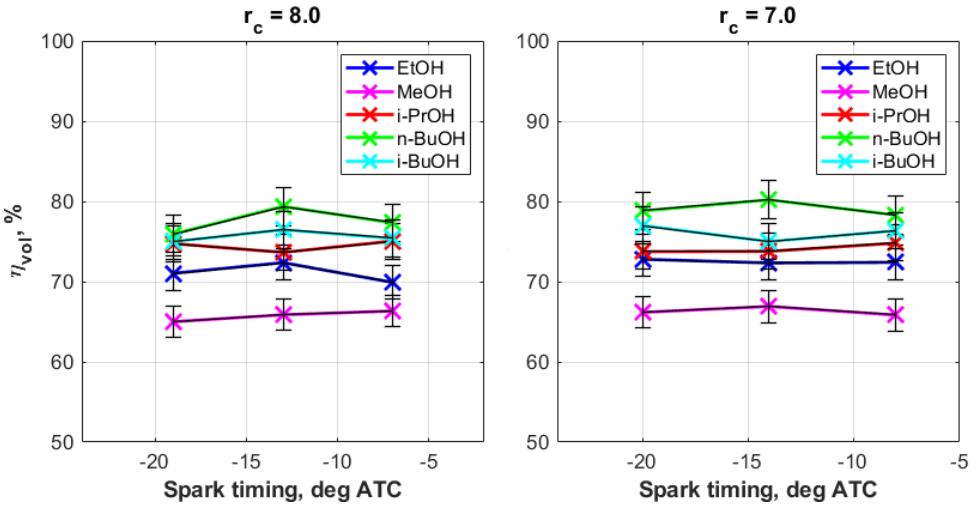

Figure 6.4: Volumetric efficiencies for all alcohols (compression ratios indicated).

These plots show a clear pattern at both compression ratios and at all spark timings. It is evident that the volumetric efficiencies decreased with decreasing molecular sizes. One possible reason is the fact that the smallest alcohols displace more air inside the cylinder, due to their higher stoichiometric *fuel/air* ratios (therefore, lower stoichiometric *air/fuel* ratios). This phenomenon was more pronounced in the case of methanol, since it has the lowest stoichiometric air/fuel ratio (AFR) of all alcohols (about 6.5:1), which may explain the lower volumetric efficiencies obtained with that fuel. Even though the high heat of vaporization of methanol could help increase the volumetric efficiency, this cooling effect was essentially absent, since the intake air temperatures were kept approximately constant throughout the tests (see Figure 6.1 above). On the other hand, the butanols, being the largest alcohols in this study, produced the highest volumetric efficiencies, since their higher stoichiometric AFRs may have caused them to displace less air inside the cylinder. The calculated uncertainties in the volumetric efficiency figures, using the method outlined in Appendix A, were in the order of 0.5%, essentially negligible.

In any case, the variation in the physicochemical properties of the different alcohols, along with those conflicting experimental conditions were not sufficient to cause significant differences in IMEP, as Figure 6.3 shows.

6.3.2 Knock Characterization

This section outlines some key aspects of engine knock and methods for evaluating its occurrence and intensity—a topic already addressed in Chapter 5—before presenting the knock-related experimental findings obtained with the neat alcohols fuels. As it was pointed out in the previous chapter, there are different criteria used for determining knock onset and, in this dissertation, an engine firing cycle was considered to be knocking if its measured MAPO (maximum amplitude of pressure oscillations) value exceeded 1.0 bar. However, it is worth mentioning again that every cycle will produce some MAPO value, ranging from background noise to severe knock and the occurrence of a single cycle with a MAPO value above the specified threshold does not necessarily indicate that the engine is knocking—thus, the statistical tools already introduced in Chapter 5 can be very useful.

Before proceeding, it is worth quickly examining the average MAPO values obtained with the different alcohols, at both compression ratios and at all spark timings, as shown in Figure 6.5 below. It should be noted that the y-scales in both plots are different. Each bar then represents the average MAPO calculated over 1000 firing engine cycles whereas, as in the previous case, the error bars show the variability observed in each measurement, represented by the standard deviation calculated from those 1000 cycles. As previously discussed, the MAPO uncertainties themselves were deemed to be related to the uncertainty in the cylinder pressures, which were found to be 0.05 bar. Once more, the variability in the measurements was far larger than the estimated uncertainties.

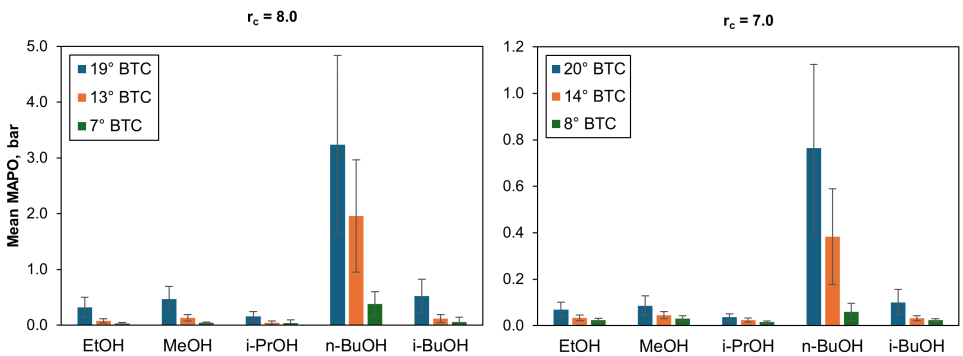

Figure 6.5: Mean values of knock intensities (MAPO) during the tests (compression ratios and spark timings indicated).

From Figure 6.5, it is evident that *n*-butanol stands out as being the fuel producing by far the highest average MAPOs among all alcohols, a fact observed at both compression ratios. The average knock intensities exhibited by the other alcohols were much lower in comparison and roughly in the same range. Also, as expected, the plots show that, the earlier the spark timing, the higher the MAPO intensity. It is interesting to note that, even under the smooth engine operating conditions obtained with the 7:0 compression ratio, it was still possible to detect some trends among the alcohols, a fact that becomes more clear with the help of cumulative frequency distributions, as discussed further below.

As already mentioned in Chapter 5, the variability in the MAPO measurements can be quite large, an example of which is illustrated in Figure 6.6, when the engine was running on *n*-butanol—the least knock-resistant fuel—at the compression ratio (r_c) of 8:0 and at a spark timing of 19° BTC, that is, a worst-case scenario for knock. In this particular case, 97% of the cycles were knocking (i.e. their measured MAPO values were above 1.0 bar).

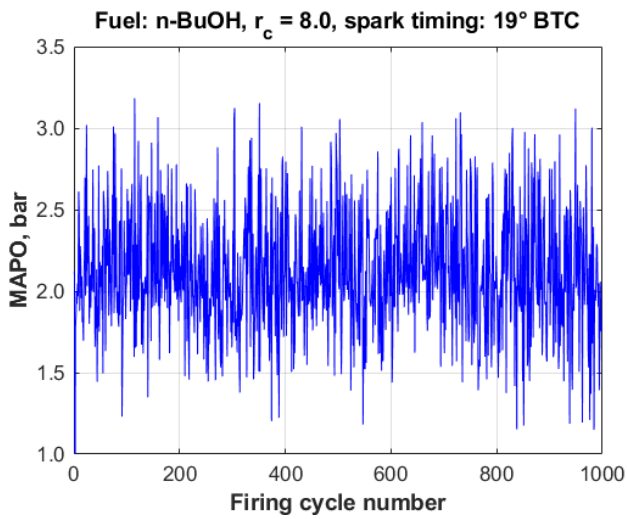

Figure 6.6: Cycle-to-cycle variations in knock intensity.

As pointed out in the previous chapter, statistical tools are useful when analyzing such large cyclic variations [230]. As a stochastic phenomenon, knock can be effectively characterized as a statistical distribution of the values of its intensity (e.g. MAPO) measured over a sufficiently large number of cycles and calculated at each individual firing cycle. Additionally, histograms are useful in visualizing and char-

acterizing random quantities, such as knock intensity [99].

The histogram shown in Figure 6.7 illustrates the effect of spark timing on the MAPO distributions obtained with *n*-butanol. It is evident that the variations in spark timing not only affected the knock intensity itself, but it also had a strong impact on the spread of the distributions, which increased as the mean MAPO increased. This behavior helps explain the large cyclic variations (hence the large error bars) observed at higher knock levels. It also helps explain why knock intensity distributions are skewed to the right, towards lower MAPO values, as observed by Chun and Heywood [99].

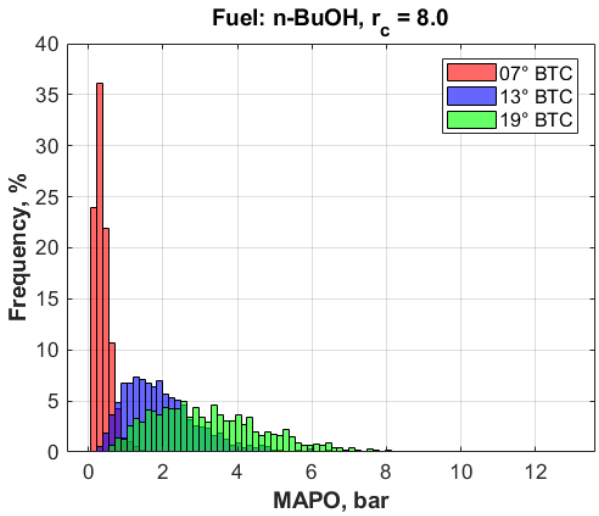

Figure 6.7: Knock intensity (MAPO) distributions, *n*-butanol, r_c = 8.0.

Cumulative Frequency Distributions

As stated in Chapter 5, empirical cumulative frequency distribution charts are a convenient way of describing knock intensity [90]. In an attempt to better illustrate the overall knock behavior of the different alcohols, the selected MAPO cumulative frequency distributions were calculated at the *earliest* and at the *latest* spark timings at each compression ratio. This choice of opposite engine operating conditions was meant to illustrate the MAPO behavior of the alcohols at both the most and the least demanding conditions. As in the previous chapter, each cumulative distribution was determined based on a minimum of 1000 firing engine cycles.

It should be kept in mind that, since no knock occurred during the less demanding tested engine conditions, the term "knock" may be misleading in those situations and the term "MAPO" itself would be more accurate to describe the in-cylinder pressure oscillations, regardless of the occurrence of knock.

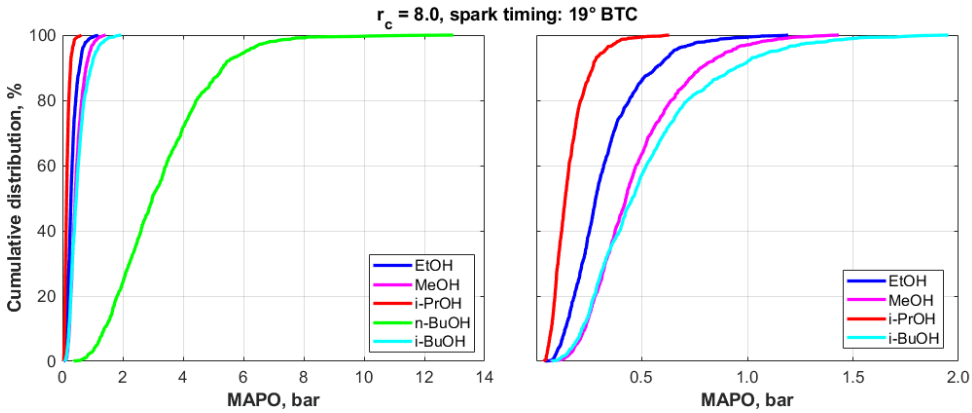

Figure 6.8: MAPO cumulative frequency distributions for the tested alcohols, earliest spark timing.

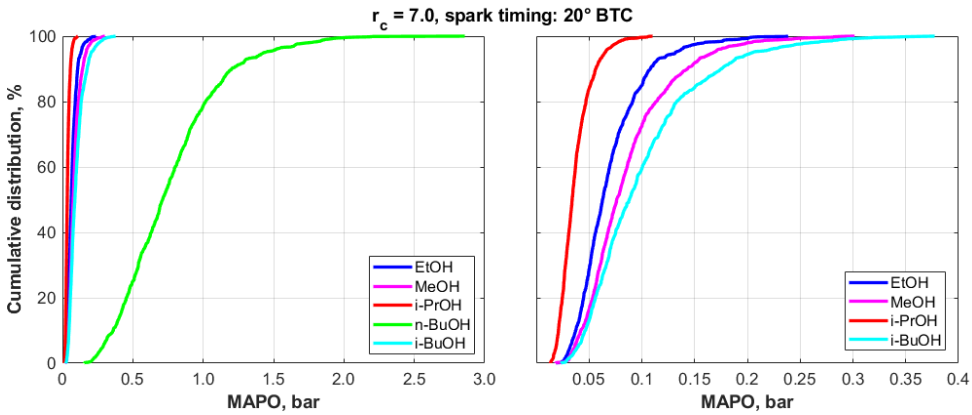

Figure 6.9: MAPO cumulative frequency distributions for the tested alcohols, earliest spark timing.

Figures 6.8 and 6.9 show the MAPO cumulative frequency distributions obtained with all tested alcohols at the earliest spark timings, namely 19° and 20° BTC, corresponding to the 8:1 and 7:1 compression ratios, respectively. These plots represent the most demanding operating conditions—knock-wise—at both compression ratios. The CFDs for *n*-butanol immediately stand out at both compression ratios due to the significantly higher MAPO values produced by that fuel. Because of

that, the *n*-butanol CFDs were removed in the plots on the right in each figure, to better visualize the distributions of the other alcohols. In this case, it is interesting to note that there seem to be well-defined patterns among them, in which they display clearly distinct behaviors, even when the measured MAPO values were very low, as in the case of the 7:1 compression ratio.

A Mann–Whitney *U* test was performed on those distributions and the results indicated that there is a statistical difference between them, implying that their behaviors were distinct.

Another interesting feature is that, in this particular case, the same patterns are observed with both compression ratios, in which isopropanol produced the lowest MAPO values, followed by ethanol, methanol, isobutanol—and *n*-butanol, as the least knock-resistant alcohol. These results do not correlate well with the average IMEP values obtained with the alcohols, suggesting that the differences in MAPO can be attributed to differences in fuel properties, as opposed to fuel intake energy.

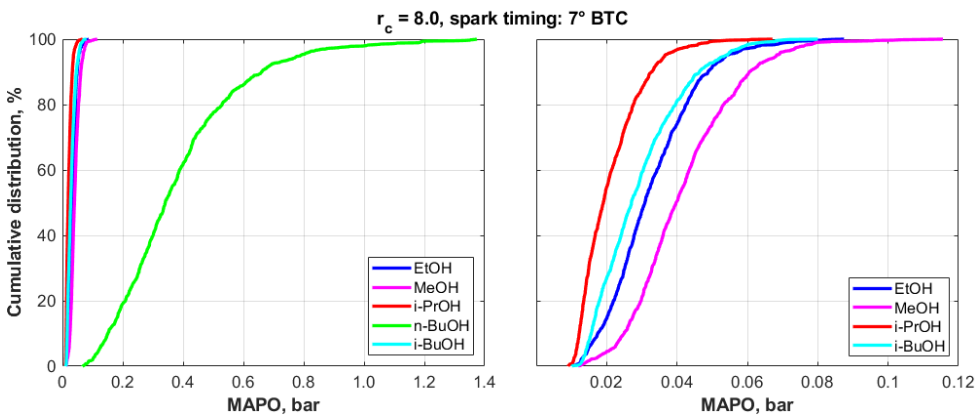

Figure 6.10: MAPO cumulative frequency distributions for the tested alcohols, latest spark timing.

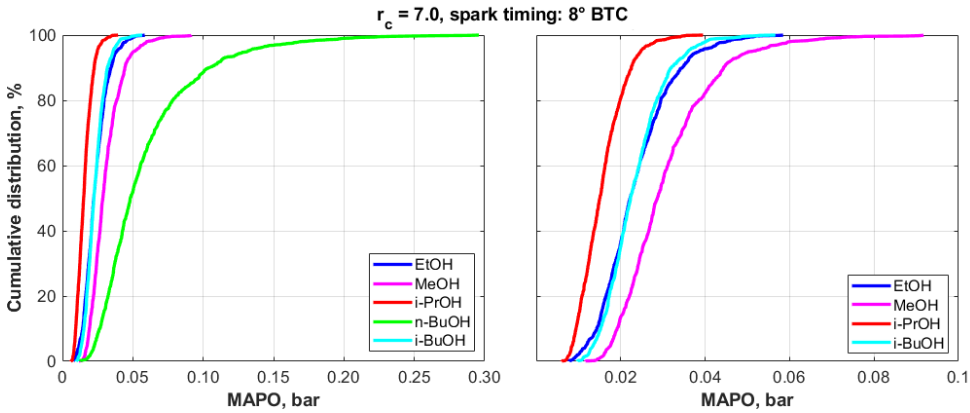

Figure 6.11: MAPO cumulative frequency distributions for the tested alcohols, latest spark timing.

Figures 6.10 and 6.11 show the MAPO CFDs obtained with the alcohol fuels at the latest spark timings of 7° and 8° BTC, corresponding to the compression ratios of 8:1 and 7:1, respectively. These plots represent the least demanding conditions tested, at both compression ratios. Compared to the previous case, the situation is very similar. Interestingly, *n*-butanol stood out again as the fuel producing the highest MAPO levels, even in this case where their values are very low overall, particularly at the 7:1 compression ratio. When *n*-butanol is excluded, as in the plots on the right in each figure, a pattern can again be discerned, where isopropanol seemed to produce the lowest MAPO levels, followed by isobutanol, ethanol, methanol, and *n*-butanol. It is also interesting to note that roughly the same trend was exhibited at both compression ratios, similarly to the previous case.

Once more, a Mann–Whitney *U* test was performed on the MAPO distributions, the results of which suggesting that their statistical behaviors were distinct—except for the 8° BTC case, in which the ethanol and isobutanol distributions were found to be statistically similar.

Based on the results described above, the most obvious takeaway is that, when compared to the other alcohols, *n*-butanol produced significantly higher MAPO values, even during engine operation regarded as knock-free. However, the fact that the intake air temperature was higher in the case of *n*-butanol (see Section 6.2.2 "Test Procedure"), might have contributed to its poor knocking behavior. In any case, this finding is unsurprising, since *n*-butanol has been shown to be the most reactive butanol isomer [237, 238]. This stands in contrast with the results

produced by isobutanol, highlighting the influence of a fuel's molecular structure on its knock behavior. Another interesting finding is the distinction among the MAPO behaviors exhibited by the other alcohols, with isopropanol producing the lowest MAPO levels overall. However, the distinctions are small, as the reactivities of the C_1–C_4 alcohols—except for *n*-butanol—are similar [175, 176].

6.3.3 Combustion Characteristics

In this section, the characteristics of the combustion process of the different alcohols that can influence knock onset and intensity are presented and discussed.

Combustion Phasing

The development of the combustion of the fuel-air mixture in the cylinder can be described by its phasing, which is determined from the heat-release profiles and is represented by the crank angle position corresponding to a certain percentage of the mixture that has been consumed following ignition. It can be interpreted as a measure of the speed of combustion of a particular fuel. The CA50 crank angle, which corresponds to half of the fuel mass that has been consumed, together with the angle representing most of the combustion duration, CA90-CA10 (representing the bulk of the combustion, in this case considered as taking 80 crank angle degrees (CAD)) are commonly used metrics for characterizing combustion phasing. The CA50 angles for the five alcohols in this study are shown in Figure 6.12, for both compression ratios and at all spark timings, whereas the corresponding CA90-CA10 angles are shown in Figure 6.13.

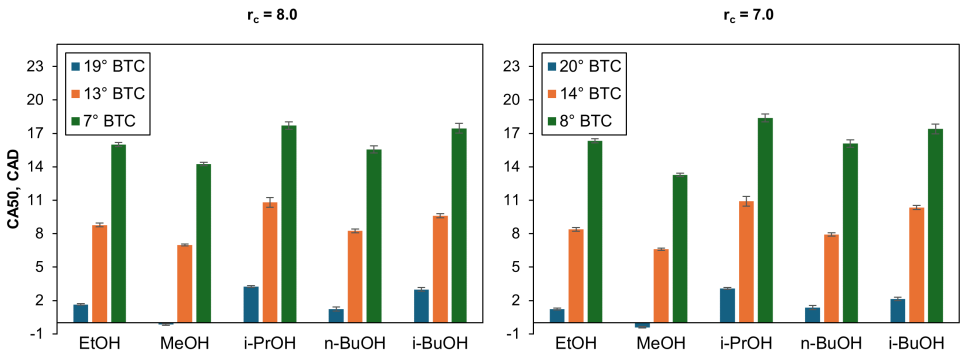

Figure 6.12: 50% mass burned fraction angles for the tested alcohols (compression ratios and spark timings indicated).

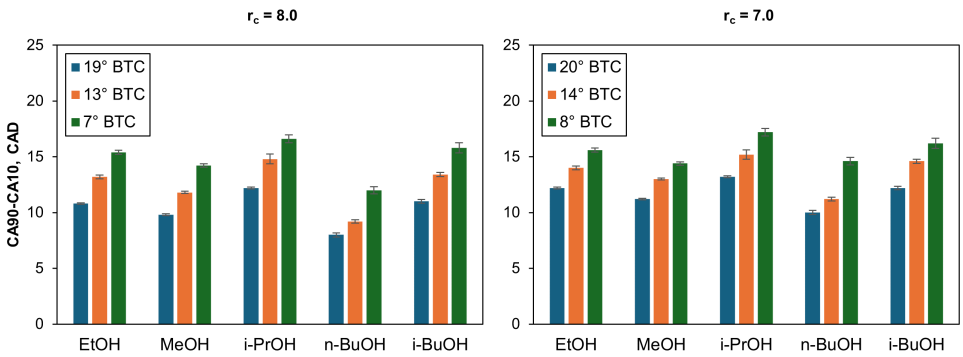

Figure 6.13: 10-90% mass burned fraction angles for the tested alcohols (compression ratios and spark timings indicated).

By inspecting the results, the values of the CA50 angles, in ascending order (that is, from earliest to latest 50% mass fraction burned) can be summarized as follows: MeOH < *n*-BuOH ≈ EtOH ≈ *i*-BuOH < *i*-PrOH.

Overall, the combustion phasing, as represented by both the CA50 and CA90-CA10 quantities, can be ranked as follows: *n*-BuOH < MeOH ≈ EtOH ≈ *i*-BuOH < *i*-PrOH, in ascending order (that is, from shortest to longest burn duration).

These results suggest that methanol and *n*-butanol were the fastest burning alcohols, followed by ethanol, whereas isopropanol and isobutanol burned at the slowest rates. These results mostly agree with studies discussed in the thorough review by Sarathy *et al.* [79]. In that article, an inspection of the presented results reveals that the laminar flame speeds of the alcohols investigated in this work, can be roughly

ranked as follows: MeOH ≈ EtOH > *n*-BuOH > *i*-PrOH ≈ *i*-BuOH. However, it should be kept in mind that laminar flame speed is an idealized combustion property that is difficult to be measured exactly at engine conditions, therefore there might exist discrepancies published by different studies.

Exhaust Gas Temperatures

The exhaust gas temperatures measured for the five alcohols in this study are shown in Figure 6.14, at both compression ratios and at all spark timings. Again, in general, the temperatures can be ranked, from lowest to highest, as follows: *n*-BuOH ≈ MeOH < EtOH < *i*-BuOH < *i*-PrOH. This is the same trend as in the combustion phasing case discussed above, which is not surprising, since later-burning fuels will tend to cause higher exhaust temperatures. Therefore, these results confirm the combustion phasing values observed with the different alcohols.

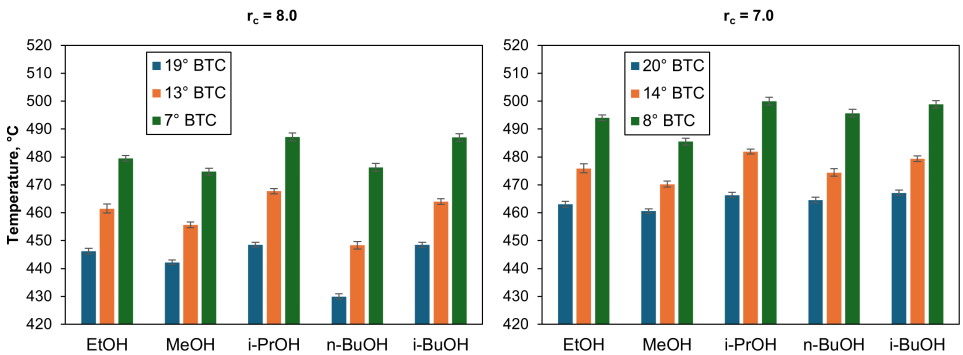

Figure 6.14: Exhaust gas temperatures for the tested alcohols (compression ratios and spark timings indicated).

Heat Release Rates

The heat release plots corresponding to the CFDs described above, representing the earliest and latest spark timings at both compression ratios, are shown in Figures 6.15 and 6.16. The main finding from the preceding knock analysis was the significantly higher knock tendency of *n*-butanol, when compared to the other alcohols. Unsurprisingly, the combustion behavior of that alcohol stands out as having a more ”abrupt” heat release shape. This fact is clearly seen in the results obtained at the earliest spark timings, especially at the higher compression ratio of 8:1, as

Figure 6.15 illustrates. On the other hand, isopropanol produced the lowest overall MAPOs, a result that is also seen in its heat release profiles. For ease of comparison, all plots have the same y-axis scale.

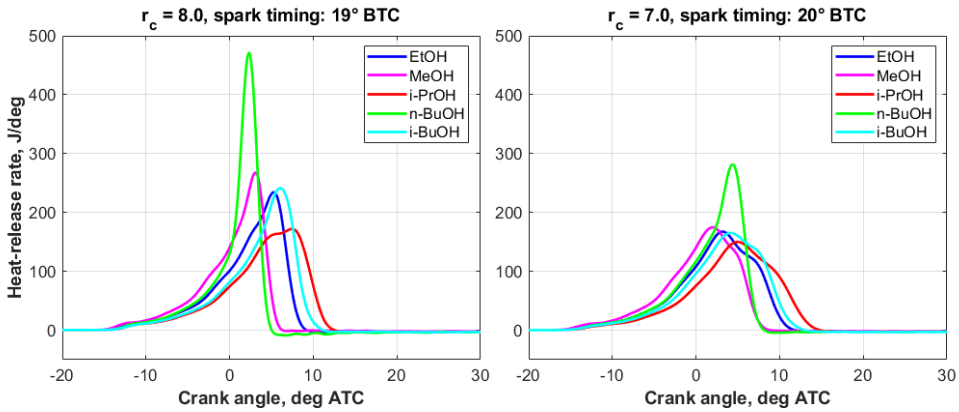

Figure 6.15: Heat release rates at the earliest spark timings.

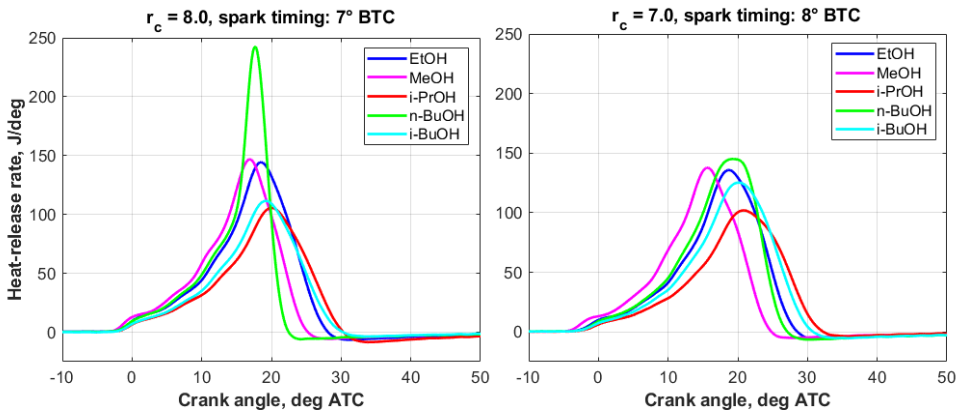

Figure 6.16: Heat release rates at the latest spark timings.

As depicted in the CFDs previously shown, the higher MAPO values exhibited by *n*-butanol was evident even in the case of the latest spark timings, that is, at the smoothest engine conditions tested. This fact is reflected in its heat release profiles, as depicted in Figure 6.16. In contrast, the gradual heat release behavior exhibited by isopropanol, at both compression ratios, once again explains the lowest knock tendency of that fuel, compared to the other alcohols.

6.3.4 Exhaust Emissions

In this section, the exhaust emissions produced by the different alcohols are presented and discussed. In each of the figures that follow, the results obtained at both compression ratios are shown, for all alcohols, as a function of spark timing. All concentrations are shown in ppm, as a function of spark timing.

Carbon Monoxide

The exhaust concentrations of carbon monoxide are shown in Figure 6.17. The CO concentration ranges differ roughly by a factor of two. Upon inspection of both plots, the following trend can be discerned: n-BuOH > EtOH > i-PrOH ≈ i-BuOH > MeOH.

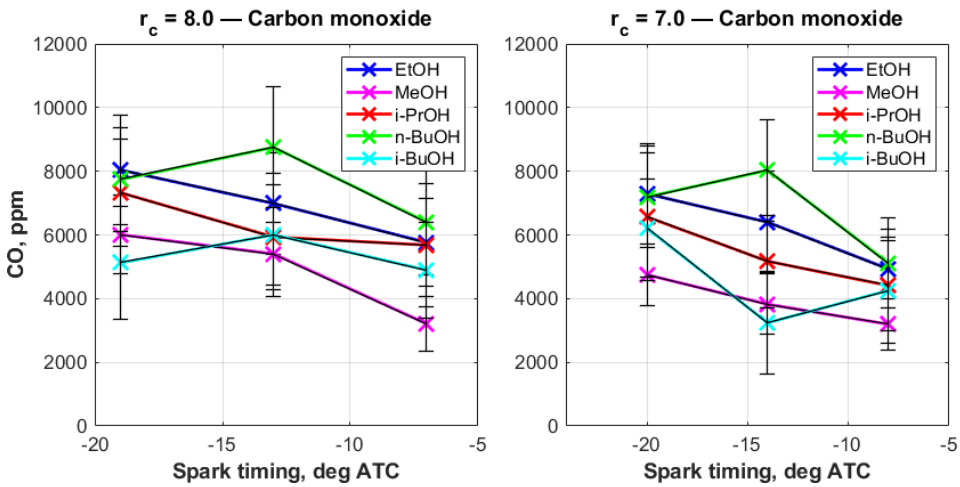

Figure 6.17: Carbon monoxide emissions (compression ratios indicated).

The average overall lambda values measured at the corresponding points are shown in Figure 6.18. By comparing these plots with the ones above, it can be seen that the CO emissions do not follow the same pattern exhibited by the lambda plots. For instance, *n*-butanol produced the highest CO concentrations, whereas its lambda values were technically the lowest. Therefore, the carbon monoxide emissions did not seem to be linked to the slight lambda variations seen in Figure 6.18. It could be speculated that the CO emissions were influenced by differences in the viscosity

and/or volatility of the alcohols, resulting in localized, slightly richer regions where fuel and air were poorly mixed.

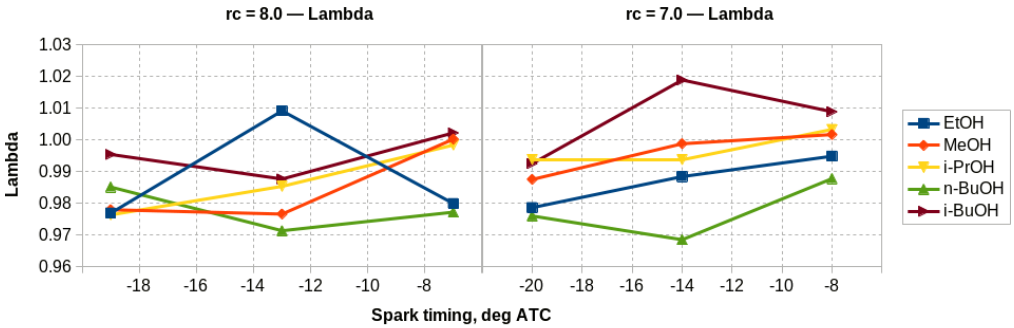

Figure 6.18: Relative air/fuel ratios (λ) (compression ratios indicated).

Hydrocarbons

The exhaust concentrations of hydrocarbons are shown in Figure 6.19. Similar to the CO emissions, the HC concentration ranges also differ roughly by a factor of two. Inspecting both plots, it can be seen that they exhibit the following trend: n-BuOH > i-BuOH > i-PrOH > MeOH > EtOH. At both compression ratios, the alcohols with the largest molecules, isobutanol and *n*-butanol, produced the highest concentrations of unburned hydrocarbons, whereas the HC emissions for the smaller alcohols ethanol, methanol, and isopropanol were the lowest. These results suggest that the volatility of the alcohols might have been responsible for the differences in the hydrocarbon concentrations, since the largest alcohols exhibit lower volatilities, a characteristic that can impair their combustion.

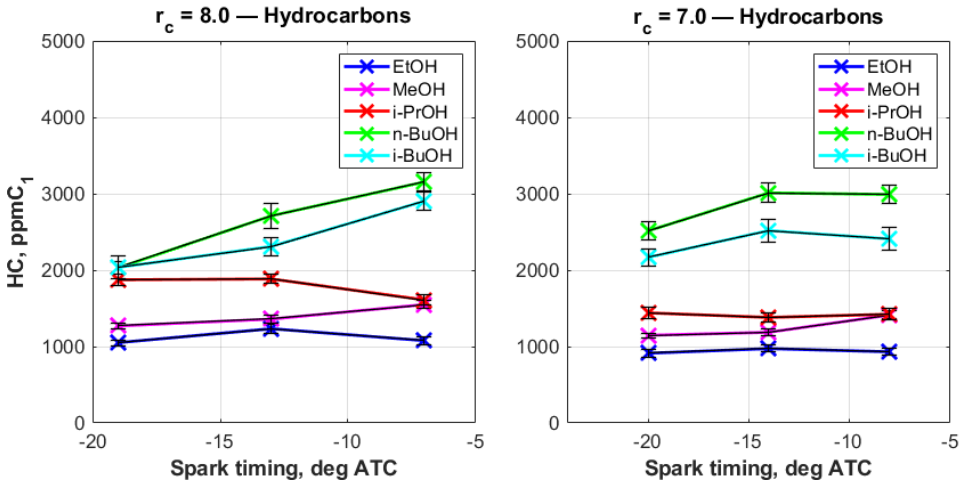

Figure 6.19: Hydrocarbon emissions (compression ratios indicated).

Nitric Oxide

Figure 6.20 shows the emissions of nitric oxide for all alcohols, at both compression ratios. The plots show a trend in the NO concentrations that can be roughly summarized as follows: i-BuOH > n-BuOH > i-PrOH ≈ MeOH ≈ EtOH. This trend is most likely related to the different peak combustion temperatures obtained with the different alcohols.

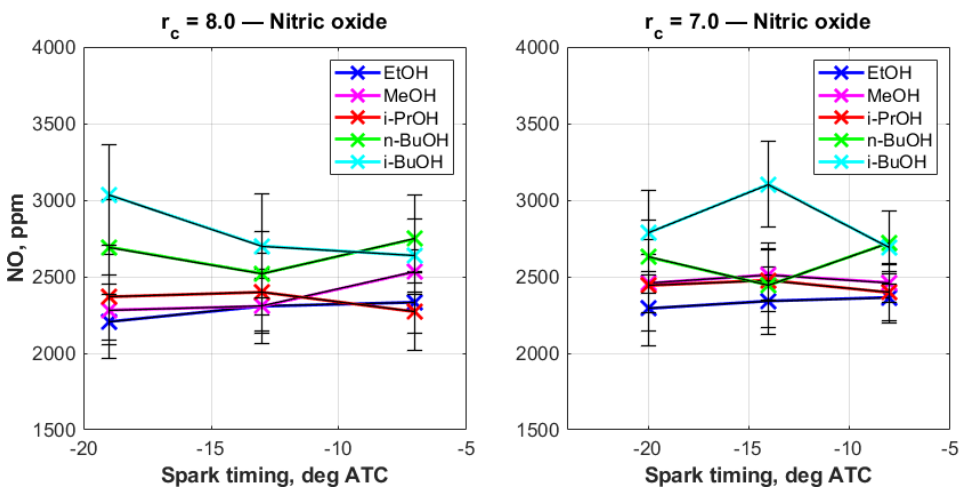

Figure 6.20: Nitric oxide emissions (compression ratios indicated).

Formaldehyde

The emissions of formaldehyde, Figure 6.21, while being low for all alcohols, is the highest in the case of methanol, since it is one of the main intermediate species produced during its combustion [79].

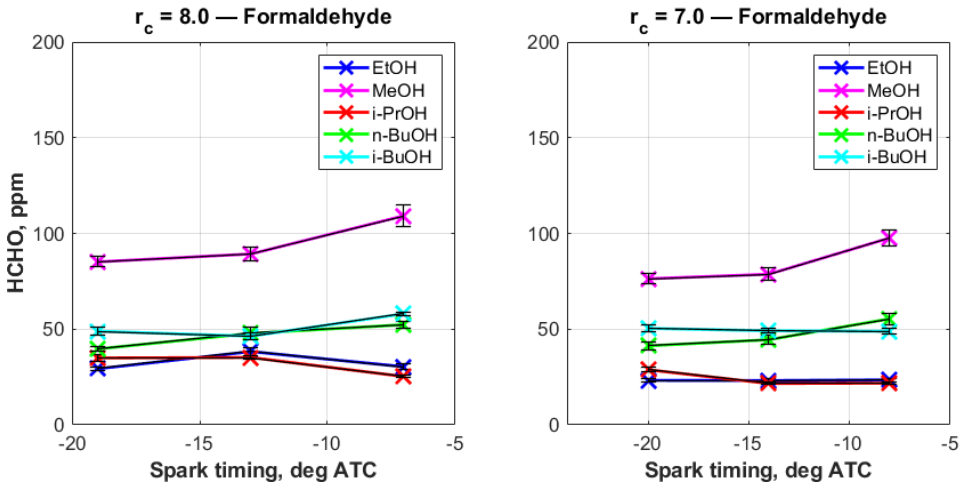

Figure 6.21: Formaldehyde emissions (compression ratios indicated).

Acetaldehyde

The acetaldehyde emissions are shown in Figure 6.22. As it can be easily seen, the acetaldehyde emissions from methanol and isopropanol were negative, which is obviously not possible. An explanation for this may be the fact that the FTIR analyzer was not able to interpret the spectra produced by the emissions from those two alcohols. Being an instrument to be primarily used by OEMs, the analyzer was most likely calibrated to measure the exhaust emissions produced by the conventional fuels gasoline and diesel—but *not* the emissions from fuels such as methanol and isopropanol [235]. Because it just could not interpret those two fuels, it produced an error in the form of negative values. Moreover, it is also probable that the acetaldehyde emissions from ethanol and the butanols, while positive, might not be correct.

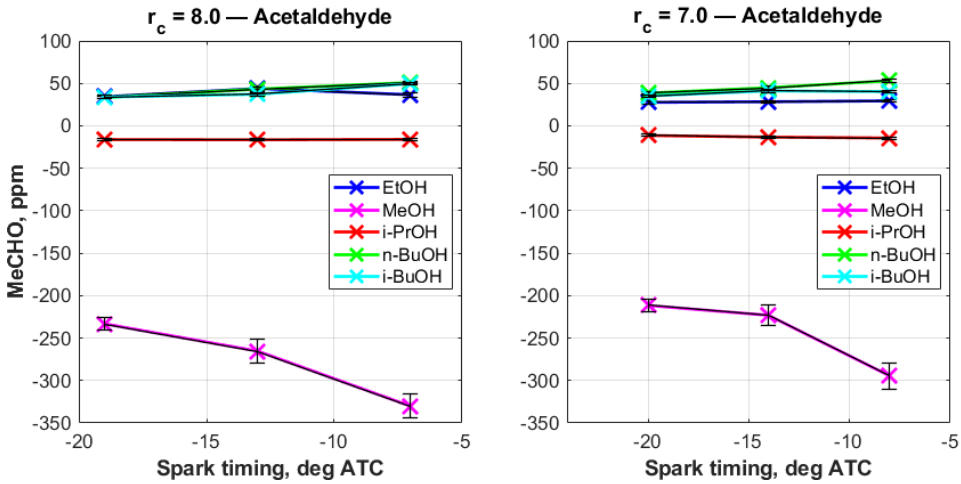

Figure 6.22: Acetaldehyde emissions (compression ratios indicated).

6.4 Summary

In this chapter, the goal was to investigate the characteristics of alcohols that can make them suitable for being used as neat fuels for spark-ignition engines. The compounds investigated were the C_1–C_4 alcohols methanol, ethanol, isopropanol, *n*-butanol, and isobutanol. Due to the fact that avoiding knock is extremely important for SI engines, the engine experiments described in this chapter focused on evaluating the knock propensities of the different neat alcohols. As in Chapter 5, in this chapter engine testing was done on a modified spark-ignition Waukesha CFR engine operating at a fixed speed, at different compression ratios and spark timings. The results showed that the different alcohols exhibited distinguishable behaviors regarding their resistance to autoignition. Even so, they performed roughly equally well, except for *n*-butanol, whose knock tendency, as measured using the maximum amplitude of pressure oscillations (MAPO), was significantly and consistently the highest among the alcohols. This finding is in line with the results from the previous chapter, in which *n*-butanol, as a gasoline oxygenate, produced the worst results, based on its MAPO behavior. On the other end, isopropanol seemed to produce the lowest MAPOs overall, highlighting its potential as a neat SI fuel. This is evidenced by its octane ratings (both RON and MON, see Table 6.1), the highest of all alcohols tested. As stated above, propanol is the smallest alcohol existing as different isomers, which means that isopropanol is the smallest alcohol molecule

exhibiting a branched structure, characteristics that help explain its seemingly superior knock resistance. However, as previously stated, even though it is possible to synthesize isopropanol from renewable sources, the available techniques for doing so still do not seem feasible for its large-scale production. Isobutanol is another interesting alcohol emerging from the present study. Its branched structure translates into good autoignition resistance while its larger molecule results in a higher heating value, when compared to the most common alcohol fuel, ethanol. Compared to ethanol, isobutanol also gives additional benefits, such as lower corrosiveness and lower water affinity.

Given the fact that the available techniques for obtaining isobutanol from biomass have matured to the point of making its large-scale manufacture feasible, there seems to be little doubt that it has the potential to become an alternative to ethanol, either as a gasoline oxygenate, as discussed in the previous chapter or, as shown in the present one, as a neat fuel.

Chapter 7

Conclusions and Outlook

7.1 Overview

The research work described in this dissertation investigated the use of alternative fuels for internal combustion engines (ICEs), having the possibility to be produced from renewable sources. More specifically, this work studied the potential of certain types of glycerol-derived chemicals and C_1–C_4 alcohols to be used as fuels for ICEs. The research activities described in this study originated from the *BioRen* project, an E.U.-funded, *Horizon 2020* project of which the author was a member. The *BioRen* project had the main goal of producing fuels from the organic fraction of municipal solid waste (MSW), essentially a cellulosic feedstock, via fermentation routes. The target fuels included ethanol, isobutanol and, most notably, glycerol *tert*-butyl ether (GTBE), a chemical compound with the potential to be used as fuel component (i.e. additive) for both gasoline and diesel fuels. Part of the purpose of GTBE production is that it can be obtained using the waste glycerol that is the by-product of the biodiesel transesterification process. By doing that, the *BioRen* project aimed at not only producing biofuels, but also at tackling waste-management issues, in the framework of the circular economy. Finally, the residues of the fermentation process were then turned into biocoal through a hydrothermal carbonization (HTC) process. The overall tasks of the project, which were allocated to the different members as work packages, ranged from MSW sorting and pretreatment, to isobutanol and GTBE production, to the evaluation of the biofuels though engine testing, the package that was assigned to Lund University.

The present work is based on such activities. However, to increase its relevance, the scope of the engine tests was expanded to include other types of glycerol derivatives in addition to GTBE, such as solketal and triacetin, with the potential to be used as fuel components. Moreover, besides ethanol and isobutanol, methanol, isopropanol, and *n*-butanol were included in the tests.

The tests described in this work promote the *diversification* of the available fuel options for the transport sector. As discussed in the introductory chapter of this monograph, fuel diversification is an important step towards a decarbonized transport. To that end, the various chemical compounds discussed in this study were evaluated as fuel components by preparing their blends with either a gasoline surrogate (for the SI tests) or commercial diesel fuel (for the diesel tests), depending on the fuel and the test type. The diesel tests were performed on both a light-duty and a heavy-duty diesel engine, while the spark-ignition tests were carried out on a CFR engine, an engine especially designed for fuel testing. Besides evaluating fuel *blends*, this study also evaluated the performance of *neat* C_1–C_4 alcohols on the CFR engine, since such compounds have properties that make them particularly suited to SI engine operation. For all tests and all fuels, combustion characteristics and exhaust emissions were the main focus, whereas for the SI engine tests, the knock propensity of the alcohols (either in blends with the gasoline surrogate or in neat form) was also relevant. Due to the fact that several compounds were tested, at a number of operating conditions, and using three different engines, the results were extensive, but the following paragraphs should provide a quick insight into them.

7.2 Key Takeaways

The light-duty diesel engine tests of **Chapter 3** served as an initial screening of GTBE and isobutanol as additives for diesel fuel, as a prelude to the subsequent heavy-duty engine tests. The GTBE was mixed with diesel at a concentration of 5 vol.% and the isobutanol blend, mixed at 6.5 vol.%, was prepared to match that same oxygen content. In addition, a 10 vol.% GTBE blend was prepared, but tested at only one operating condition. A four-cylinder Volvo passenger car engine was used for the tests. As a preliminary set of experiments, the tests described in Chapter 3 showed that the addition of GTBE or isobutanol did not compromise

engine performance, at those relatively low blending concentrations. In addition, the presence of fuel-bound oxygen meant that both compounds were able to reduce soot emissions, an effect that was most pronounced at light loads. Regarding NO_x emissions, the oxygenated blends, in general, were able to lower the soot emissions while keeping the NO_x levels relatively constant, a pattern that was not visible at full load (in which the soot-reducing benefits of the oxygenated blends were less evident).

Chapter 4 discussed the heavy-duty diesel tests. Those tests were more extensive and were divided into two parts, depending on the concentrations at which the oxygenates were mixed with diesel fuel. In the first part, the blends were prepared to match the oxygen content of a 5 vol.% di-GTBE blend. On the other hand, in the second part, all oxygenated compounds were mixed at a fixed concentration of 4 vol.%. In addition to B7 diesel (i.e. diesel fuel containing 7 vol.% of biodiesel), additional compounds were tested in Chapter 4: a 75%/25% mixture of mono- and di-GTBE, pure di-GTBE, pure tri-GTBE, solketal, and triacetin. The inclusion of these extra compounds showed that they have potential to be mixed with diesel fuels in low concentrations, thus contributing to displacing fossil fuel usage. Besides not impairing engine performance, the overall results showed that, in general, the oxygenated compounds seemed to reduce the emissions of soot, hydrocarbons, and carbon monoxide, without increasing the NO_x emissions appreciably (due to the well-known soot-NO_x trade-off).

The part of this work dealing with spark-ignition tests starts with **Chapter 5**. A modified Waukesha CFR engine was used throughout the experiments. Moreover, the main focus of the SI tests was to evaluate the knock tendency of the different fuels, since knock can be a significant constraint on the performance of SI engines, and also because the CFR engine was specifically designed for assessing the octane rating (i.e. the knock resistance) of fuels. For these tests, a gasoline surrogate comprised of iso-octane, *n*-heptane, and toluene, having an octane rating (RON) of 91, was used as baseline fuel. To that surrogate, the glycerol derivatives and alcohols were blended, at two different concentration levels, matching the oxygen content of a blend of 10 vol.% and 20 vol.% ethanol (commonly known as "E10" and "E20", respectively), for a total of 16 different fuels that were tested. The chosen knock metric was the so-called maximum amplitude of pressure oscillations (MAPO) and knock propensity was evaluated with the use of empirical cumulative frequency distributions, based on the MAPO results logged over 1000 engine cycles. The results

showed that, among the glycerol derivatives, the GTBE types were the most effective in reducing the MAPO intensity, as shown by the cumulative distributions. On the other hand, solketal gave the poorest performance. Among the alcohols, in general, all of them performed well, with the notable exception of *n*-butanol, whose MAPO values were consistently the highest, even at very mild, essentially knock-free, engine operating conditions. On the other hand, isopropanol and isobutanol performed particularly well.

Finally, **Chapter 6** addressed the topic of using neat alcohols as SI fuels. In that chapter, methanol, ethanol, isopropanol, *n*-butanol, and isobutanol were evaluated according to their knock tendencies. The CFR engine was again used and the test procedure was very similar to that of Chapter 5. The results, based on the cumulative frequency distributions, showed that the alcohols exhibited distinguishable behaviors regarding their knock resistance. As in Chapter 5, *n*-butanol clearly had the worst performance. The remaining alcohols performed well, particularly isopropanol, since the MAPO levels it produced seemed to be the lowest among all alcohols. This is unsurprising, as isopropanol has the highest octane rating among the alcohols (see Table 6.1). Isobutanol also exhibited good knock resistance, which, along with its higher heating value, lower water affinity and corrosiveness, and improved biochemical routes to produced it from biomass, makes it a uniquely good alternative to ethanol, as a gasoline oxygenate.

The findings presented in this work were the results of extensive engine testing, carried out using several different fuels, on three different engines, and at many different engine operating conditions. The overall results showed that the main target fuels of the *BioRen* project, isobutanol and GTBE have the potential to be used as fuel components. In the case of diesel fuel, the blending levels of either compound should be restricted to lower concentrations, since the cetane ratings of both are expected to be low, making the use of high-concentration blends unfeasible for diesel applications. In any case, if isobutanol and GTBE were to be used as diesel oxygenates, the mixing levels should be kept at low values, in order to conform to existing fuel standards (such as the U.S. standard ASTM D975 [239] and the European norm EN 590 [200]). In that aspect, the glycerol compounds should be more suitable for SI applications, so it is not surprising that many of the available studies investigate their potential as octane boosters. The inferior knock-inhibiting performance of *n*-butanol—either as an oxygenate or as a neat fuel—highlights the fact that straight-chain compounds tend to have inferior knock resistance, when com-

pared to their branched-molecule counterparts. This characteristic was evidenced in the case of isopropanol, the smallest tertiary (and as such, branched) alcohol, since its overall knock resistance was shown to be highest among the alcohols, both when used as an oxygenate, mixed with the surrogate, or in neat form. Unfortunately, even though there have been advances in the field, the routes for producing isopropanol from renewable sources still seem to be problematic, which precludes its use as an SI fuel and helps explain the limited number of engine studies found in the literature devoted to it. On the other hand, the production of isobutanol from biomass seems to have reached a level that is mature enough to allow it to be manufactured at commercial scale. From the results, isobutanol exhibited good knock resistance. In addition to that, when compared to ethanol—the biofuel *par excellence*—it has advantages such as a higher heating value, much lower affinity for water, lower corrosiveness and a lower impact on the distillation properties and volatility of the base gasoline (which simplifies its blending with it). When considering all these advantages together, it becomes clear that, from a purely technical perspective, isobutanol is a superior gasoline oxygenate, compared to ethanol. Those favorable characteristics, especially its lower corrosiveness, also mean that it has a very good potential to be used as neat fuel. Lastly, the fact it has a lower oxygen content, when compared to ethanol, means that a larger volume of isobutanol can be blended with gasoline to achieve a fixed maximum blend oxygen content, alleviating the "blend wall" problem that exists in some markets (for instance, the U.S.[1] and the E.U.[2]). When produced from renewable feedstocks, it also means that larger volumes of fossil gasoline can be displaced, contributing even further to the goal of decarbonizing transport.

7.3 Limitations of the Study

It needs to be taken into account that, being an academic study with a limited availability of glycerol derivatives, the use of a larger multi-cylinder engine (such as a production heavy-duty diesel) was not an option. That, in addition to single-cylinder-engine experiments, could have provided additional valuable insights regarding the use of the oxygenates in a more realistic "real-world" application. Furthermore, it should be kept in mind that the results presented in this dissertation

[1]According to the ASTM standard D4814 [240].
[2]According to the European standard EN 228 [241].

are based on a limited number of experiments and, as such, care should be taken when making generalizations of the study's main findings. Lastly, being an academic study, the conclusions obtained from it were based on experiments done on engines operating in controlled settings and not under more realistic conditions.

7.4 Suggestions for Future Work

The results presented in this work were based on engine tests carried out on three different engines, at several different operating conditions. As mentioned above, the possibility of using a multi-cylinder heavy-duty diesel engine could provide additional information on the behavior of the different fuel blends under more severe and realistic conditions. On the spark-ignition side, while the CFR engine is a very valuable tool for engine testing—especially when investigating the knock resistance of fuels—it is far different from modern spark-ignition engines. As mentioned in Chapter 2, the CFR engine was originally designed in the 1920s with the goal of measuring and characterizing knock. While conventional engines are designed to avoid the occurrence of knock at any cost, the CFR engine was designed to induce it, so it can be measured and characterized. This very fact in itself puts the CFR engine at odds with any conventional spark-ignition engine. Therefore, a valuable suggestion for future work would be to, in addition to using the CFR engine, evaluate the performance of the glycerol derivatives and the C_1–C_4 alcohols on a modern production SI engine, featuring characteristics such as downsizing and high boosting levels, direct fuel injection, variable valve timing, among others. It would be interesting to compare the knock behaviors of the different fuels obtained with the CFR engine and with a modern production engine. That could provide valuable additional insights into the knock performance of the different fuels.

Appendix A

Uncertainty Assessment

Analyzing uncertainties is about predicting the uncertainty interval associated with an experimental result, based on the *scatter* observed in the raw data that were used to calculate such result [242]. Uncertainties in the measured data can be assessed based on the accuracies of the measuring instruments. However, when physical quantities cannot be measured directly, those uncertainties "propagate" through the calculations, making it necessary to quantify this propagation process in order to evaluate the uncertainty in the final answer. In that way, the overall uncertainties associated to an experimental result can be estimated.

Thus, if N quantities x_1, x_2, …, x_N are measured with uncertainties δx_1, δx_2, …, δx_N, and the measured quantity q is any function of the variables x_1, x_2, …, x_N, then the uncertainty in q is expressed as follows [243]:

$$\delta R = \sqrt{\left(\frac{\partial R}{\partial x_1}\delta x_1\right)^2 + \left(\frac{\partial R}{\partial x_2}\delta x_2\right)^2 + \cdots + \left(\frac{\partial R}{\partial x_N}\delta x_N\right)^2} \tag{A.1}$$

In this equation, each term represents the contribution made by the uncertainty in one variable, δx_i, to the overall uncertainty in the result, δR. Each term has the same form: the partial derivative of R with respect to x_i multiplied by the uncertainty interval for that variable.

Equation (A.1) is the basic equation of uncertainty analysis [244] and, as such, it can estimate the the uncertainty in a computed result with good accuracy for most

functions of engineering importance [245].

In the present work, most of the plots have error bars showing the *standard deviation* of the logged data. Therefore, those bars represent the variability of the measured data around their mean value and not the "true" errors, or uncertainties, in the narrow sense of the word.

However, as Taylor pointed out in his textbook [243], the standard deviation proves to be a useful way of characterizing the reliability of measurements. For a normally-distributed quantity that has been measured N times with separate measurements $x_1, x_2, \ldots, x_N$, the mean $\bar{x}$ represents the best estimate of the "true" value of the quantity in question, whereas the standard deviation obtained from those $x_1, x_2, \ldots, x_N$ measurements is an estimate of the average uncertainty in the *individual* measurements $x_1, x_2, \ldots, x_N$.

Moreover, as long as systemic measurement errors are negligible, the *standard deviation of the mean* of those $x_1, x_2, \ldots, x_N$ measurements, defined as

$$\bar{\sigma}_x = \frac{\sigma_x}{N} \tag{A.2}$$

represents the uncertainty in the best estimate for x, that is, the uncertainty in $\bar{x}$.

Therefore, the quantity x can be expressed as:

$$x = \bar{x} \pm \bar{\sigma}_x$$

In summary, if the measurement of a quantity has been made (i.e. logged) enough times, the scatter of the measured values, as represented by their standard deviation, should still give an indication of the uncertainties involved (although the standard deviation of the mean will produce a smaller, less conservative, value).

References

[1] WUEBBLES, DJ. and JAIN, AK. Concerns about climate change and the role of fossil fuel use. *Fuel Processing Technology*, June 2001, vol. 71, no. 1-3, p. 99–119, doi:10.1016/S0378-3820(01)00139-4.

[2] US DEPARTMENT OF COMMERCE, NOAA. Global Monitoring Laboratory - Carbon Cycle Greenhouse Gases. Available from: `https://gml.noaa.gov/ccgg/trends/`

[3] RITCHIE, HANNAH. Sector by sector: where do global greenhouse gas emissions come from? https://ourworldindata.org/ghg-emissions-by-sector. *Our World in Data*, 2020.

[4] DI RATTALMA, MF. (ed.). *The Dieselgate: A Legal Perspective*. Doi:10.1007/978-3-319-48323-8. Cham (Switzerland): Springer International Publishing, 2017. ISBN 978-3-319-48322-1.

[5] MAHMOUDZADEH ANDWARI, A., PESIRIDIS, A., RAJOO, S., *et al.* A review of Battery Electric Vehicle technology and readiness levels. *Renewable and Sustainable Energy Reviews*, Oct. 2017, vol. 78, p. 414–430, doi:10.1016/j.rser.2017.03.138.

[6] WEISS, M., PATEL, MK., JUNGINGER, M., *et al.* On the electrification of road transport - Learning rates and price forecasts for hybrid-electric and battery-electric vehicles. *Energy Policy*, Sept. 2012, vol. 48, p. 374–393, doi:10.1016/j.enpol.2012.05.038.

[7] SENECAL, K. and LEACH, F. *Racing Toward Zero: The Untold Story of Driving Green*. Warrendale: SAE International, 2021. 280 p. ISBN 978-1-4686-0146-6.

[8] ZHANG, R. and FUJIMORI, S. The role of transport electrification in global climate change mitigation scenarios. *Environmental Research Letters*, Feb. 2020, vol. 15, no. 3, p. 034019, doi:10.1088/1748-9326/ab6658.

[9] KALGHATGI, G. Is it really the end of internal combustion engines and petroleum in transport? *Applied Energy*, Sept. 2018, vol. 225, p. 965–974, doi:10.1016/j.apenergy.2018.05.076.

[10] QIAO, Q., ZHAO, F., LIU, Z., *et al.* Cradle-to-gate greenhouse gas emissions of battery electric and internal combustion engine vehicles in China. *Applied Energy*, May 2017, vol. 204, p. 1399–1411, doi:10.1016/j.apenergy.2017.05.041.

[11] OLIVETTI, EA., CEDER, G., GAUSTAD, GG., *et al.* Lithium-Ion Battery Supply Chain Considerations: Analysis of Potential Bottlenecks in Critical Metals. *Joule*, Oct. 2017, vol. 1, no. 2, p. 229–243, doi:10.1016/j.joule.2017.08.019.

[12] DUMMETT, M. The Dark Side of Electric Cars: Exploitative Labor Practices. *TIME*, Sept. 2017. Available from: `https://time.com/4939738/electric-cars-human-rights-congo/`

[13] INTERNATIONAL, AMNESTY. Electric cars: Running on child labour? Sept. 2016. Available from: `https://www.amnesty.org/en/latest/press-release/2016/09/electric-cars-running-on-child-labour/`

[14] ONORATI, A., PAYRI, R., VAGLIECO, BM., *et al.* The role of hydrogen for future internal combustion engines. *International Journal of Engine Research*, Apr. 2022, vol. 23, no. 4, p. 529–540, doi:10.1177/14680874221081947.

[15] DESANTES, JM., NOVELLA, R., PLA, B., *et al.* Impact of fuel cell range extender powertrain design on greenhouse gases and NOx emissions in automotive applications. *Applied Energy*, Nov. 2021, vol. 302, p. 117526, doi:10.1016/j.apenergy.2021.117526.

[16] OLAH, GA., GOEPPERT, A., and PRAKASH, GKS. Chemical Recycling of Carbon Dioxide to Methanol and Dimethyl Ether: From Greenhouse Gas to Renewable, Environmentally Carbon Neutral Fuels and Synthetic Hydrocarbons. *The Journal of Organic Chemistry*, Jan. 2009, vol. 74, no. 2, p. 487–498, doi:10.1021/jo801260f.

[17] NO AUTHOR, . The death of the internal combustion engine. *The Economist*, Aug. 2017, vol. 424, no. 9053, p. 7–8.

[18] MAYERSOHN, N. The Internal Combustion Engine Is Not Dead Yet. *The New York Times*, Aug. 2017, ISSN 0362-4331.

[19] STATISTA, DAILY DATA. Infographic: E-Mobility: Norway Races Ahead. Jan. 2023. Available from: `https://www.statista.com/chart/23863/electric-car-share-in-norway`

[20] REITZ, RD., OGAWA, H., PAYRI, R., *et al.* IJER editorial: The future of the internal combustion engine. *International Journal of Engine Research*, Jan. 2020, vol. 21, no. 1, p. 3–10, doi:10.1177/1468087419877990.

[21] U.S. ENERGY INFORMATION ADMINISTRATION, (EIA). Biomass explained - U.S. Energy Information Administration (EIA). Available from: `https://www.eia.gov/energyexplained/biomass/`

[22] REIJNDERS, L. and HUIJBREGTS, M. *Biofuels for Road Transport: A Seed to Wheel Perspective*. London: Springer, 2009. Green Energy and Technology. ISBN 978-1-84882-137-8.

[23] KLEMM, D., HEUBLEIN, B., FINK, H-P., *et al.* Cellulose: Fascinating Biopolymer and Sustainable Raw Material. *Angewandte Chemie International Edition*, May 2005, vol. 44, no. 22, p. 3358–3393, doi:10.1002/anie.200460587.

[24] CRAWFORD, RL. *Lignin Biodegradation and Transformation*. New York: Wiley, 1981. ISBN 978-0-471-05743-7.

[25] MICHEL, HARTMUT. Editorial: The Nonsense of Biofuels. *Angewandte Chemie International Edition*, Mar. 2012, vol. 51, no. 11, p. 2516–2518, doi:10.1002/anie.201200218.

[26] APPELS, L., LAUWERS, J., DEGRÈVE, J., *et al.* Anaerobic digestion in global bio-energy production: Potential and research challenges. *Renewable and Sustainable Energy Reviews*, Dec. 2011, vol. 15, no. 9, p. 4295–4301, doi:10.1016/j.rser.2011.07.121.

[27] SELIN, NE. and LEHMAN, C. Biofuel. *Encyclopædia Britannica*, Sept. 2024. Available from: `https://www.britannica.com/technology/biofuel`

[28] OECD, and FAO, . *OECD-FAO Agricultural Outlook 2024-2033*. doi:10.1787/4c5d2cfb-en. Paris: OECD Publishing, July 2024. 335 p. ISBN 978-92-64-72259-0. Available from: `https://www.oecd-ilibrary.org/content/publication/4c5d2cfb-en`

[29] KNOTHE, G. and RAZON, LF. Biodiesel fuels. *Progress in Energy and Combustion Science*, Jan. 2017, vol. 58, p. 36–59, doi:10.1016/j.pecs.2016.08.001.

[30] RANTANEN, L., LINNAILA, R., AAKKO, P., *et al.* NExBTL - Biodiesel Fuel of the Second Generation. SAE paper 2005-01-3771. *SAE Technical Paper Series*, Oct. 2005, doi:10.4271/2005-01-3771.

[31] TIMILSINA, GR. and SHRESTHA, A. How much hope should we have for biofuels? *Energy*, Apr. 2011, vol. 36, no. 4, p. 2055–2069, doi:10.1016/j.energy.2010.08.023.

[32] CHISTI, Y. Biodiesel from microalgae. *Biotechnology Advances*, May 2011, vol. 25, no. 3, p. 294–306, doi:10.1016/j.biotechadv.2007.02.001.

[33] MAROUŠEK, J., MAROUŠKOVÁ, A., GAVUROVÁ, B., *et al.* Competitive algae biodiesel depends on advances in mass algae cultivation. *Bioresource Technology*, Apr. 2023, vol. 374, p. 128802, doi:10.1016/j.biortech.2023.128802.

[34] HUTCHINGS, G, DAVIDSON, M., ATKINS, P., *et al. Sustainable synthetic carbon based fuels for transport: Policy Briefing*. London: The Royal Society, Sept. 2019. 44 p. ISBN 978-17-82-52422-9.

[35] BRYNOLF, S., TALJEGÅRD, M., GRAHN, M., *et al.* Electrofuels for the transport sector: A review of production costs. *Renewable and Sustainable Energy Reviews*, Jan. 2018, vol. 81, p. 1887–1905, doi:10.1016/j.rser.2017.05.288.

[36] RAMIREZ, A., SARATHY, SM., and GASCON, J. CO2 Derived E-Fuels: Research Trends, Misconceptions, and Future Directions. *Trends in Chemistry*, Sept. 2020, vol. 2, no. 9, p. 785–795, doi:10.1016/j.trechm.2020.07.005.

[37] GLENK, G. and REICHELSTEIN, S. Economics of converting renewable power to hydrogen. *Nature Energy*, Feb. 2019, vol. 4, no. 3, p. 216–222, doi:10.1038/s41560-019-0326-1.

[38] FARGIONE, J., HILL, J., TILMAN, D., *et al.* Land Clearing and the Biofuel Carbon Debt. *Science*, Feb. 2008, vol. 319, no. 5867, p. 1235–1238, doi:10.1126/science.1152747.

[39] SEARCHINGER, T., HEIMLICH, R., HOUGHTON, RA., *et al.* Use of U.S. Croplands for Biofuels Increases Greenhouse Gases Through Emissions from Land-Use Change. *Science*, Feb. 2008, vol. 319, no. 5867, p. 1238–1240, doi:10.1126/science.1151861.

[40] DANIELSEN, F., BEUKEMA, H., BURGESS, ND., *et al.* Biofuel Plantations on Forested Lands: Double Jeopardy for Biodiversity and Climate. *Conservation Biology*, Apr. 2009, vol. 23, no. 2, p. 348–358, doi:10.1111/j.1523-1739.2008.01096.x.

[41] FARGIONE, JE., PLEVIN, RJ., and HILL, JD. The Ecological Impact of Biofuels. *Annual Review of Ecology, Evolution, and Systematics*, Dec. 2010, vol. 41, no. 1, p. 351–377, doi:10.1146/annurev-ecolsys-102209-144720.

[42] COMMISSION, EUROPEAN. BioRen - Development of competitive, next generation biofuels from municipal solid waste. 2020. Available from: `https://www.bioren.be`

[43] CORDIS, EUROPEAN COMMISSION. Development of competitive, next generation biofuels from municipal solid waste | BioRen Project | Fact Sheet | H2020. Available from: `https://cordis.europa.eu/project/id/818310`

[44] KOWALSKI, Z., KULCZYCKA, J., VERHÉ, R., *et al.* Second-generation biofuel production from the organic fraction of municipal solid waste. *Frontiers in Energy Research*, Aug. 2022, vol. 10, p. 919415, doi:10.3389/fenrg.2022.919415.

[45] VERHÉ, R., VARGHESE, S., THEVELEIN, JM., *et al.* Production of Bio-Ethanol from the Organic Fraction of Municipal Solid Waste and Refuse-Derived Fuel. *Biomass*, Dec. 2022, vol. 2, no. 4, p. 224–236, doi:10.3390/biomass2040015.

[46] SENECAL, PK. and LEACH, F. Diversity in transportation: Why a mix of propulsion technologies is the way forward for the future fleet. *Results in Engineering*, Dec. 2019, vol. 4, p. 100060, doi:10.1016/j.rineng.2019.100060.

[47] BOURNE JR., JK. Green Dream. *National Geographic Magazine*, Oct. 2007, vol. 212, no. 4, p. 38–59.

[48] FOUNTAIN, H. Corn Ethanol Makers Weigh Switch to Butanol. *The New York Times*, Oct. 2012, ISSN 0362-4331.

[49] SMITH, OI. Fundamentals of soot formation in flames with application to diesel engine particulate emissions. *Progress in Energy and Combustion Science*, Jan. 1981, vol. 7, no. 4, p. 275–291, doi:10.1016/0360-1285(81)90002-2.

[50] TREE, DR. and SVENSSON, KI. Soot processes in compression ignition engines. *Progress in Energy and Combustion Science*, June 2007, vol. 33, no. 3, p. 272–309, doi:10.1016/j.pecs.2006.03.002.

[51] CHOI, MY., HAMINS, A., MULHOLLAND, GW., *et al.* Simultaneous optical measurement of soot volume fraction and temperature in premixed flames. *Combustion and Flame*, Oct. 1994, vol. 99, no. 1, p. 174–186, doi:10.1016/0010-2180(94)90088-4.

[52] HAYNES, BS. and WAGNER, HGG. Soot formation. *Progress in Energy and Combustion Science*, Jan. 1981, vol. 7, no. 4, p. 229–273, doi:10.1016/0360-1285(81)90001-0.

[53] GLASSMAN, I., YETTER, RA., and GLUMAC, NG. *Combustion*. 5th ed. Waltham, San Diego, London, Kidlington: Academic Press, 2015. 774 p. ISBN 978-0-12-407913-7.

[54] AMANN, CA. and SIEGLA, DC. Diesel Particulates—What They Are and Why. *Aerosol Science and Technology*, Jan. 1982, vol. 1, no. 1, p. 73–101, doi:10.1080/02786828208958580.

[55] KITTELSON, DB. Engines and nanoparticles: a review. *Journal of Aerosol Science*, June 1998, vol. 29, no. 5-6, p. 575–588, doi:10.1016/S0021-8502(97)10037-4.

[56] KITTELSON, DB., SUN, R., BLACKSHEAR, PL., *et al.* Oxidation of Soot Agglomerates in a Direct Injection Diesel Engine. SAE paper 920111. *SAE Technical Paper Series*, Feb. 1992, doi:10.4271/920111.

[57] DEC, JE. A Conceptual Model of Dl Diesel Combustion Based on Laser-Sheet Imaging. SAE paper 970873. *SAE Technical Paper Series*, Feb. 1997, doi:10.4271/970873.

[58] WESTBROOK, CK., PITZ, WJ., and CURRAN, HJ. Chemical Kinetic Modeling Study of the Effects of Oxygenated Hydrocarbons on Soot Emissions from Diesel Engines. *The Journal of Physical Chemistry A*, June 2006, vol. 110, no. 21, p. 6912–6922, doi:10.1021/jp056362g.

[59] SIEBERS, DL. and HIGGINS, B. Flame Lift-Off on Direct-Injection Diesel Sprays Under Quiescent Conditions. SAE paper 2001-01-0530. *SAE Technical Paper Series*, Mar. 2001, doi:10.4271/2001-01-0530.

[60] MIYAMOTO, N., OGAWA, H., ARIMA, T., *et al.* Improvement of Diesel Combustion and Emissions with Addition of Various Oxygenated Agents to Diesel Fuels. SAE paper 962115. *SAE Technical Paper Series*, Oct. 1996, doi:10.4271/962115.

[61] MIYAMOTO, N., OGAWA, H., NURUN, NM., *et al.* Smokeless, Low NOx, High Thermal Efficiency, and Low Noise Diesel Combustion with Oxygenated Agents as Main Fuel. SAE paper 980506. *SAE Technical Paper Series*, Feb. 1998, doi:10.4271/980506.

[62] NABI, MN., MINAMI, M., OGAWA, H., *et al.* Ultra Low Emission and High Performance Diesel Combustion with Highly Oxygenated Fuel. SAE paper 2000-01-0231. *SAE Technical Paper Series*, Mar. 2000, doi:10.4271/2000-01-0231.

[63] HALLGREN, BE. and HEYWOOD, JB. Effects of Oxygenated Fuels on DI Diesel Combustion and Emissions. SAE paper 2001-01-0648. *SAE Technical Paper Series*, Mar. 2001, doi:10.4271/2001-01-0648.

[64] FLYNN, PF., DURRETT, RP., HUNTER, GL., *et al.* Diesel Combustion: An Integrated View Combining Laser Diagnostics, Chemical Kinetics, And Empirical Validation. SAE paper 1999-01-0509. *SAE Technical Paper Series*, Mar. 1999, doi:10.4271/1999-01-0509.

[65] CURRAN, HJ., FISHER, EM., GLAUDE, P-A., *et al.* Detailed Chemical Kinetic Modeling of Diesel Combustion with Oxygenated Fuels. SAE paper 2001-01-0653. *SAE Technical Paper Series*, Mar. 2001, doi:10.4271/2001-01-0653.

[66] CHENG, AS., DIBBLE, RW., and BUCHHOLZ, BA. The Effect of Oxygenates on Diesel Engine Particulate Matter. SAE paper 2002-01-1705. *SAE Technical Paper Series*, May 2002, doi:10.4271/2002-01-1705.

[67] MCENALLY, CS. and PFEFFERLE, LD. Experimental study of fuel decomposition and hydrocarbon growth processes for practical fuel components in nonpremixed flames: MTBE and related alkyl ethers. *International Journal of Chemical Kinetics*, June 2004, vol. 36, no. 6, p. 345–358, doi:10.1002/kin.20005.

[68] MCENALLY, CS. and PFEFFERLE, LD. Fuel decomposition and hydrocarbon growth processes for oxygenated hydrocarbons: butyl alcohols. *Proceedings of the Combustion Institute*, Jan. 2005, vol. 30, no. 1, p. 1363–1370, doi:10.1016/j.proci.2004.07.033.

[69] MCNESBY, KL., MIZIOLEK, AW., NGUYEN, T., *et al.* Experimental and computational studies of oxidizer and fuel side addition of ethanol to opposed flow air/ethylene flames. *Combustion and Flame*, Sept. 2005, vol. 142, no. 4, p. 413–427, doi:10.1016/j.combustflame.2005.04.003.

[70] RUBINO, L. and THOMSON, MJ. The Effect of Oxygenated Additives on Soot Precursor Formation in a Counterflow Diffusion Flame. SAE paper 1999-01-3589. *SAE Technical Paper Series*, Oct. 1999, doi:10.4271/1999-01-3589.

[71] CORRIGAN, DJ. and FONTANESI, S. Knock: A Century of Research. *SAE International Journal of Engines*, July 2021, vol. 15, no. 1, p. 57–127, doi:10.4271/03-15-01-0004.

[72] ROBEYN, T. *An alternative pressure-oscillation-based octane rating method, for fuels below and beyond 100 RON, to aid the development of a second-generation spark-ignition biofuel*. Doctoral dissertation, Ghent University, Ghent, Belgium, July 2024, iSBN 978-94-6355-858-7.

[73] SHAHLARI, AJ. and GHANDHI, JB. A Comparison of Engine Knock Metrics. SAE paper 2012-32-0007. *SAE Technical Paper Series*, Oct. 2012, doi:10.4271/2012-32-0007.

[74] DRAPER, CS. Pressure Waves Accompanying Detonation in the Internal Combustion Engine. *Journal of the Aeronautical Sciences*, Apr. 1938, vol. 5, no. 6, p. 219–226, doi:10.2514/8.590.

[75] ENG, JA. Characterization of Pressure Waves in HCCI Combustion. SAE paper 2002-01-2859. *SAE Technical Paper Series*, Oct. 2002, doi:10.4271/2002-01-2859.

[76] PUZINAUSKAS, PV. Examination of Methods Used to Characterize Engine Knock. SAE paper 920808. *SAE Technical Paper Series*, Feb. 1992, doi:10.4271/920808.

[77] HEYWOOD, JB. *Internal Combustion Engine Fundamentals*. 2nd ed. New York: McGraw-Hill Education, 2018. 1028 p. ISBN 978-1-260-11610-6.

[78] KHOVAKH, M. (ed.). *Motor Vehicle Engines*. Translated by A. Troitsky and M. Samokhvalov. 3rd printing. Moscow: Mir Publishers, 1979. 616 p. Translation of: Avtomobil'nye dvigateli.

[79] SARATHY, SM., OßWALD, P., HANSEN, N., *et al.* Alcohol combustion chemistry. *Progress in Energy and Combustion Science*, Oct. 2014, vol. 44, p. 40–102, doi:10.1016/j.pecs.2014.04.003.

[80] TANAKA, S., AYALA, F., KECK, JC., *et al.* Two-stage ignition in HCCI combustion and HCCI control by fuels and additives. *Combustion and Flame*, Jan. 2003, vol. 132, no. 1-2, p. 219–239, doi:10.1016/S0010-2180(02)00457-1.

[81] BRADLEY, D. and HEAD, RA. Engine autoignition: The relationship between octane numbers and autoignition delay times. *Combustion and Flame*, Nov. 2006, vol. 147, no. 3, p. 171–184, doi:10.1016/j.combustflame.2006.09.001.

[82] BOOT, MD., TIAN, M., HENSEN, EJM., *et al.* Impact of fuel molecular structure on auto-ignition behavior – Design rules for future high performance gasolines. *Progress in Energy and Combustion Science*, May 2017, vol. 60, p. 1–25, doi: 10.1016/j.pecs.2016.12.001.

[83] CHENG, S., KANG, D., FRIDLYAND, A., *et al.* Autoignition behavior of gasoline/ethanol blends at engine-relevant conditions. *Combustion and Flame*, June 2020, vol. 216, p. 369–384, doi:10.1016/j.combustflame.2020.02.032.

[84] GOLDSBOROUGH, SS., CHENG, S., KANG, D., *et al.* Effects of isoalcohol blending with gasoline on autoignition behavior in a rapid compression machine: Isopropanol and isobutanol. *Proceedings of the Combustion Institute*, 2021, vol. 38, no. 4, p. 5655–5664, doi:10.1016/j.proci.2020.08.027.

[85] CHENG, S., KANG, D., GOLDSBOROUGH, SS., *et al.* Experimental and modeling study of C2–C4 alcohol autoignition at intermediate temperature conditions. *Proceedings of the Combustion Institute*, 2021, vol. 38, no. 1, p. 709–717, doi:10.1016/j.proci.2020.08.005.

[86] CHENG, S., SAGGESE, C., KANG, D., *et al.* Autoignition and preliminary heat release of gasoline surrogates and their blends with ethanol at engine-relevant conditions: Experiments and comprehensive kinetic modeling. *Combustion and Flame*, June 2021, vol. 228, p. 57–77, doi:10.1016/j.combustflame.2021.01.033.

[87] SINGH, E., TINGAS, E-A., GOUSSIS, D., *et al.* Chemical Ignition Characteristics of Ethanol Blending with Primary Reference Fuels. *Energy & Fuels*, Oct. 2019, vol. 33, no. 10, p. 10185–10196, doi:10.1021/acs.energyfuels.9b01423.

[88] TAYLOR, CF. *The Internal-Combustion Engine in Theory and Practice*. Revised ed., vol. II: Combustion, Fuels, Material, Design. Cambridge (Mass.): MIT Press, 1985. 783 p. ISBN 978-0-262-70027-6.

[89] NABER, JB., BLOUGH, JR., FRANKOWSKI, D., *et al.* Analysis of Combustion Knock Metrics in Spark-Ignition Engines. SAE paper 2006-01-0400. *SAE Technical Paper Series*, Apr. 2006, doi:10.4271/2006-01-0400.

[90] LEPPARD, WR. Individual-Cylinder Knock Occurence and Intensity in Multicylinder Engines. SAE paper 820074. *SAE Technical Paper Series*, Feb. 1982, doi: 10.4271/820074.

[91] XIAOFENG, G., STONE, R., HUDSON, C., *et al.* The Detection and Quantification of Knock in Spark Ignition Engines. SAE paper 932759. *SAE Technical Paper Series*, Oct. 1993, doi:10.4271/932759.

[92] DICKINSON, HC. The Cooperative Fuel Research and Its Results. SAE paper 290032. *SAE Technical Paper Series*, 1929, doi:10.4271/290032.

[93] HORNING, HL. The Cooperative Fuel-Research Committee Engine. SAE paper 310019. *SAE Technical Paper Series*, 1931, doi:10.4271/310019.

[94] WAUKESHA ENGINE DRESSER, INC., . Waukesha CFR F-1 & F-2 Octane Rating Units Operation & Maintenance. 2003.

[95] SWARTS, A., YATES, A, VILJOEN, C., *et al.* A Further Study of Inconsistencies between Autoignition and Knock Intensity in the CFR Octane Rating Engine. SAE paper 2005-01-2081. *SAE Technical Paper Series*, May 2005, doi:10.4271/2005-01-2081.

[96] BELLMAN, DR., MOECKEL, WE., and EVVARD, JC. Knock-Limited Power Outputs from a CFR Engine Using Internal Coolants II - Six Aliphatic Amines. Advance Confidential Report E5H31, National Advisory Committee for Aeronautics, Washington, DC, Oct. 1945.

[97] ASTM INTERNATIONAL, . ASTM D2699-23a — Test Method for Research Octane Number of Spark-Ignition Engine Fuel. doi:10.1520/D2699-23A.

[98] ASTM INTERNATIONAL, . ASTM D2700-16 — Test Method for Motor Octane Number of Spark-Ignition Engine Fuel. doi:10.1520/D2700-16.

[99] CHUN, KM. and HEYWOOD, JB. Characterization of Knock in a Spark-Ignition Engine. SAE paper 890156. *SAE Technical Paper Series*, Feb. 1989, doi:10.4271/890156.

[100] WANG, Z., LIU, H., and REITZ, RD. Knocking combustion in spark-ignition engines. *Progress in Energy and Combustion Science*, July 2017, vol. 61, p. 78–112, doi:10.1016/j.pecs.2017.03.004.

[101] TURNER, JWG., POPPLEWELL, A., PATEL, R., *et al.* Ultra Boost for Economy: Extending the Limits of Extreme Engine Downsizing. SAE paper 2014-01-1185. *SAE International Journal of Engines*, Apr. 2014, vol. 7, no. 1, p. 387–417, doi:10.4271/2014-01-1185.

[102] DEMIRBAS, A., BALUBAID, MA., BASAHEL, AM., *et al.* Octane Rating of Gasoline and Octane Booster Additives. *Petroleum Science and Technology*, June 2015, vol. 33, no. 11, p. 1190–1197, doi:10.1080/10916466.2015.1050506.

[103] DABELSTEIN, W., REGLITZKY, A., SCHÜTZE, A., *et al.* Automotive Fuels. In WILEY-VCH (ed.). *Ullmann's Encyclopedia of Industrial Chemistry*. Weinheim: Wiley-VCH, 2016. p. 1–41. ISBN 978-3-527-30385-4.

[104] SQUILLACE, PJ., ZOGORSKI, JS., WILBER, WG., *et al.* Preliminary Assessment of the Occurrence and Possible Sources of MTBE in Groundwater in the United States, 1993–1994. *Environmental Science & Technology*, Apr. 1996, vol. 30, no. 5, p. 1721–1730, doi:10.1021/es9507170.

[105] HARTLEY, WR., ENGLANDE, AJ., and HARRINGTON, DJ. Health risk assessment of groundwater contaminated with methyl tertiary butyl ether (MTBE). *Water Science and Technology*, May 1999, vol. 39, no. 10-11, p. 305–310, doi:10.2166/wst.1999.0671.

[106] GOLDEMBERG, J. and MACEDO, IC. Brazilian alcohol program: an overview. *Energy for Sustainable Development*, May 1994, vol. 1, no. 1, p. 17–22, doi:10.1016/S0973-0826(08)60009-5.

[107] MOREIRA, JR. and GOLDEMBERG, J. The alcohol program. *Energy Policy*, Apr. 1999, vol. 27, no. 4, p. 229–245, doi:10.1016/S0301-4215(99)00005-1.

[108] DIETLER, M. Alcohol: Anthropological/Archaeological Perspectives. *Annual Review of Anthropology*, Oct. 2006, vol. 35, no. 1, p. 229–249, doi:10.1146/annurev.anthro.35.081705.123120.

[109] OLSON, AL., TUNÉR, M., and VERHELST, S. A concise review of glycerol derivatives for use as fuel additives. *Heliyon*, Jan. 2023, vol. 9, no. 1, p. e13041, doi:10.1016/j.heliyon.2023.e13041.

[110] CHRISTOPH, R., SCHMIDT, B., STEINBERNER, U., *et al.* Glycerol. In *Ullmann's Encyclopedia of Industrial Chemistry*, vol. 17. Weinheim: Wiley-VCH, 2012. p. 67–82. ISBN 978-3-527-30385-4.

[111] NICOL, RW., MARCHAND, K., and LUBITZ, WD. Bioconversion of crude glycerol by fungi. *Applied Microbiology and Biotechnology*, Mar. 2012, vol. 93, no. 5, p. 1865–1875, doi:10.1007/s00253-012-3921-7.

[112] CHRISTOPH, R., SCHMIDT, B., STEINBERNER, U., *et al.* Glycerol. In *Ullmann's Encyclopedia of Industrial Chemistry*, vol. 17. Weinheim: Wiley-VCH, Apr. 2006. p. 67–82. Doi:10.1002/14356007.a12_477.pub2. ISBN 978-3-527-30673-2.

[113] MCNEIL, J., DAY, P., and SIROVSKI, F. Glycerine from biodiesel: The perfect diesel fuel. *Process Safety and Environmental Protection*, May 2012, vol. 90, no. 3, p. 180–188, doi:10.1016/j.psep.2011.09.006.

[114] EATON, SJ., HARAKAS, GN., KIMBALL, RW., *et al.* Formulation and Combustion of Glycerol–Diesel Fuel Emulsions. *Energy & Fuels*, June 2014, vol. 28, no. 6, p. 3940–3947, doi:10.1021/ef500670d.

[115] BOHON, MD., METZGER, BA., LINAK, WP., *et al.* Glycerol combustion and emissions. *Proceedings of the Combustion Institute*, Sept. 2011, vol. 33, no. 2, p. 2717–2724, doi:10.1016/j.proci.2010.06.154.

[116] BEAUCHAMP, RO., ANDJELKOVICH, DA., KLIGERMAN, AD., *et al.* A critical review of the literature on acrolein toxicity. *CRC Critical Reviews in Toxicology*, Jan. 1985, vol. 14, no. 4, p. 309–380, doi:10.3109/10408448509037461.

[117] KOHSE□HÖINGHAUS, K., OßWALD, P., COOL, TA., *et al.* Biofuel Combustion Chemistry: From Ethanol to Biodiesel. *Angewandte Chemie International Edition*, May 2010, vol. 49, no. 21, p. 3572–3597, doi:10.1002/anie.200905335.

[118] ASTM, . Standard Specification for Biodiesel Fuel Blend Stock (B100) for Middle Distillate Fuels. Available from: `https://www.astm.org/d6751-20a.html`

[119] DOMINGOS, AM., PITT, FD., and CHIVANGA BARROS, AA. Purification of residual glycerol recovered from biodiesel production. *South African Journal of Chemical Engineering*, July 2019, vol. 29, p. 42–51, doi:10.1016/j.sajce.2019.06.001.

[120] DUTTA, A. Impact of carbon emission trading on the European Union biodiesel feedstock market. *Biomass and Bioenergy*, Sept. 2019, vol. 128, p. 105328, doi:10.1016/j.biombioe.2019.105328.

[121] OECD, . Agriculture and fisheries. Available from: `https://www.oecd.org/en/topics/policy-areas/agriculture-and-fisheries.html`

[122] VICENTE, G., MARTÍNEZ, M., and ARACIL, J. Integrated biodiesel production: a comparison of different homogeneous catalysts systems. *Bioresource Technology*, May 2004, vol. 92, no. 3, p. 297–305, doi:10.1016/j.biortech.2003.08.014.

[123] SINGH, SP. and SINGH, D. Biodiesel production through the use of different sources and characterization of oils and their esters as the substitute of diesel: A review. *Renewable and Sustainable Energy Reviews*, Jan. 2010, vol. 14, no. 1, p. 200–216, doi:10.1016/j.rser.2009.07.017.

[124] DEMIRBAS, A. Biofuels securing the planet's future energy needs. *Energy Conversion and Management*, Sept. 2009, vol. 50, no. 9, p. 2239–2249, doi:10.1016/j.enconman.2009.05.010.

[125] DEMIRBAS, A. *Biofuels: Securing the Planet's Future Energy Needs*. Doi:10.1007/978-1-84882-011-1. London: Springer, 2009. Green Energy and Technology. ISBN 978-1-84882-010-4.

[126] CORNEJO, A., BARRIO, I., CAMPOY, M., *et al.* Oxygenated fuel additives from glycerol valorization. Main production pathways and effects on fuel properties and engine performance: A critical review. *Renewable and Sustainable Energy Reviews*, Nov. 2017, vol. 79, p. 1400–1413, doi:10.1016/j.rser.2017.04.005.

[127] JOHNSON, DT. and TACONI, KA. The glycerin glut: Options for the value□added conversion of crude glycerol resulting from biodiesel production. *Environmental Progress*, Dec. 2007, vol. 26, no. 4, p. 338–348, doi:10.1002/ep.10225.

[128] MONTEIRO, MR., KUGELMEIER, CL., PINHEIRO, RS., *et al.* Glycerol from biodiesel production: Technological paths for sustainability. *Renewable and Sustainable Energy Reviews*, May 2018, vol. 88, p. 109–122, doi:10.1016/j.rser.2018.02.019.

[129] GHOLAMI, Z., ABDULLAH, AZ., and LEE, K-T. Dealing with the surplus of glycerol production from biodiesel industry through catalytic upgrading to polyglycerols and other value-added products. *Renewable and Sustainable Energy Reviews*, Nov. 2014, vol. 39, p. 327–341, doi:10.1016/j.rser.2014.07.092.

[130] BROCK, D., KODER, A., RABL, H-P., *et al.* Optimising the biodiesel production process: Implementation of glycerol derivatives into biofuel formulations and their potential to form hydrofuels. *Fuel*, Mar. 2020, vol. 264, p. 116695, doi:10.1016/j.fuel.2019.116695.

[131] DODSON, JR., LEITE, TDCM., S. PONTES, N., *et al.* Green Acetylation of Solketal and Glycerol Formal by Heterogeneous Acid Catalysts to Form a Biodiesel Fuel Additive. *ChemSusChem*, Sept. 2014, vol. 7, no. 9, p. 2728–2734, doi:10.1002/cssc.201402070.

[132] OZORIO, LP., PIANZOLLI, R., MOTA, MBS., *et al.* Reactivity of glycerol/acetone ketal (solketal) and glycerol/formaldehyde acetals toward acid-catalyzed hydrolysis. *Journal of the Brazilian Chemical Society*, May 2012, vol. 23, no. 5, p. 931–937, doi: 10.1590/S0103-50532012000500019.

[133] RODRIGUES, R., GONÇALVES, M., MANDELLI, D., *et al.* Solvent-free conversion of glycerol to solketal catalysed by activated carbons functionalised with acid groups. *Catalysis Science & Technology*, Mar. 2014, vol. 4, no. 8, p. 2293–2301, doi:10.1039/C4CY00181H.

[134] SAMOILOV, VO., ONISHCHENKO, MO., RAMAZANOV, DN., *et al.* Glycerol Isopropyl Ethers: Direct Synthesis from Alcohols and Synthesis by the Reduction of Solketal. *ChemCatChem*, July 2017, vol. 9, no. 14, p. 2839–2849, doi:10.1002/cctc.201700108.

[135] *Process and product relating to tertiary ethers*. Patent US1968033A.

[136] DOELLING, GL. *Ethers of glycerol*. Patent US2255916A, Sept. 1941.

[137] ARCO CHEMICAL TECHNOLOGY LP, . *Glycerine ditertiary butyl ether preparation*. Inventor: VP. Gupta. Patent US5476971A, Dec. 1995.

[138] GTBE CO N.V., . *Method of preparing glycerol alkyl ethers*. Inventors: GF. Versteeg, P. Ijben, WN. Wermink, K. Klepáčová, S. van Loo, and W. Kesber. Patent US9000230B2, Apr. 2015.

[139] BEHR, A. and OBENDORF, L. Development of a Process for the Acid-Catalyzed Etherification of Glycerine and Isobutene Forming Glycerine Tertiary Butyl Ethers. *Engineering in Life Sciences*, July 2002, vol. 2, no. 7, p. 185, doi:10.1002/1618-2863(20020709)2:7<185::AID-ELSC185>3.0.CO;2-4.

[140] KLEPÁČOVÁ, K., MRAVEC, D., and BAJUS, M. tert-Butylation of glycerol catalysed by ion-exchange resins. *Applied Catalysis A: General*, Oct. 2005, vol. 294, no. 2, p. 141–147, doi:10.1016/j.apcata.2005.06.027.

[141] CANNILLA, C., BONURA, G., FRUSTERI, L., *et al.* Batch reactor coupled with water permselective membrane: Study of glycerol etherification reaction with butanol. *Chemical Engineering Journal*, Dec. 2015, vol. 282, p. 187–193, doi: 10.1016/j.cej.2015.03.013.

[142] IZQUIERDO, JF., MONTIEL, M., PALÉS, I., *et al.* Fuel additives from glycerol etherification with light olefins: State of the art. *Renewable and Sustainable Energy Reviews*, Dec. 2012, vol. 16, no. 9, p. 6717–6724, doi:10.1016/j.rser.2012.08.005.

[143] CANNILLA, C., BONURA, G., MAISANO, S., *et al.* Zeolite-assisted etherification of glycerol with butanol for biodiesel oxygenated additives production. *Journal of Energy Chemistry*, Sept. 2020, vol. 48, p. 136–144, doi:10.1016/j.jechem.2020.01.002.

[144] KOUSEMAKER, MA. AND THIELE, KD., . *Method for producing an oxygen-containing compound used as fuel additive, in particular in diesel fuels, gasoline, and rapeseed methyl ester*. Patent US20090270643A1, Oct. 2009.

[145] SAMOILOV, VO., RAMAZANOV, DN., NEKHAEV, AI., *et al.* Heterogeneous catalytic conversion of glycerol to oxygenated fuel additives. *Fuel*, May 2016, vol. 172, p. 310–319, doi:10.1016/j.fuel.2016.01.024.

[146] INDUSTRIAL MANAGEMENT, S.A., . *Process for the production of triacetin, alkyl esters of fatty acids*. Inventors: JD. Puche. Patent WO2016180498A1, Nov. 2016.

[147] GAINEY, B., O'DONNELL, P., YAN, Z., *et al.* LTC performance of C1–C4 water-alcohol blends with the same cooling potential. *Fuel*, June 2021, vol. 293, p. 120480, doi:10.1016/j.fuel.2021.120480.

[148] KOSARIC, N., DUVNJAK, Z., FARKAS, A., *et al.* Ethanol. In *Ullmann's Encyclopedia of Industrial Chemistry*, vol. 13. Weinheim: Wiley-VCH, 2012. p. 333–403. ISBN 978-3-527-30385-4.

[149] ROGERS, PL., LEE, KJ., SKOTNICKI, ML., *et al.* Ethanol production by Zymomonas mobilis. In FIECHTER, A., AIBA, S., ATKINSON, B., *et al.* (eds.). *Microbial Reactions*, *Advances in Biochemical Engineering/Biotechnology*, vol. 23. Berlin, Heidelberg: Springer, 1982. p. 37–84. Doi:10.1007/3540116982_2. ISBN 978-3-540-11698-1.

[150] ZABED, H., SAHU, JN., BOYCE, AN., *et al.* Fuel ethanol production from lignocellulosic biomass: An overview on feedstocks and technological approaches. *Renewable and Sustainable Energy Reviews*, Dec. 2016, vol. 66, p. 751–774, doi:10.1016/j.rser.2016.08.038.

[151] ZABED, H., SAHU, JN., SUELY, A., *et al.* Bioethanol production from renewable sources: Current perspectives and technological progress. *Renewable and Sustainable Energy Reviews*, May 2017, vol. 71, p. 475–501, doi:10.1016/j.rser.2016.12.076.

[152] WHITE, TL. Alcohol as a Fuel for the Automobile Motor. SAE paper 070002. *SAE Technical Paper Series*, Jan. 1907, doi:10.4271/070002.

[153] LUCKE, CE. and WOODWARD, SM. The Use of Alcohol and Gasoline in Farm Engines. Technical report Farmers' Bulletin No. 277, U.S. Department of Agriculture, Washington, DC, Feb. 1907.

[154] MENDIBURU, AZ., LAUERMANN, CH., HAYASHI, TC., *et al.* Ethanol as a renewable biofuel: Combustion characteristics and application in engines. *Energy*, Oct. 2022, vol. 257, p. 124688, doi:10.1016/j.energy.2022.124688.

[155] OTT, J., GRONEMANN, V., PONTZEN, F., *et al.* Methanol. In *Ullmann's Encyclopedia of Industrial Chemistry*. Weinheim: Wiley-VCH, 2012. p. 1–27. ISBN 978-3-527-30385-4.

[156] SHELDON, D. Methanol Production – A Technical History. *Johnson Matthey Technology Review*, July 2017, vol. 61, no. 3, p. 172–182, doi:10.1595/205651317X695622.

[157] MOLINO, A., CHIANESE, S., and MUSMARRA, D. Biomass gasification technology: The state of the art overview. *Journal of Energy Chemistry*, Jan. 2016, vol. 25, no. 1, p. 10–25, doi:10.1016/j.jechem.2015.11.005.

[158] SAFARIAN, S., UNNÞÓRSSON, R., and RICHTER, C. A review of biomass gasification modelling. *Renewable and Sustainable Energy Reviews*, Aug. 2019, vol. 110, p. 378–391, doi:10.1016/j.rser.2019.05.003.

[159] CRI, CARBON RECYCLING INTERNATIONAL. Global Leader in Carbon Capture and Utilization & E-methanol. Available from: `https://carbonrecycling.com`

[160] LANDÄLV, I. Methanol as a renewable fuel – a knowledge synthesis. Technical Report 2015:08, f3 The Swedish Knowledge Centre for Renewable Transportation Fuels, Sweden, Sept. 2017.

[161] VERHELST, S., TURNER, JWG., SILEGHEM, L., *et al.* Methanol as a fuel for internal combustion engines. *Progress in Energy and Combustion Science*, Jan. 2019, vol. 70, p. 43–88, doi:10.1016/j.pecs.2018.10.001.

[162] KLABUNDE, J., BISCHOFF, C., and PAPA, AJ. Propanols. In *Ullmann's Encyclopedia of Industrial Chemistry*. Weinheim, Germany: Wiley-VCH, 2018. p. 1–14. ISBN 978-3-527-30385-4.

[163] MCDONNELL, G. and RUSSELL, AD. Antiseptics and Disinfectants: Activity, Action, and Resistance. *Clinical Microbiology Reviews*, Jan. 1999, vol. 12, no. 1, p. 147–179, doi:10.1128/CMR.12.1.147.

[164] GASPAR, D. Top Ten Blendstocks for Turbocharged Gasoline Engines: Bioblendstocks with the Potential to Deliver the Highest Engine Efficiency. Technical Report PNNL-28713, Pacific Northwest National Laboratory, Richland, WA (United States), Sept. 2019, doi: 10.2172/1567705. Available from: `https://www.osti.gov/servlets/purl/1567705`

[165] SCHUBERT, T. Production routes of advanced renewable C1 to C4 alcohols as biofuel components – a review. *Biofuels, Bioproducts and Biorefining*, July 2020, vol. 14, no. 4, p. 845–878, doi:10.1002/bbb.2109.

[166] DÜRRE, P. New insights and novel developments in clostridial acetone/butanol/isopropanol fermentation. *Applied Microbiology and Biotechnology*, June 1998, vol. 49, no. 6, p. 639–648, doi:10.1007/s002530051226.

[167] INOKUMA, K., LIAO, JC., OKAMOTO, M., *et al.* Improvement of isopropanol production by metabolically engineered Escherichia coli using gas stripping. *Journal of Bioscience and Bioengineering*, Dec. 2010, vol. 110, no. 6, p. 696–701, doi:10.1016/j.jbiosc.2010.07.010.

[168] JANG, Y-S., MALAVIYA, A., LEE, J., *et al.* Metabolic engineering of *Clostridium acetobutylicum* for the enhanced production of isopropanol□butanol□ethanol fuel mixture. *Biotechnology Progress*, July 2013, vol. 29, no. 4, p. 1083–1088, doi:10.1002/btpr.1733.

[169] KOPPOLU, V. and VASIGALA, VKR. Role of Escherichia coli in Biofuel Production. *Microbiology Insights*, Jan. 2016, vol. 9, doi:10.4137/MBI.S10878.

[170] KO, YJ., CHA, J., JEONG, W-Y., *et al.* Bio-isopropanol production in Corynebacterium glutamicum: Metabolic redesign of synthetic bypasses and two-stage fermentation with gas stripping. *Bioresource Technology*, June 2022, vol. 354, p. 127171, doi:10.1016/j.biortech.2022.127171.

[171] LIEW, FE., NOGLE, R., ABDALLA, T., *et al.* Carbon-negative production of acetone and isopropanol by gas fermentation at industrial pilot scale. *Nature Biotechnology*, Mar. 2022, vol. 40, no. 3, p. 335–344, doi:10.1038/s41587-021-01195-w.

[172] GONG, J., CAI, J., and TANG, C. A Comparative Study of Emissions Characteristics of Propanol Isomers/Gasoline Blends Combined with EGR. SAE paper 2014-01-1454. *SAE Technical Paper Series*, Apr. 2014, doi:10.4271/2014-01-1454.

[173] SIVASUBRAMANIAN, H., POCHAREDDY, YK., DHAMODARAN, G., *et al.* Performance, emission and combustion characteristics of a branched higher mass, C3 alcohol (isopropanol) blends fuelled medium duty MPFI SI engine. *Engineering Science and Technology, an International Journal*, Apr. 2017, vol. 20, no. 2, p. 528–535, doi:10.1016/j.jestch.2016.11.013.

[174] KUMAR, N., JAIN, S., BAGLA, A., *et al.* Study of Performance and Emission Characteristics of Propan-2-ol and Gasoline Fuel Blends in an Unmodified Spark Ignition Engine. SAE paper 2019-01-0793. *SAE Technical Paper Series*, Apr. 2019, doi:10.4271/2019-01-0793.

[175] GAINEY, B. and LAWLER, B. The role of alcohol biofuels in advanced combustion: An analysis. *Fuel*, Jan. 2021, vol. 283, p. 118915, doi:10.1016/j.fuel.2020.118915.

[176] GAINEY, B., YAN, Z., and LAWLER, B. Autoignition characterization of methanol, ethanol, propanol, and butanol over a wide range of operating conditions in LTC/HCCI. *Fuel*, Mar. 2021, vol. 287, p. 119495, doi:10.1016/j.fuel.2020.119495.

[177] HAHN, H-D., DÄMBKES, G., RUPPRICH, N., *et al.* Butanols. In *Ullmann's Encyclopedia of Industrial Chemistry*. Weinheim, Germany: Wiley-VCH, 2013. p. 1–13. ISBN 978-3-527-30385-4.

[178] OLSON, AL., TUNÉR, M., and VERHELST, S. A Review of Isobutanol as a Fuel for Internal Combustion Engines. *Energies*, Nov. 2023, vol. 16, no. 22, p. 7470, doi:10.3390/en16227470.

[179] JONES, DT. and WOODS, DR. Acetone-Butanol Fermentation Revisited. *Microbiological Reviews*, Dec. 1986, vol. 50, no. 4, p. 484–524, doi:10.1128/mr.50.4.484-524.1986.

[180] EZEJI, TC., QURESHI, N., and BLASCHEK, HP. Bioproduction of butanol from biomass: from genes to bioreactors. *Current Opinion in Biotechnology*, June 2007, vol. 18, no. 3, p. 220–227, doi:10.1016/j.copbio.2007.04.002.

[181] SU, Y., ZHANG, W., ZHANG, A., *et al.* Biorefinery: The Production of Isobutanol from Biomass Feedstocks. *Applied Sciences*, Nov. 2020, vol. 10, no. 22, p. 8222, doi:10.3390/app10228222.

[182] NOZZI, NE., DESAI, SH., CASE, AE., *et al.* Metabolic engineering for higher alcohol production. *Metabolic Engineering*, Sept. 2014, vol. 25, p. 174–182, doi:10.1016/j.ymben.2014.07.007.

[183] DEDOV, AG., KARAVAEV, AA., LOKTEV, AS., *et al.* Bioisobutanol as a Promising Feedstock for Production of "Green" Hydrocarbons and Petrochemicals (A Review). *Petroleum Chemistry*, Nov. 2021, vol. 61, no. 11, p. 1139–1157, doi:10.1134/S0965544121110165.

[184] BP/DuPont launches Butamax biobutanol. *Focus on Catalysts*, Dec. 2009, vol. 2009, no. 12, p. 5, ISSN 13514180, doi:10.1016/S1351-4180(09)70514-8. Available from: `https://linkinghub.elsevier.com/retrieve/pii/S1351418009705148`

[185] Biofuels: biobutanol fuel prepares for launch. *Focus on Catalysts*, Oct. 2010, vol. 2010, no. 10, p. 2, ISSN 13514180, doi:10.1016/S1351-4180(10)

70381-0. Available from: https://linkinghub.elsevier.com/retrieve/pii/S1351418010703810

[186] Retrofit produces isobutanol. *Focus on Catalysts*, Jan. 2010, vol. 2010, no. 1, p. 5–6, ISSN 13514180, doi:10.1016/S1351-4180(09)70571-9. Available from: https://linkinghub.elsevier.com/retrieve/pii/S1351418009705719

[187] Gevo produces isobutanol, hydrocarbons, and jet fuel from cellulosic biomass. *Focus on Catalysts*, Sept. 2010, vol. 2010, no. 9, p. 4, ISSN 13514180, doi:10.1016/S1351-4180(10)70344-5. Available from: https://linkinghub.elsevier.com/retrieve/pii/S1351418010703445

[188] KAMEOKA, A., NAGAI, K., SUGIYAMA, G., *et al.* Effect of Alcohol Fuels on Fuel-Line Materials of Gasoline Vehicles. SAE paper 2005-01-3708. *SAE Technical Paper Series*, Oct. 2005, doi:10.4271/2005-01-3708.

[189] SATHISH KUMAR, T. and ASHOK, B. Material compatibility of SI engine components towards corrosive effects on methanol-gasoline blends for flex fuel applications. *Materials Chemistry and Physics*, Feb. 2023, vol. 296, p. 127344, doi:10.1016/j.matchemphys.2023.127344.

[190] BELINCANTA, J., ALCHORNE, JA., and TEIXEIRA DA SILVA, M. The Brazilian Experience With Ethanol Fuel: Aspects of Production, Use, Quality and Distribution Logistics. *Brazilian Journal of Chemical Engineering*, Dec. 2016, vol. 33, no. 4, p. 1091–1102, doi:10.1590/0104-6632.20160334s20150088.

[191] FUREY, RL. Volatility Characteristics of Gasoline-Alcohol and Gasoline-Ether Fuel Blends. SAE paper 852116. *SAE Technical Paper Series*, Oct. 1985, doi:10.4271/852116.

[192] ANDERSEN, VF., ANDERSON, JE., WALLINGTON, TJ., *et al.* Distillation Curves for Alcohol–Gasoline Blends. *Energy & Fuels*, Apr. 2010, vol. 24, no. 4, p. 2683–2691, doi:10.1021/ef9014795.

[193] ANDERSEN, VF., ANDERSON, JE., WALLINGTON, TJ., *et al.* Vapor Pressures of Alcohol–Gasoline Blends. *Energy & Fuels*, June 2010, vol. 24, no. 6, p. 3647–3654, doi:10.1021/ef100254w.

[194] CORPORATION, VOLVO CAR. Dear diesel, it's time to say goodbye. Apr. 2024. Available from: https://www.volvocars.com/intl/news/sustainability/dear-diesel-its-time-to-say-goodbye/

[195] TUNESTÅL, P. TDC Offset Estimation from Motored Cylinder Pressure Data based on Heat Release Shaping. *Oil & Gas Science and Technology – Revue d'IFP Energies nouvelles*, July 2011, vol. 66, no. 4, p. 705–716, doi:10.2516/ogst/2011144.

[196] LODI, F., JAFARI, M., BROWN, R., *et al.* Statistical Analysis of the Results Obtained by Thermodynamic Methods for the Determination of TDC Offset in an Internal Combustion Engine. SAE paper 2020-01-1350. *SAE Technical Paper Series*, Apr. 2020, doi:10.4271/2020-01-1350.

[197] GARCIA, P. *Experimental Investigations on Natural Gas-Diesel Dual Fuel Combustion*. Doctoral dissertation, Lund University, Lund, Sweden, June 2018.

[198] GATOWSKI, JA., BALLES, EN., CHUN, KM., *et al.* Heat Release Analysis of Engine Pressure Data. SAE paper 841359. *SAE Technical Paper Series*, Oct. 1984, doi:10.4271/841359.

[199] WOSCHNI, G. A Universally Applicable Equation for the Instantaneous Heat Transfer Coefficient in the Internal Combustion Engine. SAE paper 670931. *SAE Technical Paper Series*, Feb. 1967, doi:10.4271/670931.

[200] FOR STANDARDIZATION, EUROPEAN COMMITTEE. EN 590:2013 - Automotive fuels - Diesel - Requirements and test methods. 2013.

[201] PROCEDE HOLDING B.V., . *GTBE compositions, methods and installations for enhanced octane boosting*. Inventors: GF. Versteeg and WN. Wermink. Patent WO2017105246A2, June 2017.

[202] CANDEIA, RA., SILVA, MCD., CARVALHO FILHO, JR., *et al.* Influence of soybean biodiesel content on basic properties of biodiesel–diesel blends. *Fuel*, Apr. 2009, vol. 88, no. 4, p. 738–743, doi:10.1016/j.fuel.2008.10.015.

[203] INTERNATIONAL ENERGY AGENCY, IEA. Fatty Acid Esters (biodiesel) : Properties - AMF. 2024. Available from: `https://www.iea-amf.org/content/fuel_information/fatty_acid_esters/properties`

[204] BEATRICE, C., DI BLASIO, G., LAZZARO, M., *et al.* Technologies for energetic exploitation of biodiesel chain derived glycerol: Oxy-fuels production by catalytic conversion. *Applied Energy*, Feb. 2013, vol. 102, p. 63–71, doi:10.1016/j.apenergy.2012.08.006.

[205] FRUSTERI, F., CANNILLA, C., BONURA, G., *et al.* Glycerol Ethers Production and Engine Performance with Diesel/Ethers Blend. *Topics in Catalysis*, May 2013, vol. 56, no. 1-8, p. 378–383, doi:10.1007/s11244-013-9983-7.

[206] DI BLASIO, G., BONURA, G., FRUSTERI, F., *et al.* Experimental Characterization of Diesel Combustion Using Glycerol Derived Ethers Mixtures. SAE paper 2013-24-0104. *SAE International Journal of Fuels and Lubricants*, Sept. 2013, vol. 6, no. 3, p. 940–950, doi:10.4271/2013-24-0104.

[207] BEATRICE, C., DI BLASIO, G., GUIDO, C., *et al.* Mixture of glycerol ethers as diesel bio-derivable oxy-fuel: Impact on combustion and emissions of an automotive engine combustion system. *Applied Energy*, Nov. 2014, vol. 132, p. 236–247, doi: 10.1016/j.apenergy.2014.07.006.

[208] TAN, YR., ZHU, Q., ZONG, Y., *et al.* The influence of alcohol, carbonate and polyethers as oxygenated fuels on the soot characteristics from a CI engine. *Fuel*, Apr. 2023, vol. 338, p. 127296, doi:10.1016/j.fuel.2022.127296.

[209] DELFORT, B., DURAND, I., JAECKER-VOIROL, A., *et al.* Oxygenated Compounds and Diesel Engine Pollutant Emissions Performances of New Generation of Products. SAE paper 2002-01-2852. *SAE Technical Paper Series*, Oct. 2002, doi: 10.4271/2002-01-2852.

[210] FRUSTERI, F., SPADARO, L., BEATRICE, C., *et al.* Oxygenated additives production for diesel engine emission improvement. *Chemical Engineering Journal*, Nov. 2007, vol. 134, no. 1-3, p. 239–245, doi:10.1016/j.cej.2007.03.042.

[211] SPOONER-WYMAN, JK., APPLEBY, DB., and YOST, DM. Evaluation of Di-Butoxy Glycerol (DBG) for Use As a Diesel Fuel Blend Component. SAE paper 2003-01-2281. *SAE Technical Paper Series*, June 2003, doi:10.4271/2003-01-2281.

[212] IIDA, N., SUZUKI, Y., SATO, GT., *et al.* Effects of Intake Oxygen Concentration on the Characteristics of Particulate Emissions from a D.I. Diesel Engine. SAE paper 861233. *SAE Technical Paper Series*, Sept. 1986, doi:10.4271/861233.

[213] SCHMIDT, K. and VAN GERPEN, J. The Effect of Biodiesel Fuel Composition on Diesel Combustion and Emissions. SAE paper 961086. *SAE Technical Paper Series*, May 1996, doi:10.4271/961086.

[214] SONG, J., ZELLO, V., BOEHMAN, AL., *et al.* Comparison of the Impact of Intake Oxygen Enrichment and Fuel Oxygenation on Diesel Combustion and Emissions. *Energy & Fuels*, Sept. 2004, vol. 18, no. 5, p. 1282–1290, doi:10.1021/ef034103p.

[215] LAPUERTA, M., ARMAS, O., and RODRÍGUEZ-FERNÁNDEZ, J. Effect of biodiesel fuels on diesel engine emissions. *Progress in Energy and Combustion Science*, Apr. 2008, vol. 34, no. 2, p. 198–223, doi:10.1016/j.pecs.2007.07.001.

[216] TRUEDSSON, I., TUNER, M., JOHANSSON, B., *et al.* Pressure Sensitivity of HCCI Auto-Ignition Temperature for Primary Reference Fuels. SAE paper 2012-01-1128. *SAE International Journal of Engines*, Apr. 2012, vol. 5, no. 3, p. 1089–1108, doi:10.4271/2012-01-1128.

[217] FOONG, TM., MORGANTI, KJ., BREAR, MJ., *et al.* The octane numbers of ethanol blended with gasoline and its surrogates. *Fuel*, Jan. 2014, vol. 115, p. 727–739, doi:10.1016/j.fuel.2013.07.105.

[218] AHMED, A., GOTENG, G., SHANKAR, VSB., *et al.* A computational methodology for formulating gasoline surrogate fuels with accurate physical and chemical kinetic properties. *Fuel*, Mar. 2015, vol. 143, p. 290–300, doi:10.1016/j.fuel.2014.11.022.

[219] SARATHY, SM., FAROOQ, A., and KALGHATGI, GT. Recent progress in gasoline surrogate fuels. *Progress in Energy and Combustion Science*, Mar. 2018, vol. 65, p. 67–108, doi:10.1016/j.pecs.2017.09.004.

[220] GAUTHIER, BM., DAVIDSON, DF., and HANSON, RK. Shock tube determination of ignition delay times in full-blend and surrogate fuel mixtures. *Combustion and Flame*, Dec. 2004, vol. 139, no. 4, p. 300–311, doi:10.1016/j.combustflame.2004.08.015.

[221] CHECKEL, MD. and DALE, JD. Computerized Knock Detection from Engine Pressure Records. SAE paper 860028. *SAE Technical Paper Series*, Mar. 1986, doi:10.4271/860028.

[222] SCHOLL, D., DAVIS, C., RUSS, S., *et al.* The Volume Acoustic Modes of Spark-Ignited Internal Combustion Chambers. SAE paper 980893. *SAE Technical Paper Series*, Feb. 1998, doi:10.4271/980893.

[223] BENSON, G., FLETCHER, EA., MURPHY, TE., *et al.* Knock (Detonation) Control by Engine Combustion Chamber Shape. SAE paper 830509. *SAE Technical Paper Series*, Feb. 1983, doi:10.4271/830509.

[224] SWARTS, A., ANDERSON, GL., and WALLACE, JM. Comparing Knock between the CFR Engine and a Single Cylinder Research Engine. SAE paper 2019-01-2156. *SAE Technical Paper Series*, Dec. 2019, doi:10.4271/2019-01-2156.

[225] ENG, JA. Characterization of Pressure Waves in HCCI Combustion. SAE paper 2002-01-2859. *SAE Technical Paper Series*, Oct. 2002, doi:10.4271/2002-01-2859.

[226] ROCKSTROH, T., KOLODZIEJ, CP., JESPERSEN, MC., *et al.* Insights into Engine Knock: Comparison of Knock Metrics across Ranges of Intake Temperature and Pressure in the CFR Engine. SAE paper 2018-01-0210. *SAE International Journal of Fuels and Lubricants*, Apr. 2018, vol. 11, no. 4, p. 545–561, doi:10.4271/2018-01-0210.

[227] BRUNT, MFJ., POND, CR., and BLUNDO, J. Gasoline Engine Knock Analysis using Cylinder Pressure Data. SAE paper 980896. *SAE Technical Paper Series*, Feb. 1998, doi:10.4271/980896.

[228] PATTERSON, DJ. Cylinder Pressure Variations, A Fundamental Combustion Problem. SAE paper 660129. *SAE Technical Paper Series*, Feb. 1966, doi:10.4271/660129.

[229] BARTON, RK., KENEMUTH, DK., LESTZ, SS., *et al.* Cycle-by-Cycle Variations of a Spark Ignition Engine - A Statistical Analysis. SAE paper 700488. *SAE Technical Paper Series*, Feb. 1970, doi:10.4271/700488.

[230] GHANDHI, J. and KIM, KS. A Statistical Description of Knock Intensity and Its Prediction. SAE paper 2017-01-0659. *SAE Technical Paper Series*, Mar. 2017, doi:10.4271/2017-01-0659.

[231] RUPPERT, D. What is Kurtosis? An Influence Function Approach. *The American Statistician*, Feb. 1987, vol. 41, no. 1, p. 1–5, doi:10.1080/00031305.1987.10475431.

[232] BALANDA, KP. and MACGILLIVRAY, HL. Kurtosis: A Critical Review. *The American Statistician*, May 1988, vol. 42, no. 2, p. 111–119, doi:10.1080/00031305.1988.10475539.

[233] DECARLO, LT. On the meaning and use of kurtosis. *Psychological Methods*, Sept. 1997, vol. 2, no. 3, p. 292–307, doi:10.1037/1082-989X.2.3.292.

[234] HOTH, A., KOLODZIEJ, CP., ROCKSTROH, T., *et al.* Combustion Characteristics of PRF and TSF Ethanol Blends with RON 98 in an Instrumented CFR Engine. SAE paper 2018-01-1672. *SAE Technical Paper Series*, Sept. 2018, doi:10.4271/2018-01-1672.

[235] GAINEY, BJ. Personal communication. Aug. 2024.

[236] RICARDO, HR. *The High-Speed Internal-Combustion Engine*. London; Glasgow: Blackie, 1931.

[237] WEBER, BW. and SUNG, C-J. Comparative Autoignition Trends in Butanol Isomers at Elevated Pressure. *Energy & Fuels*, Mar. 2013, vol. 27, no. 3, p. 1688–1698, doi:10.1021/ef302195c.

[238] MOSS, JT., BERKOWITZ, AM., OEHLSCHLAEGER, MA., *et al.* An Experimental and Kinetic Modeling Study of the Oxidation of the Four Isomers of Butanol. *The Journal of Physical Chemistry A*, Oct. 2008, vol. 112, no. 43, p. 10843–10855, doi:10.1021/jp806464p.

[239] INTERNATIONAL, ASTM. ASTM D975 - Standard Specification for Diesel Fuel. 2021.

[240] INTERNATIONAL, ASTM. ASTM D4814 - Standard Specification for Automotive Spark-Ignition Engine Fuel. 2021.

[241] FOR STANDARDIZATION, EUROPEAN COMMITTEE. EN 228:2012 - Automotive fuels - Unleaded petrol - Requirements and test methods. 2012.

[242] MOFFAT, RJ. Contributions to the Theory of Single-Sample Uncertainty Analysis. *Journal of Fluids Engineering*, June 1982, vol. 104, no. 2, p. 250–258, doi:10.1115/1.3241818.

[243] TAYLOR, JR. *An Introduction to Error Analysis: The Study of Uncertainties in Physical Measurements*. 2nd ed. Sausalito, CA: University Science Books, 1997. ISBN 0-935702-75-X.

[244] MOFFAT, RJ. Describing the uncertainties in experimental results. *Experimental Thermal and Fluid Science*, Jan. 1988, vol. 1, no. 1, p. 3–17, doi:10.1016/0894-1777(88)90043-X.

[245] KLINE, SJ. and MCCLINTOCK, FA. Describing Uncertainties in Single-Sample Experiments. *Mechanical Engineering*, Jan. 1953, vol. 75, no. 1, p. 3–8.